C. Chryssostomidis
N.M. Patrikalakis

Theoretical and Experimental Prediction of the Response of a Marine Riser Model Subjected to Sinusoid Excitation of its Top End

MIT Sea Grant Program

Massachusetts Institute of Technology
Cambridge
Massachusetts 02139

Report Number
MITSG 83-20
August 1983

THEORETICAL AND EXPERIMENTAL PREDICTION OF THE RESPONSE OF A MARINE RISER MODEL SUBJECTED TO SINUSOID EXCITATION OF ITS TOP END

by

C. Chryssostomidis
N. M. Patrikalakis

MIT SEA GRANT REPORT NO. 83-20

AUGUST, 1983

ABSTRACT

The objective of this report is to provide:

1. An analysis of the experimental results obtained from a 3 m flexible riser model with its top end oscillated sinusoidally with amplitudes between 0.49 and 2.97 diameters.

2. A comparison of the experimental results from the flexible model with theoretical predictions of the response based on rigid and spring mounted rigid cylinder experimental results.

ACKNOWLEDGEMENTS

Funding for this research was obtained from the MIT Sea Grant College Program, Conoco, Inc. and Gulf Oil Company. All experiments were performed at the Laboratory for Hydrodynamics of the National Technical University of Athens, Greece. K. Ho and E. A. Vrakas helped in the preparation of the figures of this report. The typed manuscript was prepared by M. Staruch.

RELATED SEA GRANT REPORTS

1. "Theoretical and Experimental Prediction of the Response of a Marine Riser Model Subjected to Sinusoid Excitation of its Top End with Amplitude Equal to Two Diameters," C. Chryssostomidis, N. M. Patrikalakis, and E. A. Vrakas, MIT Sea Grant Report No. 83-2, March 1983.

2. "Theoretical and Experimental Prediction of the Response of a Marine Riser Model Subjected to Sinusoid Excitation of its Top End with Amplitude of Two Diameters Parallel to a Uniform Stream of Speed Equal to 120 mm/s," C. Chryssostomidis and N. M. Patrikalakis, MIT Sea Grant Report No. 83-3, March 1983.

3. "Theoretical and Experimental Prediction of the Response of a Marine Riser Model Subjected to Sinusoid Excitation of its Top End with Amplitude of Two Diameters Parallel to a Uniform Stream of Speed Equal to 240 mm/s," C. Chryssostomidis and N. M. Patrikalakis, MIT Sea Grant Report No. 83-4, March 1983.

4. "Theoretical and Experimental Prediction of the Response of a Marine Riser Model Subjected to Sinusoid Excitation of its Top End with Amplitude of Two Diameters Orthogonal to a Uniform Stream of Speed Equal to 120 mm/s," N. M. Patrikalakis and C. Chryssostomidis, MIT Sea Grant Report No. 83-5, March 1983.

5. "Theoretical and Experimental Prediction of the Response of a Marine Riser Model Subjected to Sinusoid Excitation of its Top End with Amplitude of Two Diameters Orthogonal to a Uniform Stream of Speed Equal to 240 mm/s," N. M. Patrikalakis and C. Chryssostomidis, MIT Sea Grant Report No. 83-6, March 1983.

6. "Theoretical and Experimental Prediction of the Response of a Marine Riser Model in a Uniform Stream," N. M. Patrikalakis and C. Chryssostomidis, MIT Sea Grant Report No. 83-15, August 1983.

7. "Theoretical and Experimental Prediction of the Response of a Marine Riser Model Subjected Sinusoid Excitation of Its Top End Orthogonal to a Uniform Stream of Speed Equal to 42 mm/s," N. M. Patrikalakis and C. Chryssostomidis, MIT Sea Grant Report No. 83-18, August 1983.

8. "Theoretical and Experimental Prediction of the Response of a Marine Riser Model Subjected to Sinusoid Excitation of Its Top End Parallel to a Uniform Stream," C. Chryssostomidis and N. M. Patrikalakis, MIT Sea Grant Report No. 83-19, August 1983.

9. "Theoretical and Experimental Prediction of the Response of a Marine Riser Model Subjected to Sinusoid Excitation of Its Top End Orthogonal to a Uniform Stream," C. Chryssostomidis and N. M. Patrikalakis, MIT Sea Grant Report No. 83-21, August 1983.

TABLE OF CONTENTS

LIST OF TABLES

LIST OF FIGURES

EXPERIMENT 15:

EXPERIMENT 18:

EXPERIMENT 21:

EXPERIMENT 48:

EXPERIMENT 24:

Figures A1, A2, and A3:

Figures A4 and A5:

1. A DESCRIPTION OF THE RISER MODEL

A brief description of the model based on the information given in Patrikalakis and Chryssostomidis (1983) is included here for the reader's convenience.

The model is made up of an aluminum tube covered externally with a sealing material. The overall model characteristics are:

- Length between ball joints (L) = 3.000 m
- Aluminum tube I. D. (D_i) = 10.92 mm
- Aluminum tube O. D. (D_o) = 12.61 mm
- External sealing (effective) diameter (D_e) = 15.3 mm
- Average mass per unit length (M) = 0.327 kg/m
- Average effective weight per unit length (We) = 1.378 N/m
- Effective overpull at the lower ball joint (Pe(0)) = 1.72 N
- Bending stiffness of a cross section (EI) = 37.6 Nm^2

The inside of the aluminum tube is filled with a glycerin solution in water of density approximately equal to 900 kg/m^3. At the ends of the model there are ball joints which minimize the end bending moments. Above the upper ball joint there is a slip joint, which is designed to minimize tension variations due to flexural motions. The riser model is also designed so it can be tensioned to the desired tension. The first four "natural frequencies" of the model in water are approximately equal to 1.57, 6.06, 13.54 and 24.02 Hz, respectively. These have been determined theoretically using c_m=1. The first two "natural frequencies" have also been verified from a decay test in quiescent water, where the initial amplitude of the response was of the order of 1/10 of the effective diameter.

The model is instrumented at ten equidistant locations, 1-10, each with two strain gage full bridges installed on the outer surface of the aluminum tube, designed to isolate bending from tension and to measure bending strains on two orthogonal directions A and B. In the vertical static equilibrium condition, planes A and B are parallel and orthogonal to the centerline of the towing tank, respectively. The actual location of each branch of the bending bridges is at approximately 9.80 degrees from planes A and B. The numbering of the bridges begins at the upper end, while their elevation is measured from the axis of the lower ball joint. The first and last bending bridges are L/11 from the axes of the top and bottom ball joints, respectively, and the separation between bending bridges is L/11. For example, bridge A6 measures bending strains created by deflections in plane A at elevation $Z=5L/11$ from the axis of the lower ball joint. In addition, the model is instrumented at two extra positions T1 and T2, 101 m from the axes of each ball joint, with specially designed full bridges isolating tension from bending. Tension bridge T2 is at the lower end of the model. Finally, the model is instrumented at an additional location, Q1, 1773 mm from the upper ball joint, with a full torsion bridge. The mass per unit length of a single wire is 0.198 grams/m, while the total mass of all wires for all 23 full bridges is approximately 2.73% of the total model mass. Their total volume is approximately equal to 5.32 cm^3. The four wires of each bridge are braided to avoid interference and are sent internally to the lower end of the model.

The oscillation of the top end of the model is created by a DC motor driven by a signal generator and controlled by a tachometer measuring angular velocities and a linear variable differential transducer, LVDT, measuring displacements. The rotational motion of the motor is converted to linear motion via a specially designed rack anti-backlash pinion system. During the experiments, measurements from a number of strain bridges and the LVDT were made simultaneously and were recorded digitally. Using the torque bridge, it was observed that the structural torsion was negligible, see Chapter III of Patrikalakis (1983). It was estimated analytically, and also confirmed by the tension bridge measurements, that the tension variation during the experiments was small approximately 5% of the effective tension. Therefore, even for the lowest excited mode, the ratio of the change of restoring force due to tension variation to the overall restoring force is very small (0.3%). This implies that the assumption of constant effective tension with time is an acceptable approximation for theoretical estimates of the response.

From calibration experiments in air, it was found that the logarithmic decrement representing the structural damping force is a nonlinear function of the modal amplitude. For the first mode, our estimate for the logarithmic decrement representing the structural damping force in water, δ_1, is given by $\delta_1 = A + B^3/(\alpha_1^3 + C^3)$, where A=0.0664, B=0.1989, C=0.3533, and α_1 is the amplitude of the first mode in effective diameters. The corresponding estimate for the second mode, δ_2, is given by $\delta_2 = D + E^3/(\alpha_2^3 + F^3)$, where D=0.0404, E=0.0431, F=0.1186 and α_2 is the amplitude of the second mode. The range of α_1 used to estimate δ_1 is between 0.17 and 1.28 D_e and the range of α_2 used to estimate δ_2 is between 0.11 and 0.26 D_e. For the theoretical predictions orthogonal to the direction of imposed oscillation the "best fit" values for the structural damping ratios in air, ς, were used, Patrikalakis (1983). The values of ς for the first two modes are 0.016 and 0.010, respectively. This approximation does not affect our estimate of the lift response because, as it can be easily verified, typical fluid drag forces are much larger than our estimates of the structural damping forces. Our experiments in air also revealed that when the upper end of the model was oscillated in a certain plane, some flexural response orthogonal to this plane existed. This happens because our model was not rotationally uniform. When the response was primarily at the first mode, it was estimated that the flexural response orthogonal to the direction of excitation was not larger than approximately 12% of the response in the plane of applied oscillation. It was felt that such an imperfection would not substantially affect the experimental results in water.

2. PRESENTATION OF EXPERIMENTAL AND THEORETICAL RESULTS

The experiments presented in this report involve sinusoid excitation of the top end of the riser model at amplitudes between 0.49 and 2.97 effective diameters for the conditions shown in Tables 2-1 to 2-3. The experiments described in Tables 2-1 and 2-3 involve sinusoid excitation of the top end of the model parallel to plane A while the experiments described in Table 2-2 involve excitation of the top end parallel to plane B. Experiments similar to the ones described in Table 2-2 but with excitation parallel to plane A were reported earlier in Chryssostomidis, Patrikalakis and Vrakas (1983). Comparisons between our earlier results and the results of the experiments described in Table 2-2 provide estimates of the rotational uniformity of the model and of the repeatability of the measurements. During our experiments, bending strains at positions shown in Table 2-4 and the motion of the upper end were recorded.

The experimental and theoretical results reported here include plots of:

1. The root mean square of the measured motion of the top end as a function of frequency.

2. The root mean square measured dynamic bending strains as a function of the response frequency.

3. The measured and theoretical predictions of the bending strains parallel and orthogonal to the oscillation of the top end.

4. The measured maximum bending strains parallel and orthogonal to the oscillation of the top end and independent of direction.

5. Indicative partial synchronous time traces of the motion of the top end and measured bending strains from three bridges.

The root mean square responses have been calculated using standard FFT codes from the International Mathematical and Statistical Library (IMSL) on an IBM

370/168 computer. The root mean square response is the square root of the product of the power spectral density of the response times the effective bandwidth B_e employed in the Fourier analysis of the results. The root mean square rather than the magnitude of the power spectral density was selected for presentation because, in most cases, the experimental response was practically periodic. The logarithmic representation of the power spectral density was not selected because it tends to visually exaggerate the significance of smaller components, which are not important in this problem. For each major peak of the root mean square plots, the root mean square value of the response is shown. This is computed as the square root of the sum of the squares of the rms response strains at discrete frequencies, B_e Hz apart, in the neighborhood of each peak. In addition, the overall dynamic root mean square value of the response is also shown. The Fourier and maxima calculations were performed using the record length shown in Tables 2-1 to 2-3.

The nomenclature used in the Figures and Tables 2-1 to 2-3 is defined below:

The experiment number corresponds to the numbering system employed during the performance of the experiments. BE is the effective bandwidth B_e employed in the Fourier analysis in Hz. THETA is the angle of oscillation of the top end with respect to the longer side of the towing tank in degrees. VC is the current speed V_c in mm/s. FE is the nominal frequency of excitation f_e of the top end in Hz. A/DE is the ratio of the measured amplitude A of the excitation of the top end divided by the effective diameter D_e.

The Figures of the root mean square motion of the top end are referred to by the experiment number and the letters LVDT. The Figures of root mean square measured bending strains are referred to by the experiment identification number and the bridge name. The Figures showing the measured and theoretical predictions and maxima are referred to by the experiment identification number and the plane name. Figures showing the time traces are referred to by the experiment identification number and the letter T (trace).

Tables 2-1 to 2-3 include information about the theoretical prediction of the response at $f=f_e$ in the plane parallel to the oscillation of the top end, performed as described in Section IV.4.2 of Patrikalakis (1983). The procedure for computing $\hat{c}_m$ and $\hat{c}_d$ shown in Table 2-1 to 3-2 can be found in section IV.4.2 and Appendix B of Patrikalakis (1983). The estimates of the local c_m and c_d employed in the iteration procedure are based on extrapolation of rigid cylinder results shown in Figures A-1 and A-2, taken from Sarpkaya (1977). Note that the small Re for which rigid cylinder data is available is equal to 10^4.

Table 2-5 provides information about the theoretical prediction of the lift response following the method described in Sections IV.4.2 and V.4.1 of Patrikalakis (1983). The nomenclature employed in Table 2-5 is defined as follows: β, a frequency parameter defined by $\beta = f_e D_e^2/\nu$, where ν is the kinematic viscosity of fresh water; $\overline{c_{LM}^o}$, spanwise average maximum lift coefficient estimated from rigid cylinder results for the calculated KC and Re numbers in the drag direction, see Chapter IV of Patrikalakis (1983); $\overline{R_{p,n}}$, average response parameter for the nth mode defined by $\overline{R_{p,n}} = M\varsigma_n/\rho D_e^2 \overline{c_{LM}^o}$, where ρ is the density of fresh water and ς_n the structural damping ratio for the nth mode in air; a_i, the maximum amplitude of the ith mode; a_i^{max}, the maximum amplitude of the ith mode at synchronization; f_i the ith "natural frequency" of the model in water in Hz; $\overline{KC}$ the spanwise average Keulegan-Carpenter number, based on the calculated local velocity in the drag direction. Figure A-3 is used in the determination of $\overline{c_{LM}^o}$

Table 2-1: Description of experiments with an amplitude of excitation between 0.49 and 1.01 D_e parallel to plane A and information for the theoretical prediction of the response in plane A.

Experiment Number	13	16	19	22	25
Frequency of Excitation f_e in Hz	0.75	1.00	1.50	2.92	5.85
Measured A/D_e	1.01	1.01	1.01	1.00	0.49
Fresh Water Temperature in °C	13.0	13.0	13.0	13.0	13.0
Measurement Record Length in Seconds	51.150	34.100	34.100	17.050	8.525
Added Mass Coefficient $\hat{c}_m$ Used in Theoretical Prediction	0.83	0.73	0.62	1.05	1.04
Drag Coefficient $\hat{c}_d$ Used in Theoretical Prediction	1.98	2.08	2.26	1.70	1.50
Maximum Calculated Reynolds Number, Re	920	1236	2342	3549	5707
Maximum Calculated Keulegan-Carpenter Number, KC	6.35	6.38	8.07	6.28	5.05
Mean Calculated Reynolds Number, Re	564	891	1738	1390	3865
Mean Calculated Keulegan-Carpenter Number, KC	3.89	4.60	5.99	2.46	3.42

Table 2-2: Description of experiments with an amplitude of excitation of approximately $2D_e$ parallel to plane B and information for the theoretical prediction of the response in plane B.

Experiment Number	118	119
Frequency of Excitation f_e in Hz	1.50	2.92
Measured A/D_e	1.94	1.93
Fresh Water Temperature in °C	15.0	15.0
Measurement Record Length in Seconds	34.100	34.100
Added Mass Coefficient $\hat{c}_m$ Used in Theoretical Prediction	0.11	0.53
Drag Coefficient $\hat{c}_d$ Used in Theoretical Prediction	2.29	2.07
Maximum Calculated Reynolds Number, Re	3755	7270
Maximum Calculated Keulegan-Carpenter Number, KC	12.19	12.13
Mean Calculated Reynolds Number, Re	2635	2945
Mean Calculated Keulegan-Carpenter Number, KC	8.55	4.91

Table 2-3: Description of experiments with an amplitude of excitation between 2.47 and 2.97 D_e parallel to plane A and information for the theoretical prediction of the response in plane A.

Experiment Number	15	18	21	48	24
Frequency of Excitation f_e in Hz	0.75	1.00	1.50	2.30	2.92
Measured A/D_e	2.97	2.95	2.94	2.87	2.47
Fresh Water Temperature in °C	13.0	13.0	13.0	14.1	13.0
Measurement Record Length in Seconds	51.150	34.100	34.100	68.23	17.050
Added Mass Coefficient $\hat{c}_m$ Used in Theoretical Prediction	-0.06	-0.09	-0.13	0.15	0.33
Drag Coefficient $\hat{c}_d$ Used in Theoretical Prediction	2.12	2.14	2.25	2.17	2.16
Maximum Calculated Reynolds Number, Re	2708	3586	5361	8024	8767
Maximum Calculated Keulegan-Carpenter Number, KC	18.66	18.54	18.47	18.03	15.52
Mean Calculated Reynolds Number, Re	1564	2186	3225	3777	3541
Mean Calculated Keulegan-Carpenter Number, KC	10.78	11.30	11.11	8.49	6.27

Table 2-4: Elevation, Z, of bending strain measurements above the axis of the lower ball joint in multiples of L/11.

Experiment Number	Plane A	Plane B
13	3,5,8	3,6,8
16	3,5,8	3,6,8
19	3,5,8	3,6,8
22	3,5,8	3,6,8
25	3,5,8	3,6,8
118	2,4,5,8	2,5,8
119	2,4,5,8	2,5,8
15	3,5,8	3,6,8
18	3,5,8	3,6,8
21	3,5,8	3,6,8
48	3,5,8	3,5,6,8
24	3,5,8	3,6,8

EXPERIMENT NUMBER		13	19	22	25	118	119	15	21	24
β		145	290	565	1132	308	600	145	290	565
$\overline{c^{o}_{LM}}$		1.8	2.6	1.2	1.4	3.6	2.4	3.8	3.8	2.6
First Flexural Mode	$\overline{R_{p,1}}$	0.0124	0.0086	-	-	0.0062	-	0.0059	0.0059	-
	a_1^{max}/D_e	0.963	0.964	-	-	0.965	-	0.965	0.965	-
	$\overline{U_1^*}=\overline{KC}f_e/f_1$	1.86	5.72	-	-	8.17	-	5.15	10.62	-
	a_1/D_e	0.07	0.70	-	-	0.537	-	0.965	0.509	-
2nd Flexural Mode	$\overline{R_{p,2}}$	-	0.0054	0.0116	0.0100	0.0039	0.0058	-	0.0037	0.0054
	a_2^{max}/D_e	-	0.965	0.963	0.964	0.965	0.965	-	0.965	0.965
	$\overline{U_2^*}=\overline{KC}f_e/f_2$	-	1.48	1.19	3.30	2.12	2.37	-	2.75	3.02
	a_2/D_e	-	0.053	0.035	0.210	0.079	0.084	-	0.123	0.158

Table 2-5: Information for the theoretical prediction of the response orthogonal to the direction of excitation of the top end.

From all experiments analyzed in this report, it can be seen that when the frequency of imposed oscillation is not very close to one of the "natural frequencies" of the flexible system (see experiments 13, 16, 22; 119; 15, 18, 48 and 24) the strain response parallel to the oscillation of the top end is primarily concentrated at $f=f_e$, as expected from rigid cylinder results. However, some strain response exists at $f=2f_e$, $3f_e$, and $4f_e$, which, in general is not insignificant in determining the maxima of the measured response parallel to the oscillation of the top end. The relative significance of the higher harmonics of the response parallel to the oscillation increases with the amplitude of oscillation, see also Chryssostomidis, Patrikalakis and Vrakas (1983). When the frequency of the imposed oscillation is close to a "natural frequency" of the flexible system, (see experiments 19, 25; 118; 21), the strain response parallel to the excitation of the top end is almost exclusively at $f=f_e$. These results are summarized in Figures 13A, 16A, 19A, 22A, 25A; 118B, 119B; 15A, 18A, 21A, 48A and 24A, where the theoretical and experimental dynamic response strain at $f=f_e$ and maximum dynamic response strain parallel to the oscillation of the top end are shown. The theoretical maximum dynamic strain response and the theoretical dynamic strain response at $f=f_e$ parallel to the direction of excitation of the top end are the same. From these Figures we can see that the theoretical prediction of the maximum dynamic response strain is good when there is no significant response at frequencies other than f_e in the drag direction and no significant lift response. The above observations are consistent with the fact that the theoretical predictions improve with decreasing amplitude of excitation.

In the lift direction, when the frequency of imposed oscillation is not close to a "natural frequency" of the flexible system, (see experiments 13, 16, 22; 119, 15, 18, 48 and 24), the dynamic strain response is primarily at $f=2f_e$, when $2f_e$ is close to a "natural frequency" and at f_e and $2f_e$ otherwise. However, even in the first situation some strain response exists at f_e which, in general, is not insignificant in detrmining the maxima of the measured lift response. The maximum lift response for these eight experiments is comparable to the maximum drag response. When the frequency of imposed oscillation is close to a "natural frequency" of the flexible system (see experiments 19, 25; 118; 21), the dynamic lift strain response is at $f = nf_e$ and is so determined so that f is close to a "natural frequency" of the flexible system. For experiments 19, 118 and 21, n was 1 and 4, and for experiment 25 n was 1. For experiment 25 the digitization frequency was 120 Hz. The same observation was made in run 903 reported in Chryssostomidis and Patrikalakis (1982), where the model described in this report extended to 10.091 m was used. The extended model was supported by a tension leg platform subjected to surface wave excitation. In run 903 the frequency of excitation, f_e, was close to f_2, and $2f_e$ was close to f_3 and lift response was observed at both f_e and $2f_e$. The results of the present experiments are summarized in Figures 13B, 16B, 19B, 22B, 25B; 118A, 119A; 15B, 18B, 21B, 48B, and 24B.

In Figures 13B, 22B; 119A; 15B and 24B the following information is shown:

1. The measured dynamic lift response strain at $f = 2f_e$.
2. The theoretical dynamic lift response strain at $f = f_1$ for experiments 13 and 15, and $f = f_2$ for experiments 22, 119 and 24, where f_1, f_2 are the first two "natural frequencies" of our model, respectively. For experiments 13 and 15, f_1 is the "natural frequency" closer to $2f_e$ and for experiments 22, 119 and 24, f_2 is the "natural frequency" closer to $2f_e$.
3. The maximum measured dynamic lift response strain.
4. The maximum measured dynamic response strain independent of plane.
5. A theoretical estimate of the maximum dynamic response strain independent of plane. This estimate is obtained as the square root of the sum of the squares of the theoretical estimates of the response in planes A and B.

In Figures 16B, 18B and 48B, no theoretical estimate of the dynamic lift response strain can be provided because the lift response occurs at frequencies which are not close to the"natural frequencies" of the model in water. For such cases no spring mounted rigid cylinder results exist to permit estimation of lift response, Patrikalakis (1983). Therefore, the theoretical maximum dynamic response strain independent of plane in these Figures is the same as the theoretical prediction in plane A. Items 1, 3 and 4 shown in Figures 16B, 18B and 48B are the same as in Figure 13B.

For experiments 19, 25, 118, and 21 the measured dynamic lift response strain at $f=f_e$ is shown in Figures 19Ba, 19Bc; 25B; 118Aa, 118Ac; and 21Ba, 21Bc, and the response at $f=4f_e$ is shown in 19Bb, 118Ab and 21Bb, respectively. The theoretical dynamic lift response strain at $f=f_1$ is shown in Figures 19Ba, 118Aa, and 21Ba, while the theoretical dynamic lift response strain at $f=f_2$ is shown in Figures 19Bb, 25B, 118Ab, and 21Bb. In addition, the theoretical estimate of the maximum dynamic lift response strain, obtained by summing the responses at $f=f_1$ and $f=f_2$ is shown in Figures 19Bc, 118Ac, and 21Bc. A theoretical estimate of the maximum dynamic response strain independent of plane is shown in Figures 19Ba, 19Bb, 19Bc; 25B; 118Aa, 118Ab, 118Ac; and 21Ba, 21Bb, and 21Bc. This estimate is obtained as the square root of the sum of the squares of the response in the drag direction from Figures 19A, 25A, 118B and 21A, and of the lift response from Figures 19Bc, 25B, 118Ac and 21Bc, respectively. Items 3 and 4 in Figures 19B, 25B, 118A and 21B are the same as in Figure 13B.

For the lift response, unfortunately no general conclusions can be drawn because of the need to extrapolate Figures A-4 and A-5. These two Figures are taken from Sarpkaya (1980). For the theoretical estimate of the maximum response independent of plane, there is the additional complication that the phase between the response in the A and B planes is unknown, and therefore, no general statement about its accuracy can be made. A rough estimate of these phase angles can be obtained from the "T" Figures of each experiment, where the time trace of the excitation of the top end and the time traces of selected strain responses are shown.

Additional experiments for this type of flow were reported in Chryssostomidis and Patrikalakis (1982) and in Chryssostomidis, Patrikalakis, and Vrakas (1983).

EXPERIMENT 13

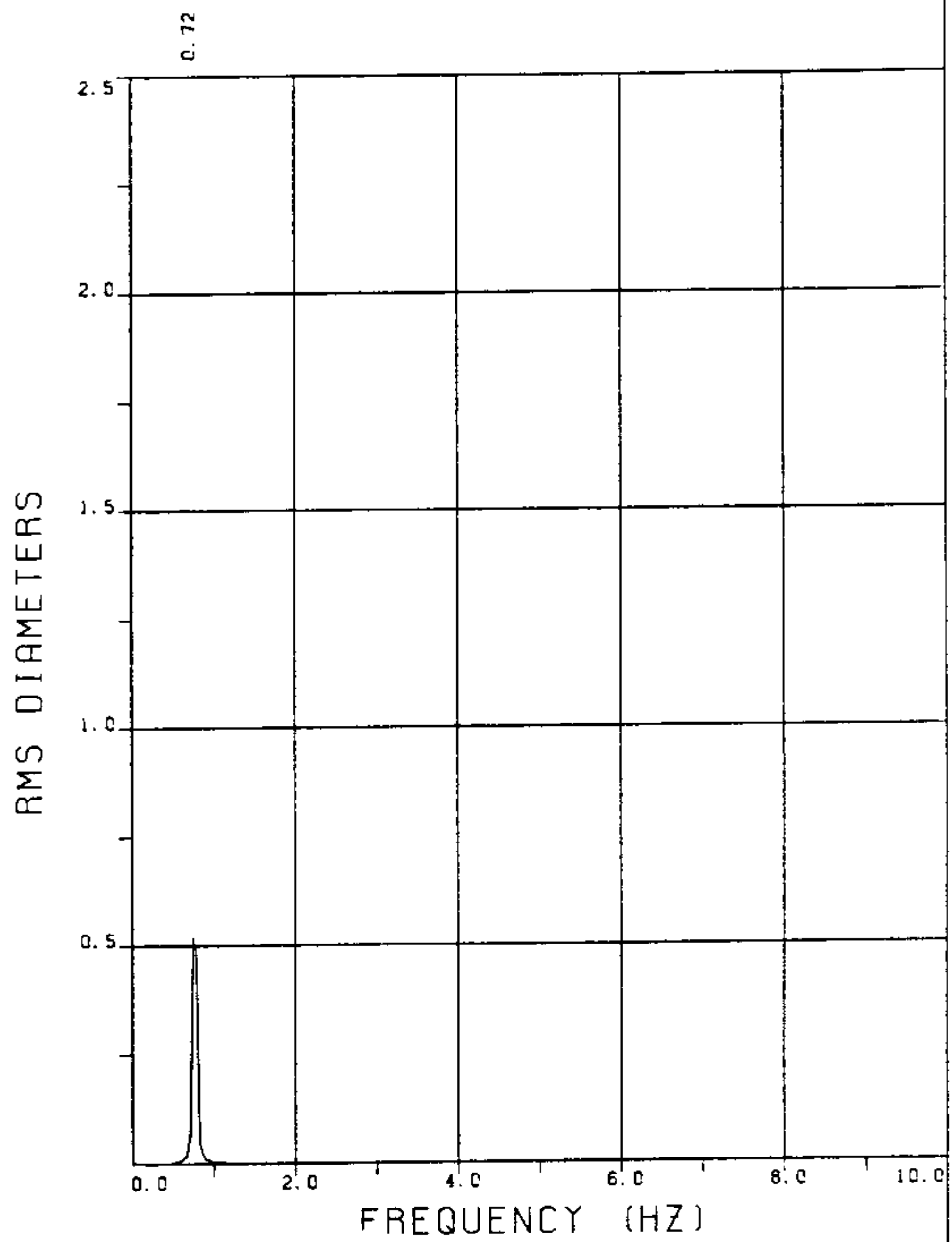

EXPERIMENT NUMBER 13

LVDT

THETA=0 VC=0 FE=0.750 BE=0.039

MEASURED A/DE=1.01

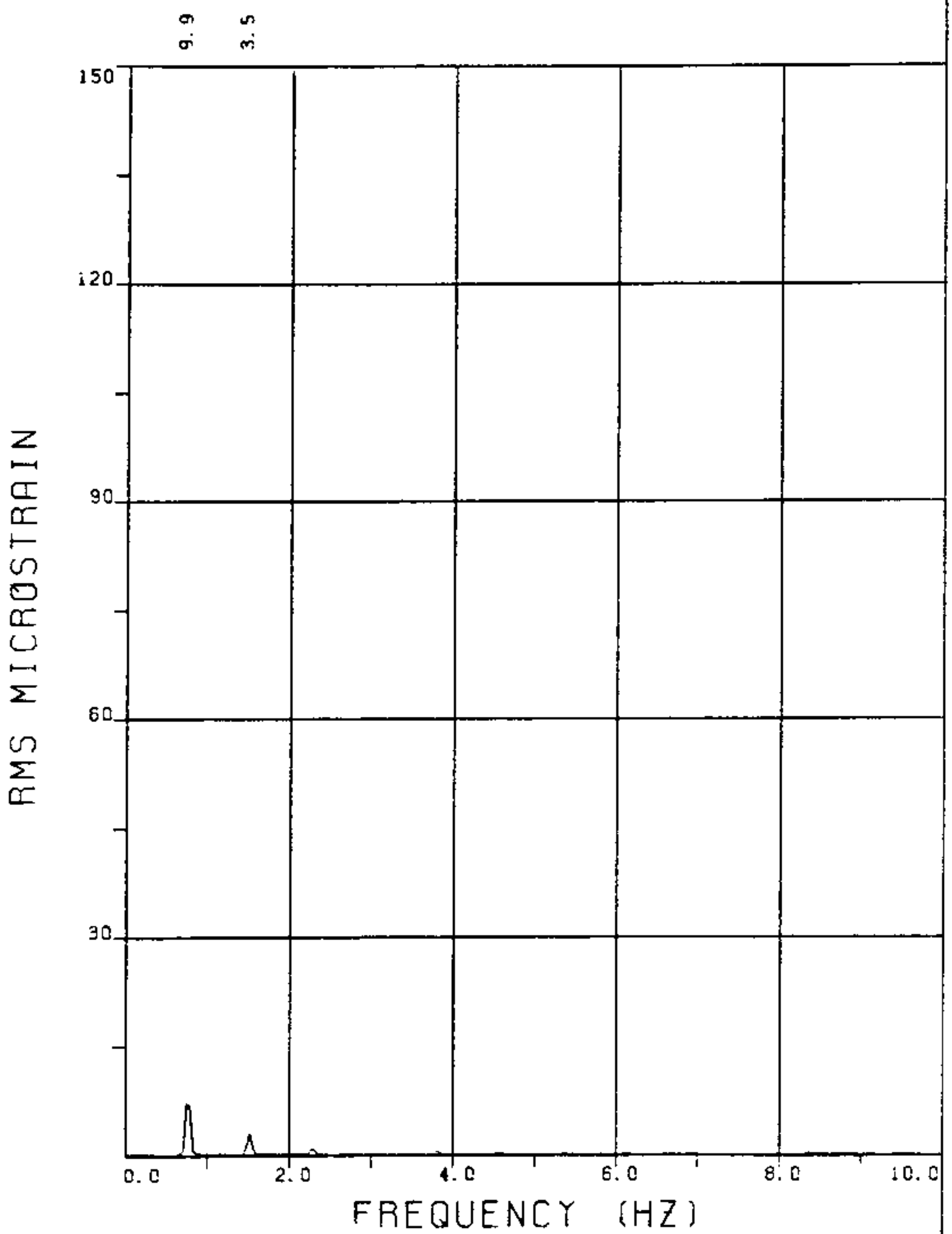

EXPERIMENT NUMBER 13

BRIDGE A8 ELEVATION=3L/11 BE=0.039

THETA=0 VC=0 FE=0.750 A/DE=1.01

MEASURED RESPONSE IN MICROSTRAIN

TOTAL DYNAMIC RMS=10.7

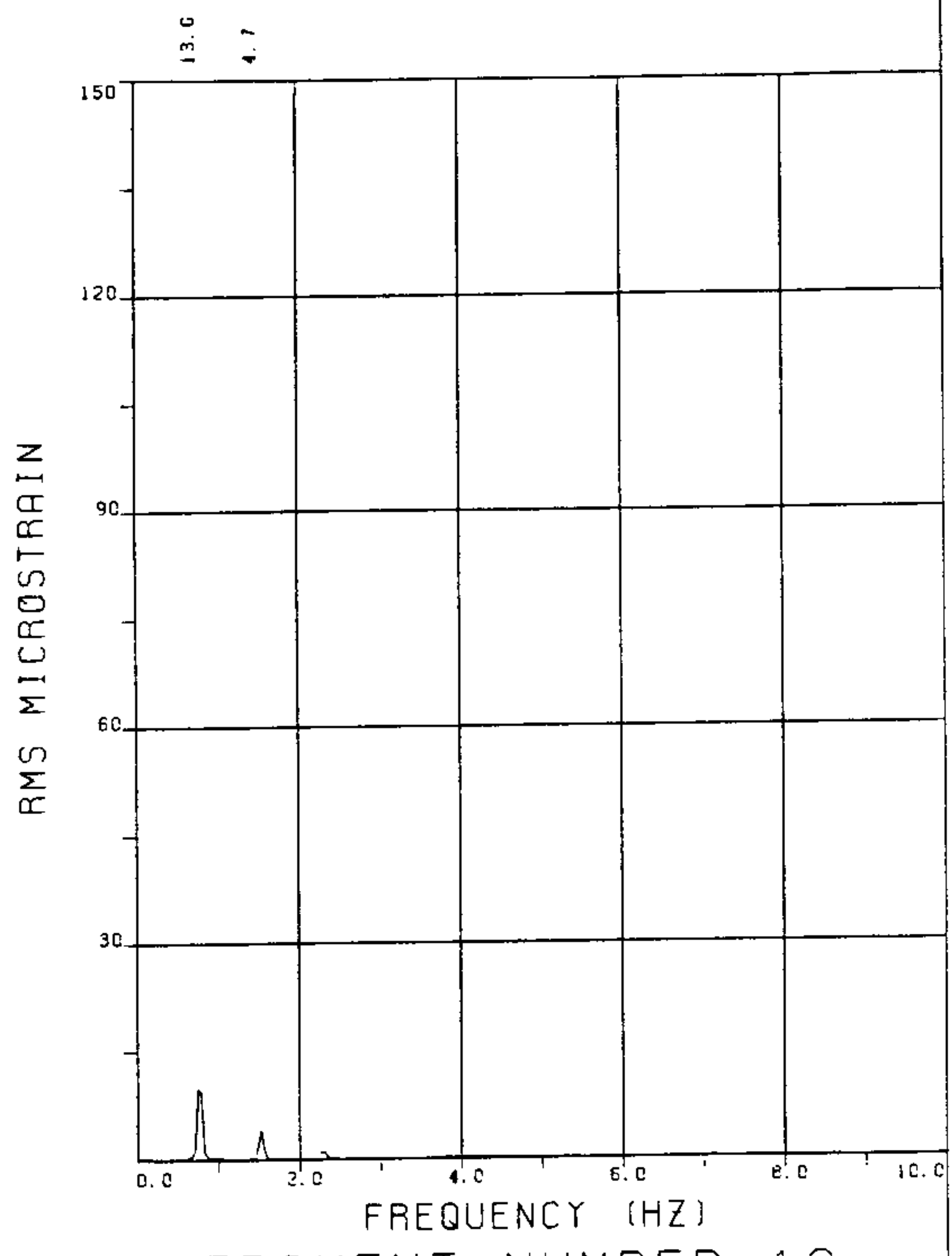

EXPERIMENT NUMBER 13

BRIDGE A6 ELEVATION=5L/11 BE=0.039

THETA=0 VC=0 FE=0.750 A/DE=1.01

MEASURED RESPONSE IN MICROSTRAIN

TOTAL DYNAMIC RMS=14.5

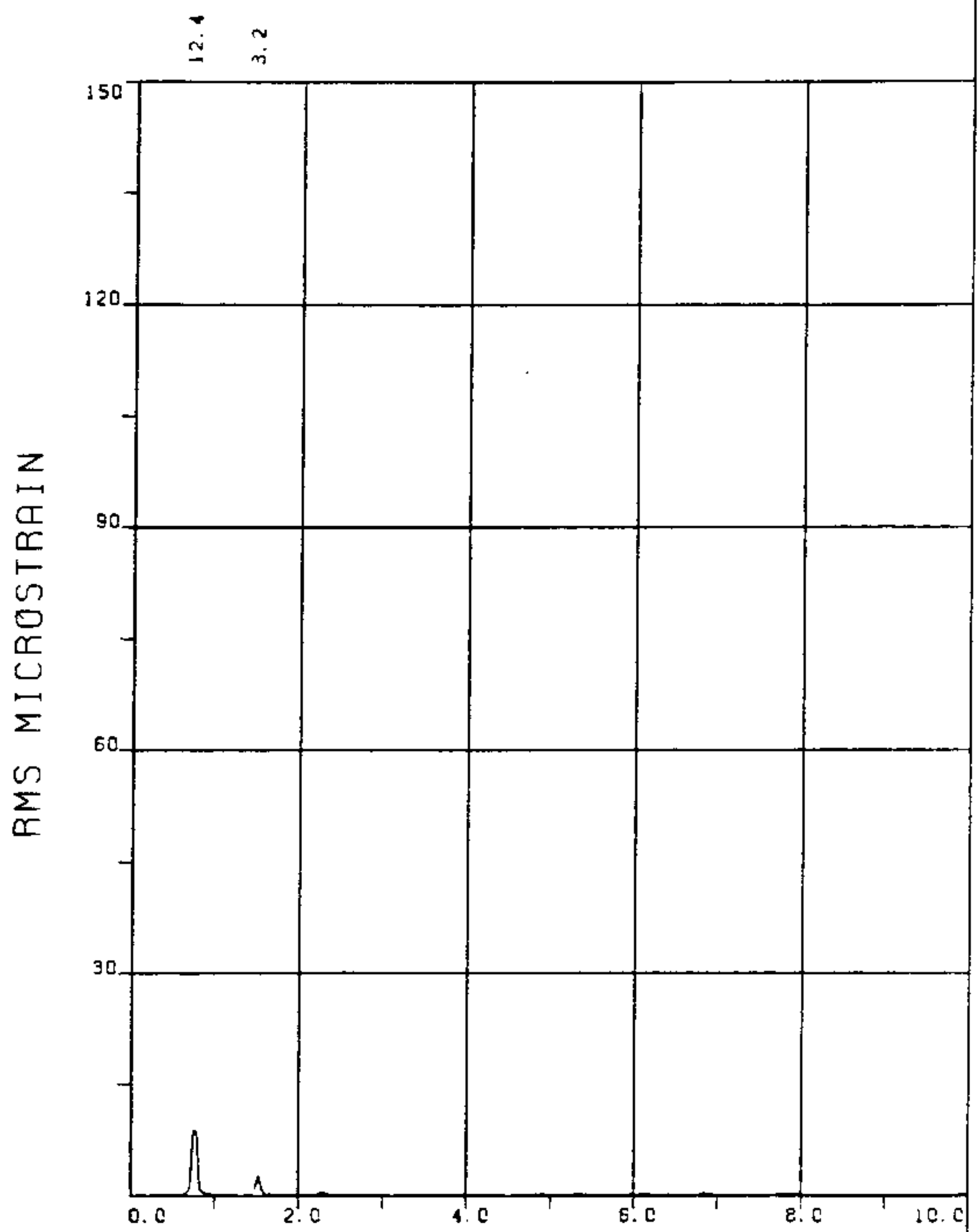

EXPERIMENT NUMBER 13

BRIDGE A3 ELEVATION=8L/11 BE=0.039

THETA=0 VC=0 FE=0.750 A/DE=1.01

MEASURED RESPONSE IN MICROSTRAIN

TOTAL DYNAMIC RMS=12.8

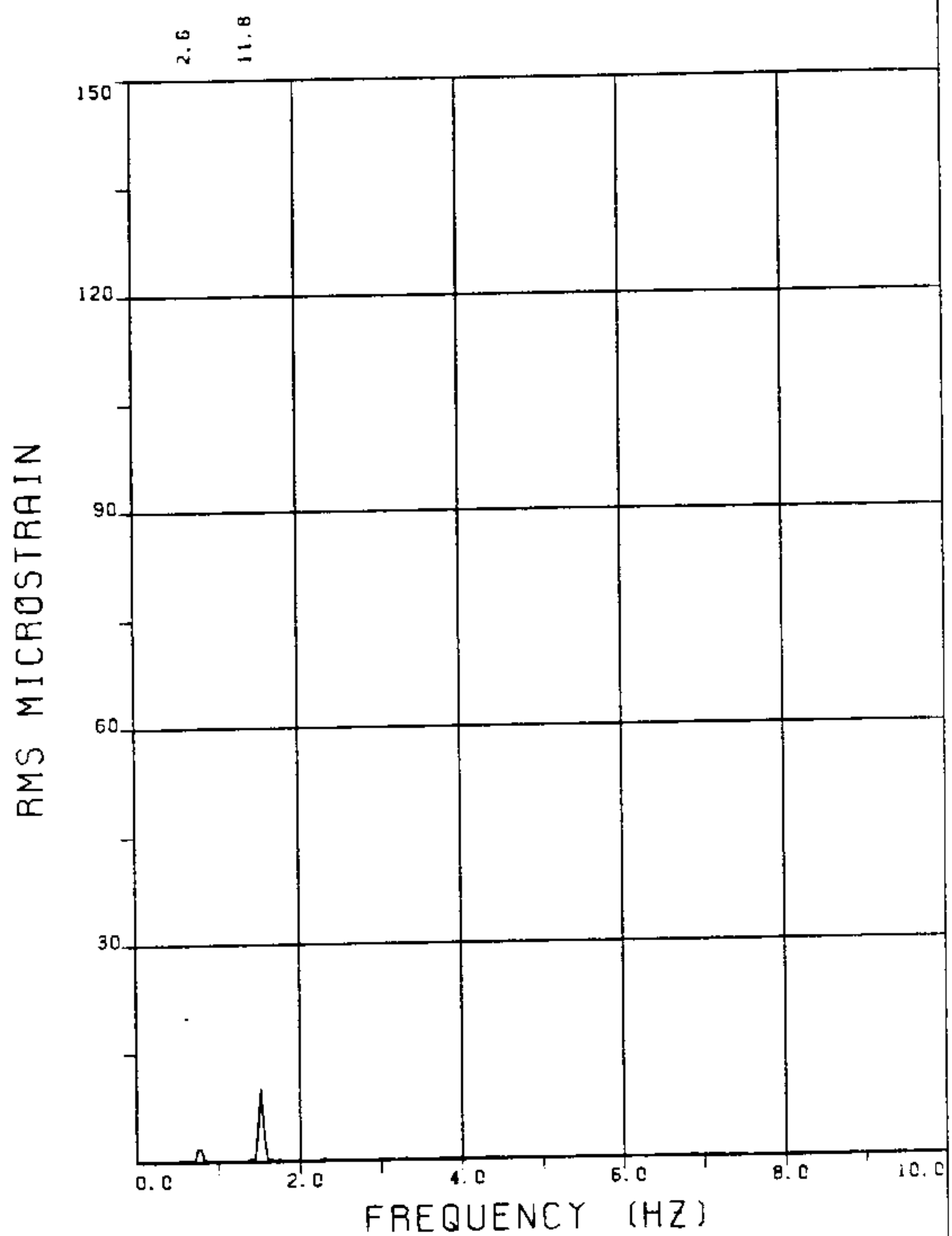

EXPERIMENT NUMBER 13

BRIDGE B8 ELEVATION=3L/11 BE=0.039

THETA=0 VC=0 FE=0.750 A/DE=1.01

MEASURED RESPONSE IN MICROSTRAIN

TOTAL DYNAMIC RMS=12.2

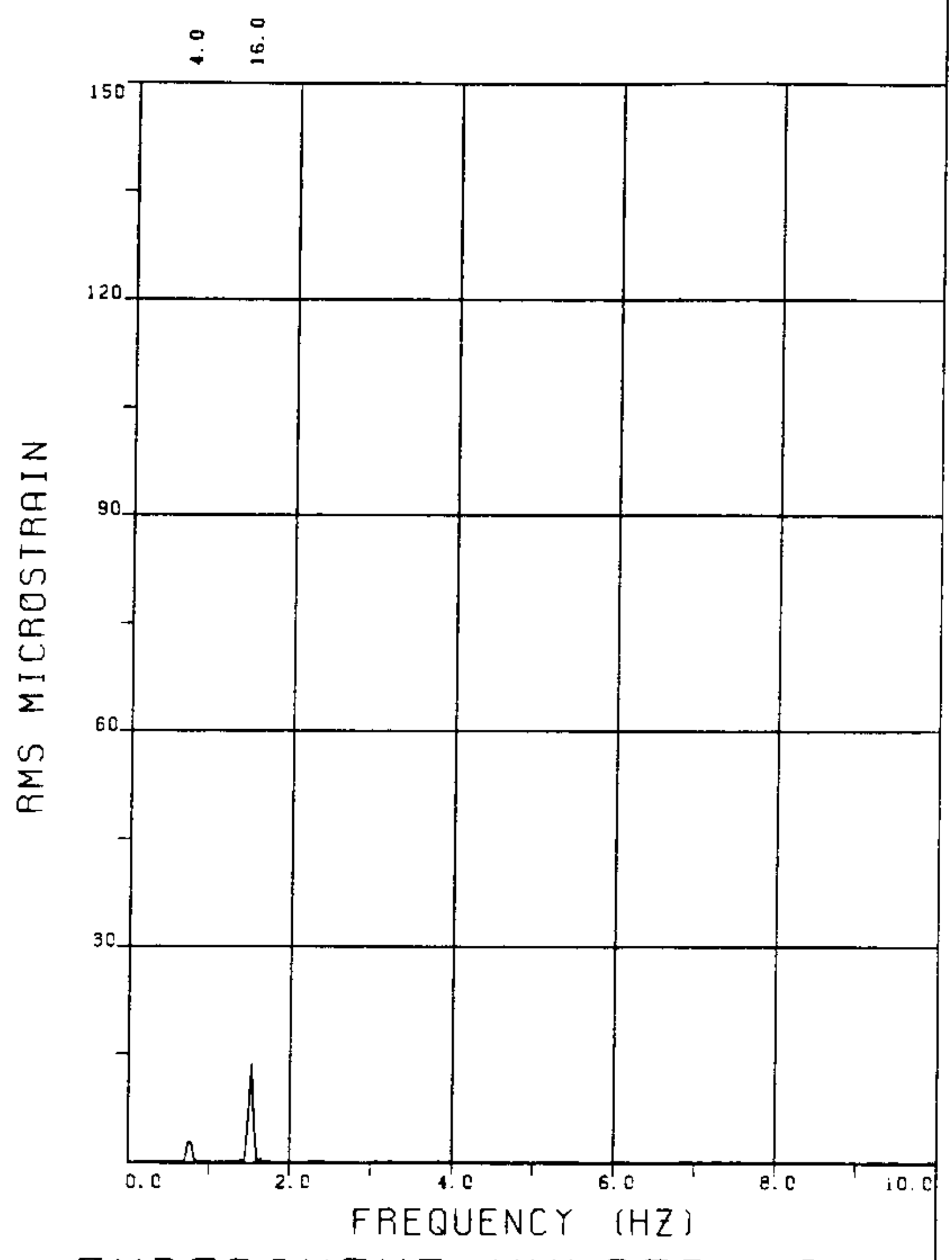

EXPERIMENT NUMBER 13

BRIDGE B5 ELEVATION=6L/11 BE=0.039

THETA=0 VC=0 FE=0.750 A/DE=1.01

MEASURED RESPONSE IN MICROSTRAIN

TOTAL DYNAMIC RMS=16.6

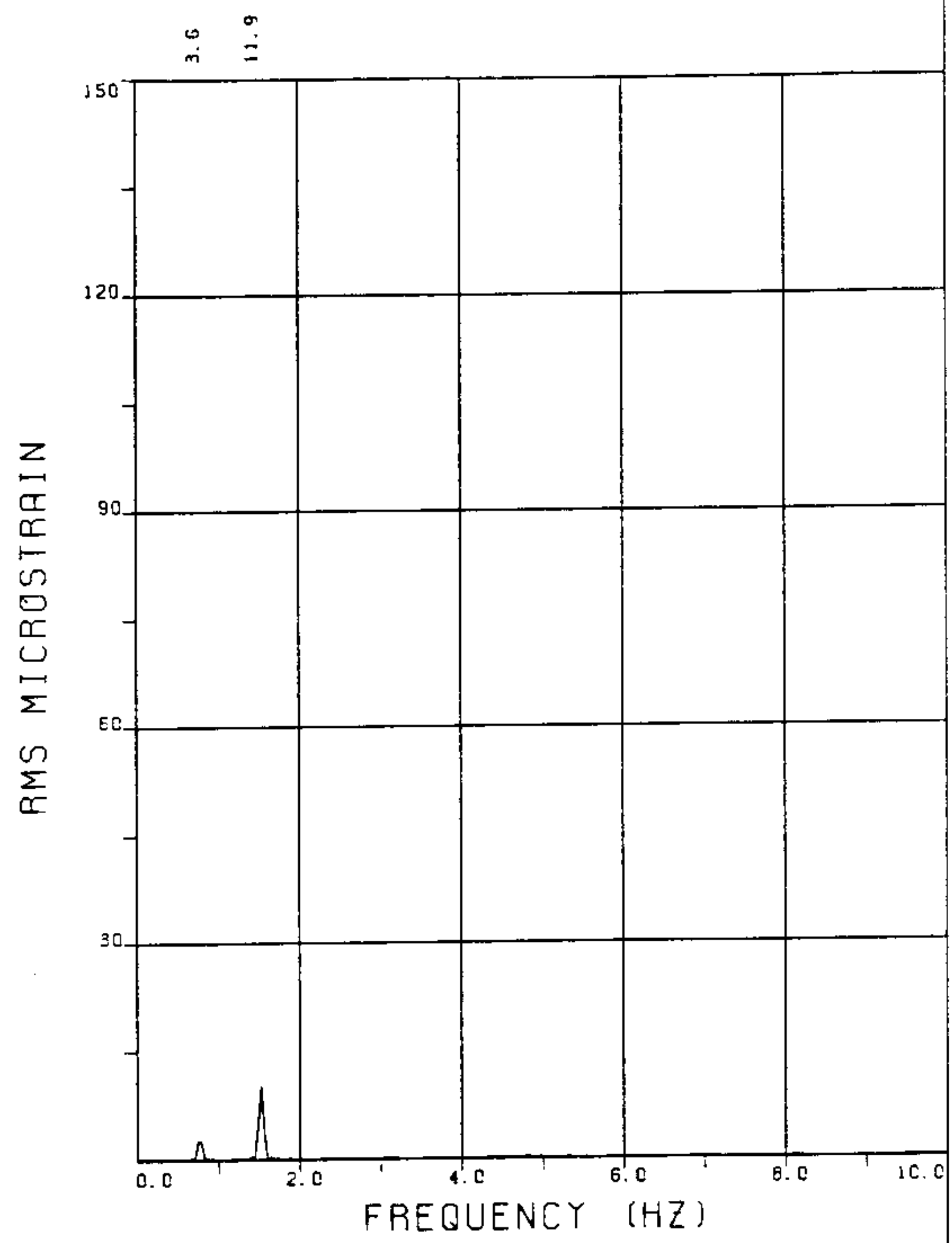

EXPERIMENT NUMBER 13

BRIDGE B3 ELEVATION=8L/11 BE=0.039

THETA=0 VC=0 FE=0.750 A/DE=1.01

MEASURED RESPONSE IN MICROSTRAIN

TOTAL DYNAMIC RMS=12.5

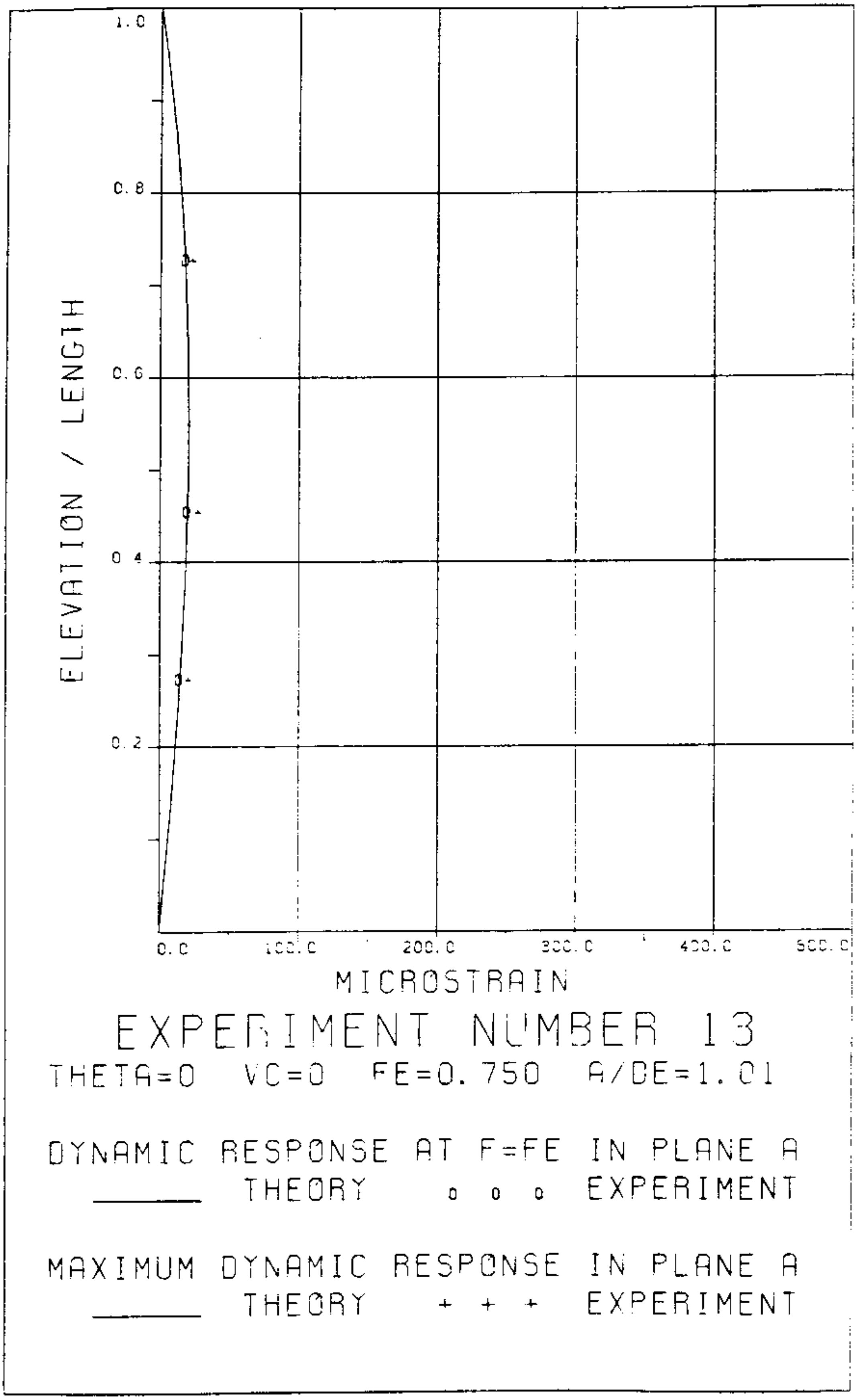
1.0
0.8
0.6
0.4
0.2
ELEVATION / LENGTH
0.0
100.0
200.0
300.0
400.0
500.0
MICROSTRAIN
EXPERIMENT NUMBER 13
THETA=0 VC=0 FE=0.750 A/DE=1.01
DYNAMIC RESPONSE AT F=FE IN PLANE A
THEORY o o o EXPERIMENT
MAXIMUM DYNAMIC RESPONSE IN PLANE A
THEORY + + + EXPERIMENT

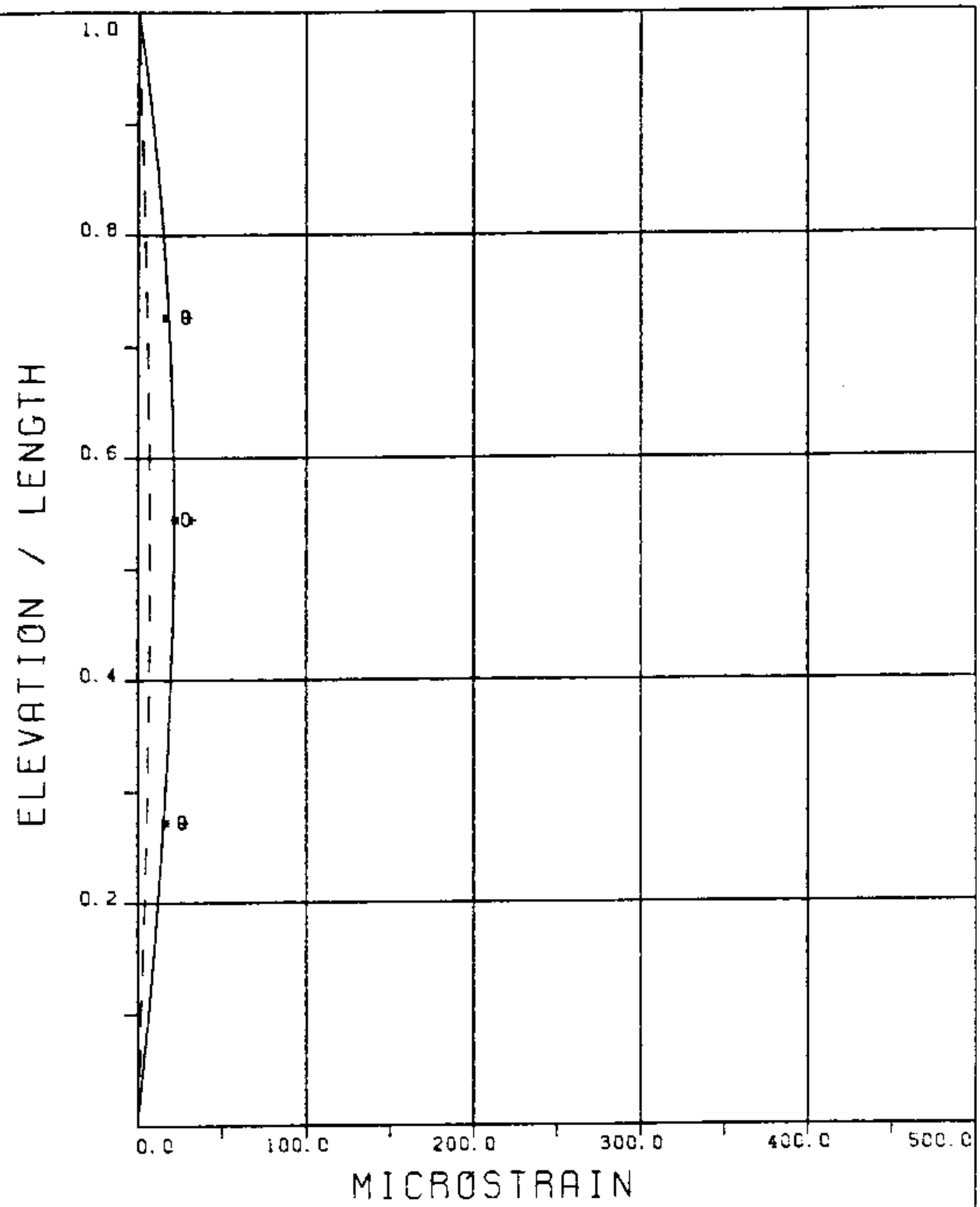

EXPERIMENT NUMBER 13

THETA=0 VC=0 FE=0.750 A/DE=1.01

DYNAMIC RESPONSE IN PLANE B AT F=2FE

----- THEORY * * * EXPERIMENT

MAXIMUM RESPONSE IN PLANE B

o o o EXPERIMENT

MAXIMUM RESPONSE

______ THEORY + + + EXPERIMENT

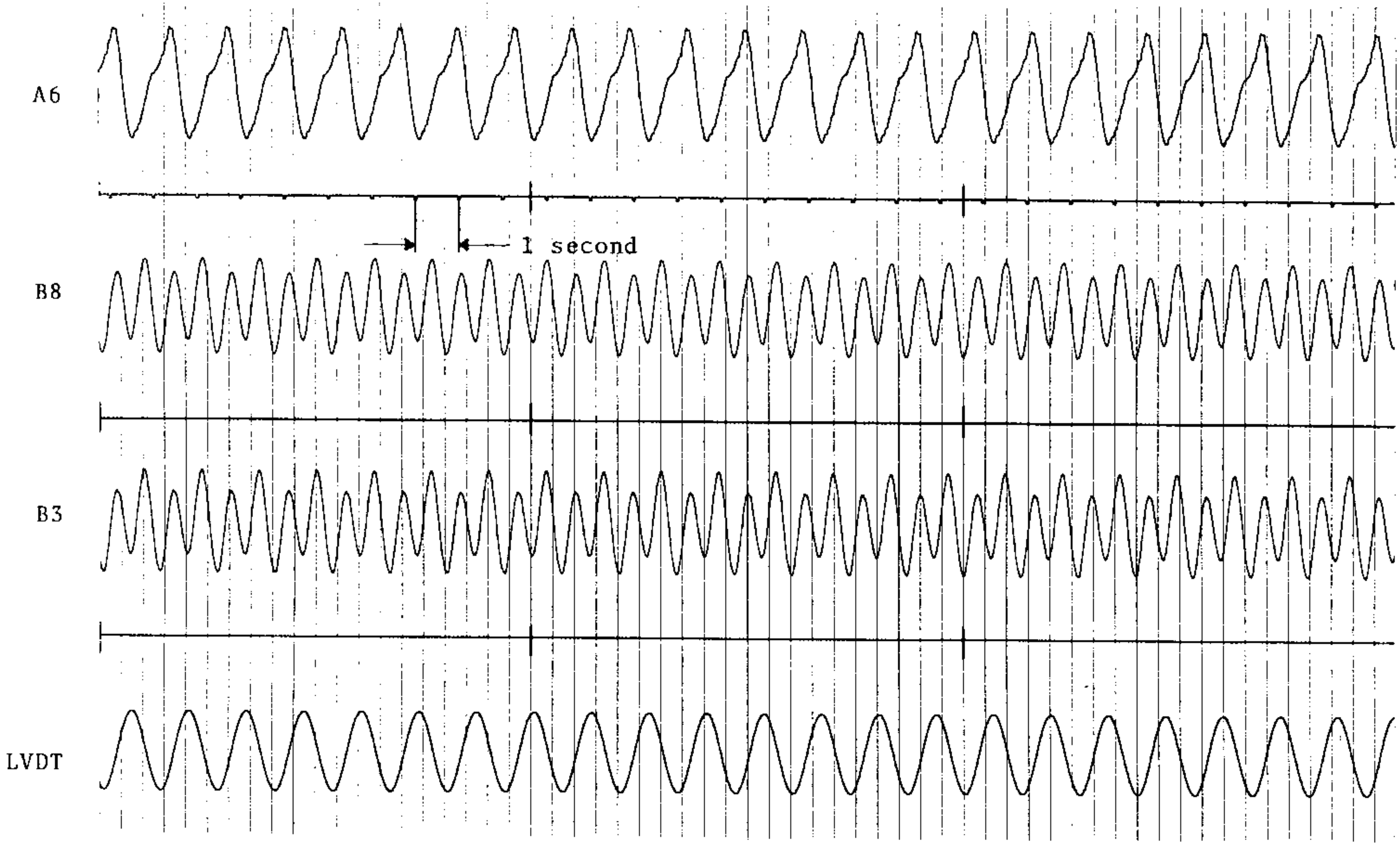

FIGURE 13T: LVDT: 0.087 D_e/DIVISION; STRAINS: 1.53 MICROSTRAIN/DIVISION

EXPERIMENT 16

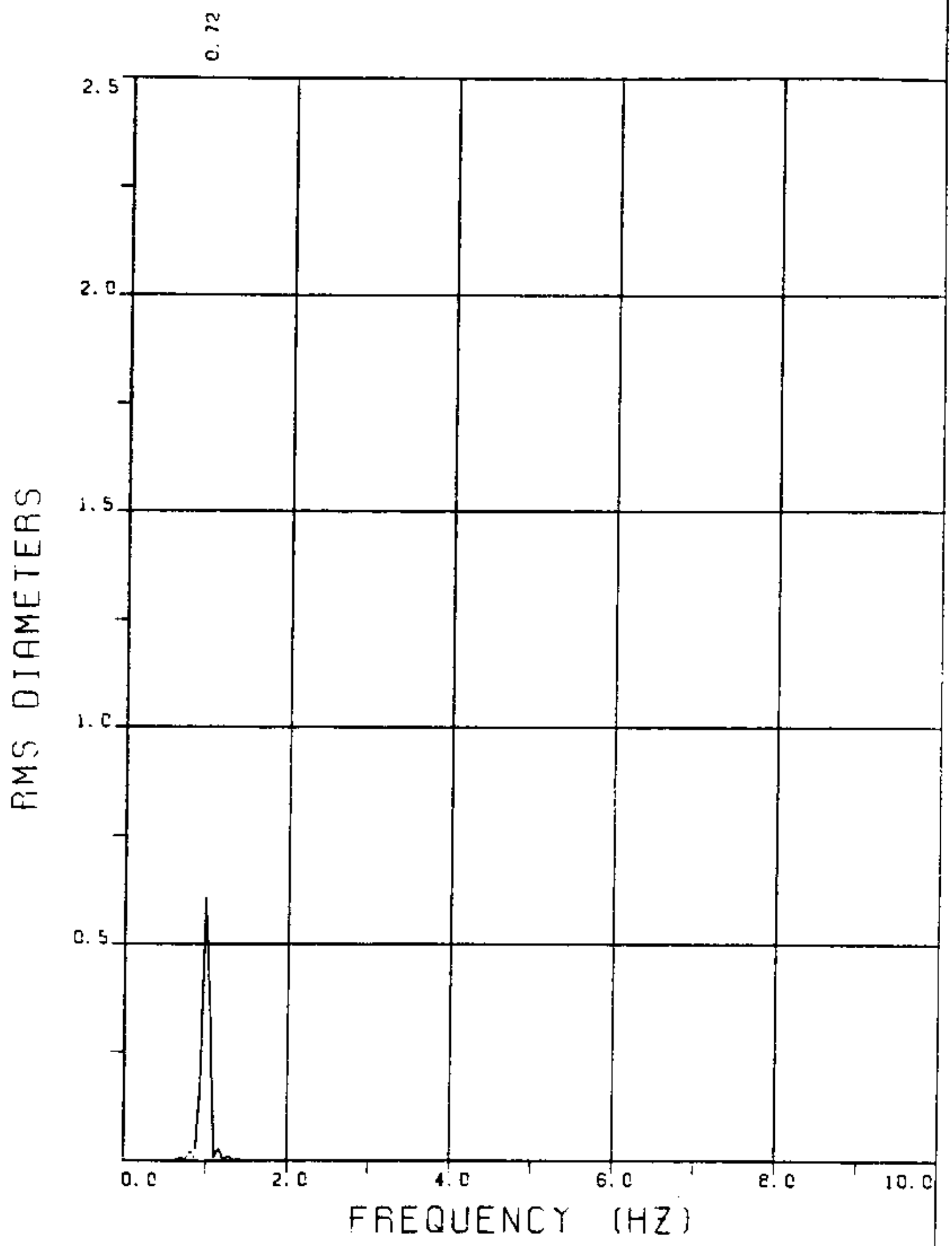

EXPERIMENT NUMBER 16

LVDT

THETA=0 VC=0 FE=1.000 BE=0.059

MEASURED A/DE=1.01

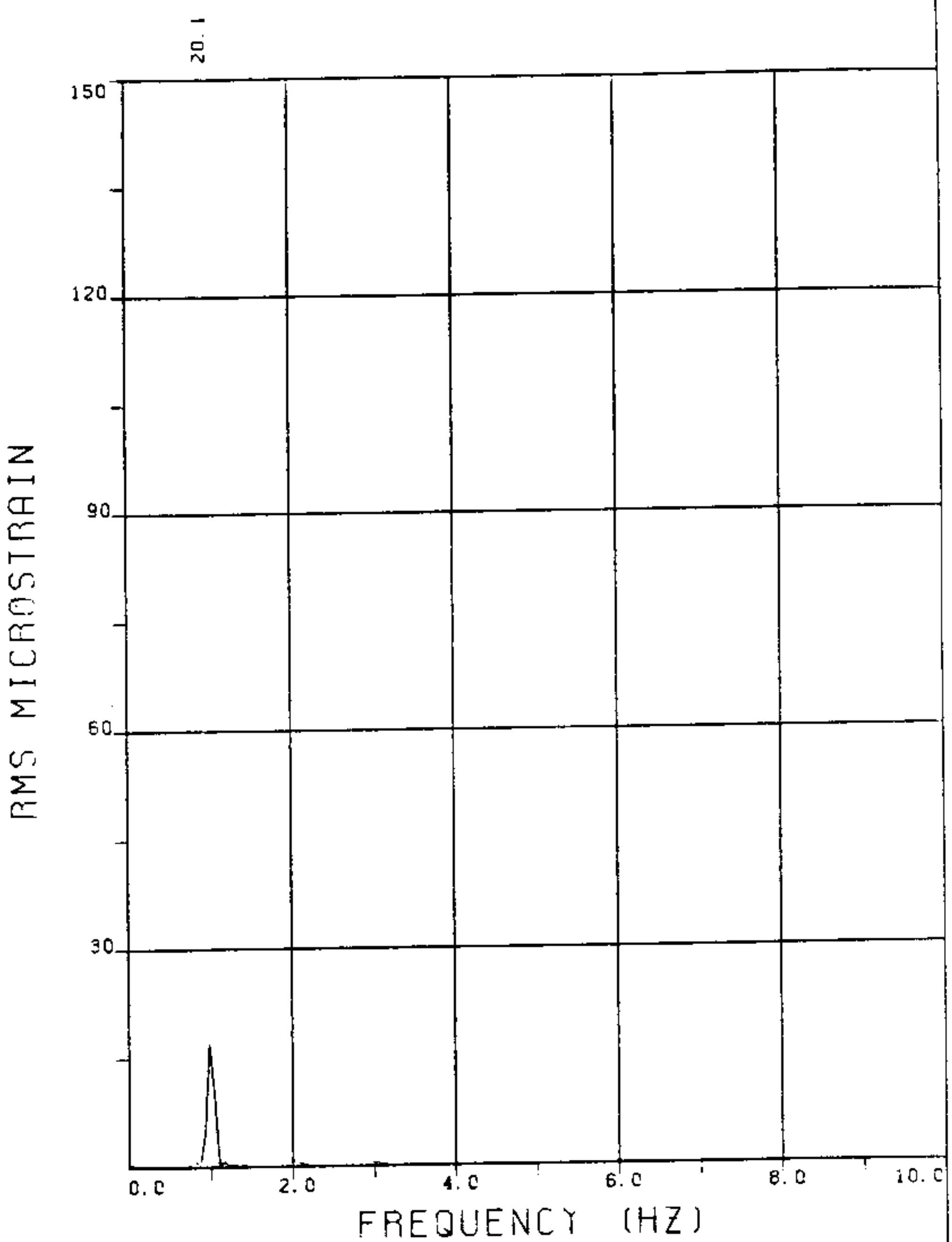

EXPERIMENT NUMBER 16

BRIDGE A8 ELEVATION=3L/11 BE=0.059

THETA=0 VC=0 FE=1.000 A/DE=1.01

MEASURED RESPONSE IN MICROSTRAIN

TOTAL DYNAMIC RMS=20.3

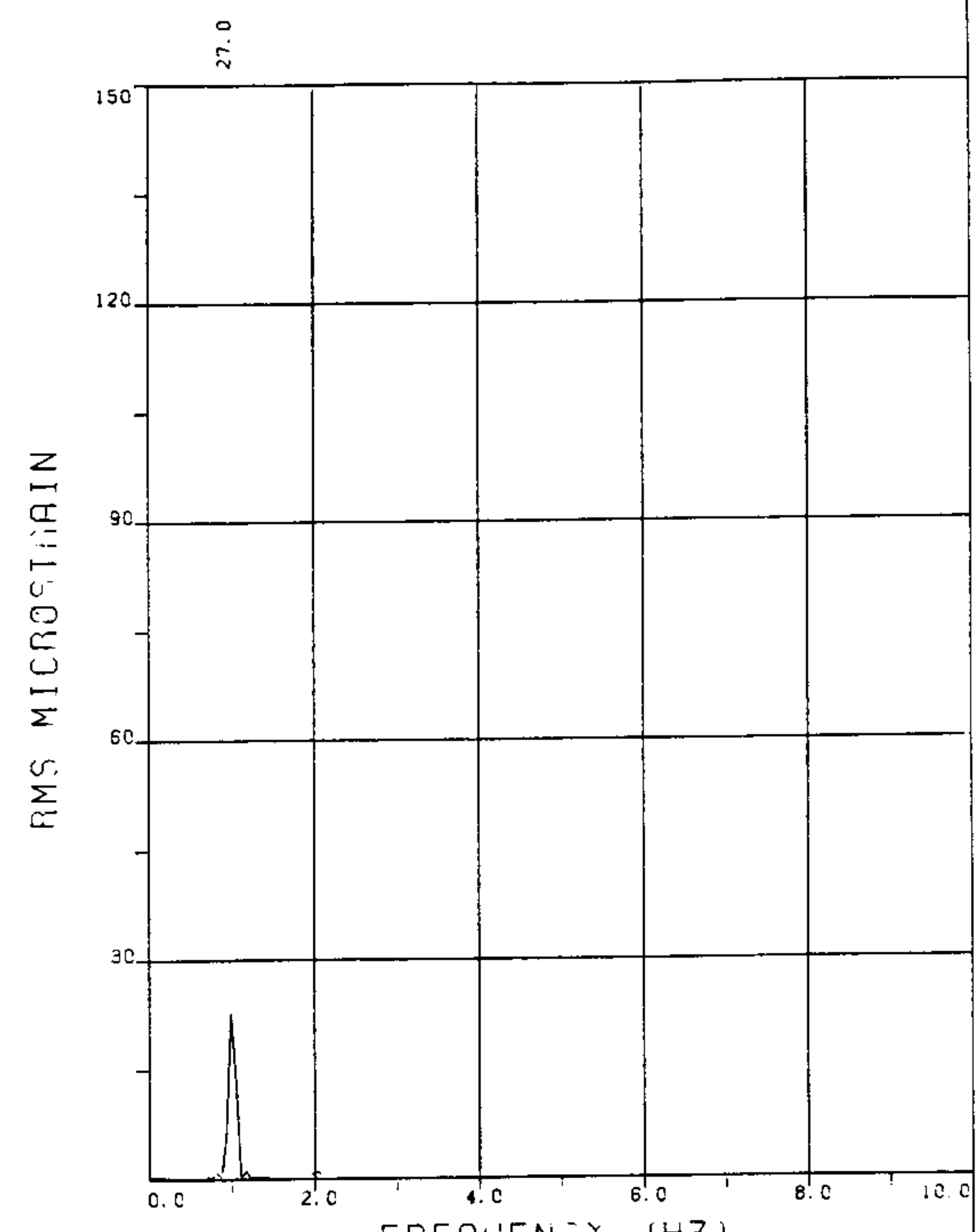

EXPERIMENT NUMBER 16

BRIDGE A6 ELEVATION=5L/11 BE=0.059

THETA=0 VC=0 FE=1.000 A/DE=1.01

MEASURED RESPONSE IN MICROSTRAIN

TOTAL DYNAMIC RMS=27.2

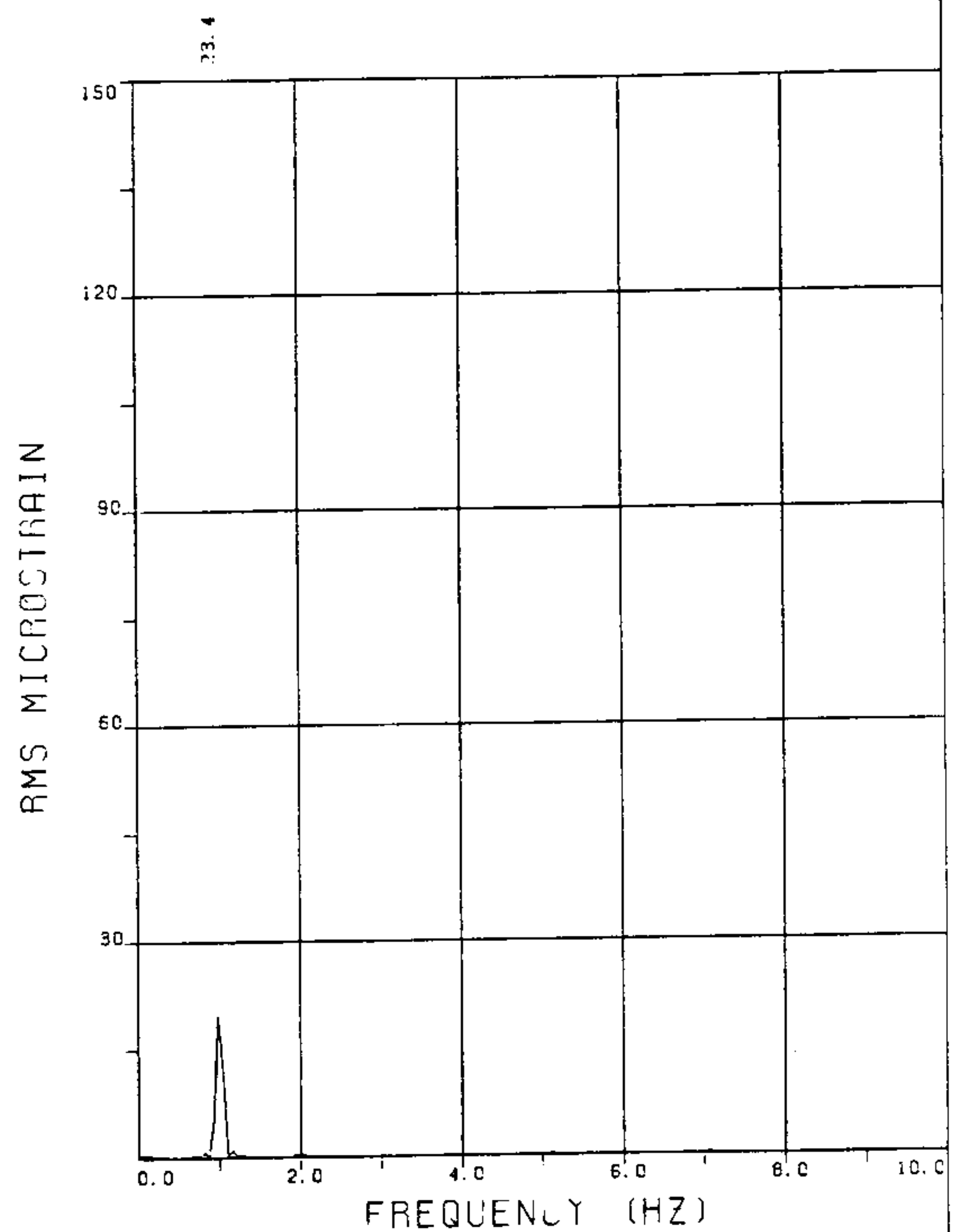

EXPERIMENT NUMBER 16

BRIDGE A3 ELEVATION=8L/11 BE=0.059

THETA=0 VC=0 FE=1.000 A/DE=1.01

MEASURED RESPONSE IN MICROSTRAIN

TOTAL DYNAMIC RMS=23.6

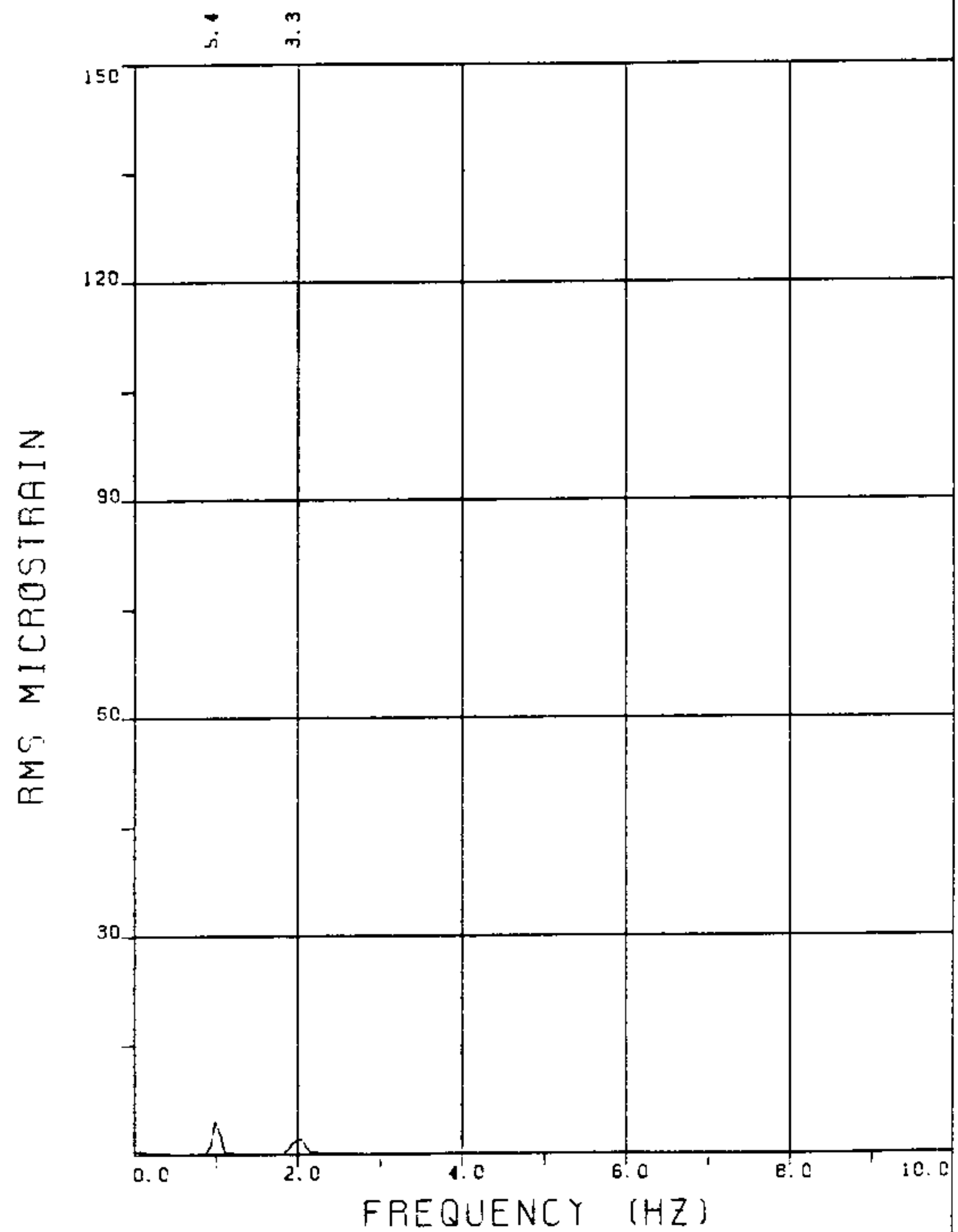

EXPERIMENT NUMBER 19

BRIDGE B8 ELEVATION=3L/11 BE=0.059

THETA=0 VC=0 FE=1.000 A/DE=1.01

MEASURED RESPONSE IN MICROSTRAIN

TOTAL DYNAMIC RMS=7.2

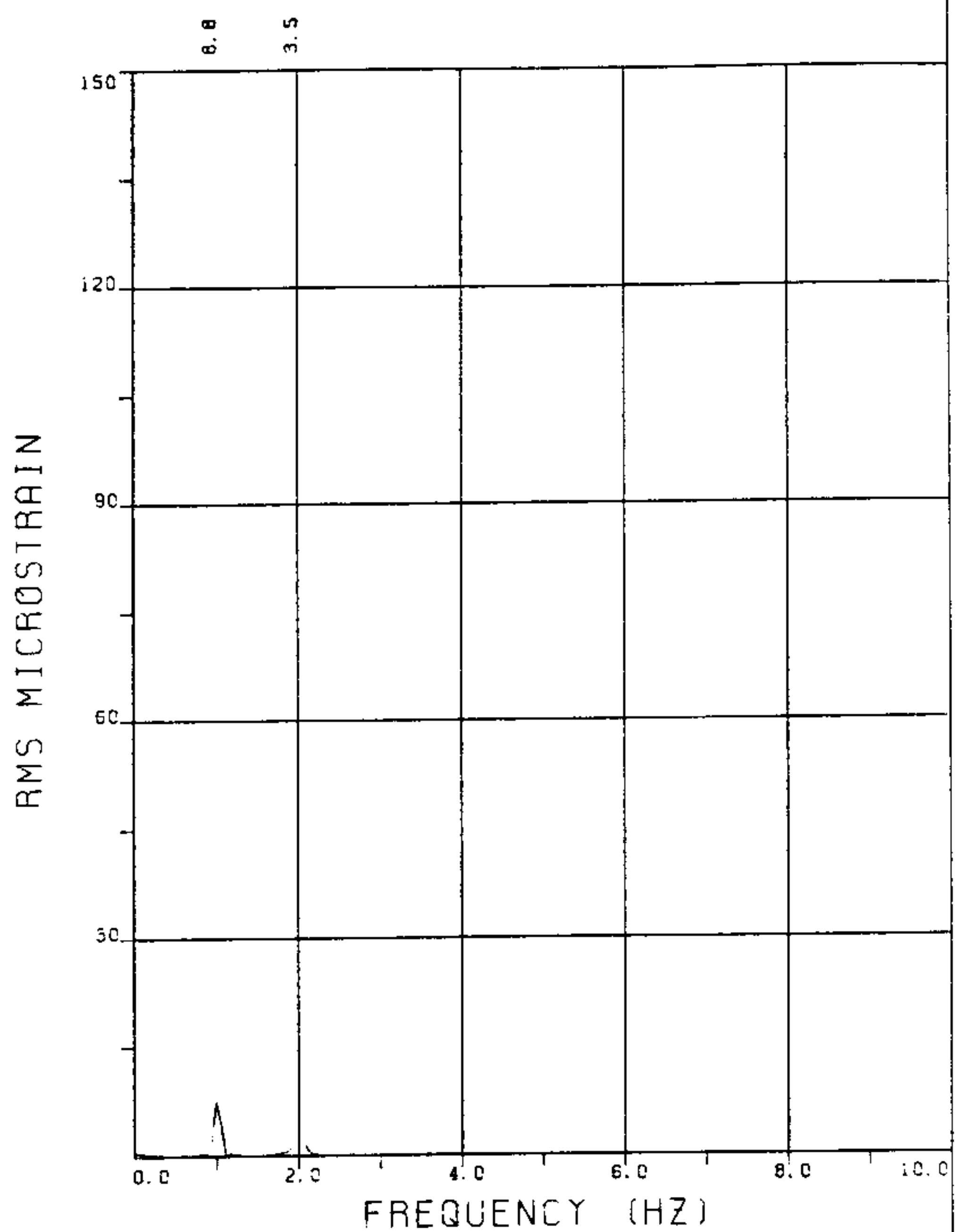

EXPERIMENT NUMBER 15

BRIDGE B5 ELEVATION=6L/11 BE=0.059

THETA=0 VC=0 FE=1.000 A/DE=1.01

MEASURED RESPONSE IN MICROSTRAIN

TOTAL DYNAMIC RMS=10.1

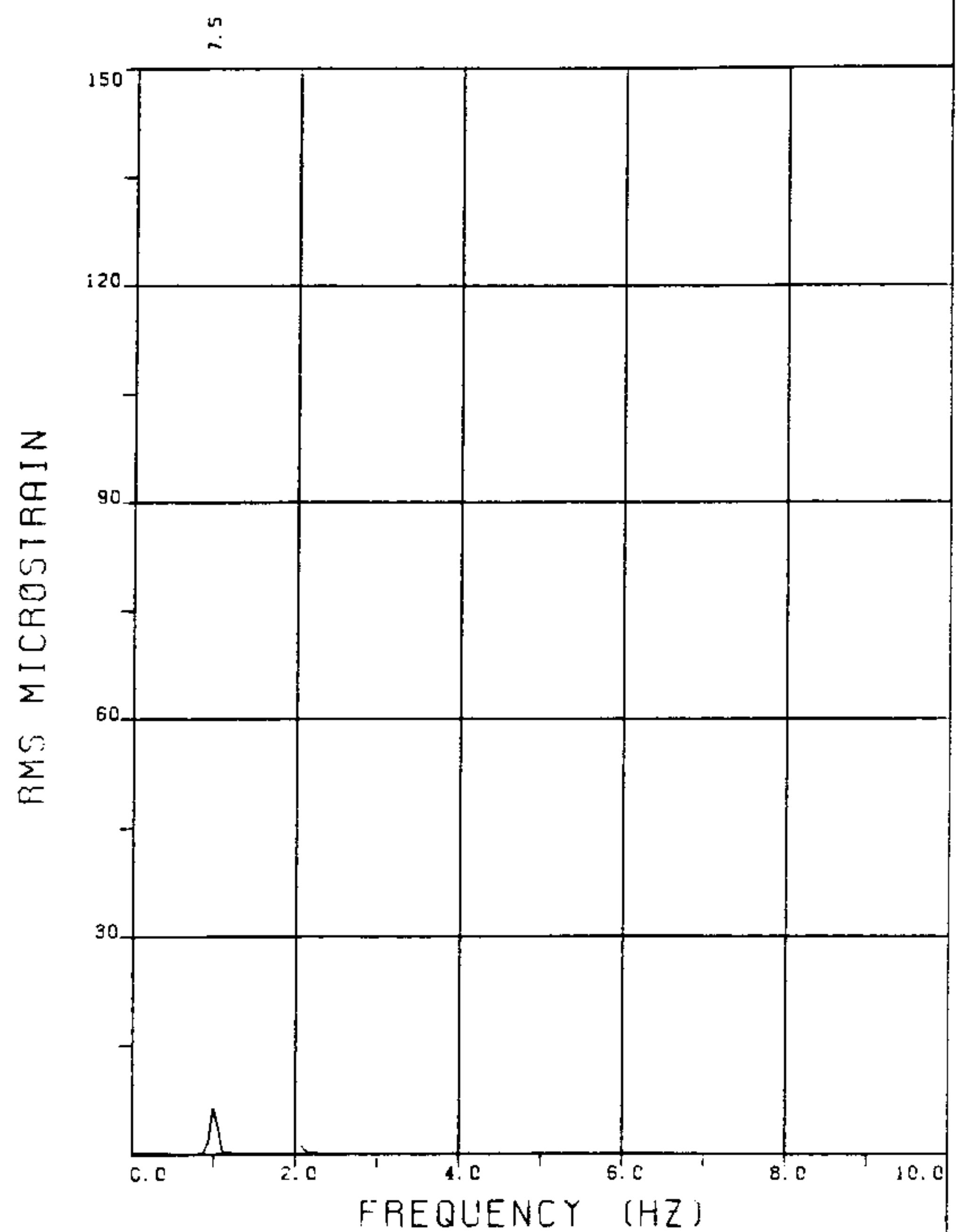

EXPERIMENT NUMBER 16

BRIDGE B3 ELEVATION=8L/11 BE=0.059

THETA=0 VC=0 FE=1.000 A/DE=1.01

MEASURED RESPONSE IN MICROSTRAIN

TOTAL DYNAMIC RMS=8.1

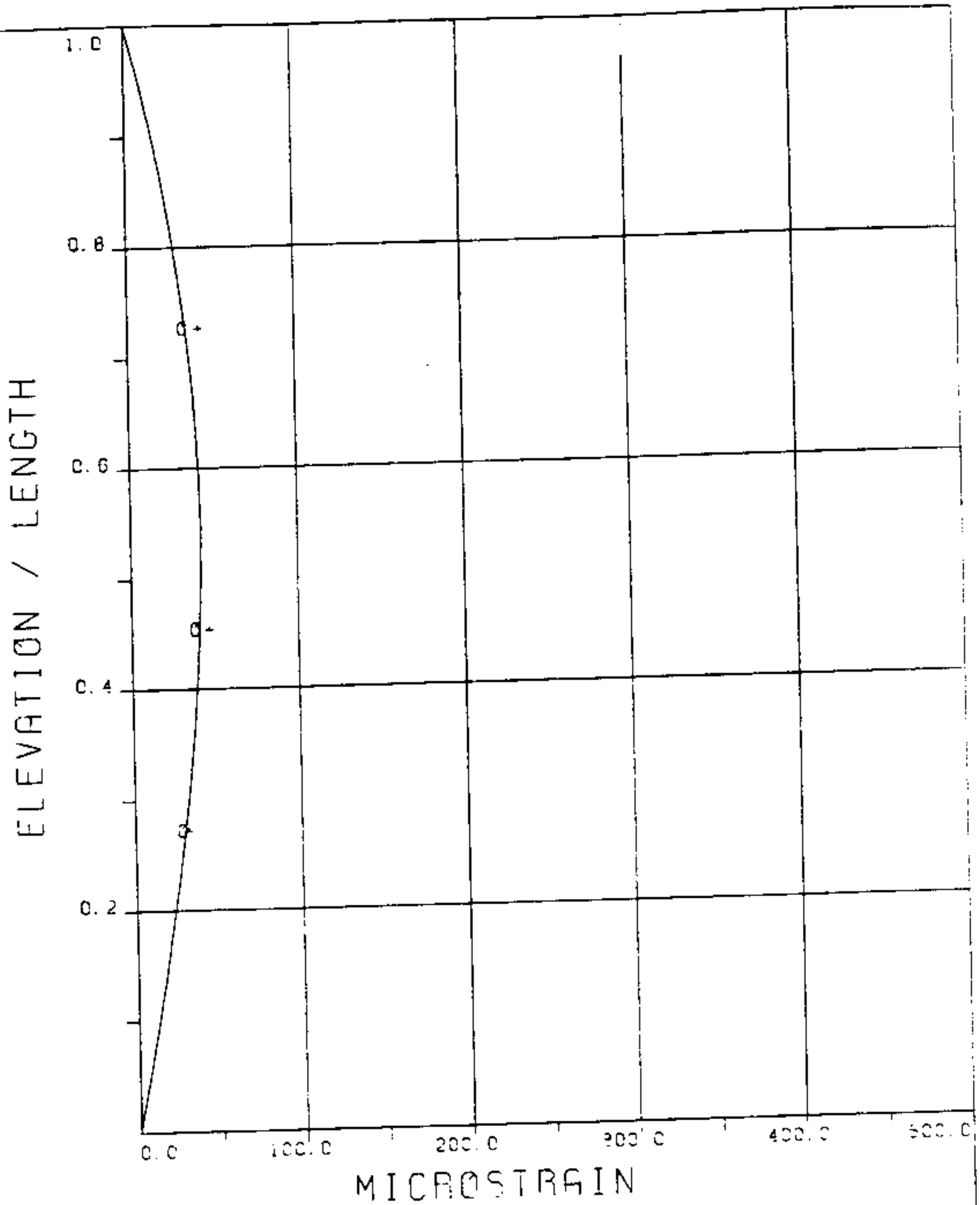

EXPERIMENT NUMBER 16

THETA=0 VC=0 FE=1.000 A/DE=1.01

DYNAMIC RESPONSE AT F=FE IN PLANE A
——— THEORY o o o EXPERIMENT

MAXIMUM DYNAMIC RESPONSE IN PLANE A
——— THEORY + + + EXPERIMENT

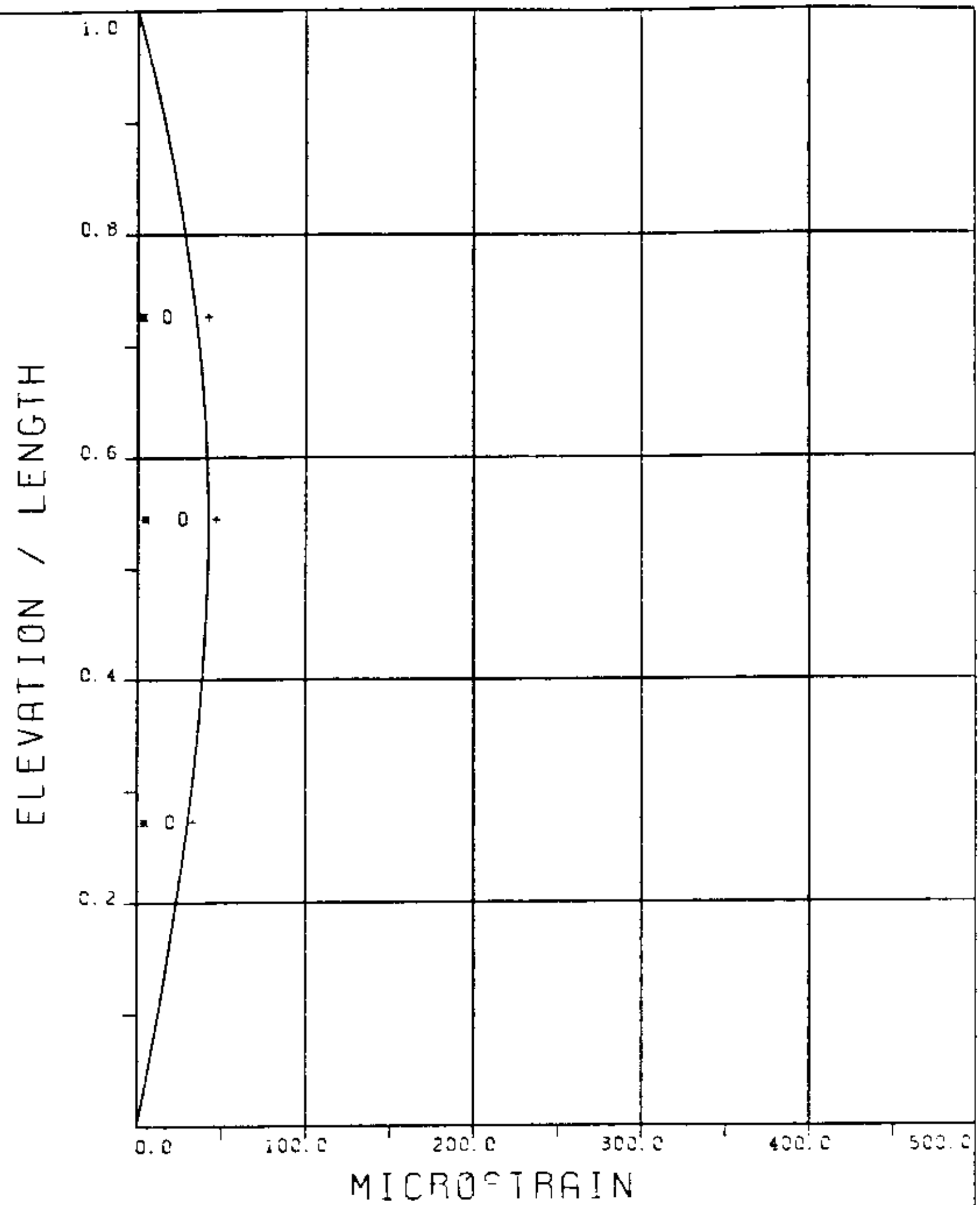

EXPERIMENT NUMBER 16

THETA=0 VC=0 FE=1.000 A/DE=1.01

DYNAMIC RESPONSE IN PLANE B AT F=2FE

* * * EXPERIMENT

MAXIMUM RESPONSE IN PLANE B

o o o EXPERIMENT

MAXIMUM RESPONSE

______ THEORY + + + EXPERIMENT

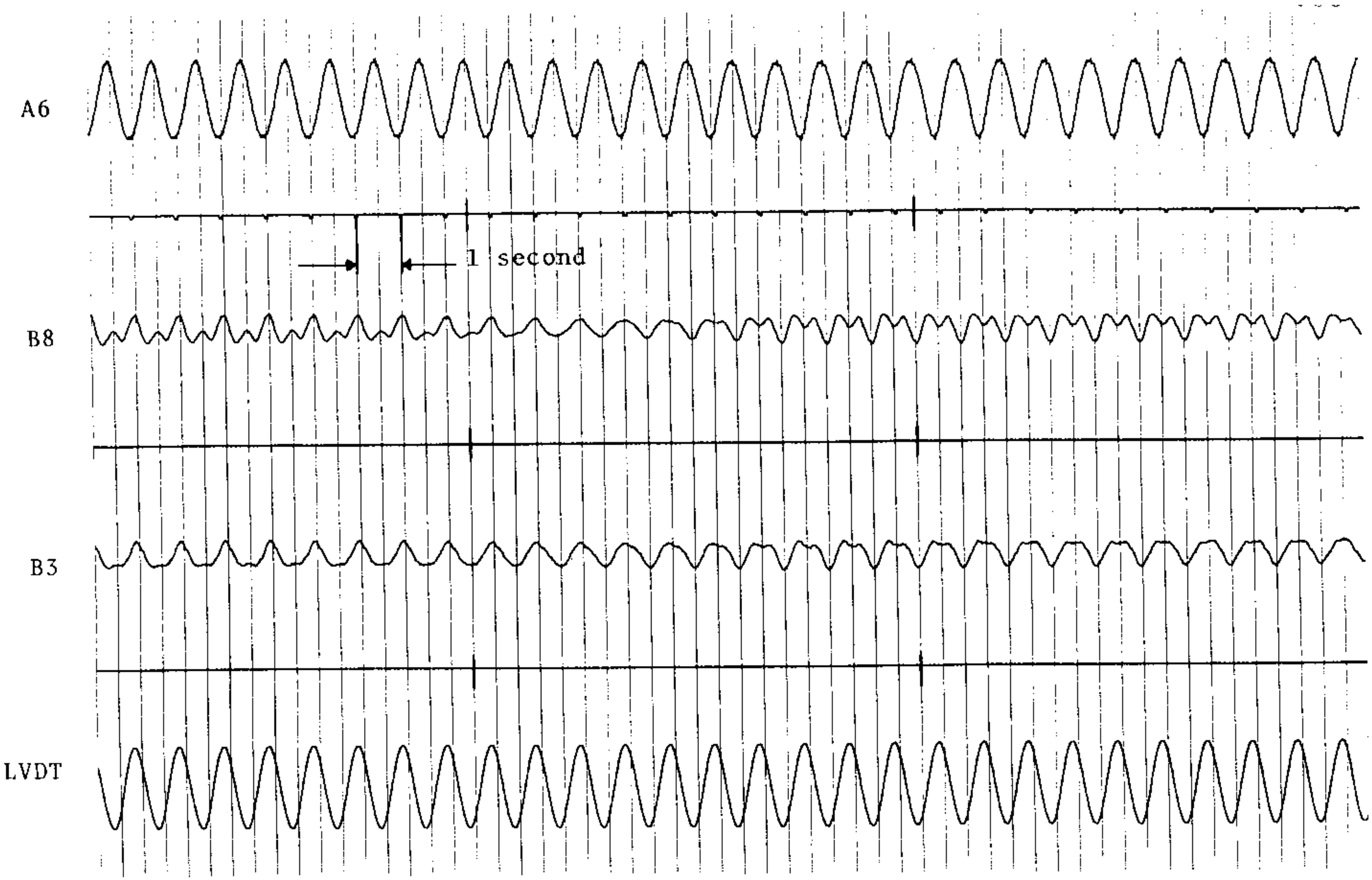

FIGURE 16Ta: LVDT: 0.087 D_e/DIVISION; STRAINS: 3.82 MICROSTRAIN/DIVISION

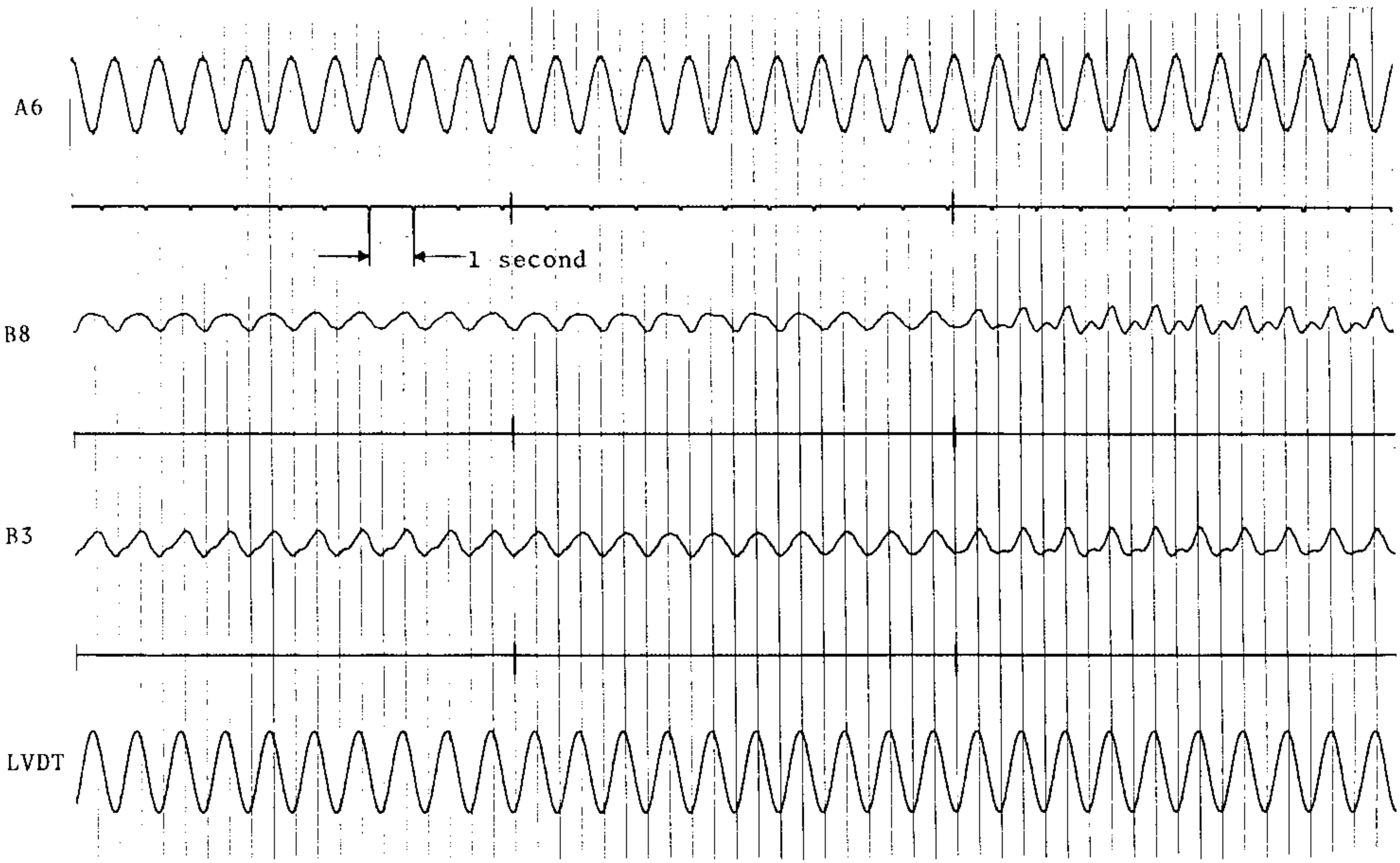

FIGURE 16Tb: LVDT: 0.087 D_e/DIVISION; STRAINS: 3.82 MICROSTRAIN/DIVISION

EXPERIMENT 19

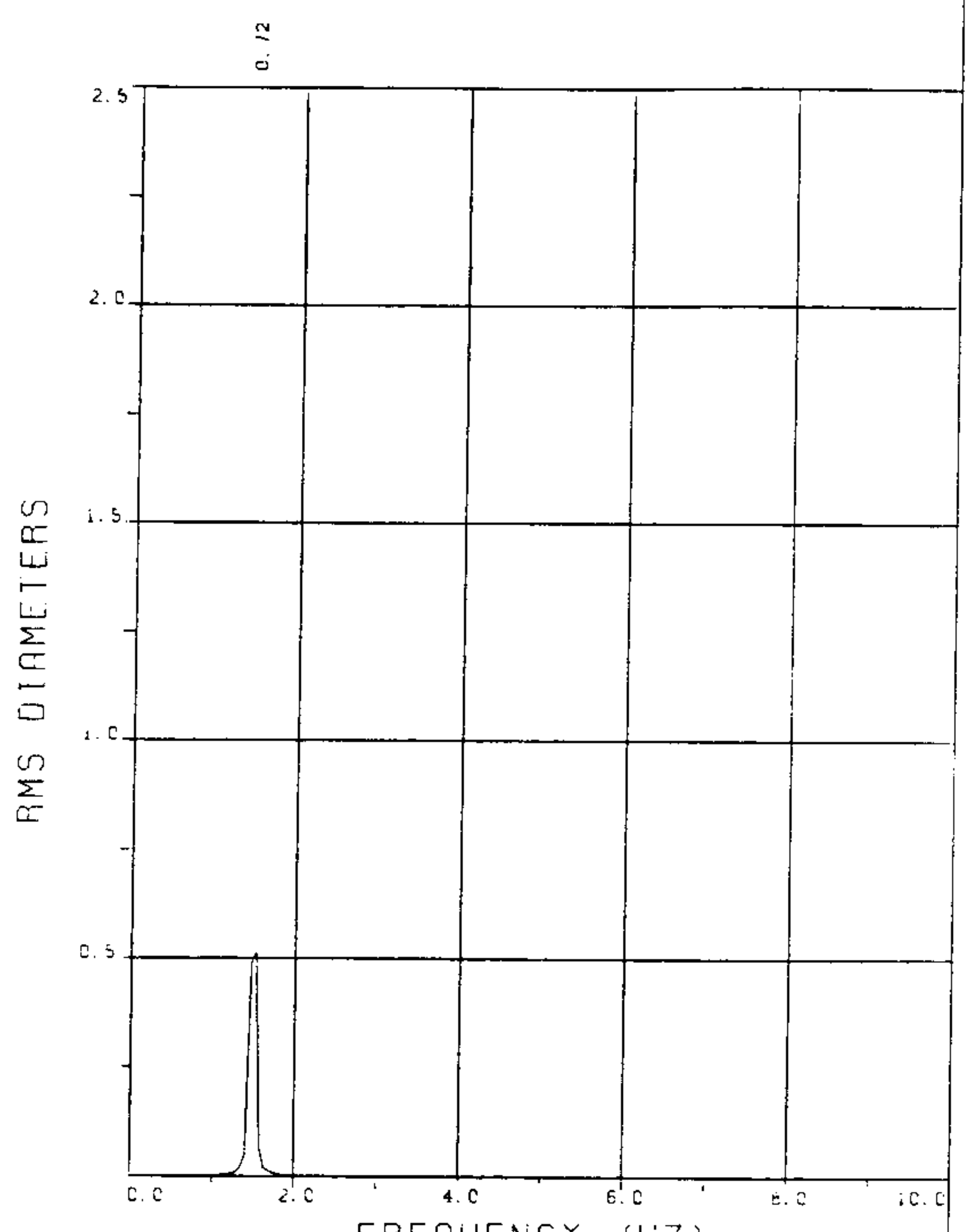

EXPERIMENT NUMBER 19

LVDT

THETA=0 VC=0 FE=1.500 BE=0.059

MEASURED A/DE=1.01

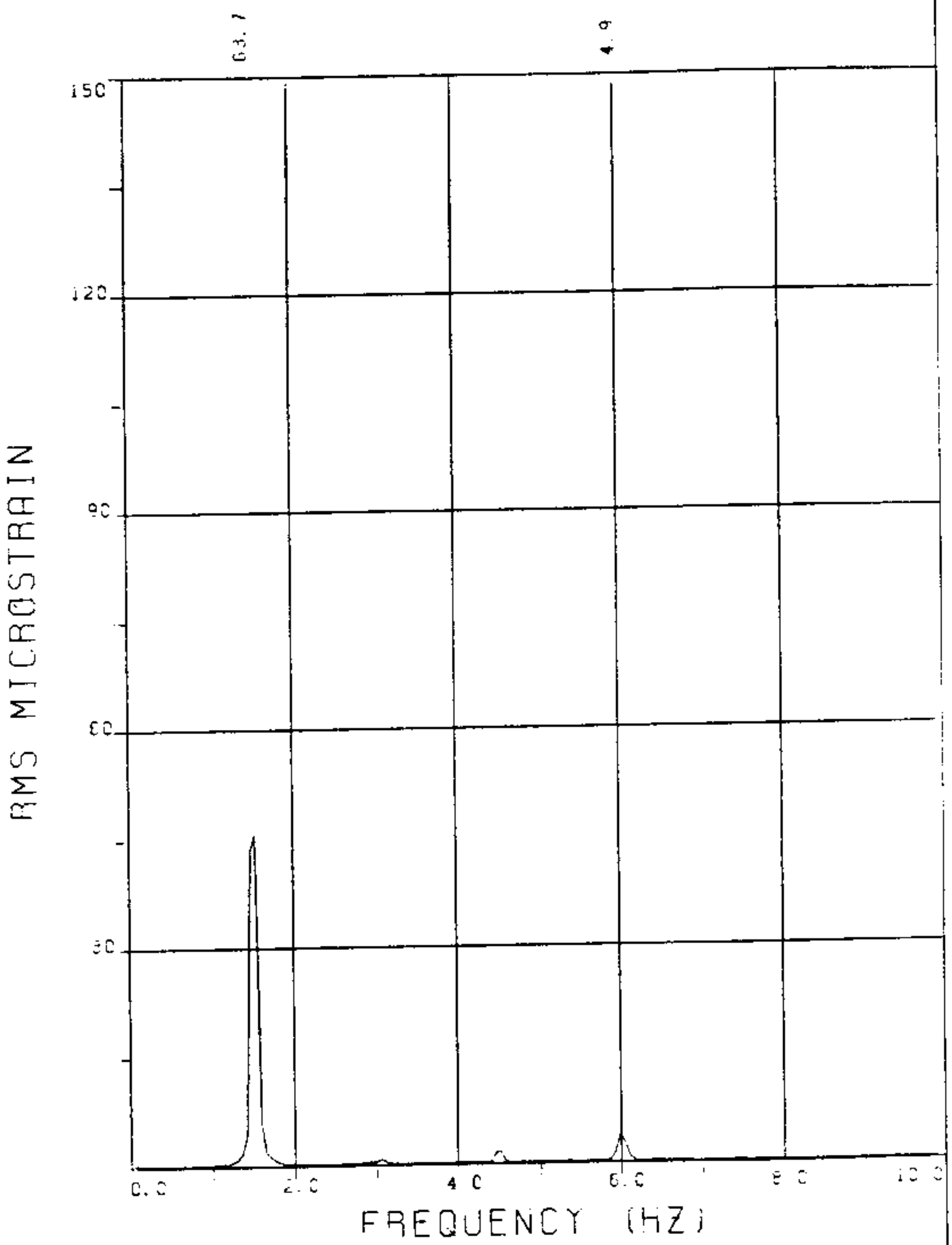

EXPERIMENT NUMBER 19

BRIDGE A8 ELEVATION=3L/11 BE=0.059

THETA=0 VC=0 FE=1.500 A/DE=1.01

MEASURED RESPONSE IN MICROSTRAIN

TOTAL DYNAMIC RMS=63.9

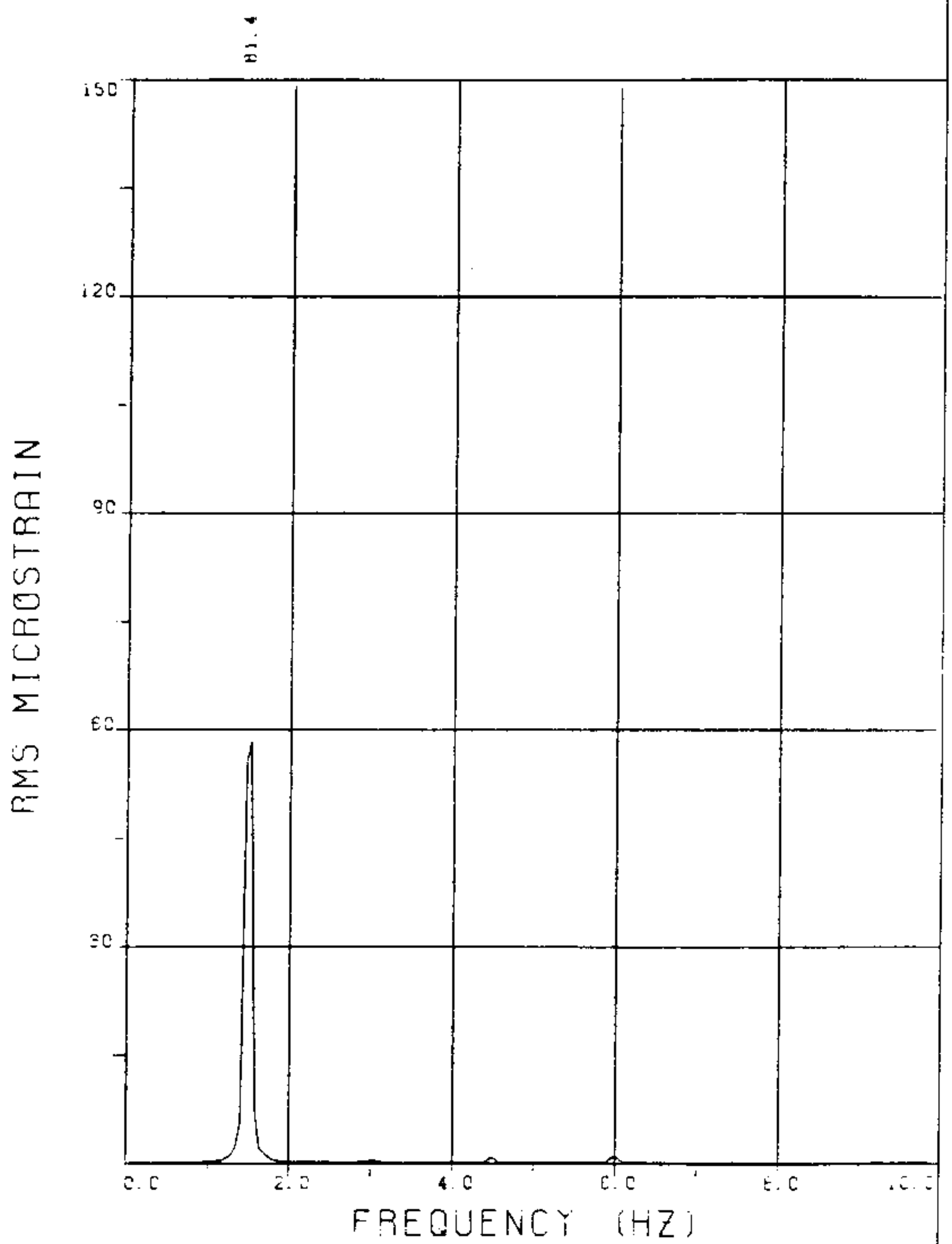

EXPERIMENT NUMBER 19

BRIDGE A6 ELEVATION=5L/11 BE=0.059

THETA=0 VC=0 FE=1.500 A/DE=1.01

MEASURED RESPONSE IN MICROSTRAIN

TOTAL DYNAMIC RMS=81.4

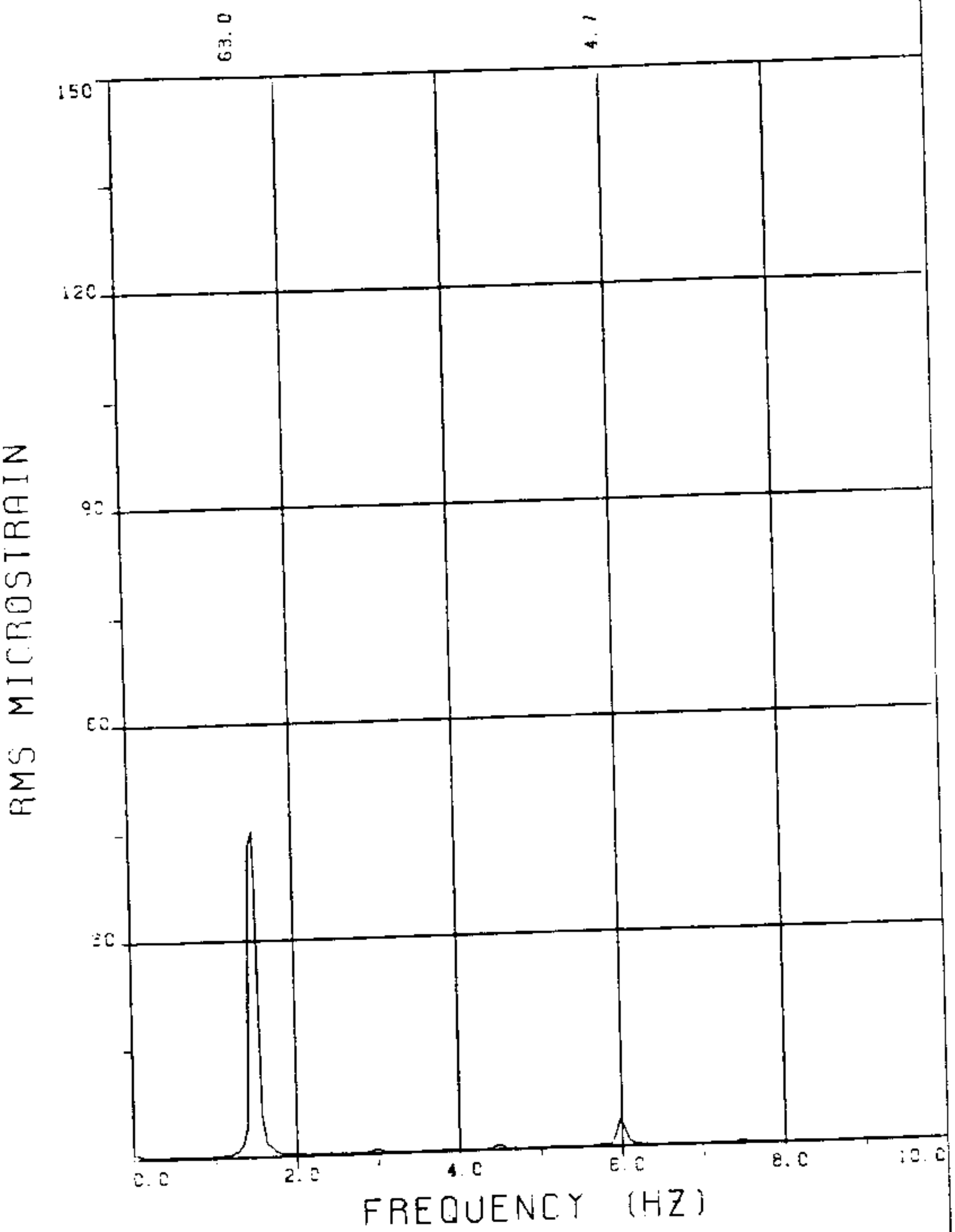

EXPERIMENT NUMBER 19

BRIDGE A3 ELEVATION=8L/11 BE=0.059

THETA=0 VC=0 FE=1.500 A/DE=1.01

MEASURED RESPONSE IN MICROSTRAIN

TOTAL DYNAMIC RMS=63.3

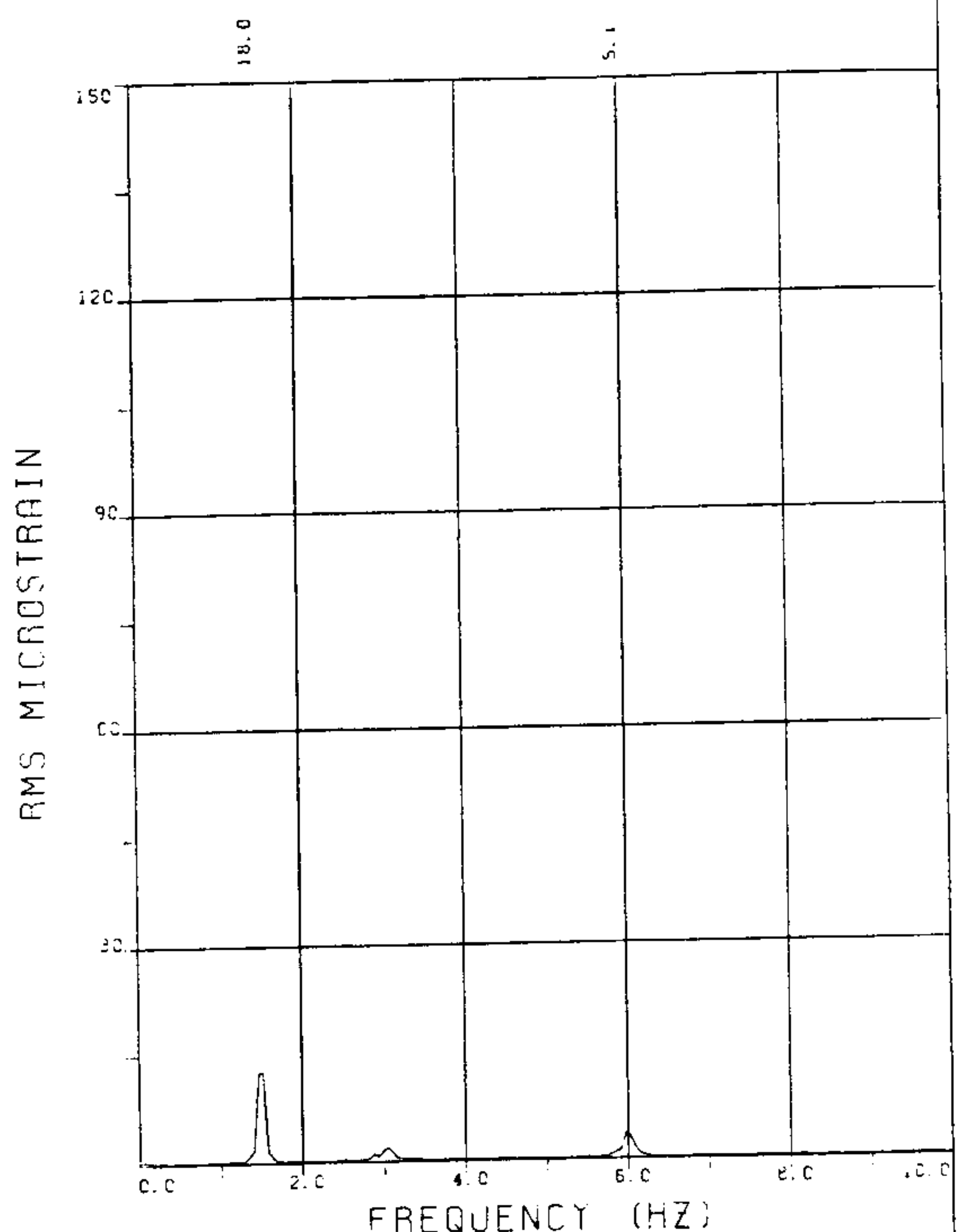

EXPERIMENT NUMBER 19

BRIDGE B8 ELEVATION=3L/11 BE=0.059

THETA=0 VC=0 FE=1.500 A/DE=1.01

MEASURED RESPONSE IN MICROSTRAIN

TOTAL DYNAMIC RMS=19.0

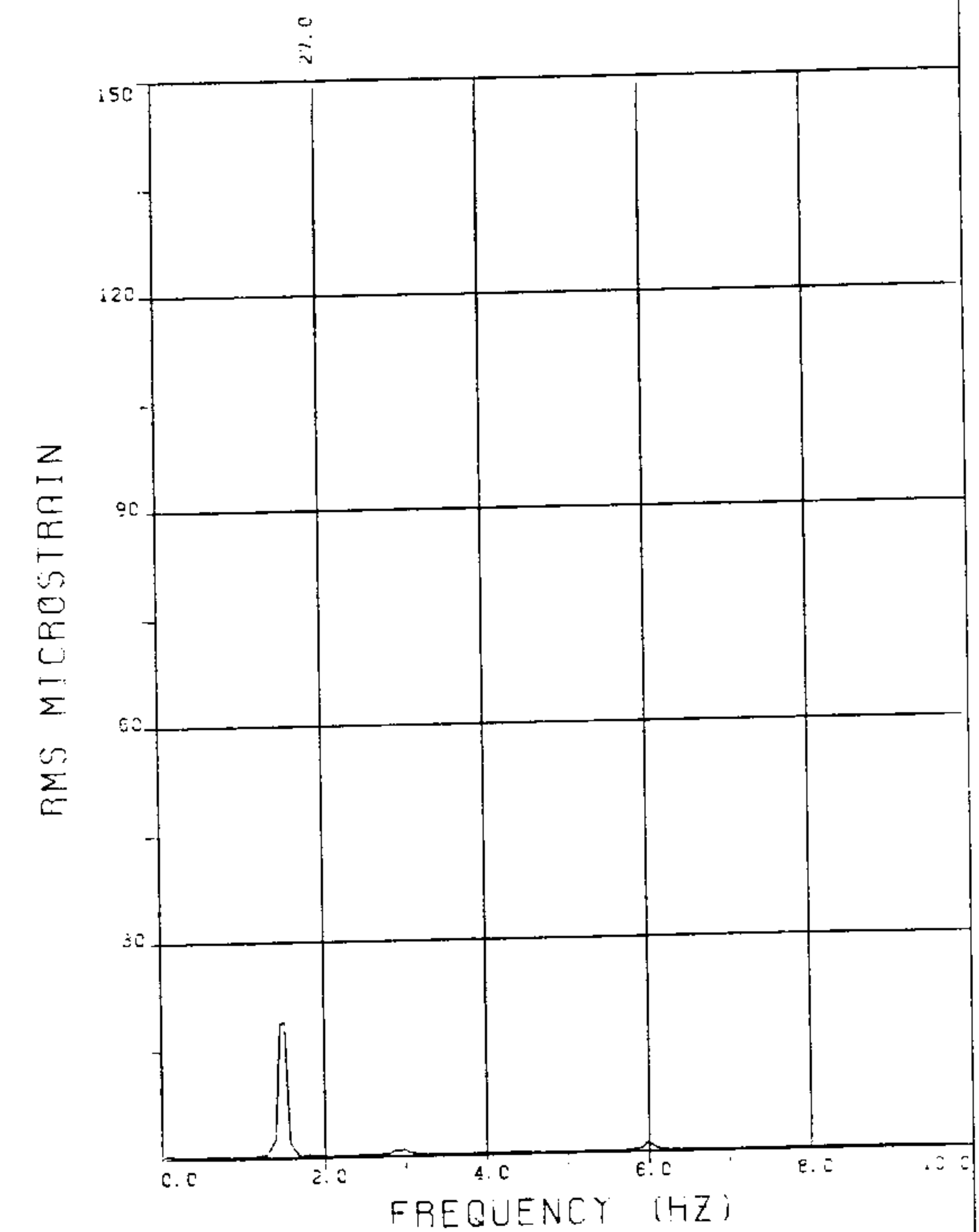

EXPERIMENT NUMBER 19

BRIDGE B5 ELEVATION=6L/11 BE=0.059

THETA=0 VC=0 FE=1.500 A/DE=1.01

MEASURED RESPONSE IN MICROSTRAIN

TOTAL DYNAMIC RMS=27.1

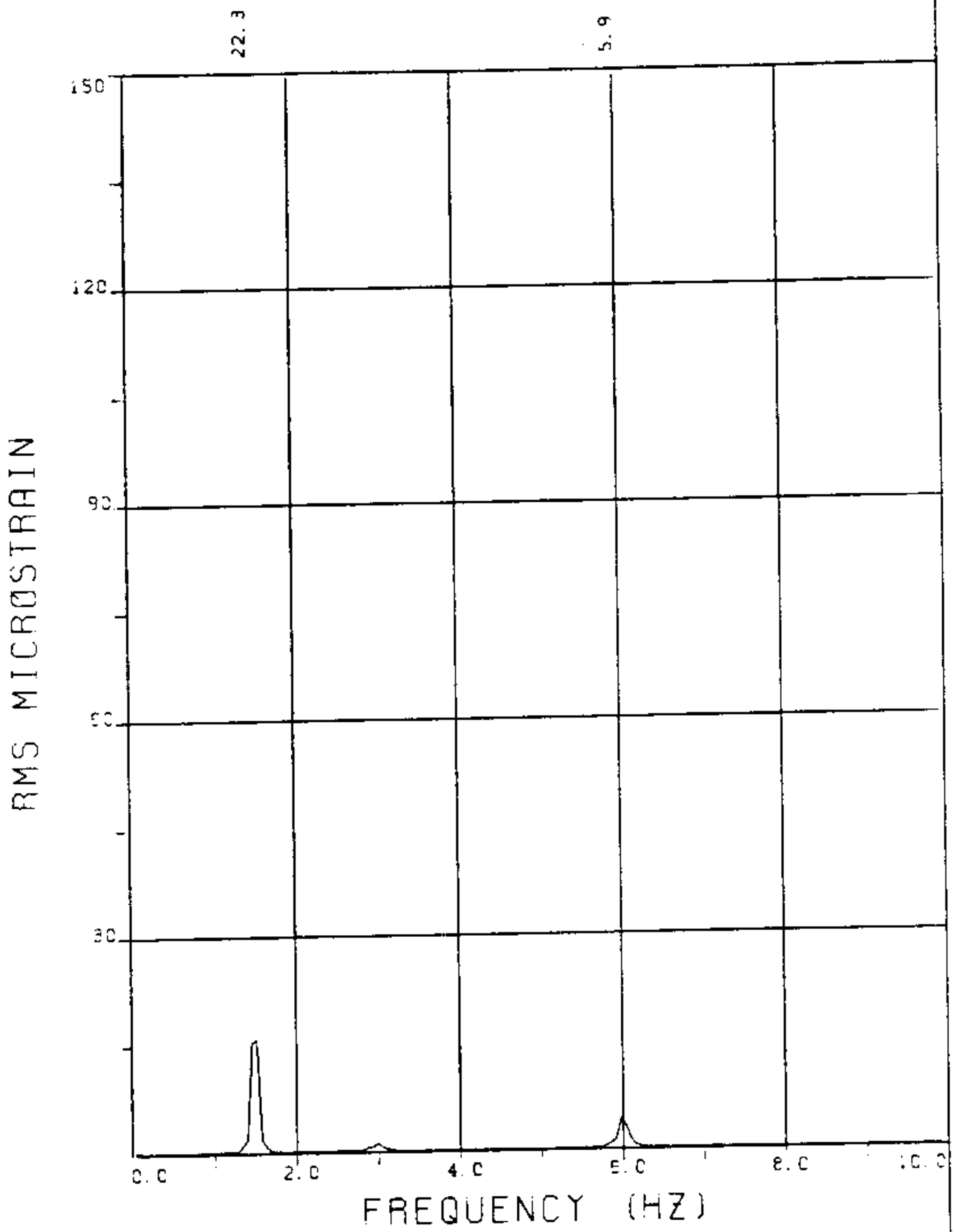

EXPERIMENT NUMBER 19

BRIDGE B3 ELEVATION=8L/11 BE=0.059

THETA=0 VC=0 FE=1.500 A/DE=1.01

MEASURED RESPONSE IN MICROSTRAIN

TOTAL DYNAMIC RMS=23.2

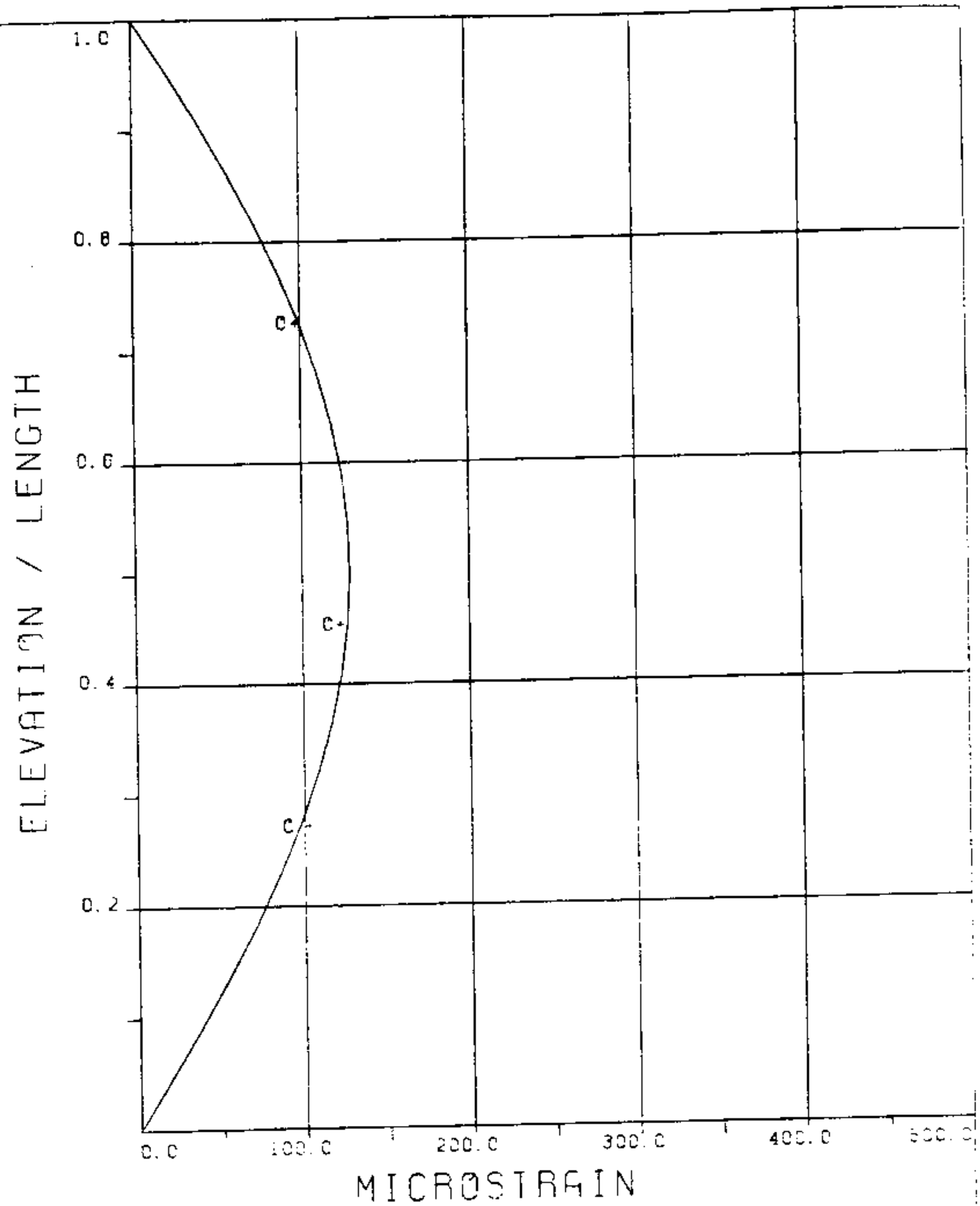

EXPERIMENT NUMBER 19

THETA=0 VC=0 FE=1.500 A/DE=1.01

DYNAMIC RESPONSE AT F=FE IN PLANE A
———— THEORY o o o EXPERIMENT

MAXIMUM DYNAMIC RESPONSE IN PLANE A
———— THEORY + + + EXPERIMENT

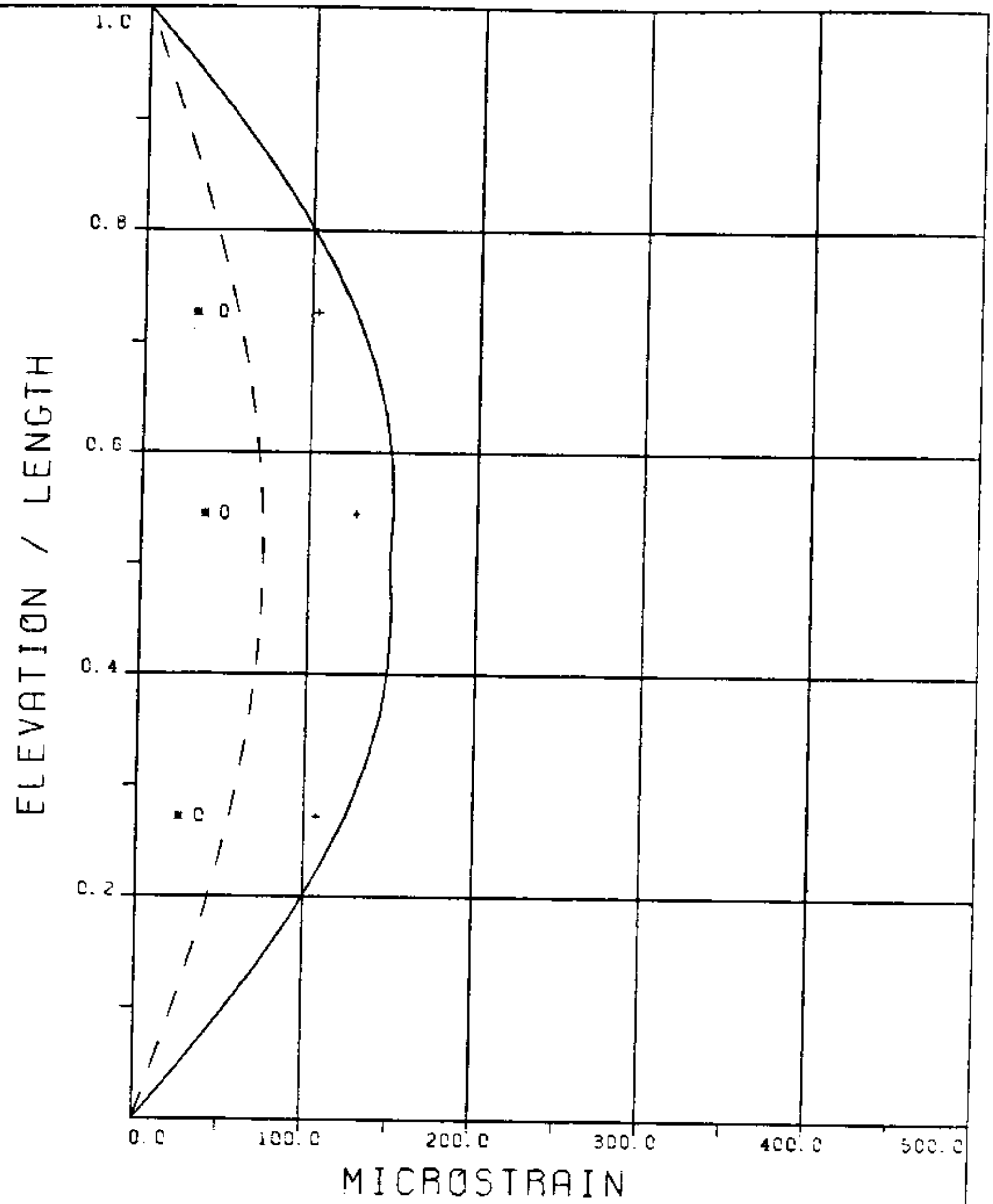

EXPERIMENT NUMBER 19

THETA=0 VC=0 FE=1.500 A/DE=1.01

DYNAMIC RESPONSE IN PLANE B AT F=FE

----- THEORY * * * EXPERIMENT

MAXIMUM RESPONSE IN PLANE B

o o o EXPERIMENT

MAXIMUM RESPONSE

——— THEORY + + + EXPERIMENT

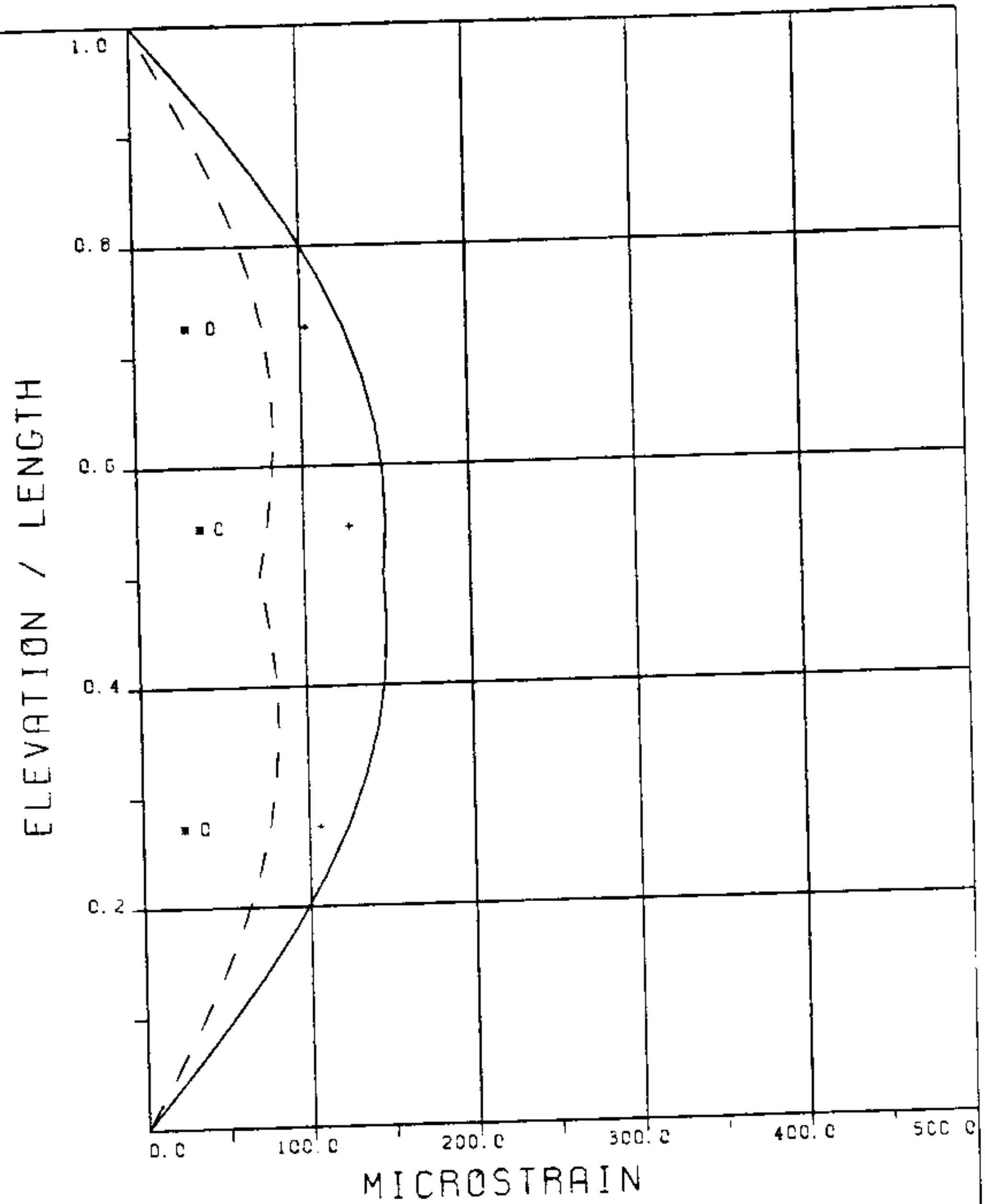

EXPERIMENT NUMBER 19

THETA=0 VC=0 FE=1.500 A/DE=1.01

DYNAMIC RESPONSE IN PLANE B AT F=FE

* * * EXPERIMENT

MAXIMUM RESPONSE IN PLANE B

----- THEORY o o o EXPERIMENT

MAXIMUM RESPONSE

——— THEORY + + + EXPERIMENT

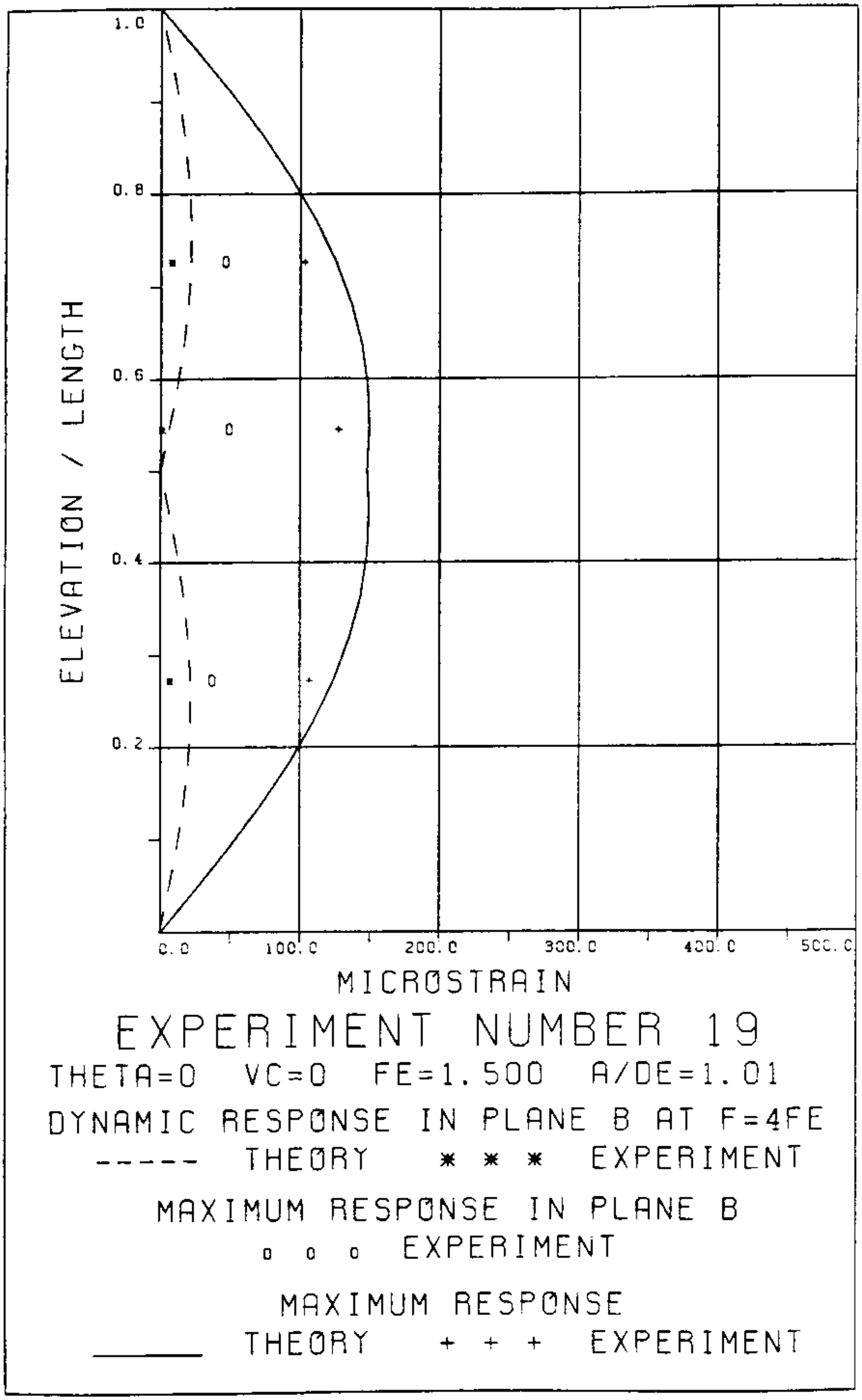
1.0
0.8
0.6
0.4
0.2
ELEVATION / LENGTH
0.0
100.0
200.0
300.0
400.0
500.0
MICROSTRAIN
EXPERIMENT NUMBER 19
THETA=0 VC=0 FE=1.500 A/DE=1.01
DYNAMIC RESPONSE IN PLANE B AT F=4FE
----- THEORY * * * EXPERIMENT
MAXIMUM RESPONSE IN PLANE B
o o o EXPERIMENT
MAXIMUM RESPONSE
THEORY + + + EXPERIMENT

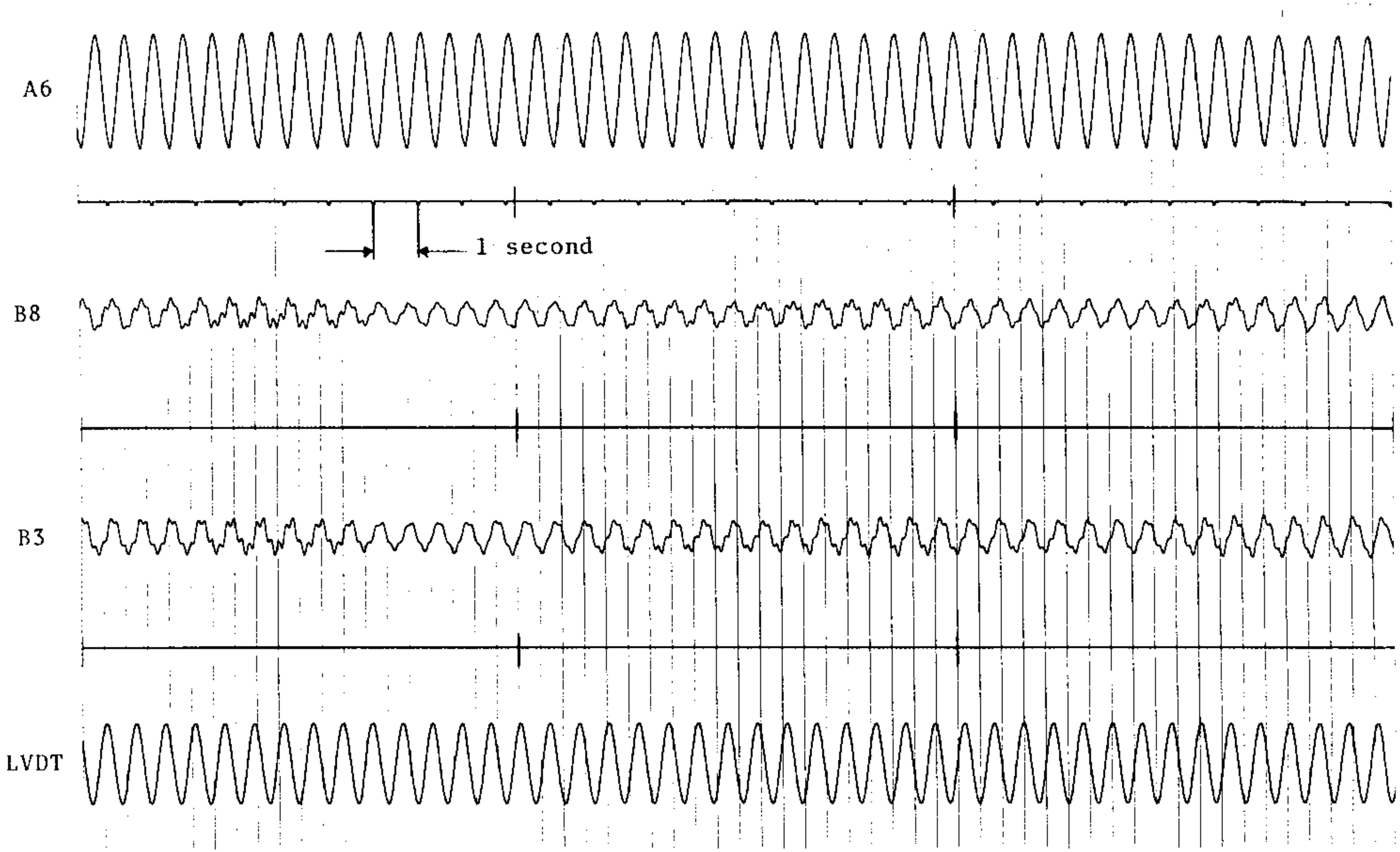

FIGURE 19Ta: LVDT: 0.087 D_e/DIVISION; STRAINS: 7.64 MICROSTRAIN/DIVISION

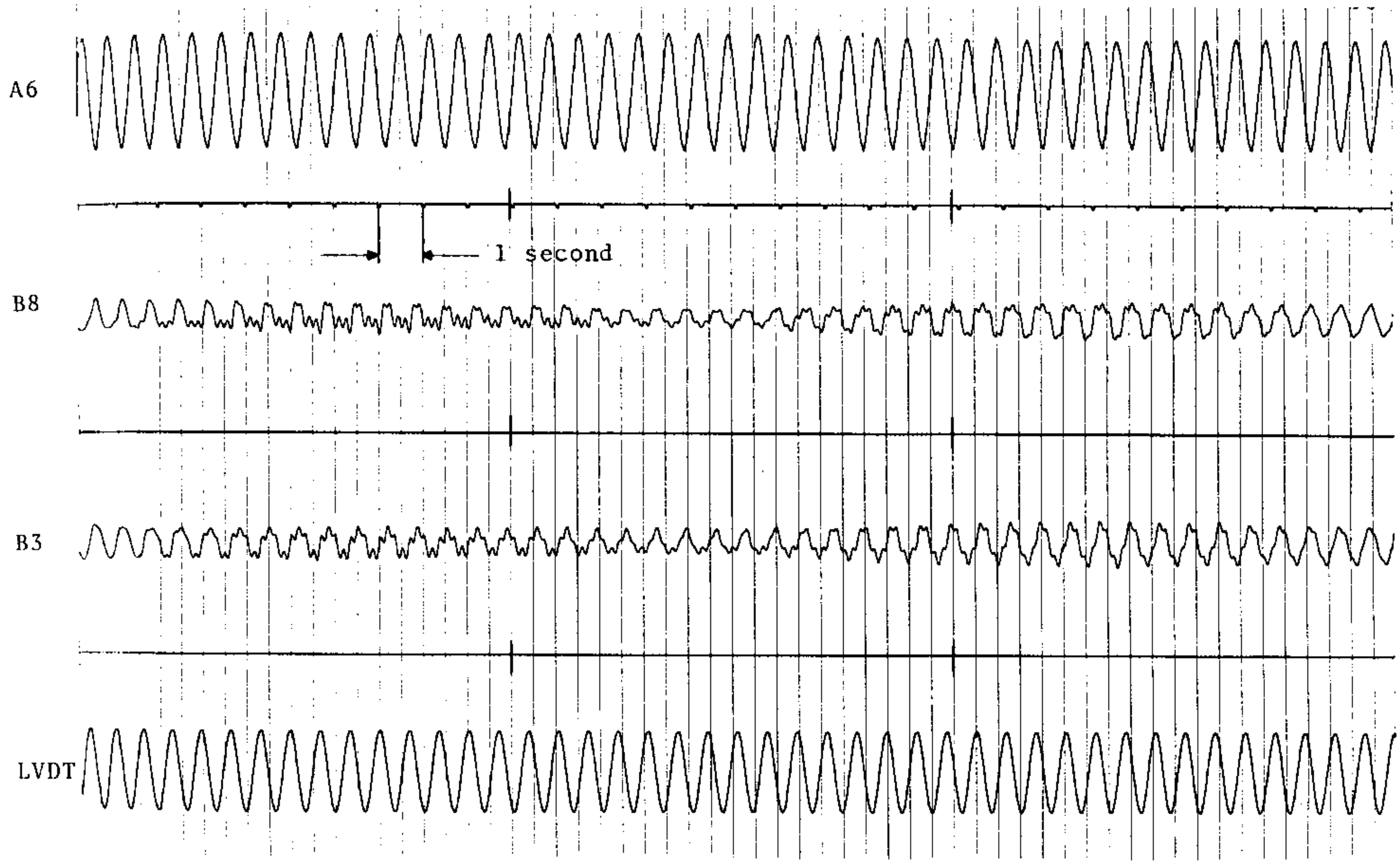

FIGURE 19Tb: LVDT: 0.087 D_c/DIVISION; STRAINS: 7.64 MICROSTRAIN/DIVISION

EXPERIMENT 22

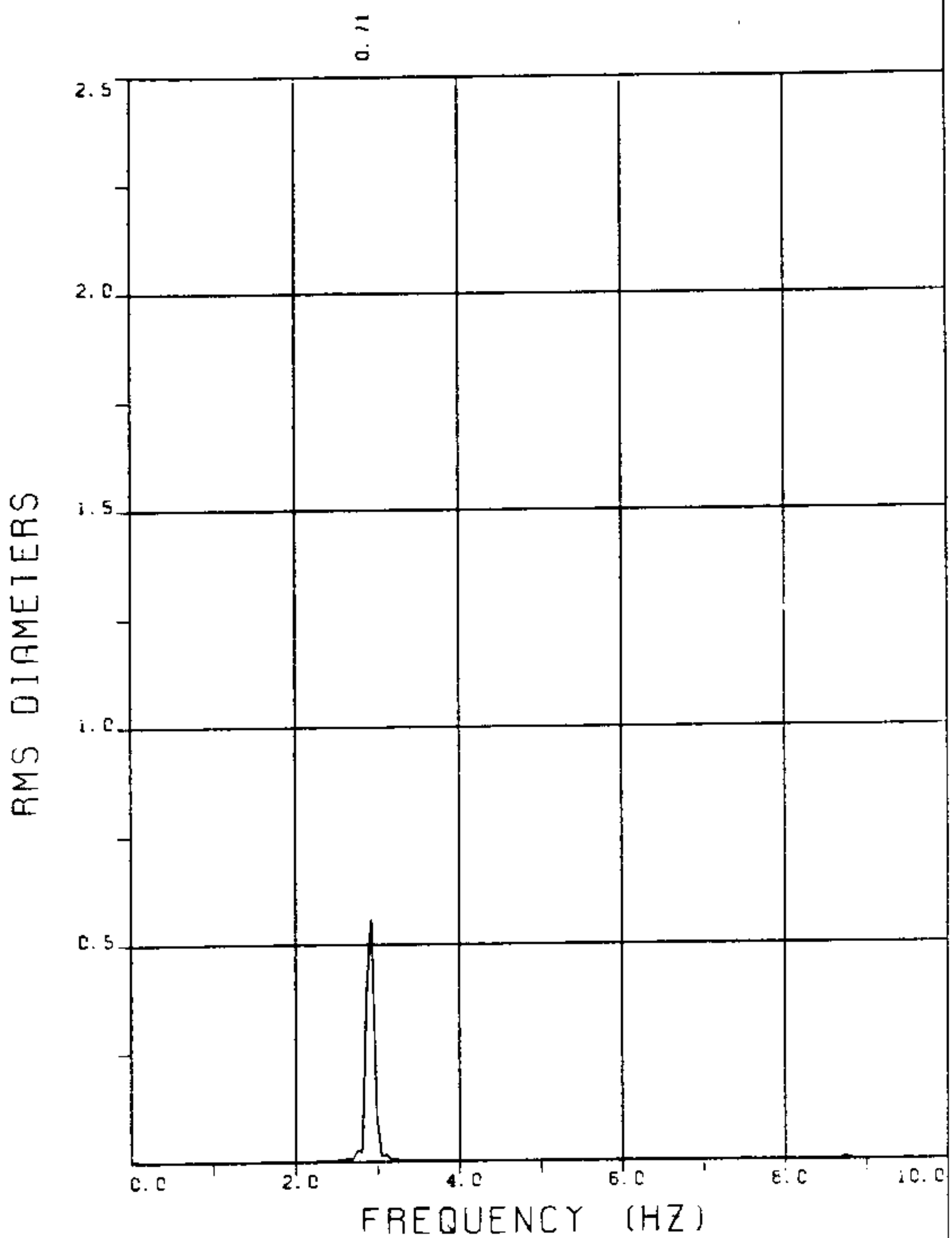

EXPERIMENT NUMBER 22

LVDT

THETA=0 VC=0 FE=2.920 BE=0.059

MEASURED A/DE=1.00

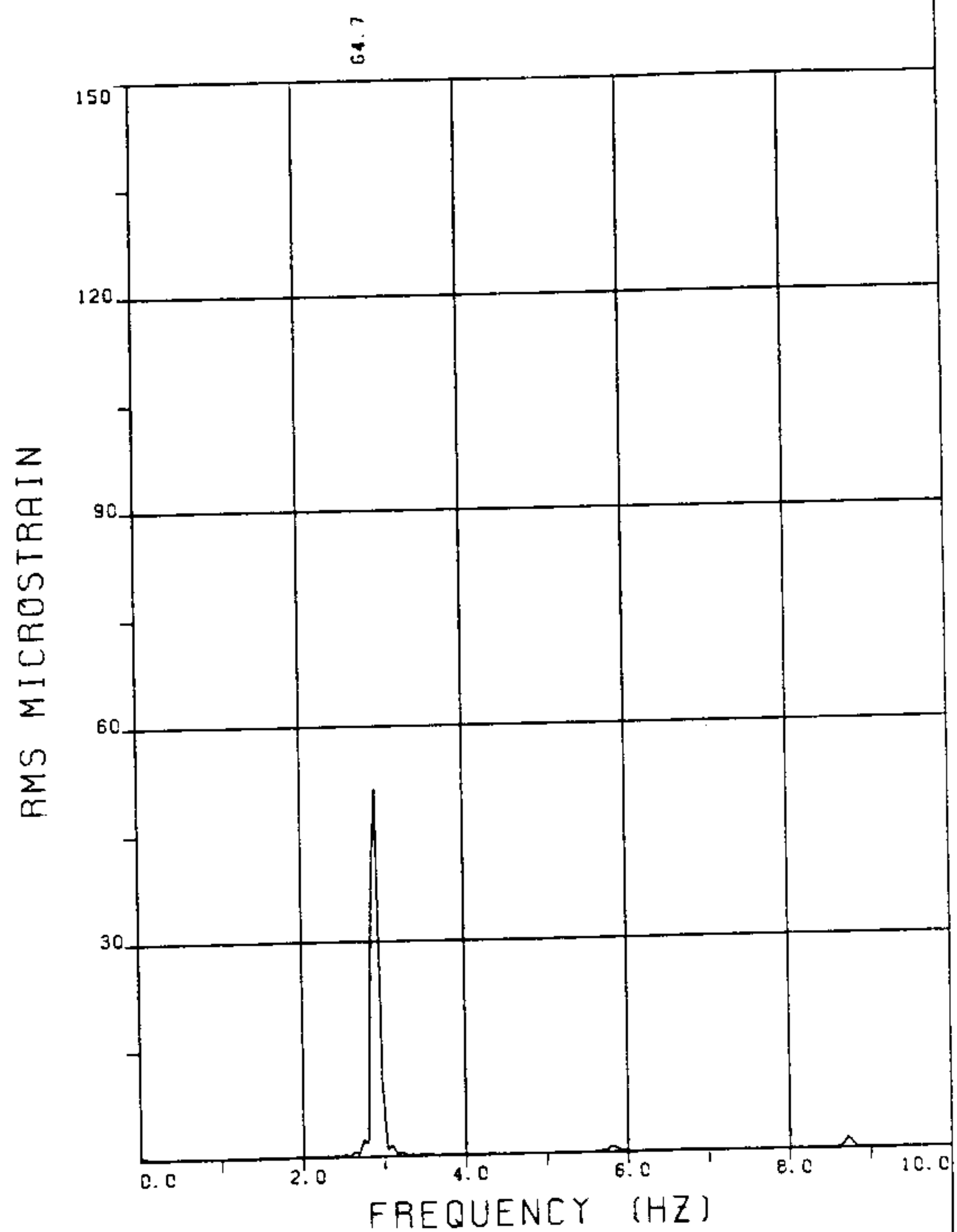

EXPERIMENT NUMBER 22

BRIDGE A8 ELEVATION=3L/11 BE=0.059

THETA=0 VC=0 FE=2.920 A/DE=1.00

MEASURED RESPONSE IN MICROSTRAIN

TOTAL DYNAMIC RMS=64.8

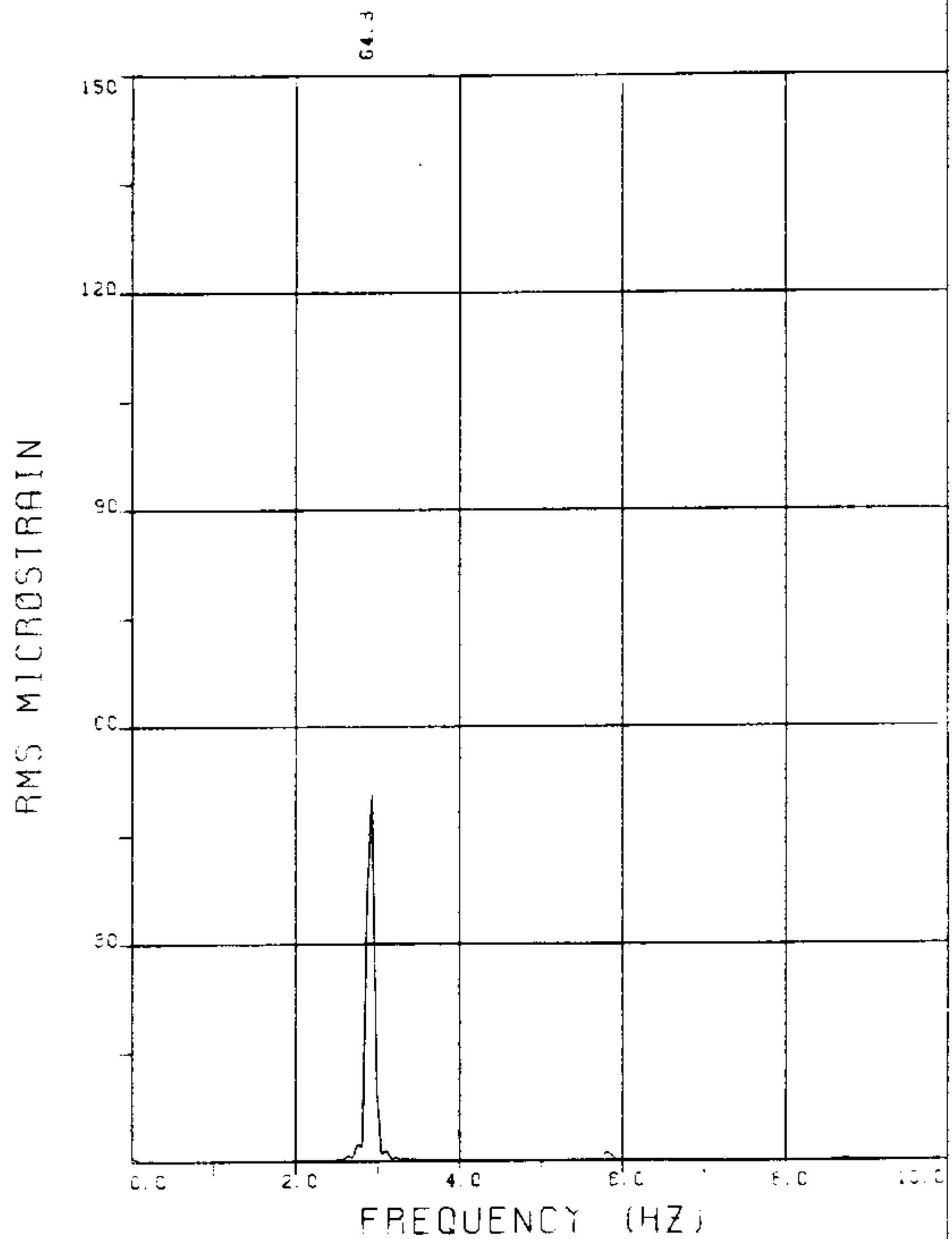

EXPERIMENT NUMBER 22

BRIDGE A6 ELEVATION=5L/11 BE=0.059

THETA=0 VC=0 FE=2.920 A/DE=1.00

MEASURED RESPONSE IN MICROSTRAIN

TOTAL DYNAMIC RMS=64.3

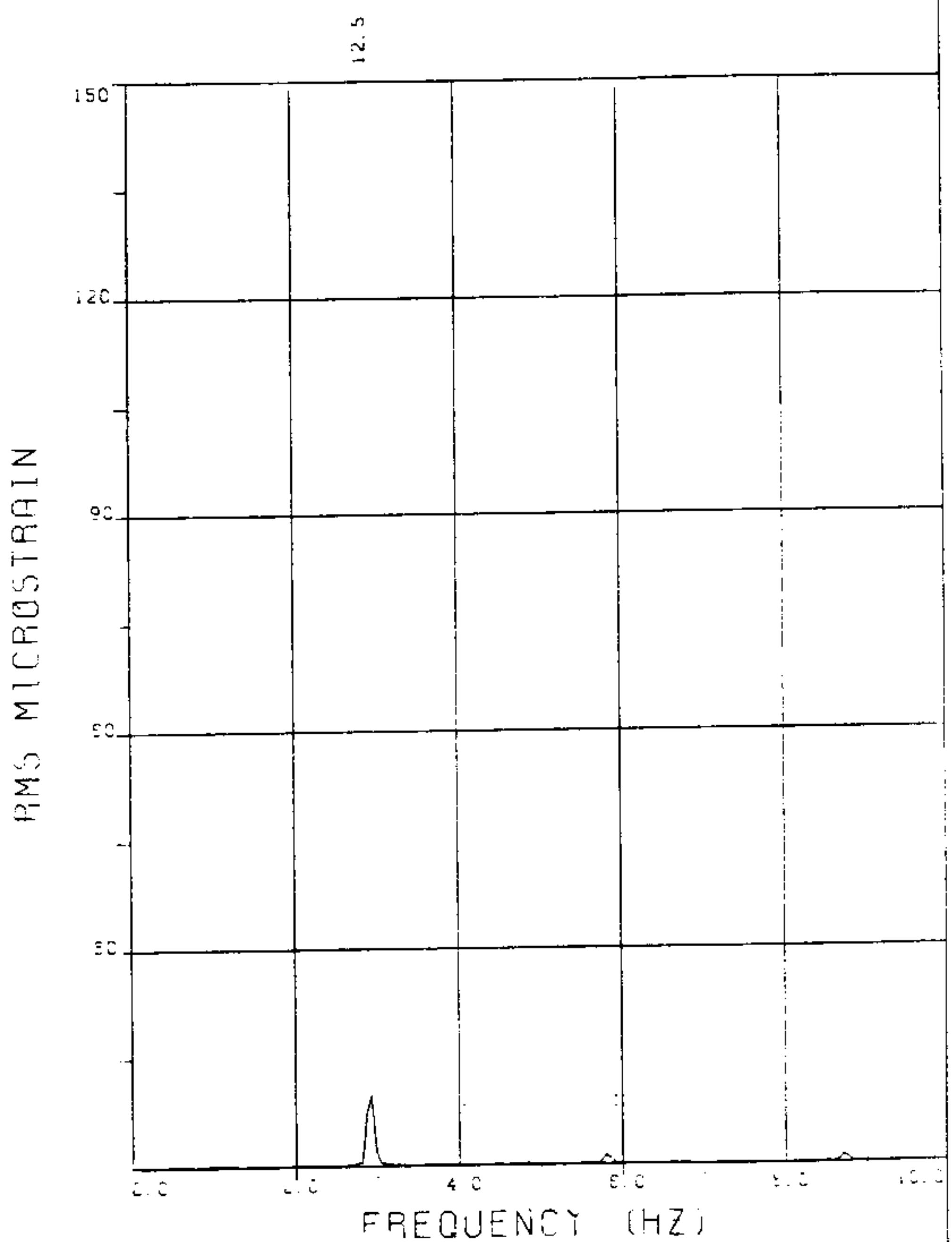

EXPERIMENT NUMBER 22

BRIDGE A3 ELEVATION=8L/11 BE=0.059

THETA=0 VC=0 FE=2.920 A/DE=1.00

MEASURED RESPONSE IN MICROSTRAIN

TOTAL DYNAMIC RMS=12.8

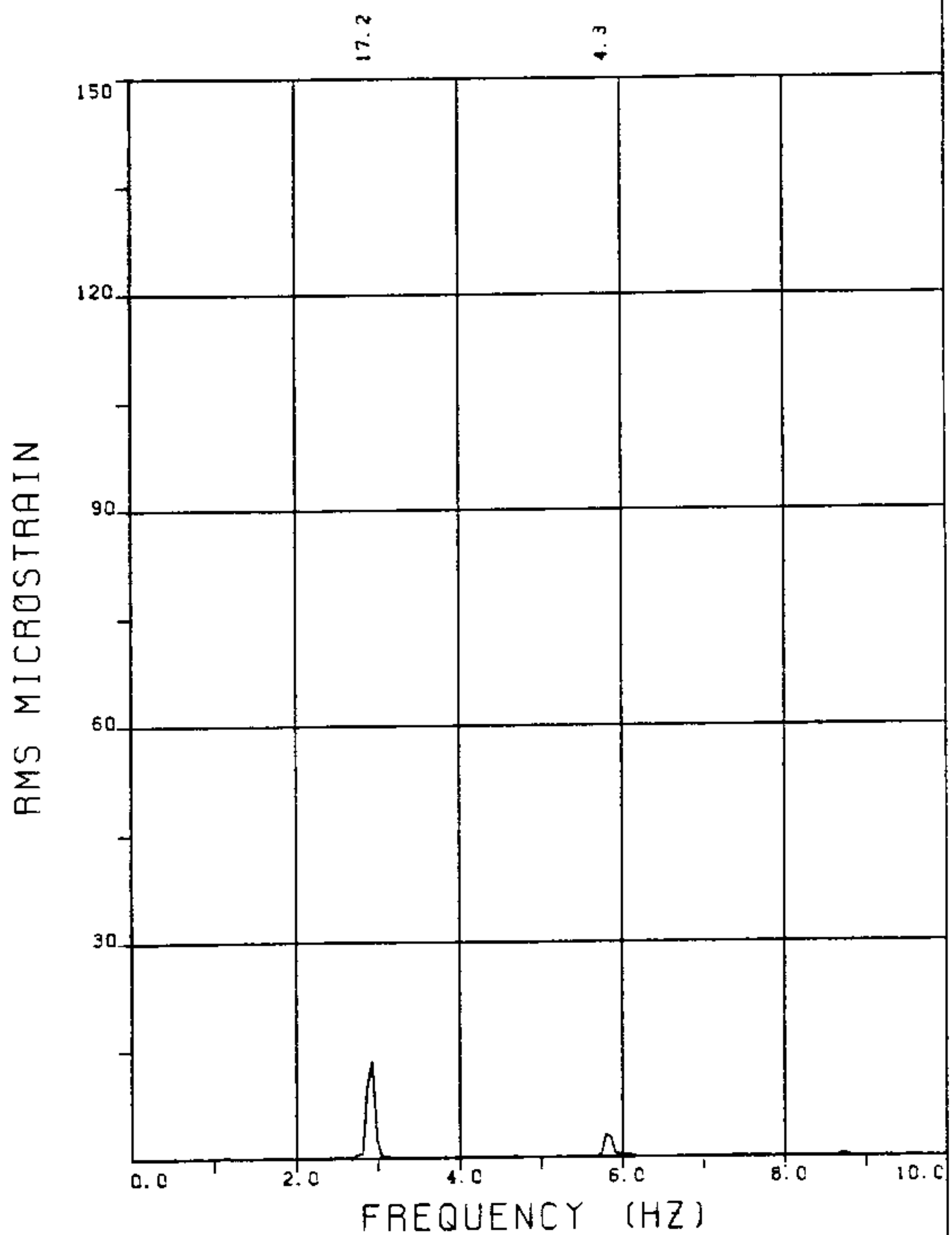

EXPERIMENT NUMBER 22

BRIDGE B8 ELEVATION=3L/11 BE=0.059

THETA=0 VC=0 FE=2.920 A/DE=1.00

MEASURED RESPONSE IN MICROSTRAIN

TOTAL DYNAMIC RMS=17.7

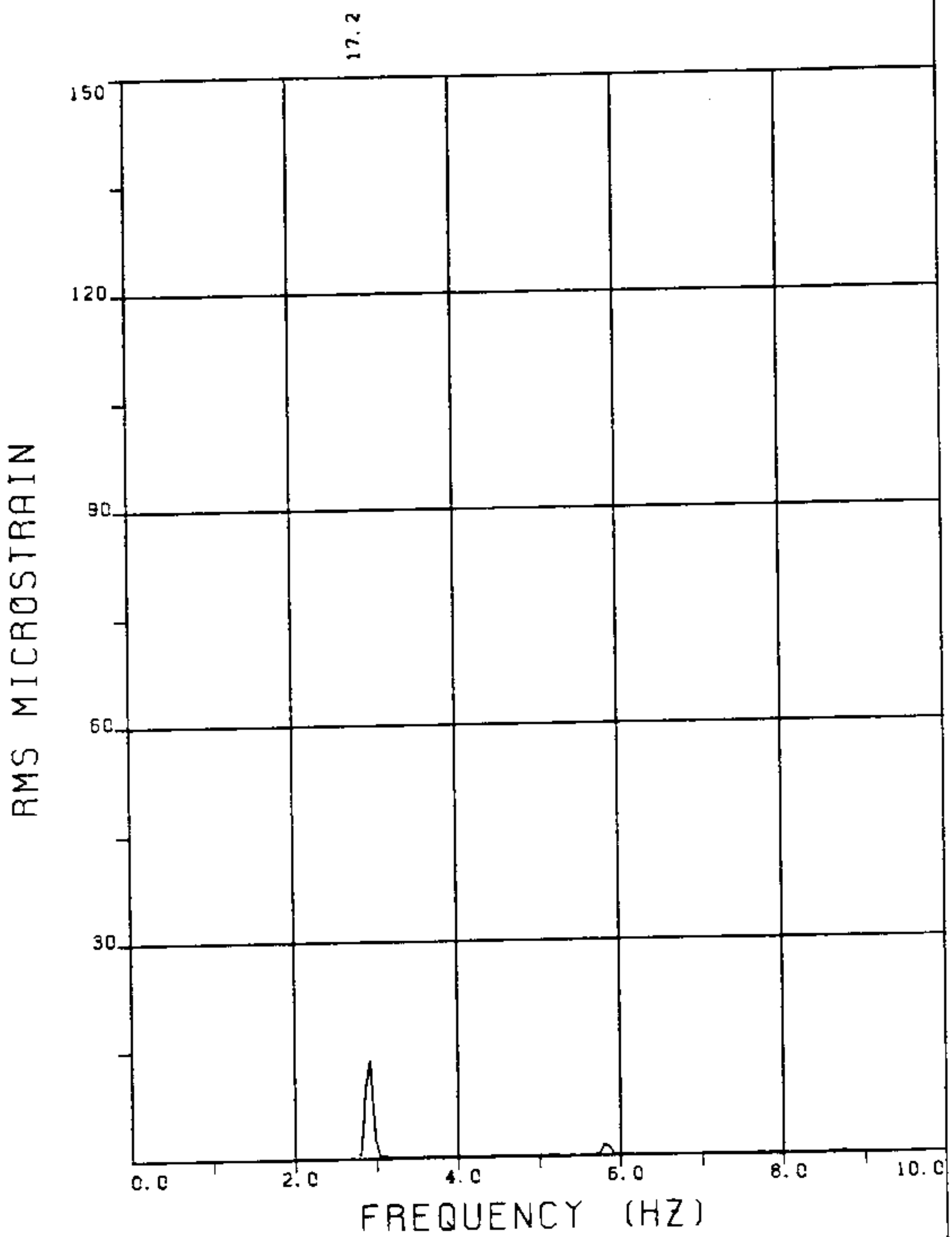

EXPERIMENT NUMBER 22

BRIDGE B5 ELEVATION=6L/11 BE=0.059

THETA=0 VC=0 FE=2.920 A/DE=1.00

MEASURED RESPONSE IN MICROSTRAIN

TOTAL DYNAMIC RMS=17.4

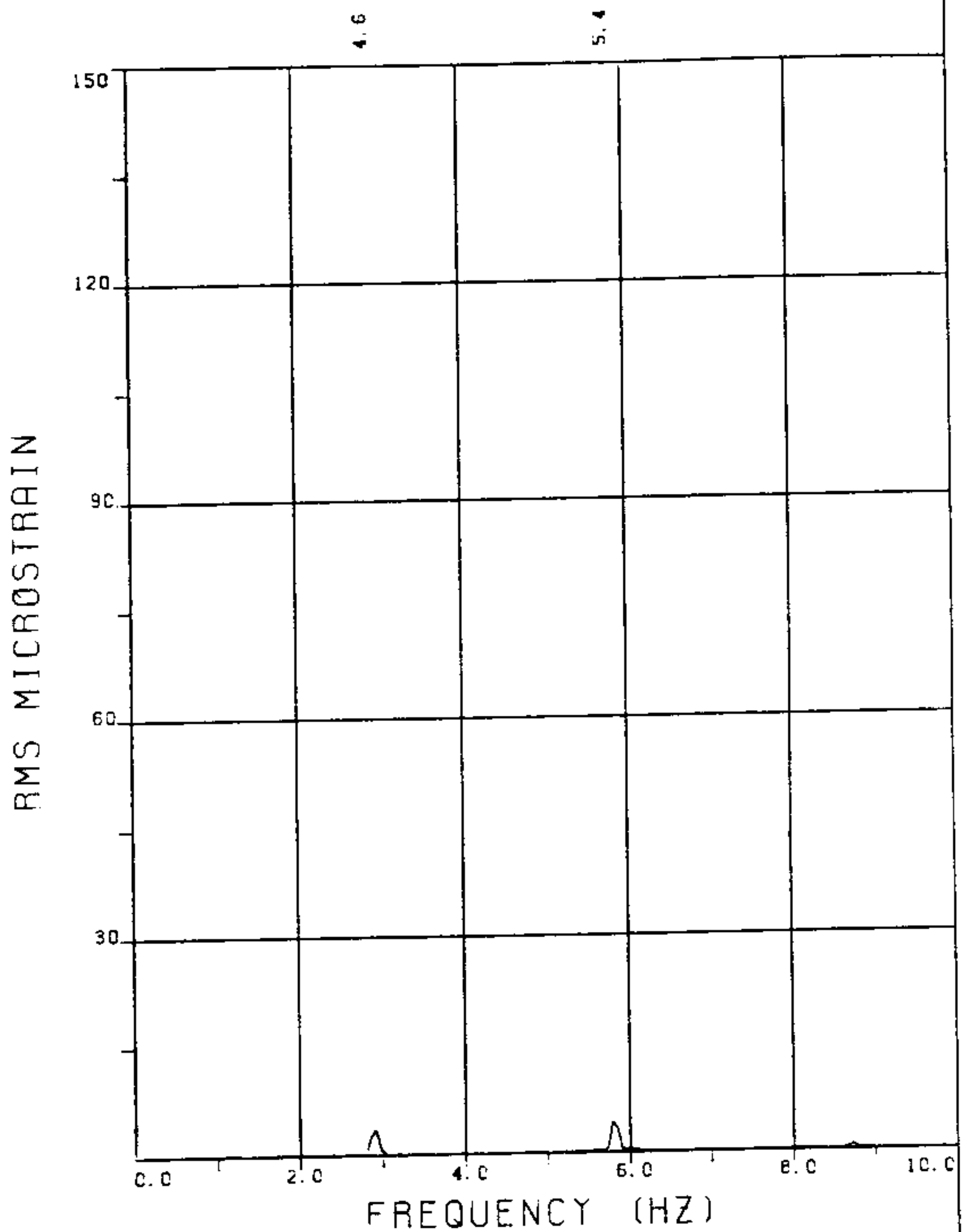

EXPERIMENT NUMBER 22

BRIDGE B3 ELEVATION=8L/11 BE=0.059

THETA=0 VC=0 FE=2.920 A/DE=1.00

MEASURED RESPONSE IN MICROSTRAIN

TOTAL DYNAMIC RMS=7.3

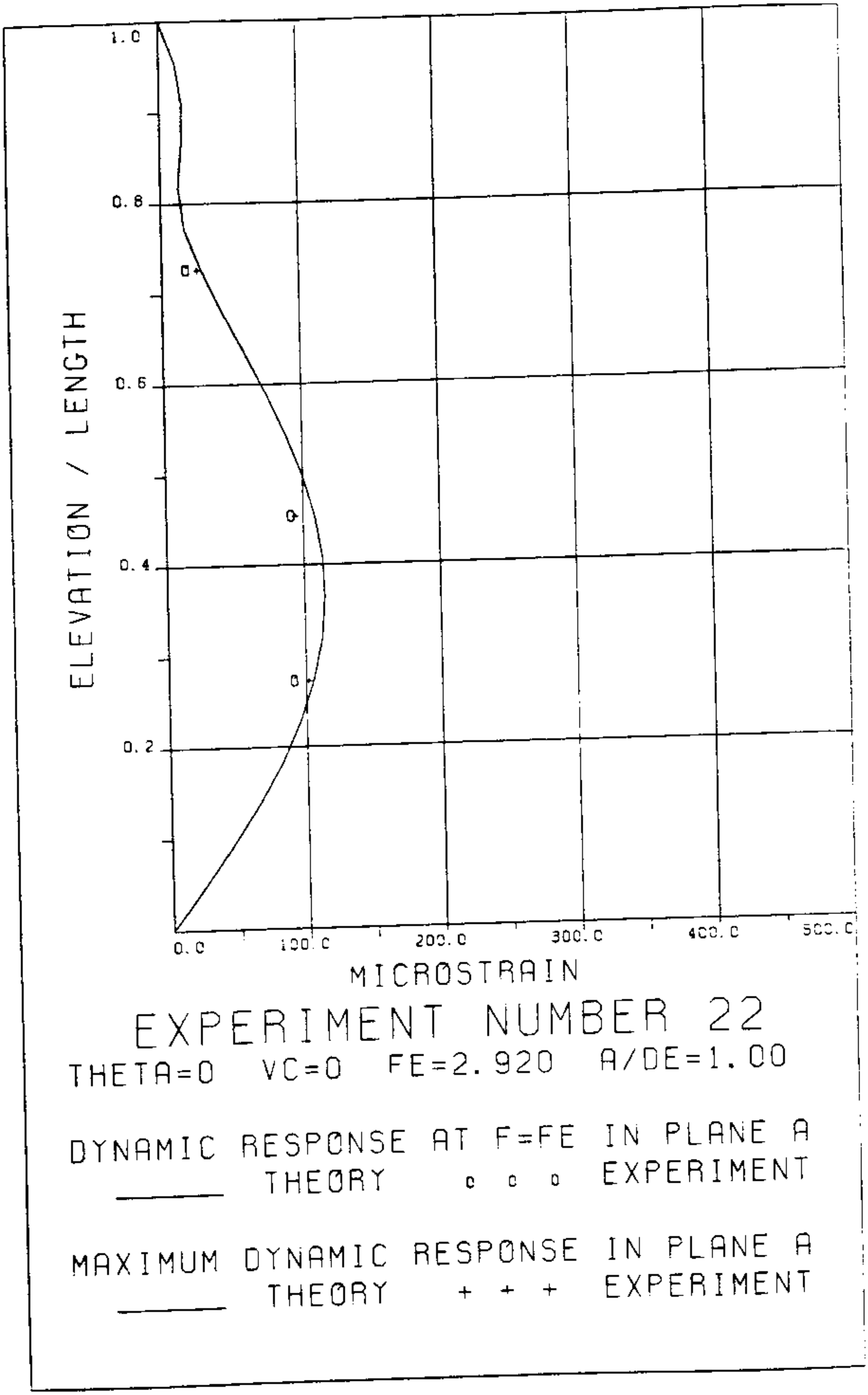
1.0
0.8
0.6
0.4
0.2
ELEVATION / LENGTH
0.0
100.0
200.0
300.0
400.0
500.0
MICROSTRAIN
EXPERIMENT NUMBER 22
THETA=0 VC=0 FE=2.920 A/DE=1.00
DYNAMIC RESPONSE AT F=FE IN PLANE A
THEORY o o o EXPERIMENT
MAXIMUM DYNAMIC RESPONSE IN PLANE A
THEORY + + + EXPERIMENT

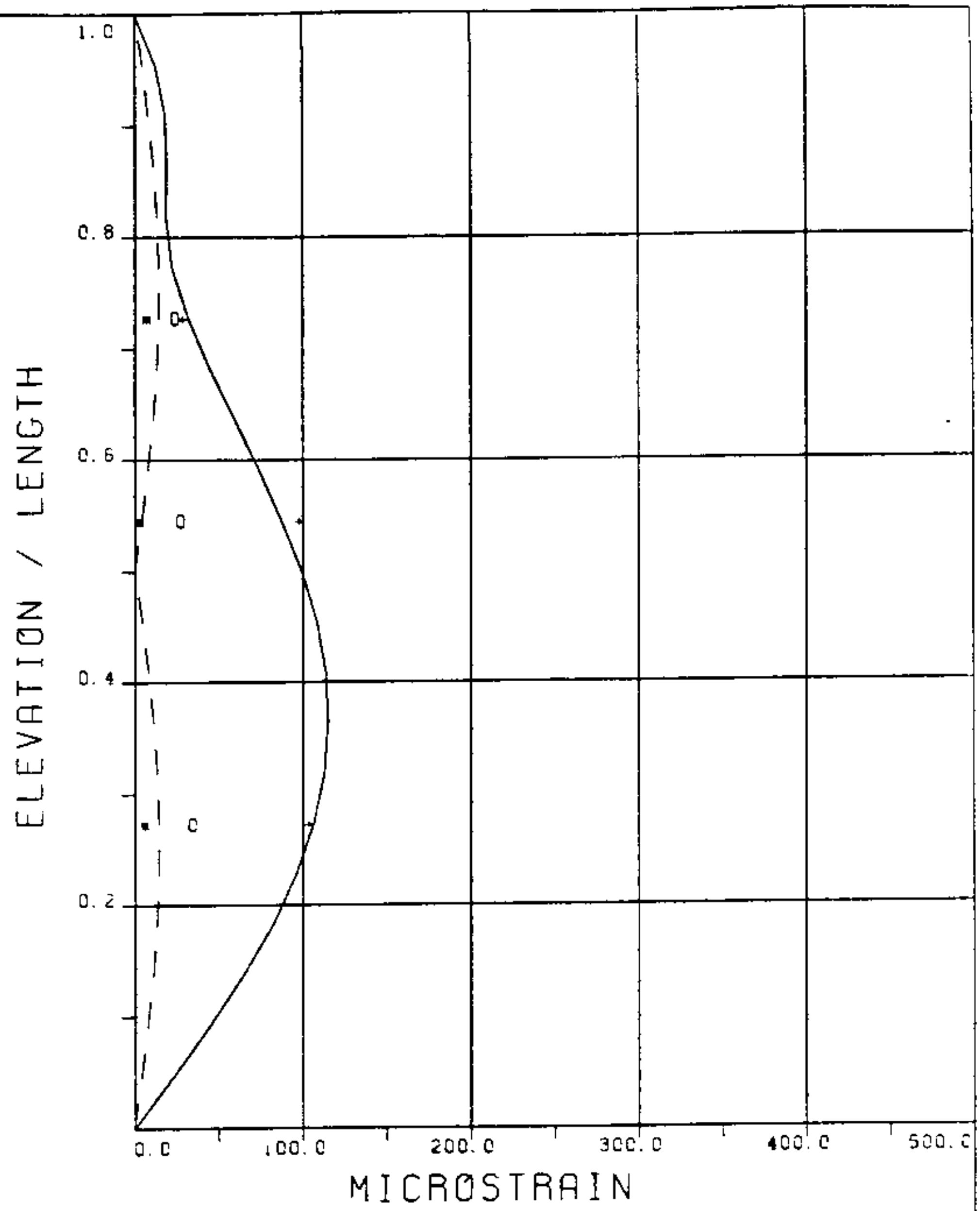

EXPERIMENT NUMBER 22

THETA=0 VC=0 FE=2.920 A/DE=1.00

DYNAMIC RESPONSE IN PLANE B AT F=2FE

----- THEORY * * * EXPERIMENT

MAXIMUM RESPONSE IN PLANE B

o o o EXPERIMENT

MAXIMUM RESPONSE

_____ THEORY + + + EXPERIMENT

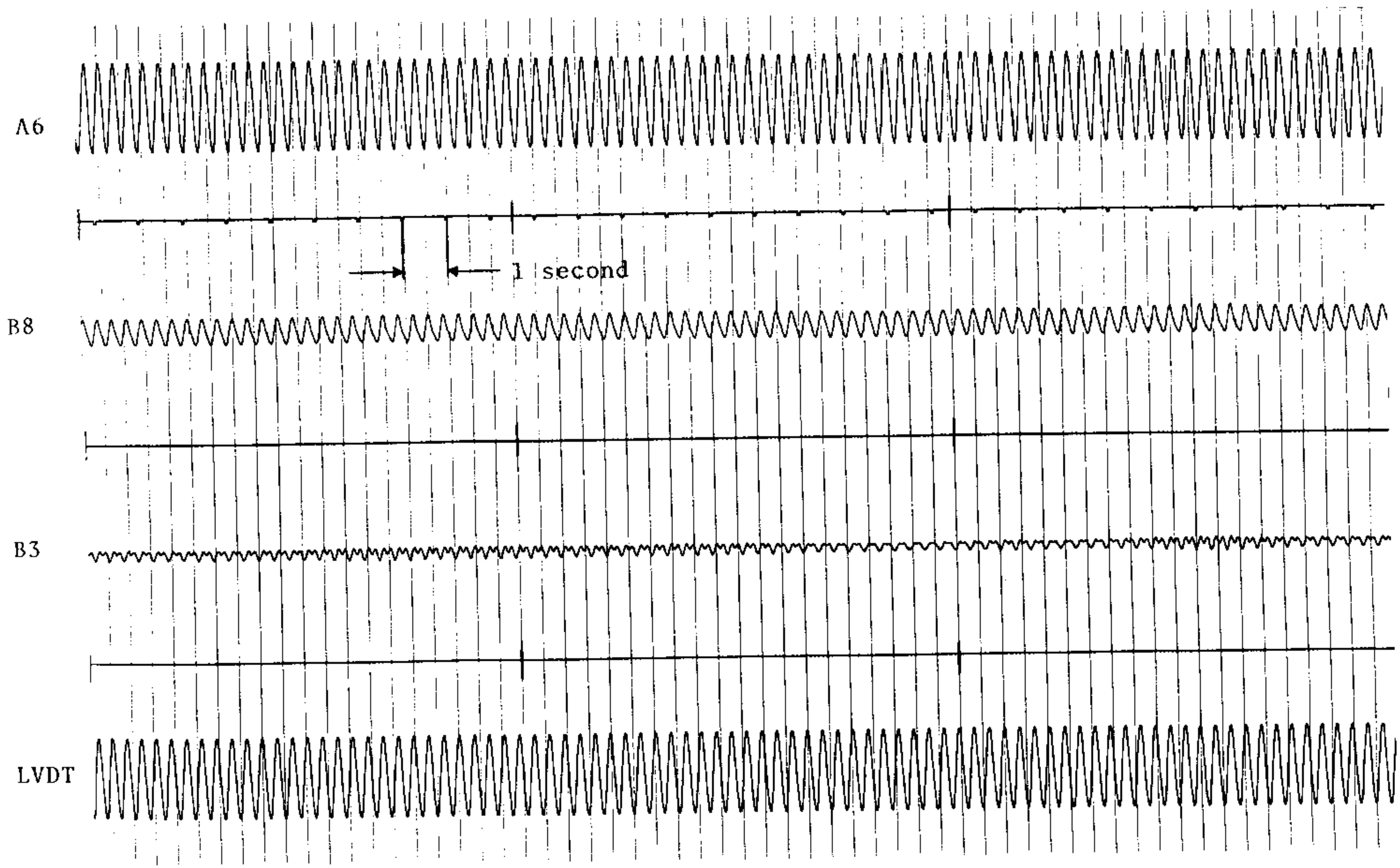

FIGURE 22T: LVDT: 0.087 D_c/DIVISION; STRAINS: 7.64 MICROSTRAIN/DIVISION

EXPERIMENT 25

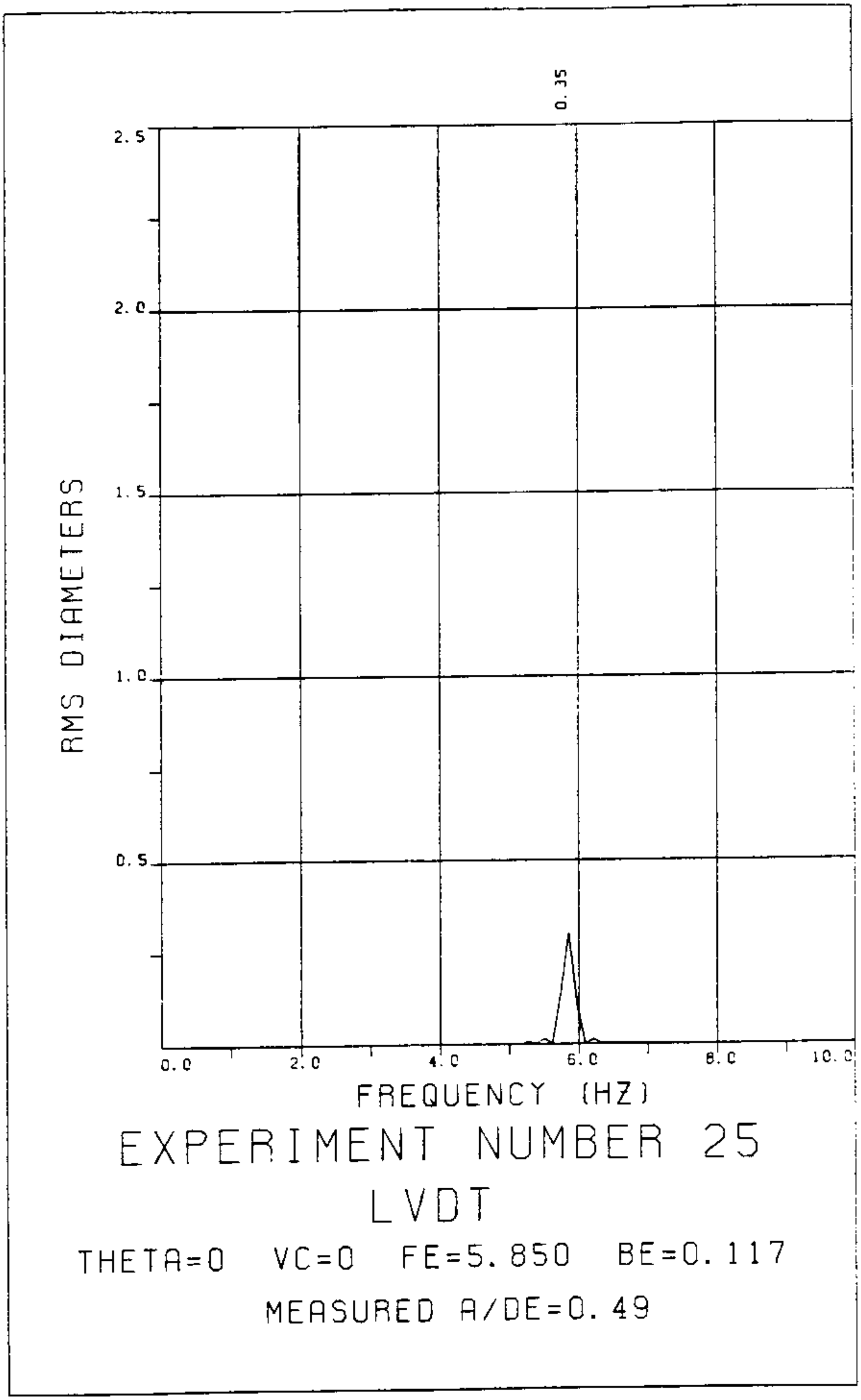
0.35
2.5
2.0
1.5
1.0
0.5
RMS DIAMETERS
0.0
2.0
4.0
6.0
8.0
10.0
FREQUENCY (HZ)
EXPERIMENT NUMBER 25
LVDT
THETA=0 VC=0 FE=5.850 BE=0.117
MEASURED A/DE=0.49

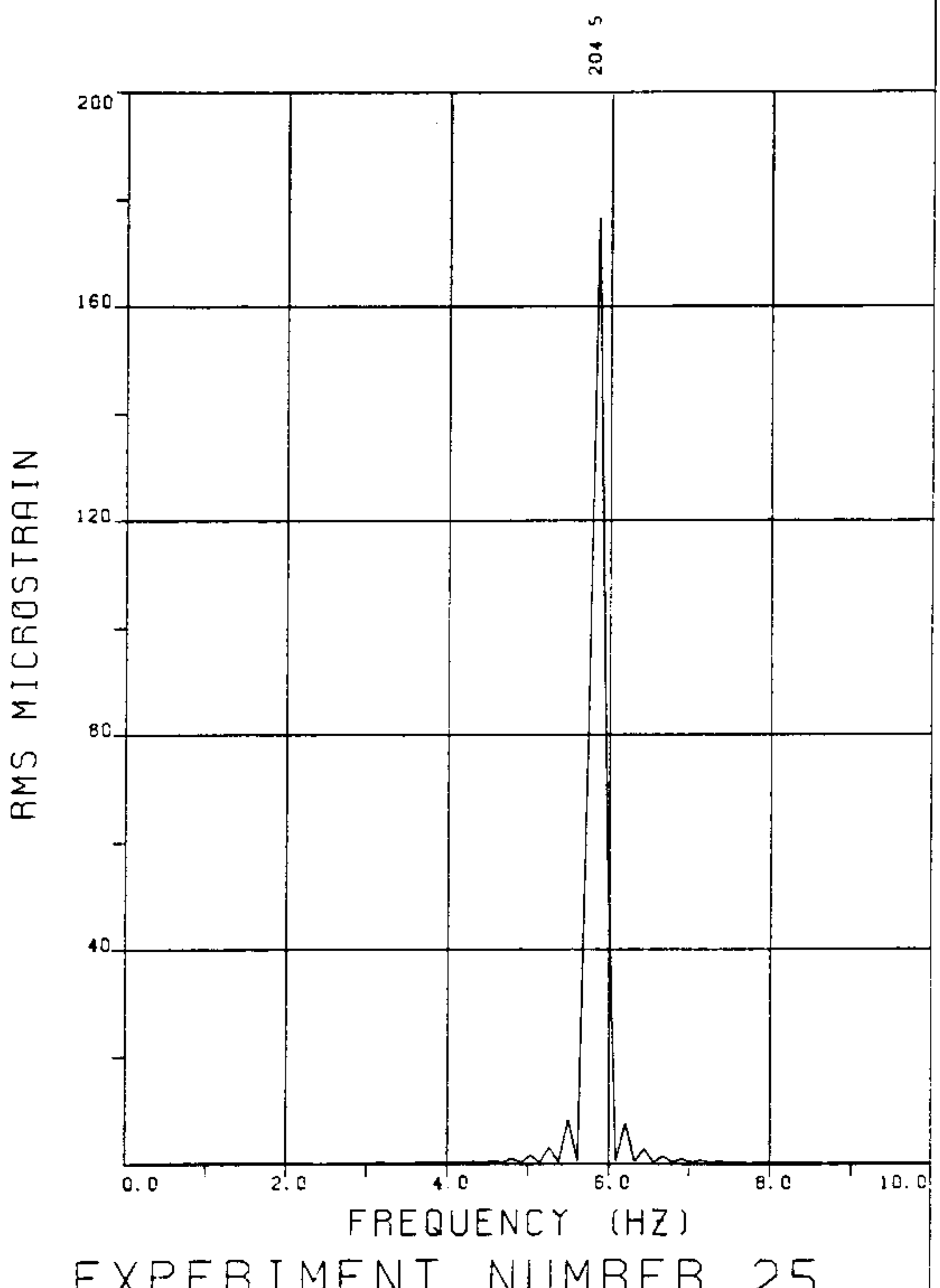

EXPERIMENT NUMBER 25

BRIDGE A8 ELEVATION=3L/11 BE=0.117

THETA=0 VC=0 FE=5.850 A/DE=0.49

MEASURED RESPONSE IN MICROSTRAIN

TOTAL DYNAMIC RMS=204.6

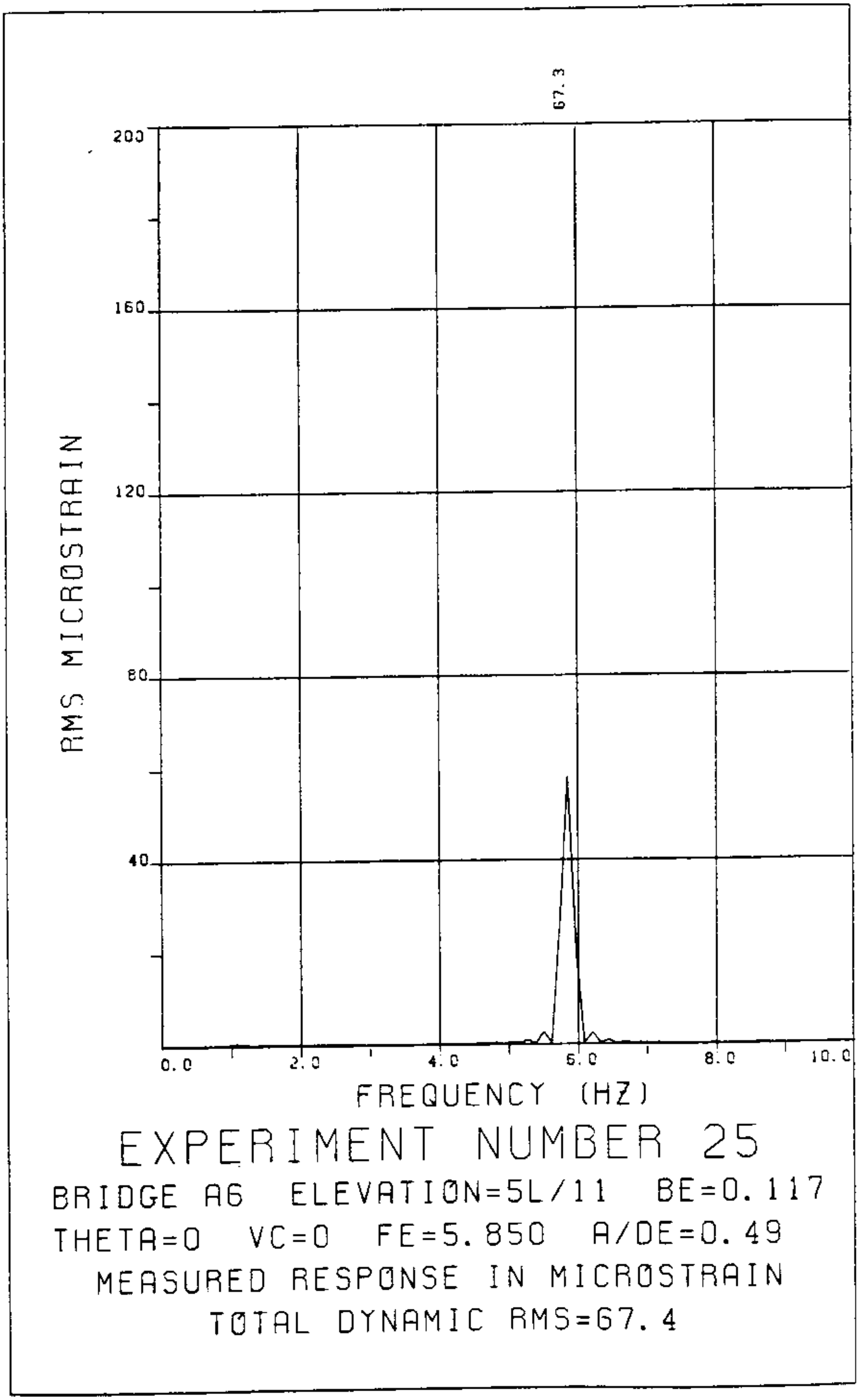
67.3
200
160
120
80
40
RMS MICROSTRAIN
0.0
2.0
4.0
6.0
8.0
10.0
FREQUENCY (HZ)
EXPERIMENT NUMBER 25
BRIDGE A6 ELEVATION=5L/11 BE=0.117
THETA=0 VC=0 FE=5.850 A/DE=0.49
MEASURED RESPONSE IN MICROSTRAIN
TOTAL DYNAMIC RMS=67.4

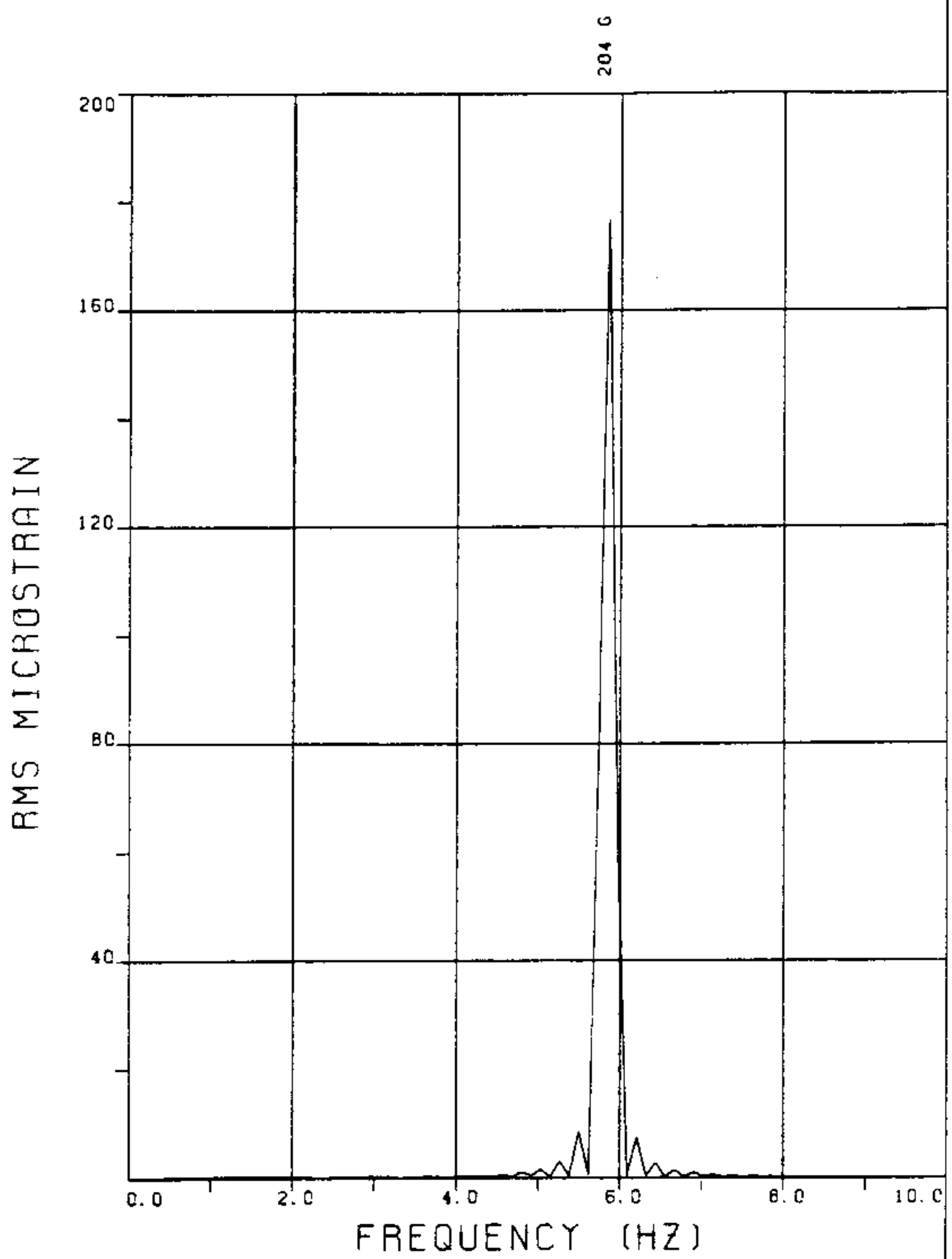

EXPERIMENT NUMBER 25

BRIDGE A3 ELEVATION=8L/11 BE=0.117

THETA=0 VC=0 FE=5.850 A/DE=0.49

MEASURED RESPONSE IN MICROSTRAIN

TOTAL DYNAMIC RMS=204.8

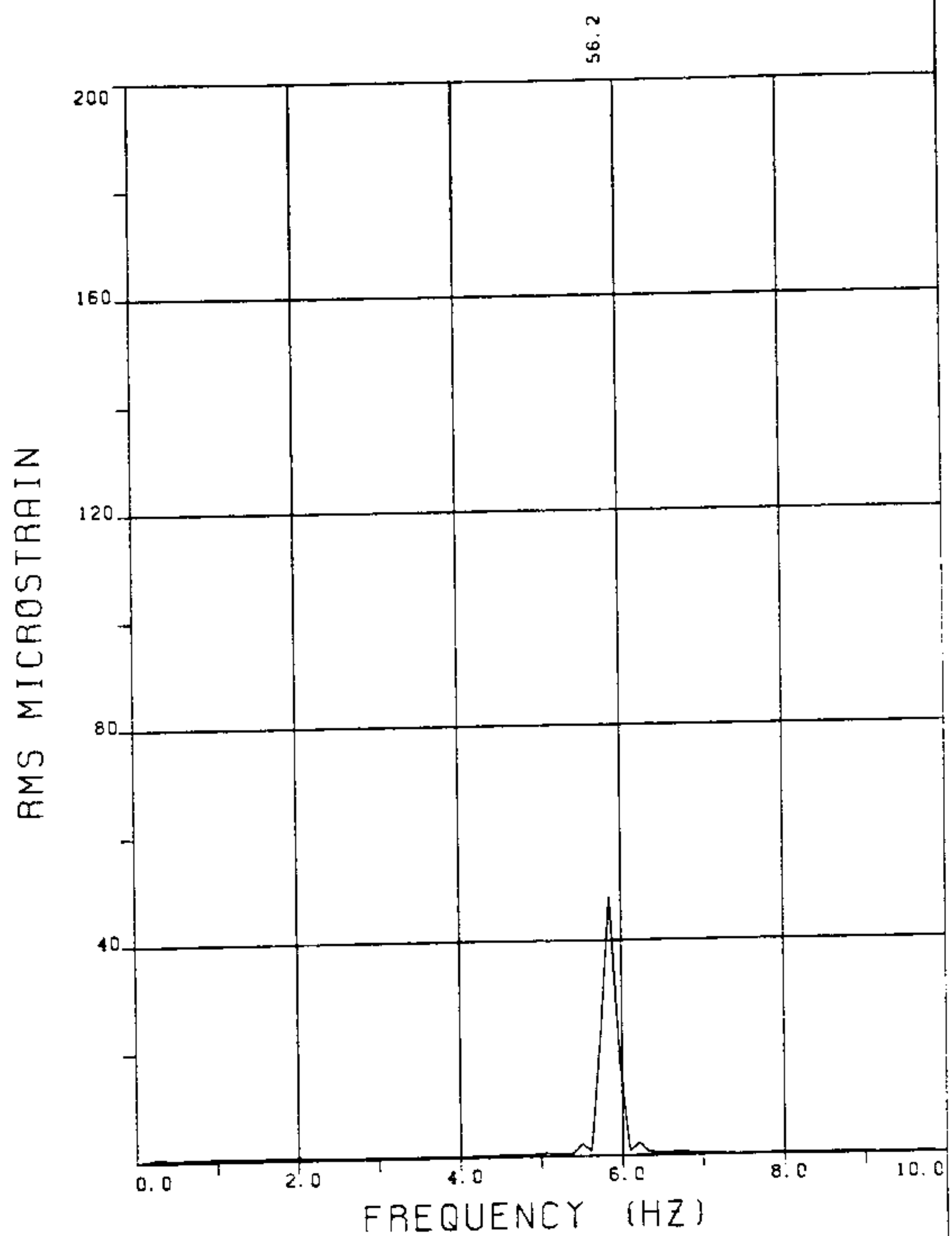

EXPERIMENT NUMBER 25

BRIDGE B8 ELEVATION=3L/11 BE=0.117

THETA=0 VC=0 FE=5.850 A/DE=0.49

MEASURED RESPONSE IN MICROSTRAIN

TOTAL DYNAMIC RMS=56.3

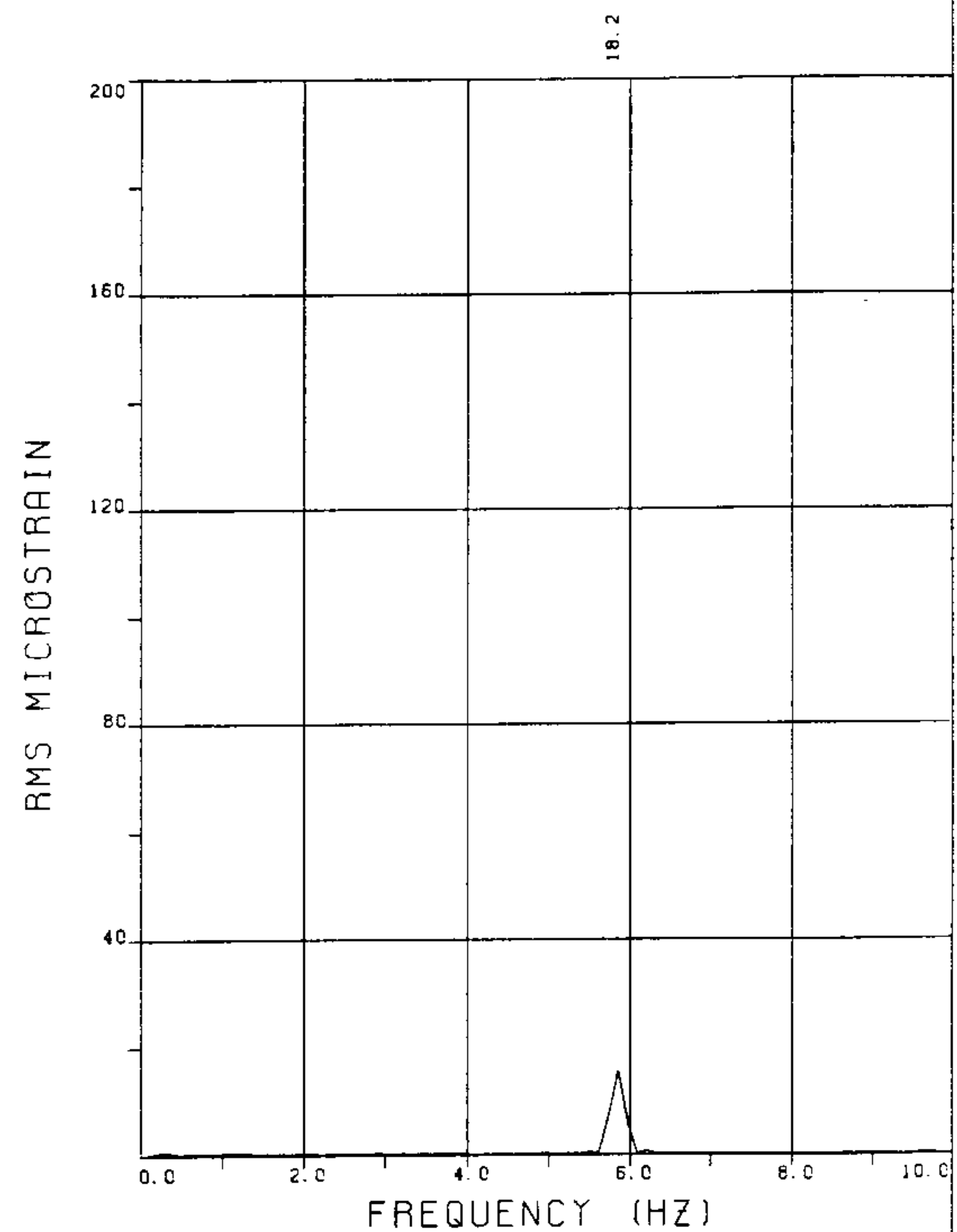

EXPERIMENT NUMBER 25

BRIDGE B5 ELEVATION=GL/11 BE=0.117

THETA=0 VC=0 FE=5.850 A/DE=0.49

MEASURED RESPONSE IN MICROSTRAIN

TOTAL DYNAMIC RMS=18.5

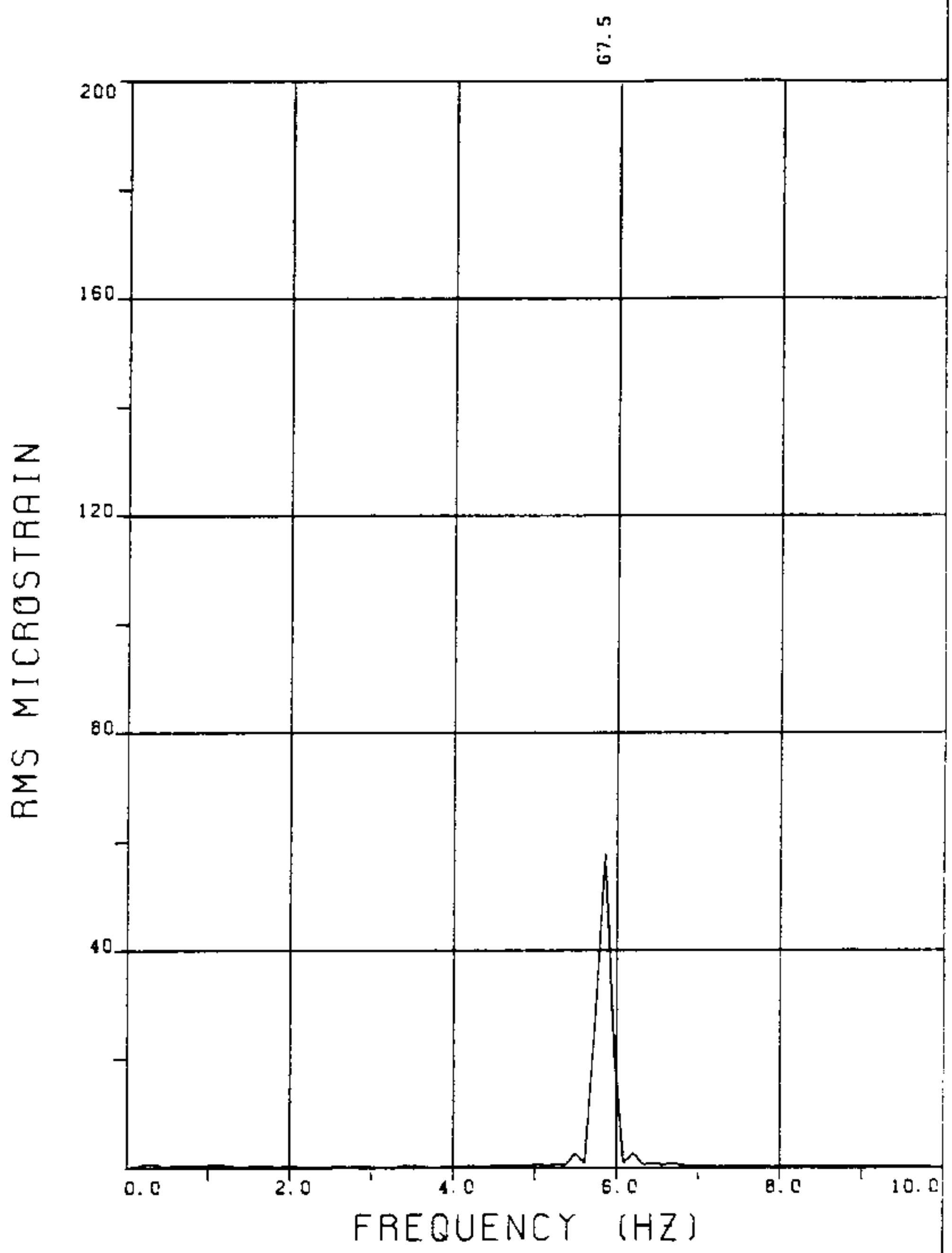

EXPERIMENT NUMBER 25

BRIDGE B3 ELEVATION=8L/11 BE=0.117

THETA=0 VC=0 FE=5.850 A/DE=0.49

MEASURED RESPONSE IN MICROSTRAIN

TOTAL DYNAMIC RMS=67.7

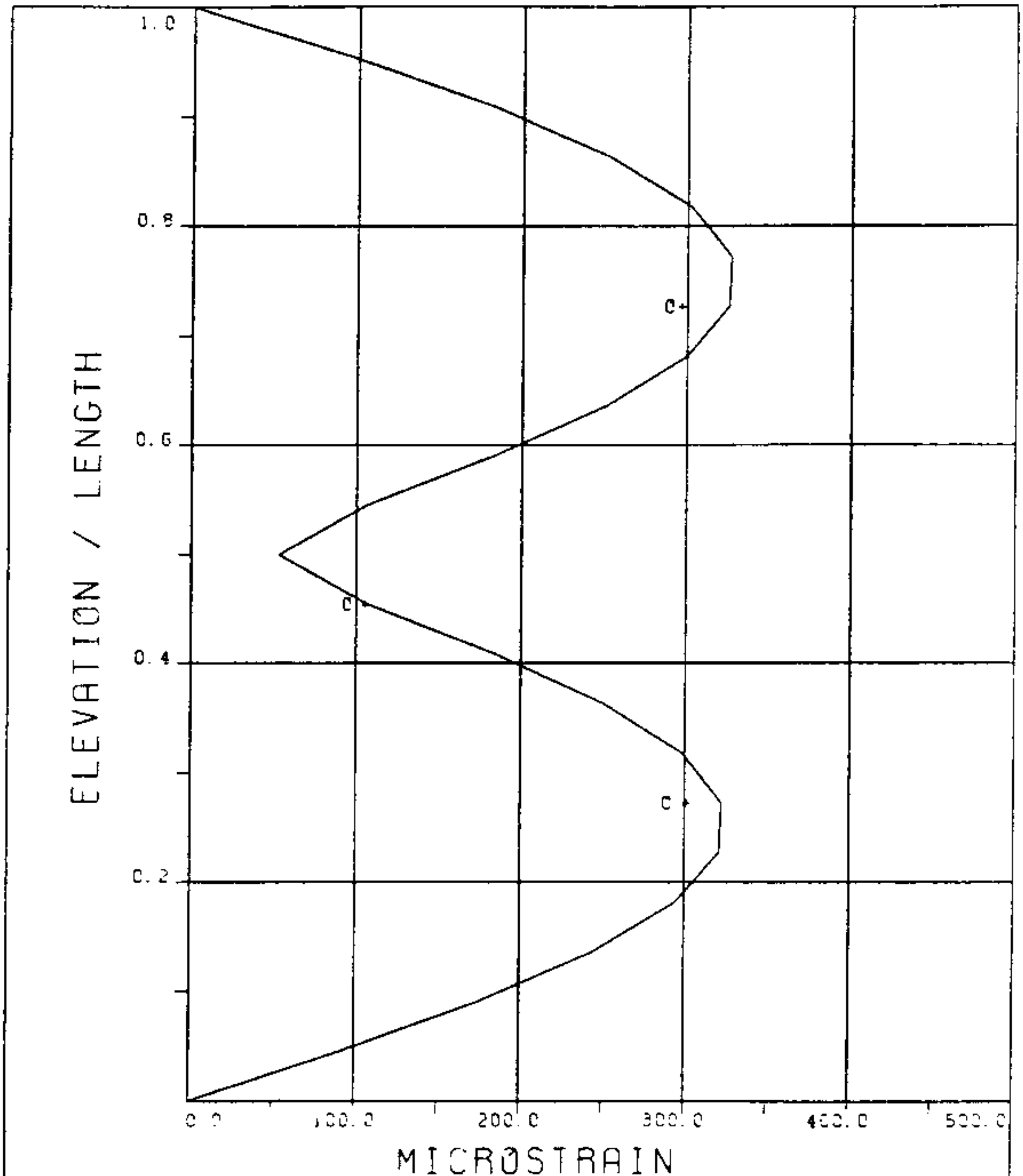

EXPERIMENT NUMBER 25

THETA=0 VC=0 FE=5.850 A/DE=0.49

DYNAMIC RESPONSE AT F=FE IN PLANE A
______ THEORY o o o EXPERIMENT

MAXIMUM DYNAMIC RESPONSE IN PLANE A
______ THEORY + + + EXPERIMENT

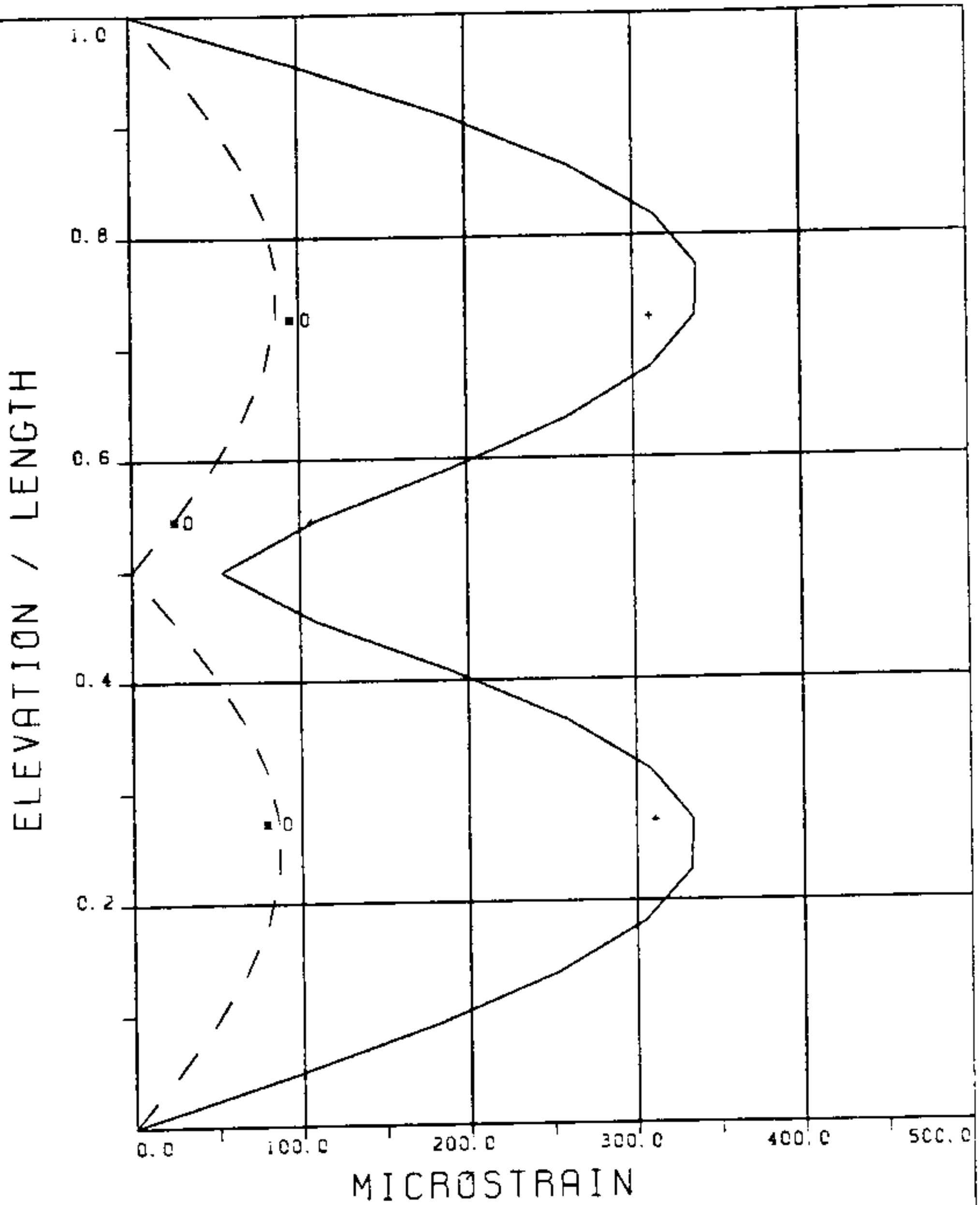

EXPERIMENT NUMBER 25

THETA=0 VC=0 FE=5.850 A/DE=0.49

DYNAMIC RESPONSE IN PLANE B AT F=FE

----- THEORY * * * EXPERIMENT

MAXIMUM RESPONSE IN PLANE B

o o o EXPERIMENT

MAXIMUM RESPONSE

——— THEORY + + + EXPERIMENT

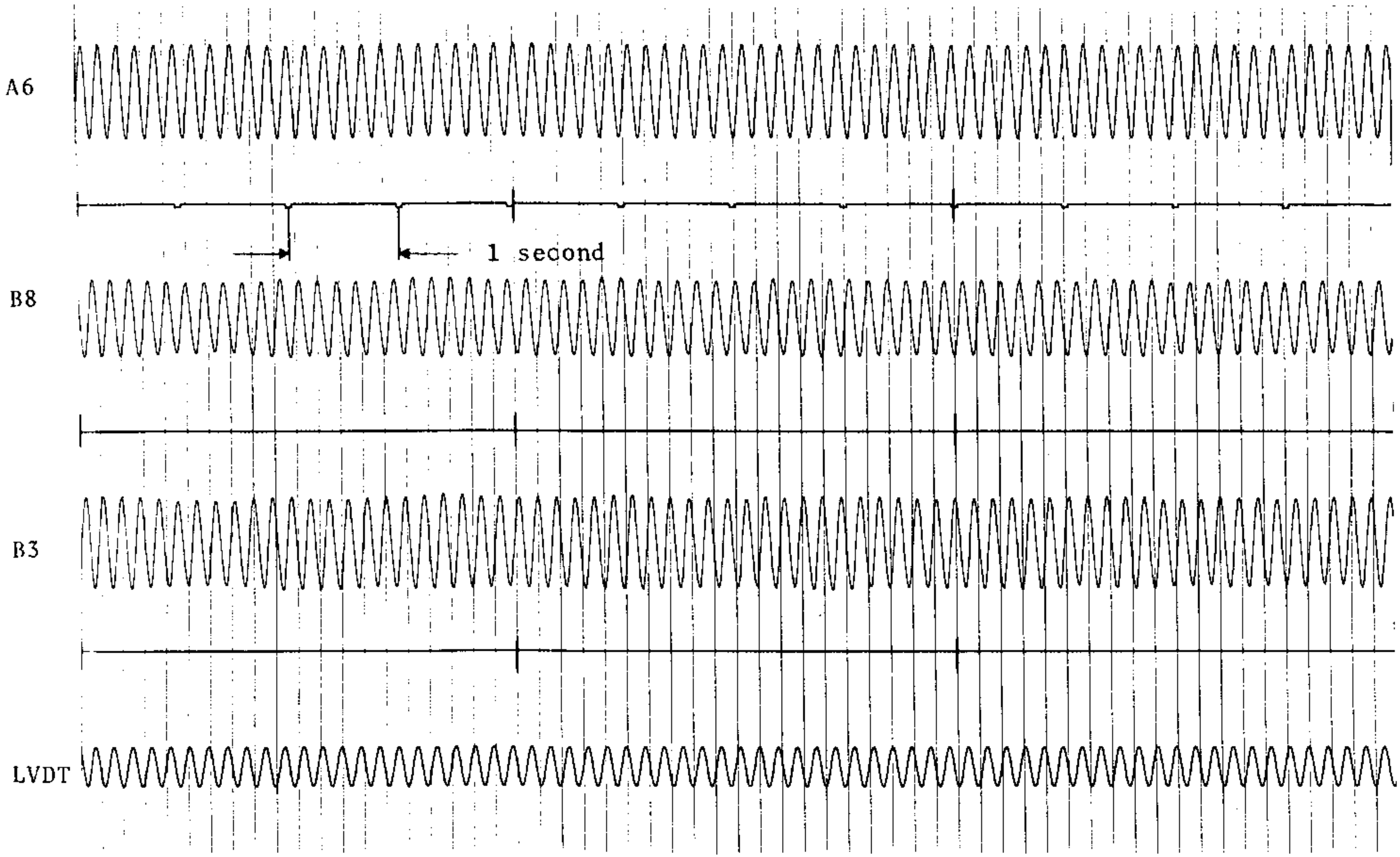

FIGURE 25T: LVDT: 0.087 D_e/DIVISION; STRAINS: 7.64 MICROSTRAIN/DIVISION

EXPERIMENT 118

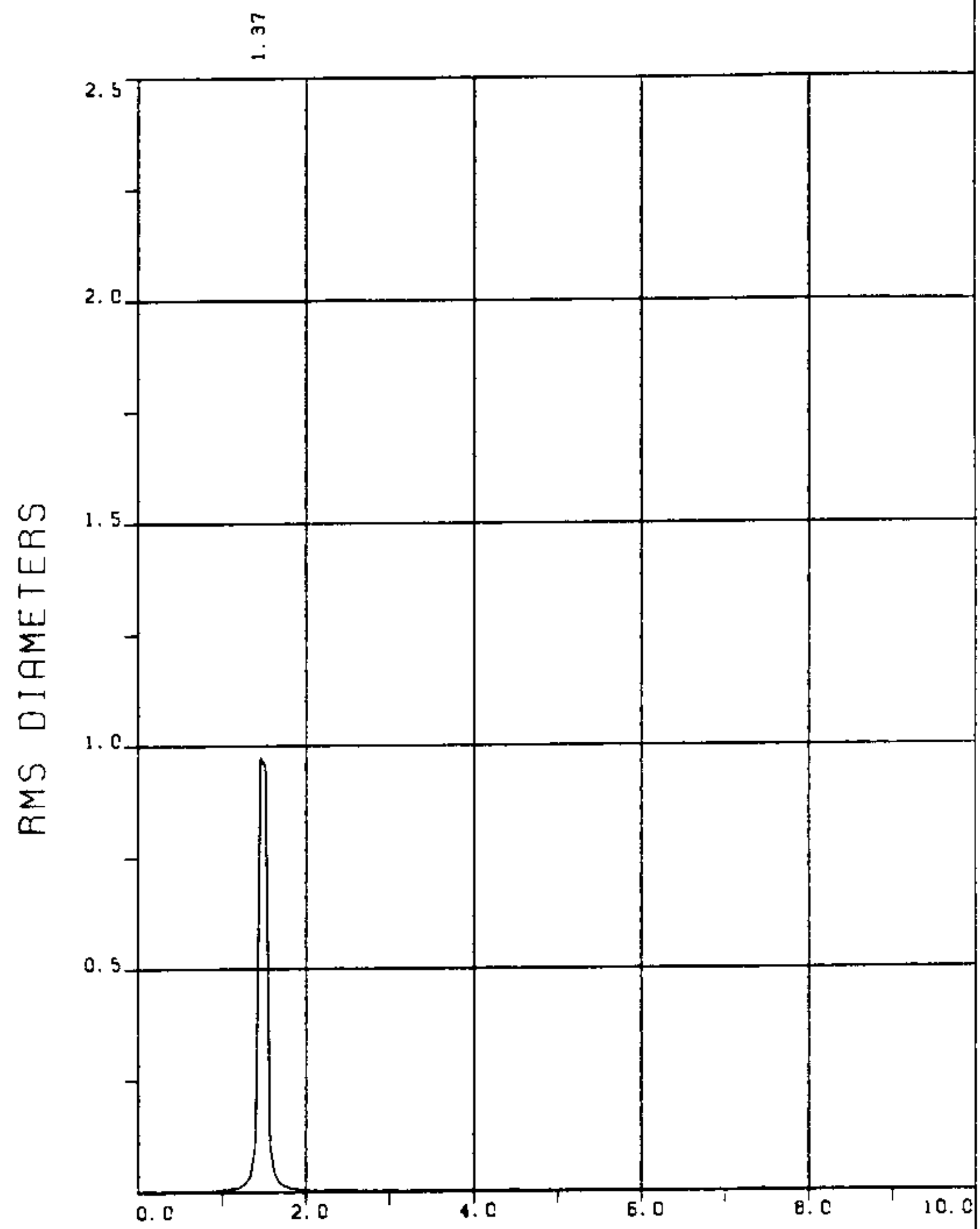

EXPERIMENT NUMBER 118

LVDT

THETA=90 VC=0 FE=1.500 BE=0.059

MEASURED A/DE=1.94

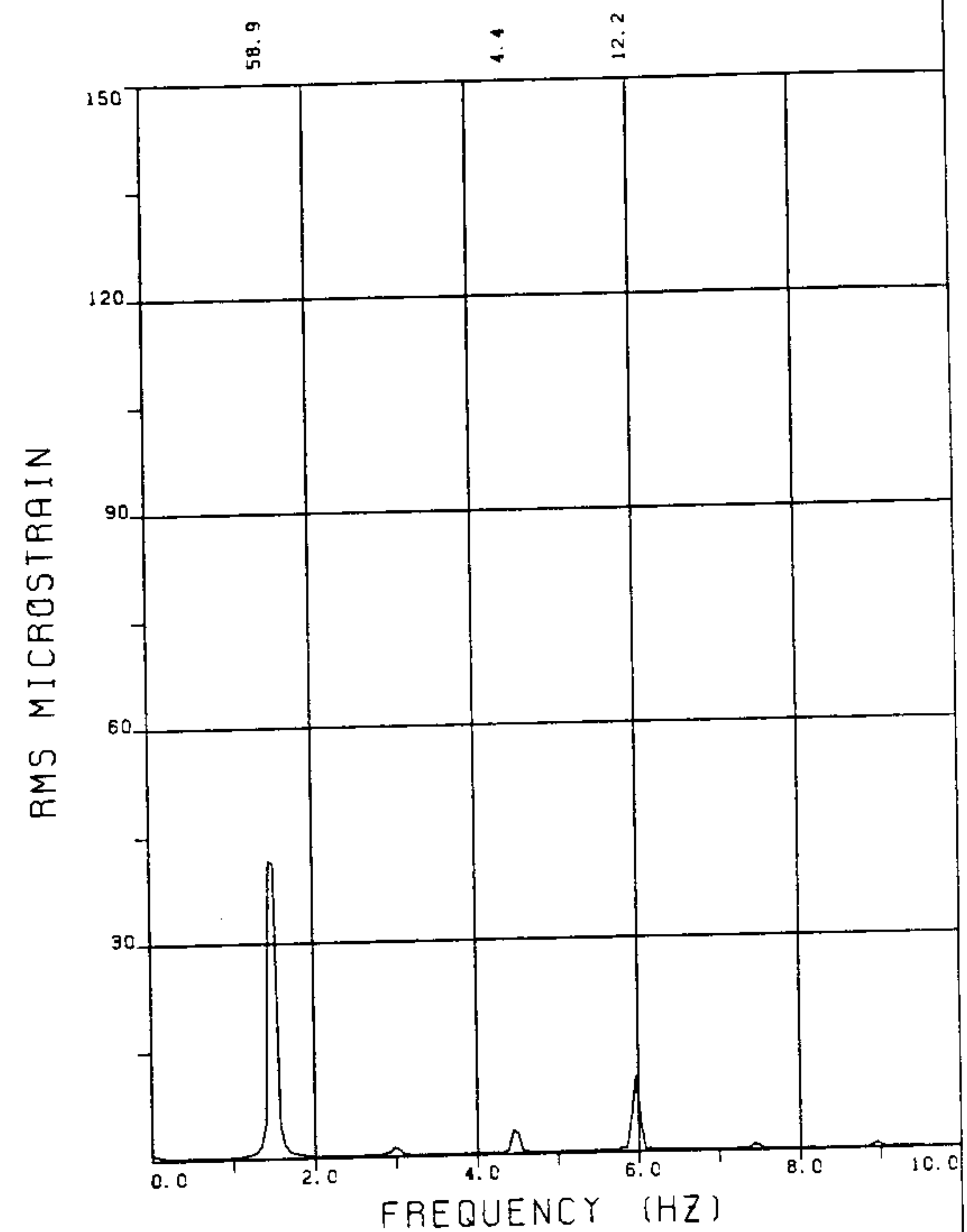

EXPERIMENT NUMBER 118

BRIDGE B9 ELEVATION=2L/11 BE=0.059

THETA=90 VC=0 FE=1.500 A/DE=1.94

MEASURED RESPONSE IN MICROSTRAIN

TOTAL DYNAMIC RMS=60.3

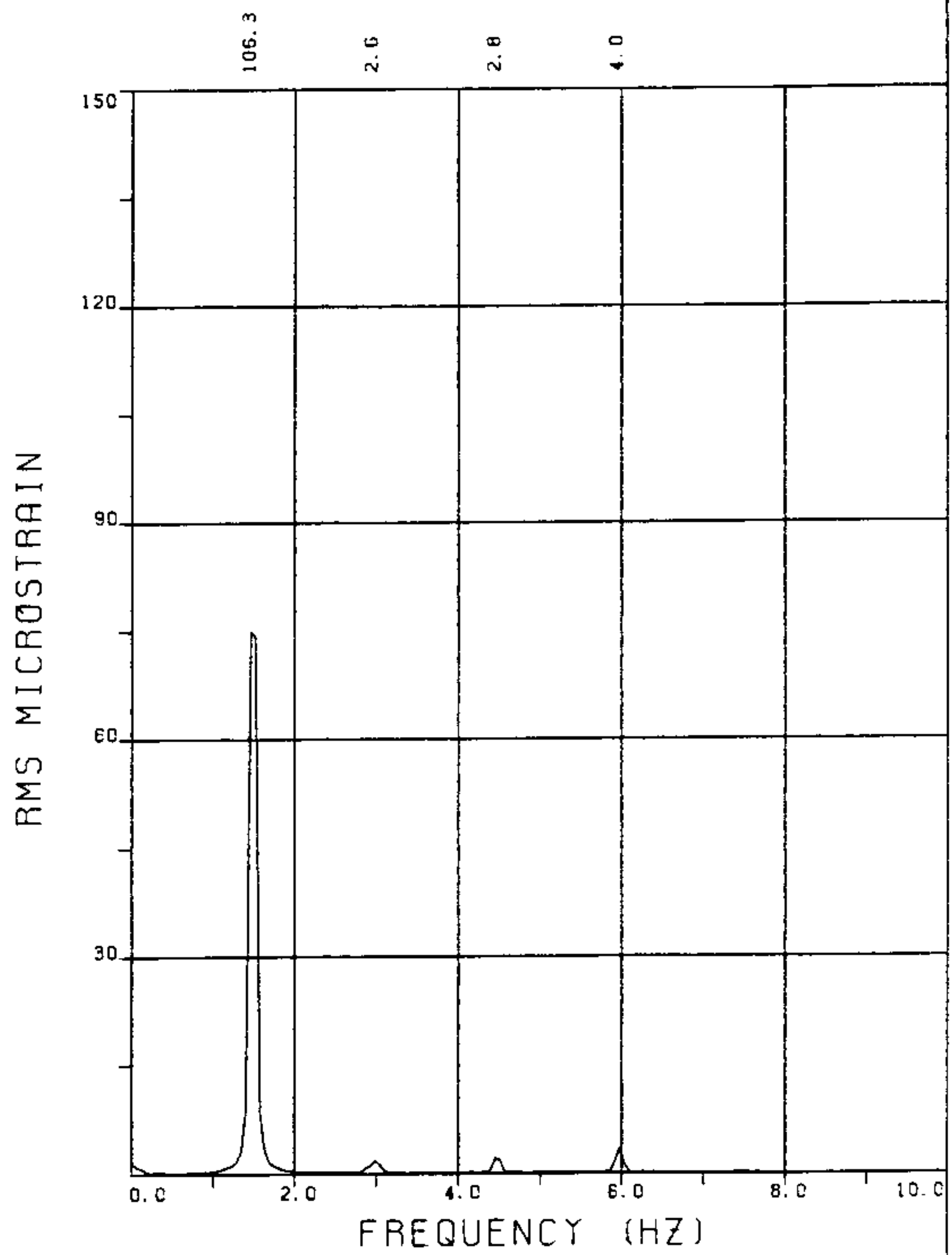

EXPERIMENT NUMBER 118

BRIDGE B6 ELEVATION=5L/11 BE=0.059

THETA=90 VC=0 FE=1.500 A/DE=1.94

MEASURED RESPONSE IN MICROSTRAIN

TOTAL DYNAMIC RMS=106.5

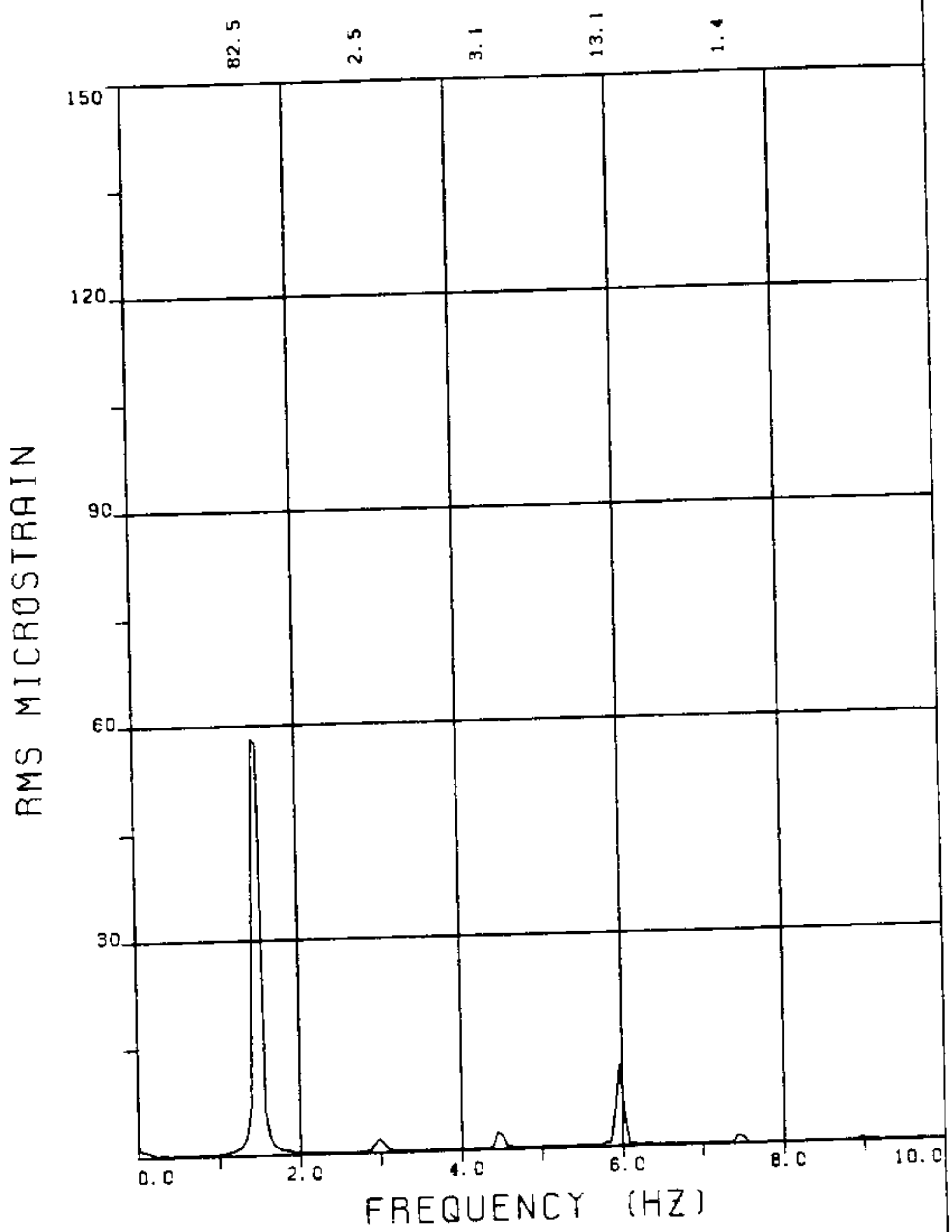

EXPERIMENT NUMBER 118

BRIDGE B3 ELEVATION=8L/11 BE=0.059

THETA=90 VC=0 FE=1.500 A/DE=1.94

MEASURED RESPONSE IN MICROSTRAIN

TOTAL DYNAMIC RMS=83.7

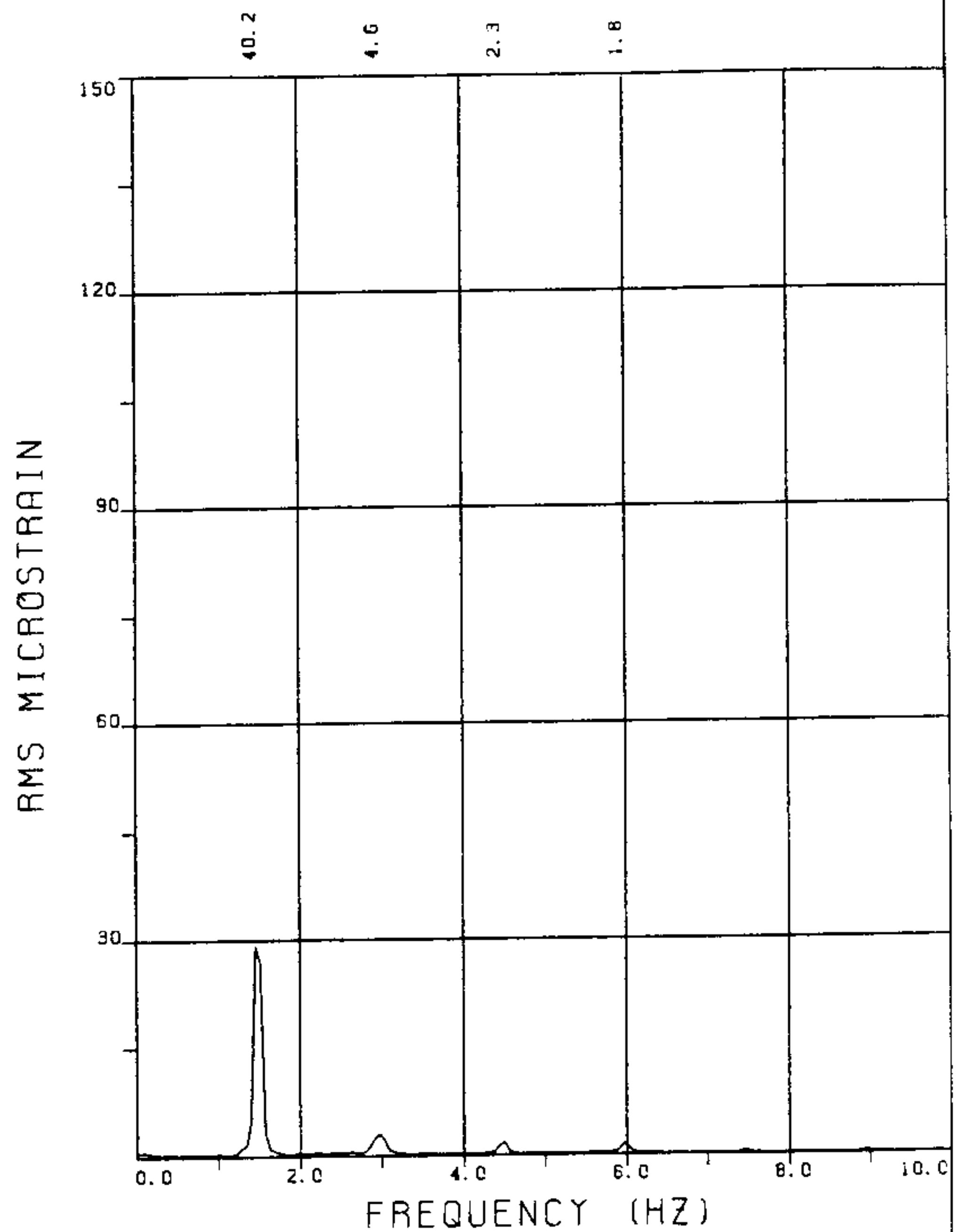

EXPERIMENT NUMBER 118

BRIDGE A9 ELEVATION=2L/11 BE=0.059

THETA=90 VC=0 FE=1.500 A/DE=1.94

MEASURED RESPONSE IN MICROSTRAIN

TOTAL DYNAMIC RMS=39.7

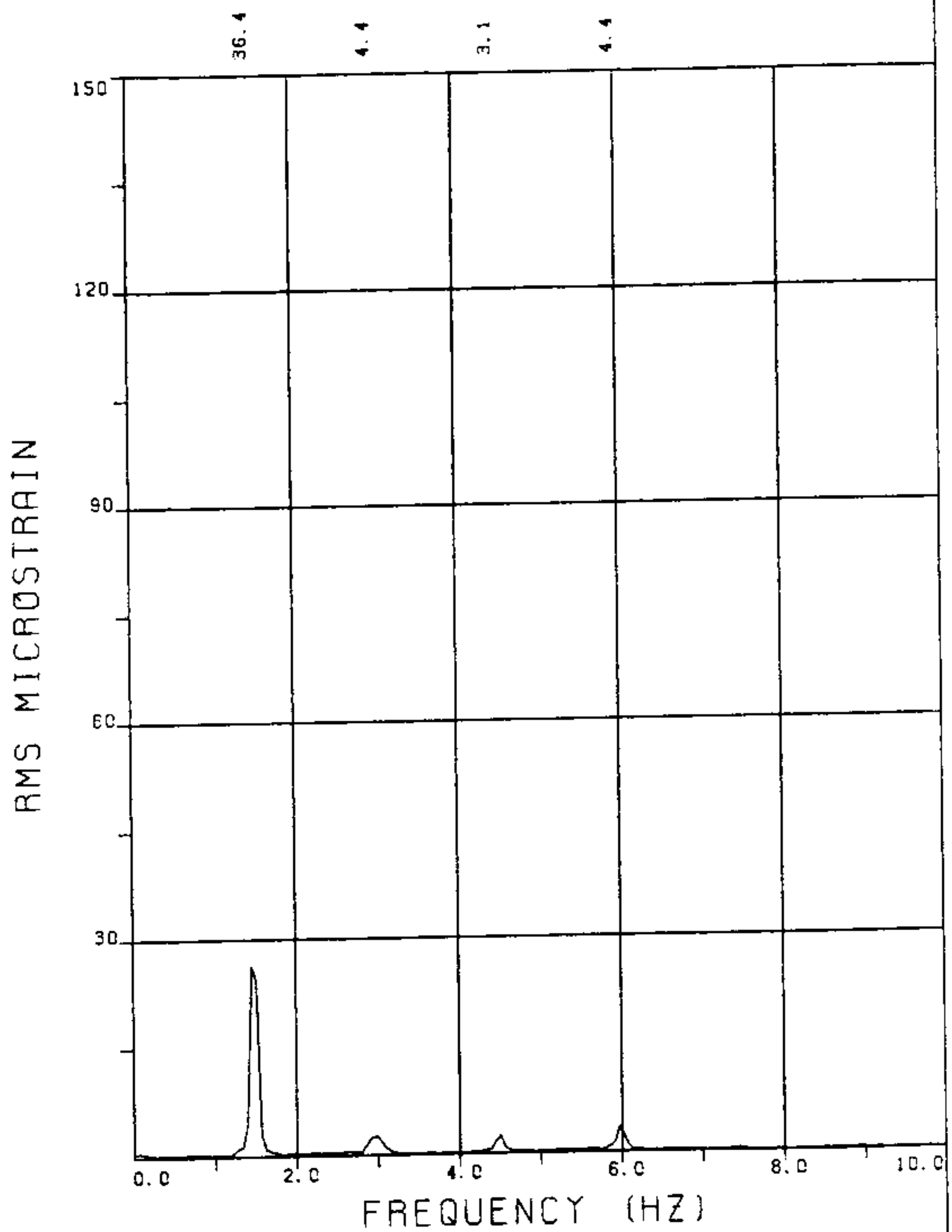

EXPERIMENT NUMBER 118

BRIDGE A7 ELEVATION=4L/11 BE=0.059

THETA=90 VC=0 FE=1.500 A/DE=1.94

MEASURED RESPONSE IN MICROSTRAIN

TOTAL DYNAMIC RMS=36.3

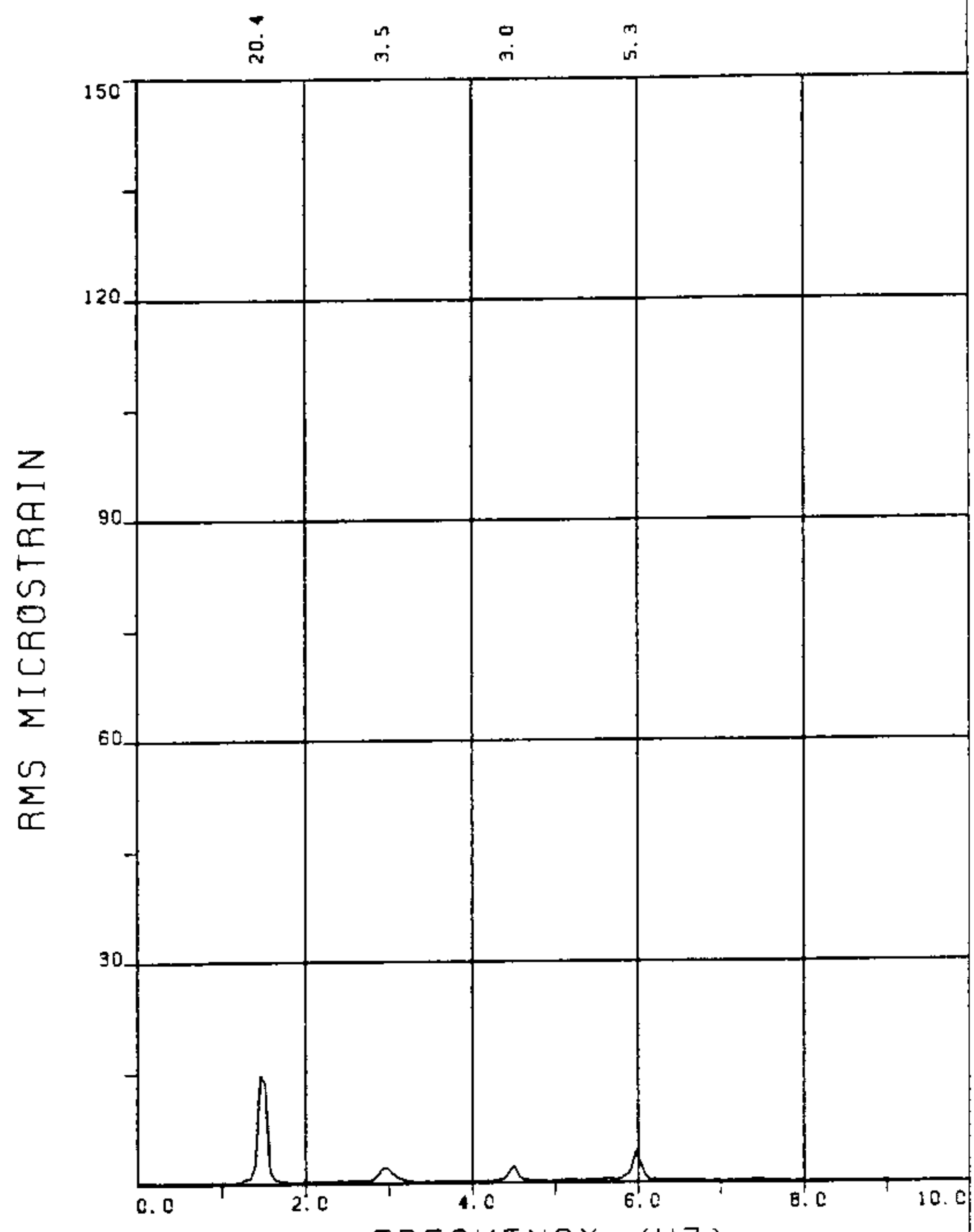

EXPERIMENT NUMBER 118

BRIDGE A6 ELEVATION=5L/11 BE=0.059

THETA=90 VC=0 FE=1.500 A/DE=1.94

MEASURED RESPONSE IN MICROSTRAIN

TOTAL DYNAMIC RMS=21.2

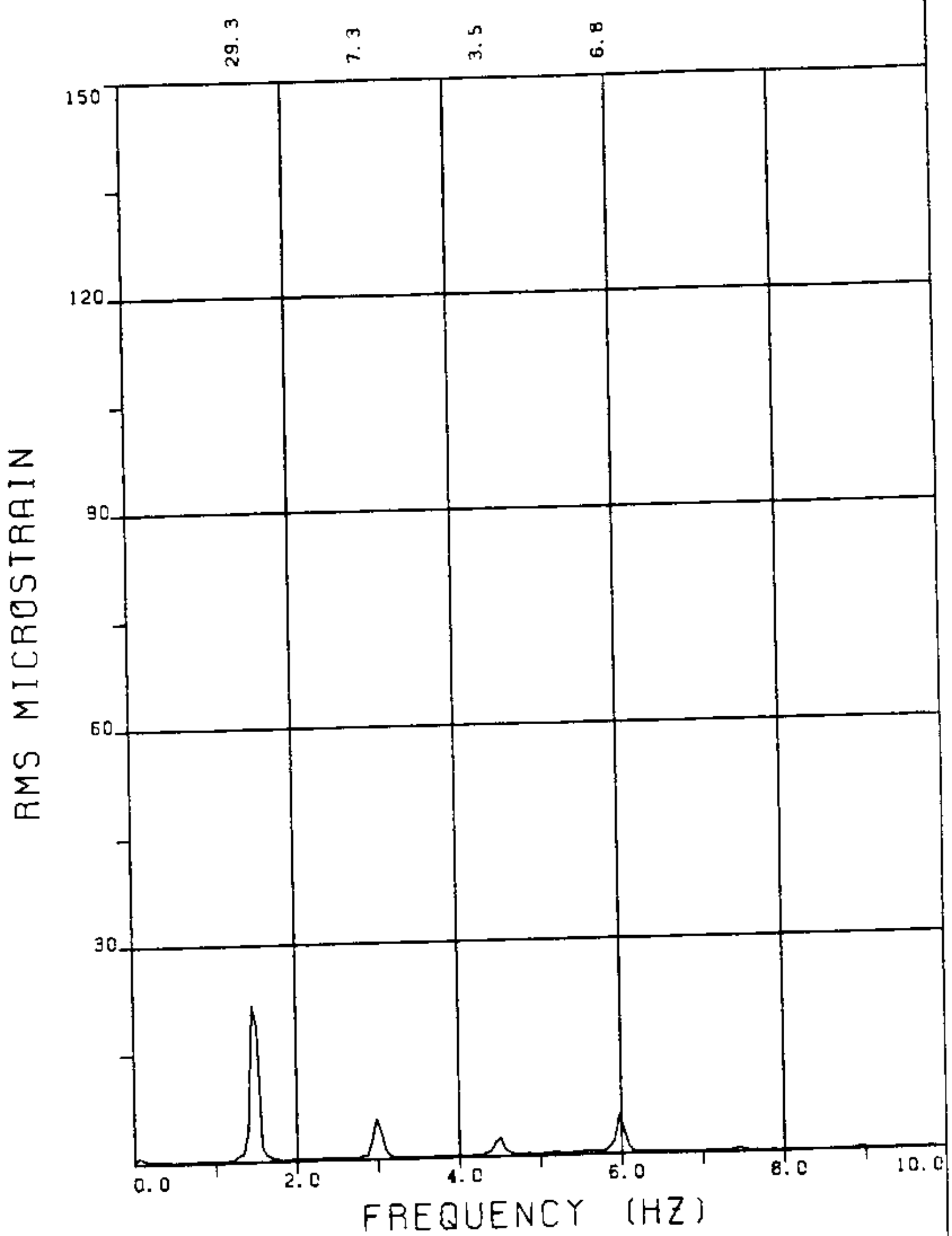

EXPERIMENT NUMBER 118

BRIDGE A3 ELEVATION=8L/11 BE=0.059

THETA=90 VC=0 FE=1.500 A/DE=1.94

MEASURED RESPONSE IN MICROSTRAIN

TOTAL DYNAMIC RMS=30.3

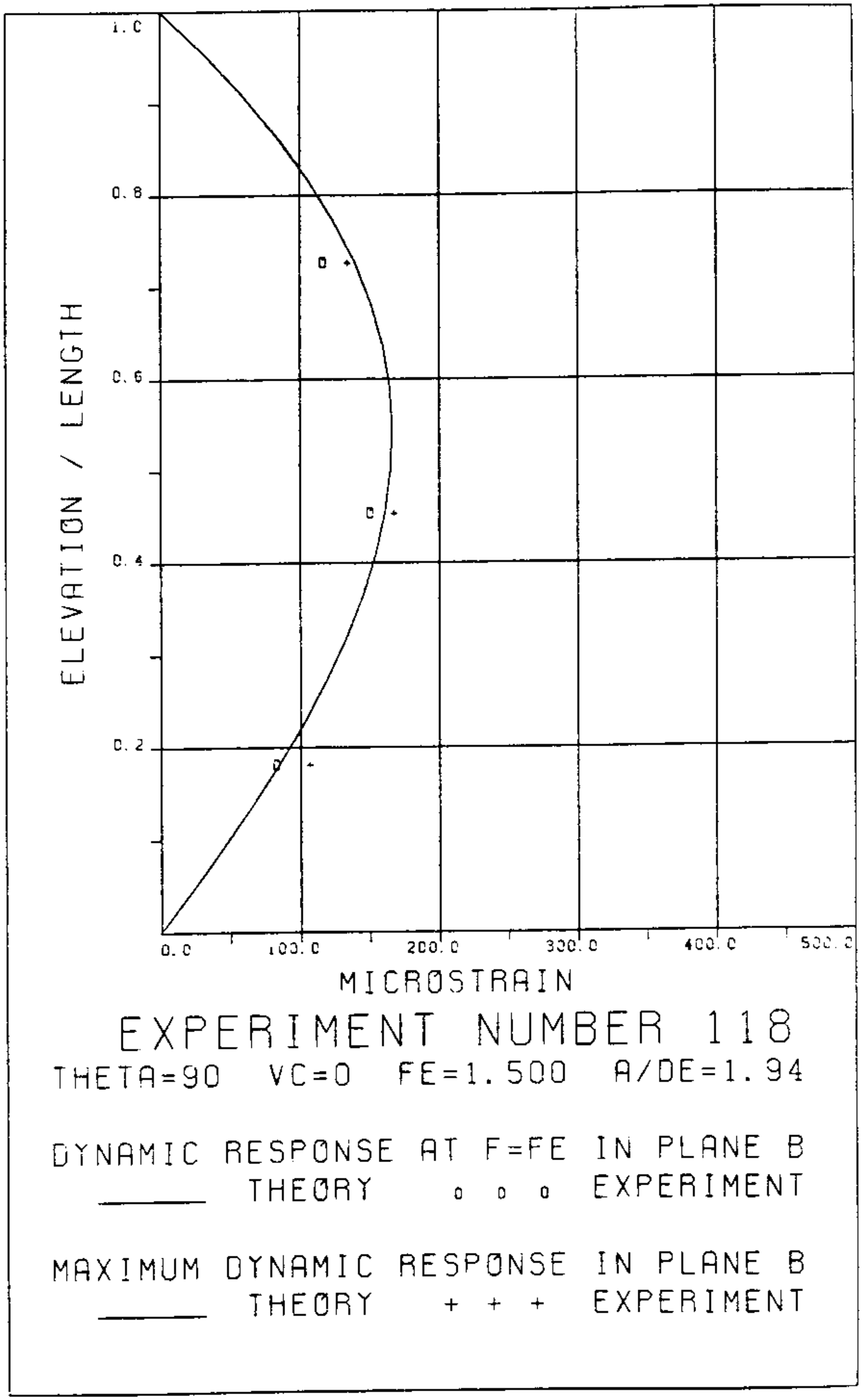
1.0
0.8
0.6
0.4
0.2
0.0
100.0
200.0
300.0
400.0
500.0
ELEVATION / LENGTH
MICROSTRAIN
EXPERIMENT NUMBER 118
THETA=90 VC=0 FE=1.500 A/DE=1.94
DYNAMIC RESPONSE AT F=FE IN PLANE B
THEORY
EXPERIMENT
MAXIMUM DYNAMIC RESPONSE IN PLANE B
THEORY
EXPERIMENT

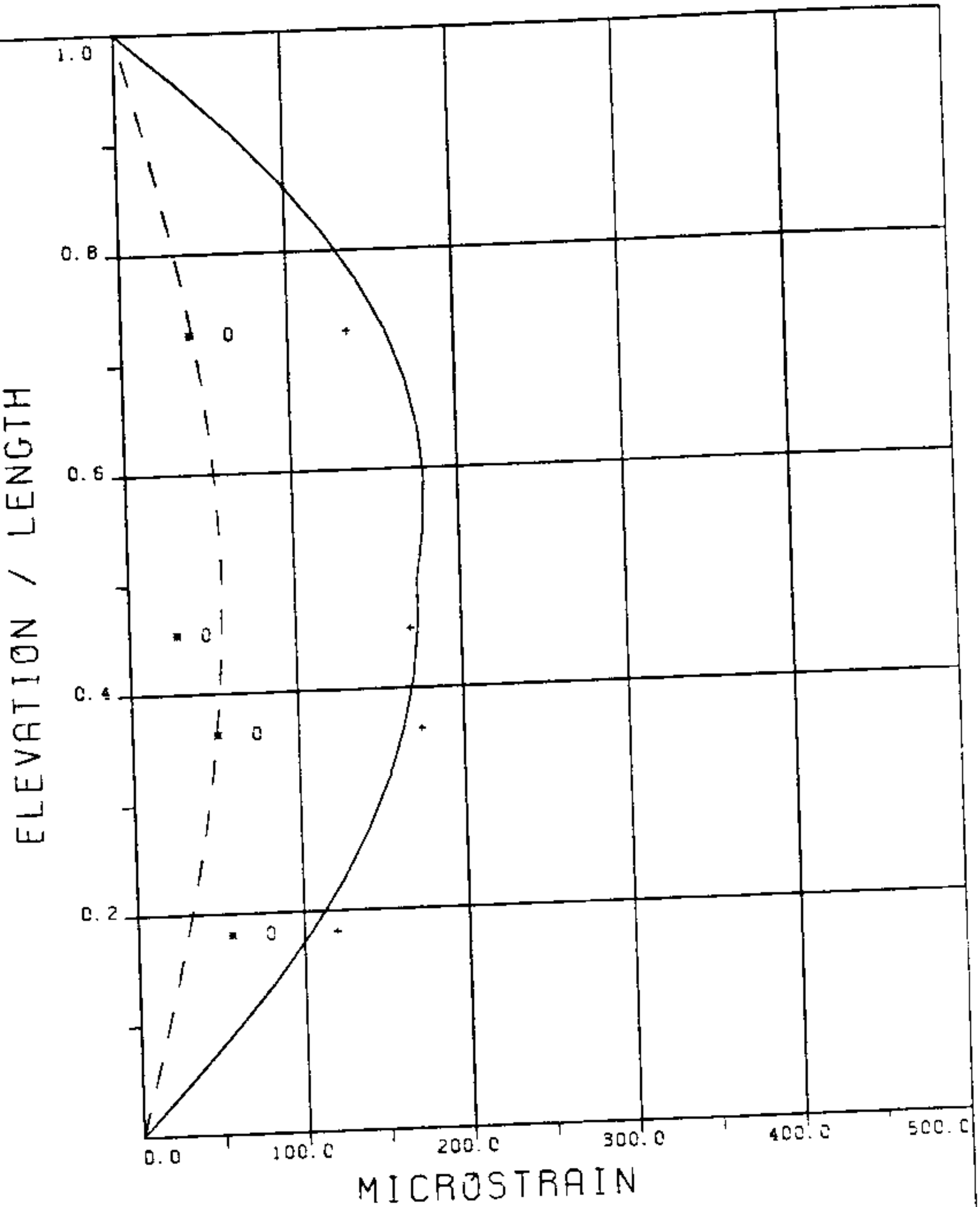

EXPERIMENT NUMBER 118

THETA=90 VC=0 FE=1.500 A/DE=1.94

DYNAMIC RESPONSE IN PLANE A AT F=FE

----- THEORY * * * EXPERIMENT

MAXIMUM RESPONSE IN PLANE A

o o o EXPERIMENT

MAXIMUM RESPONSE

——— THEORY + + + EXPERIMENT

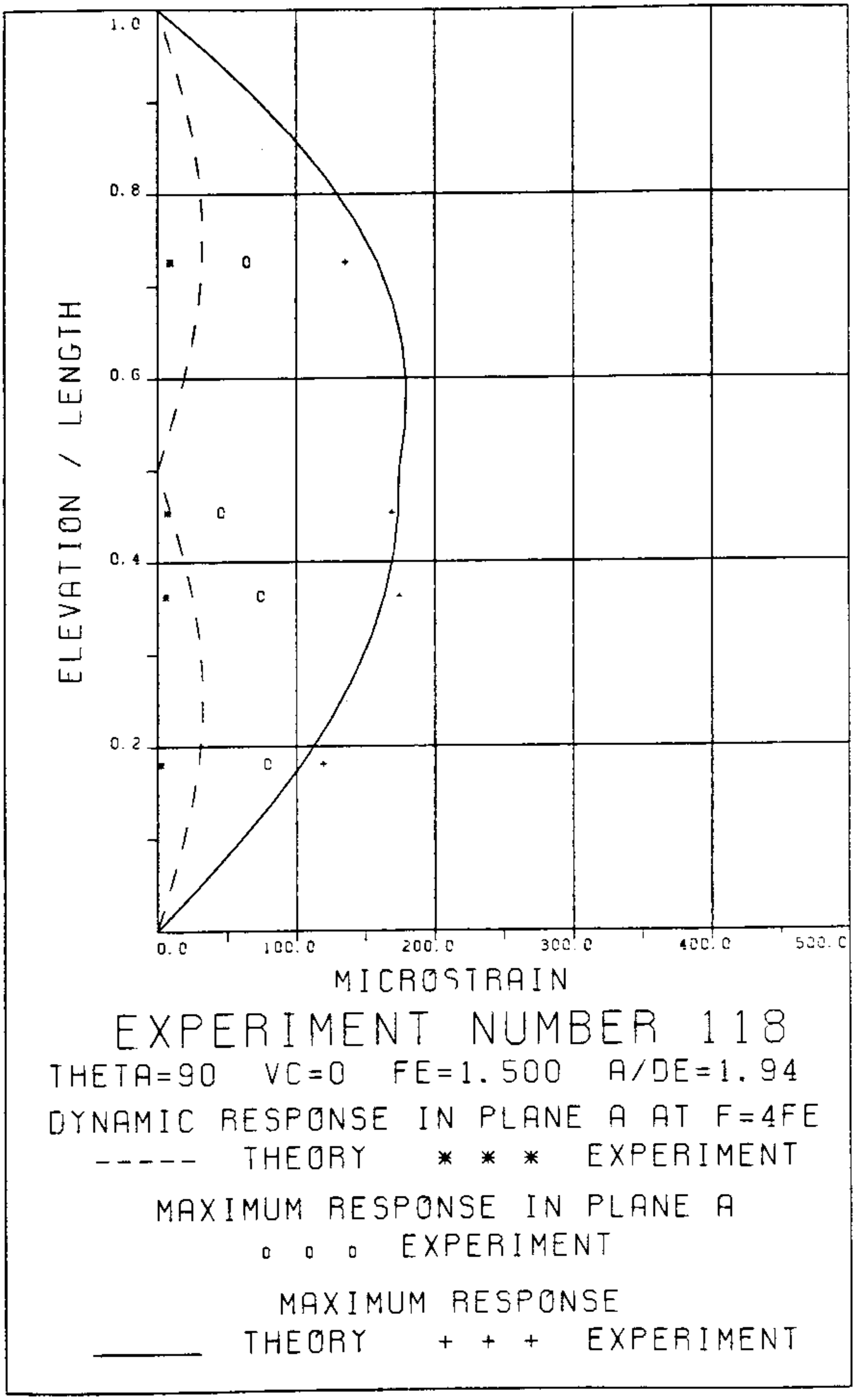
1.0
0.8
0.6
0.4
0.2
ELEVATION / LENGTH
0.0
100.0
200.0
300.0
400.0
500.0
MICROSTRAIN
EXPERIMENT NUMBER 118
THETA=90 VC=0 FE=1.500 A/DE=1.94
DYNAMIC RESPONSE IN PLANE A AT F=4FE
----- THEORY * * * EXPERIMENT
MAXIMUM RESPONSE IN PLANE A
o o o EXPERIMENT
MAXIMUM RESPONSE
THEORY + + + EXPERIMENT

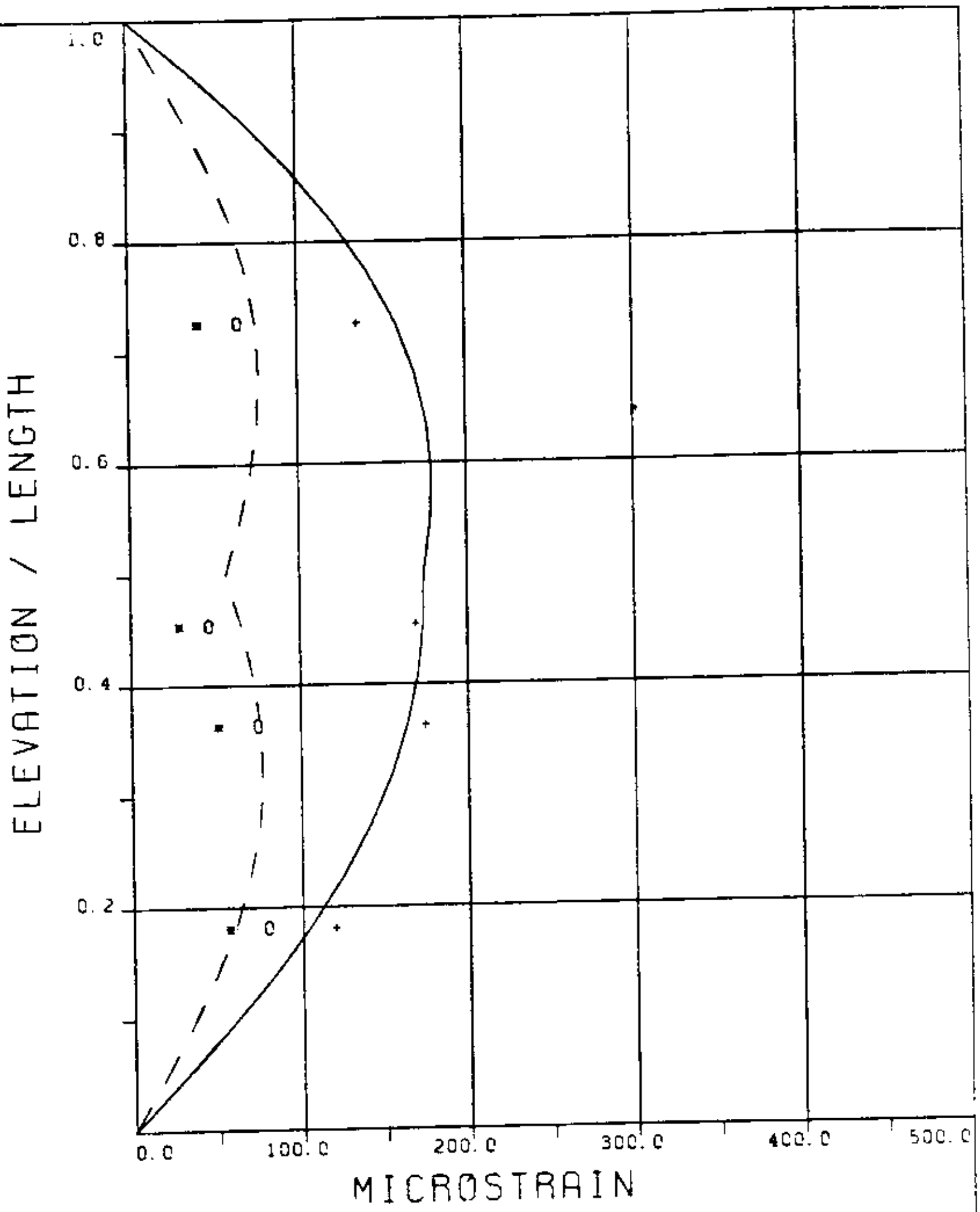

EXPERIMENT NUMBER 118

THETA=90 VC=0 FE=1.500 A/DE=1.94

DYNAMIC RESPONSE IN PLANE A AT F=FE

* * * EXPERIMENT

MAXIMUM RESPONSE IN PLANE A

----- THEORY o o o EXPERIMENT

MAXIMUM RESPONSE

_____ THEORY + + + EXPERIMENT

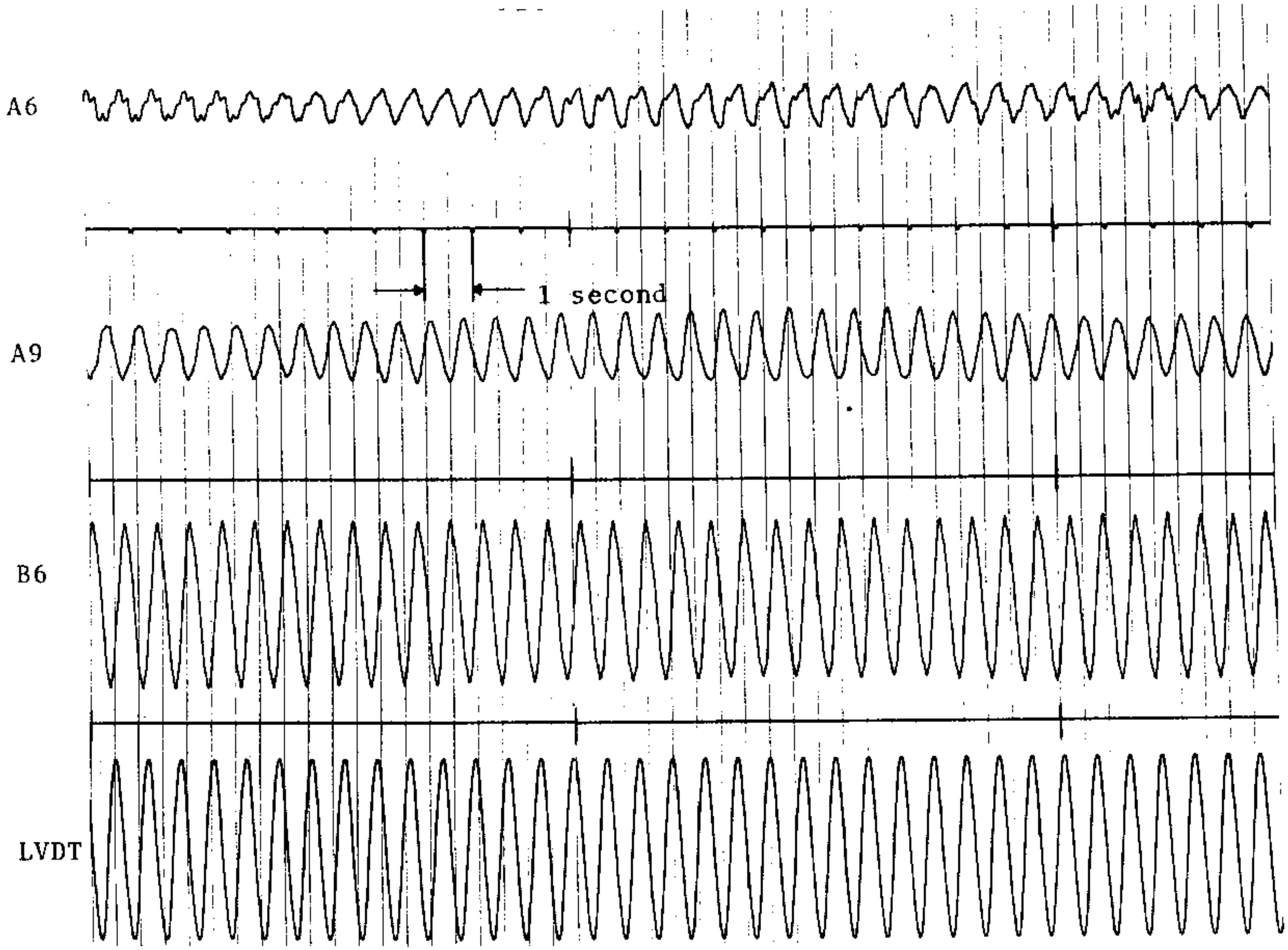

FIGURE 118Ta: LVDT: 0.087 D_e/DIVISION; STRAINS: 7.64 MICROSTRAIN/DIVISION

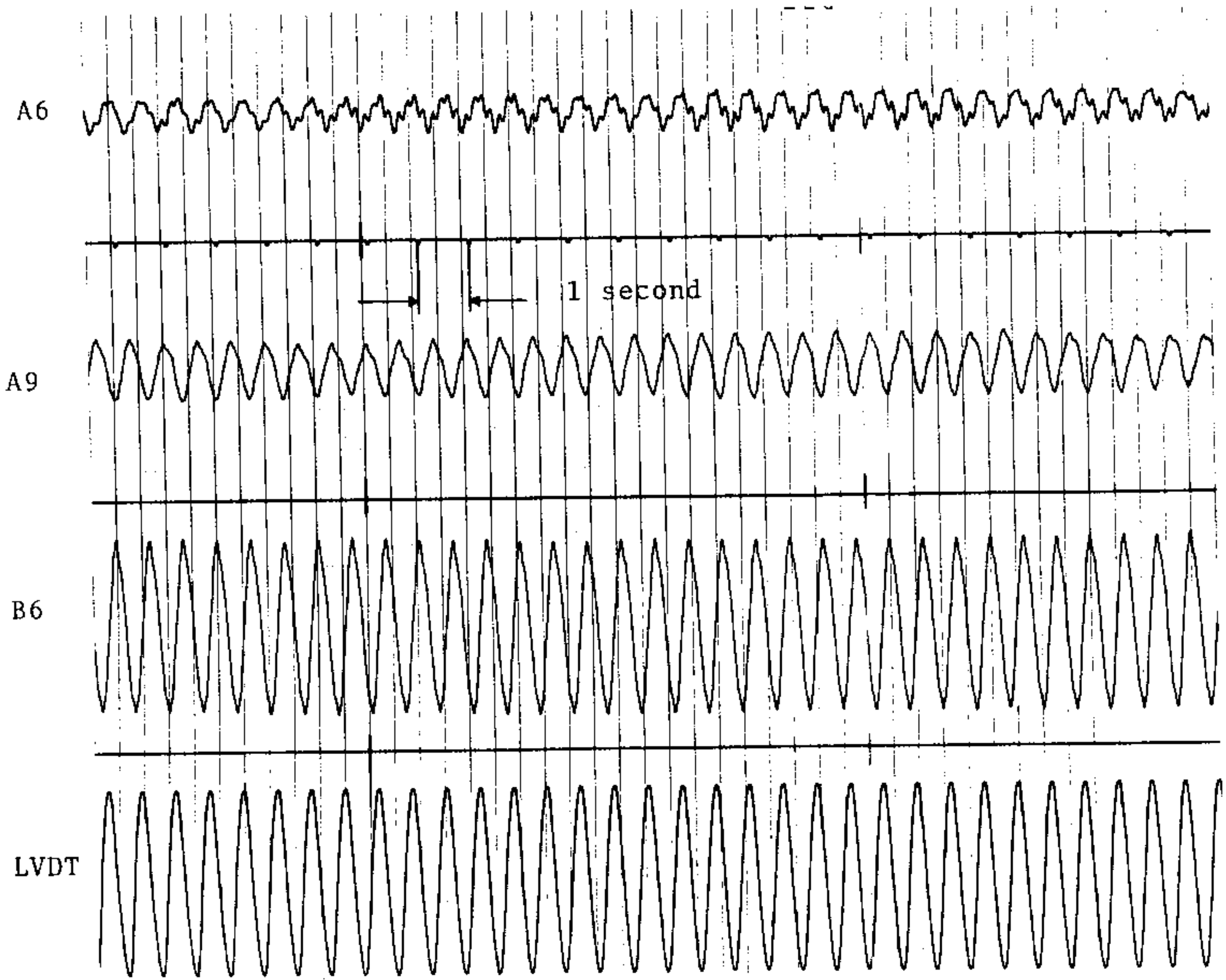

FIGURE 118Tb: LVDT: 0.087 D_e/DIVISION; STRAINS: 7.64 MICROSTRAIN/DIVISION

EXPERIMENT 119

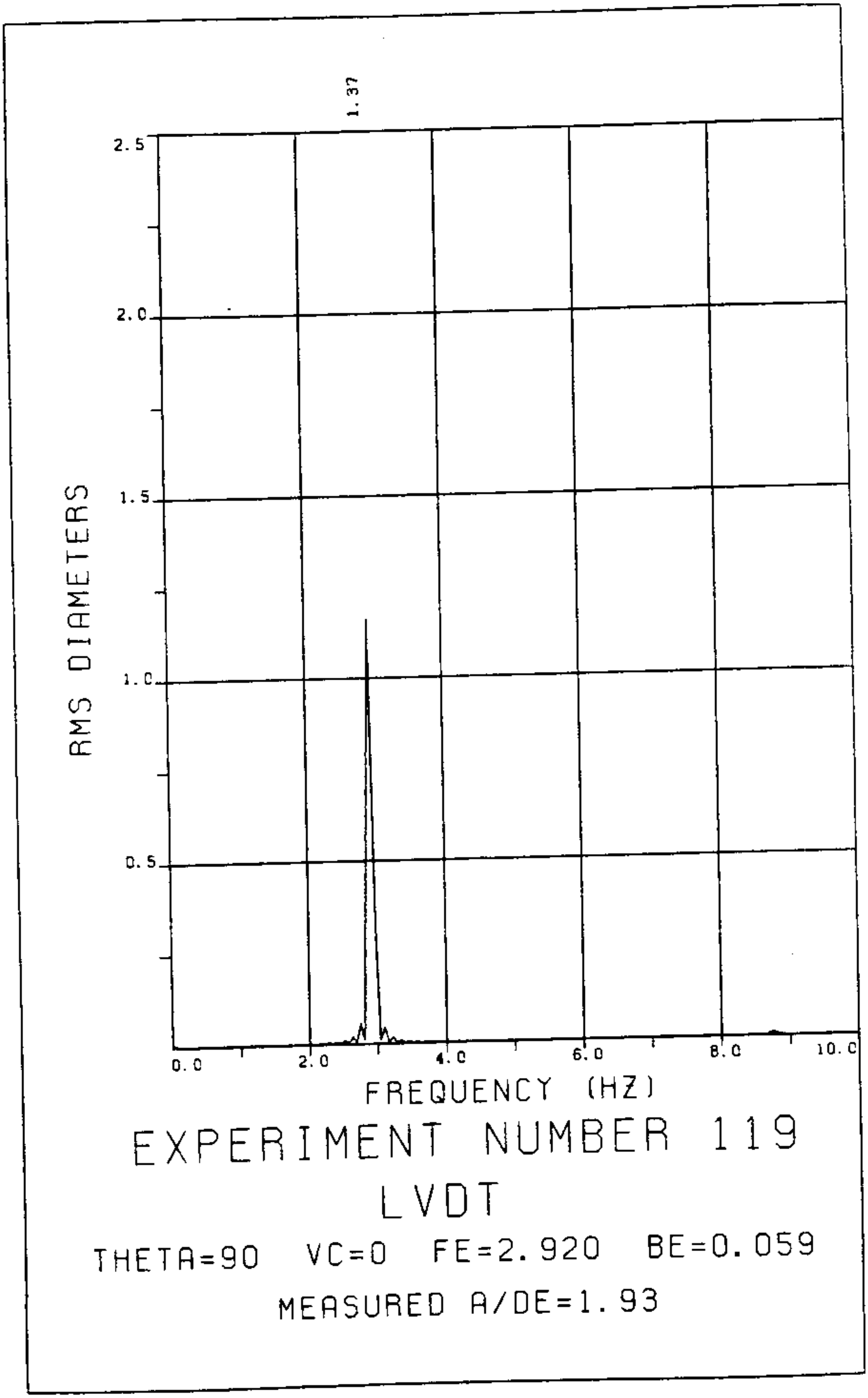
1.37
2.5
2.0
1.5
1.0
0.5
RMS DIAMETERS
0.0
2.0
4.0
6.0
8.0
10.0
FREQUENCY (HZ)
EXPERIMENT NUMBER 119
LVDT
THETA=90 VC=0 FE=2.920 BE=0.059
MEASURED A/DE=1.93

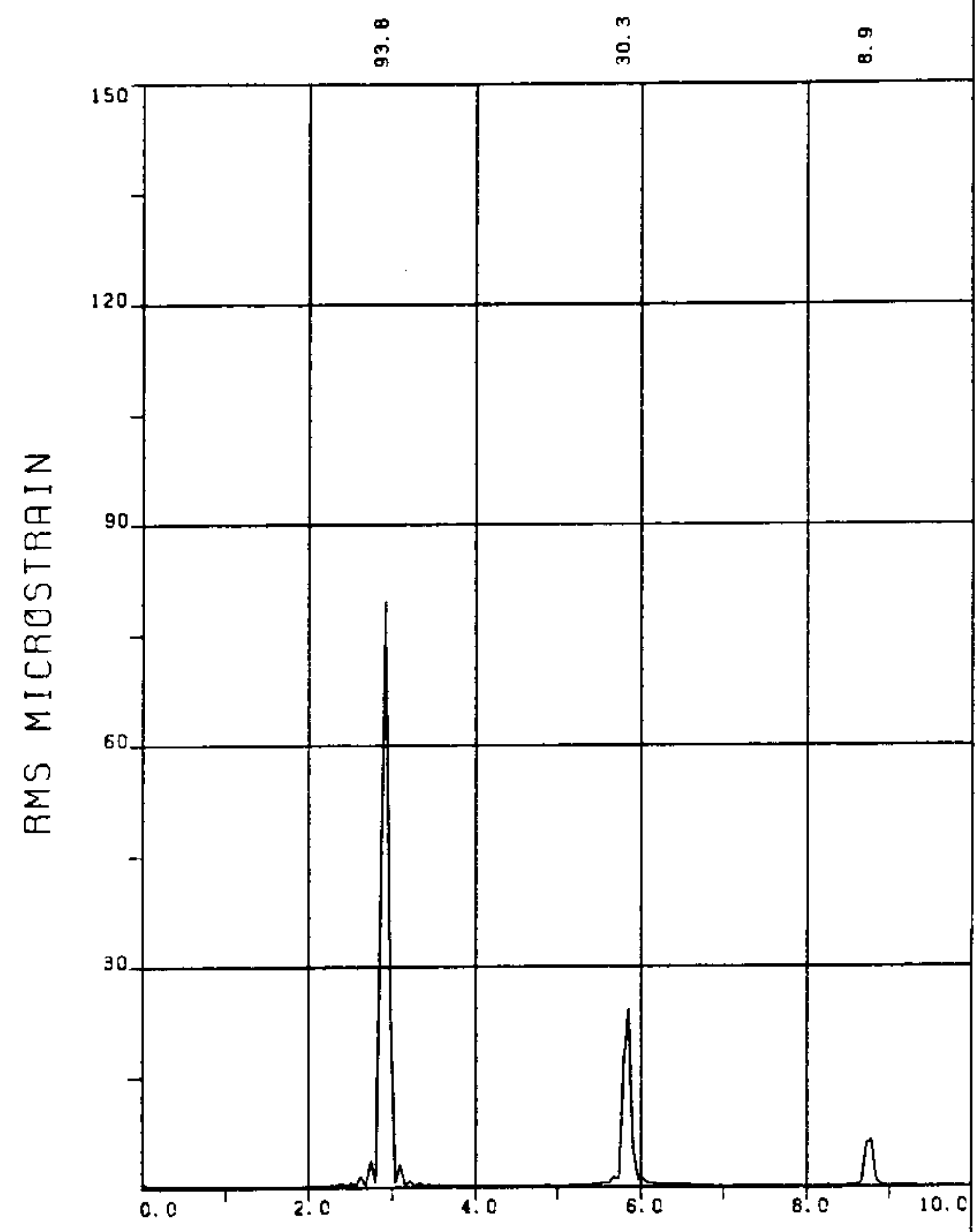

EXPERIMENT NUMBER 119

BRIDGE B9 ELEVATION=2L/11 BE=0.059

THETA=90 VC=0 FE=2.920 A/DE=1.93

MEASURED RESPONSE IN MICROSTRAIN

TOTAL DYNAMIC RMS=98.8

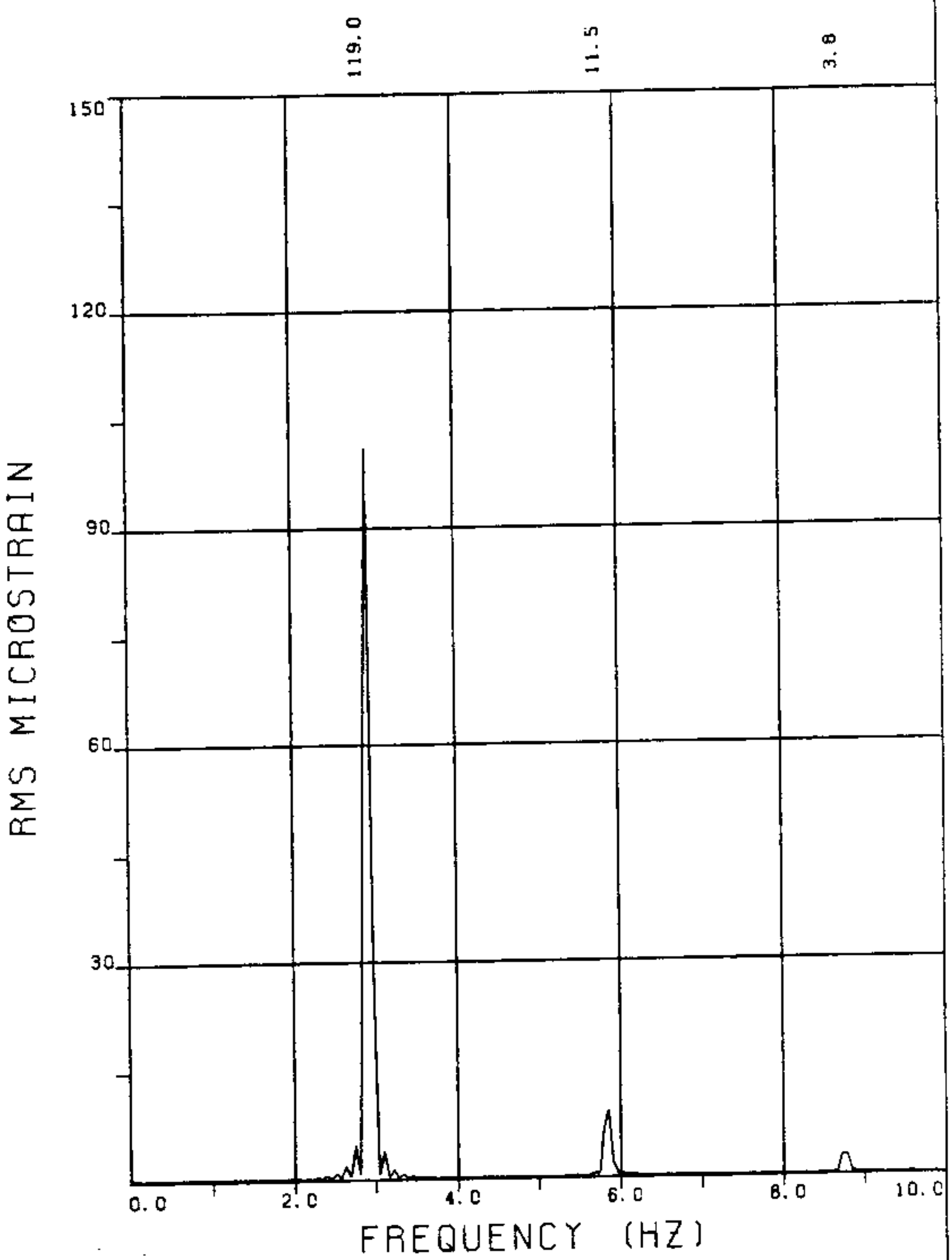

EXPERIMENT NUMBER 119

BRIDGE B6 ELEVATION=5L/11 BE=0.059

THETA=90 VC=0 FE=2.920 A/DE=1.93

MEASURED RESPONSE IN MICROSTRAIN

TOTAL DYNAMIC RMS=119.6

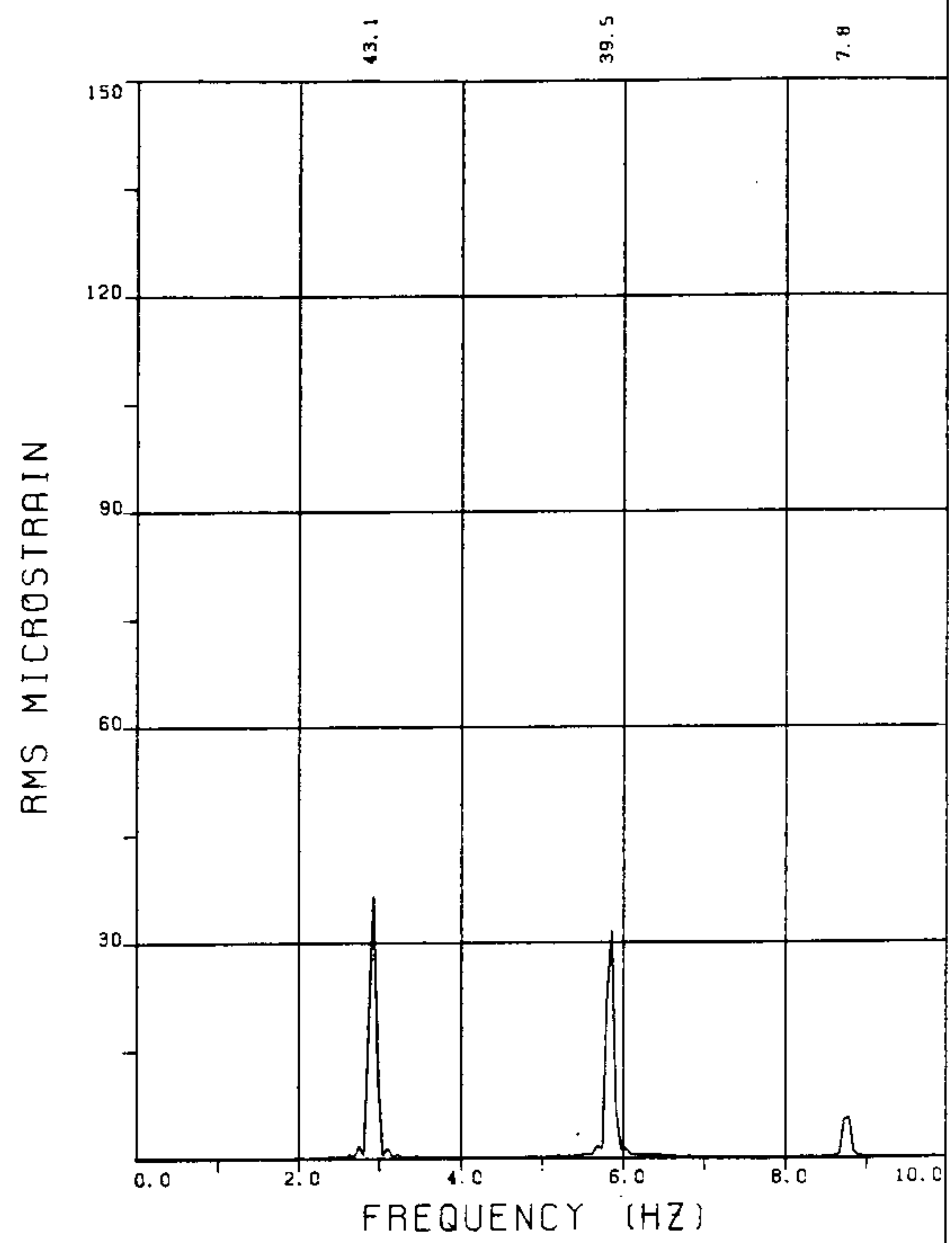

EXPERIMENT NUMBER 119

BRIDGE B3 ELEVATION=8L/11 BE=0.059

THETA=90 VC=0 FE=2.920 A/DE=1.93

MEASURED RESPONSE IN MICROSTRAIN

TOTAL DYNAMIC RMS=58.9

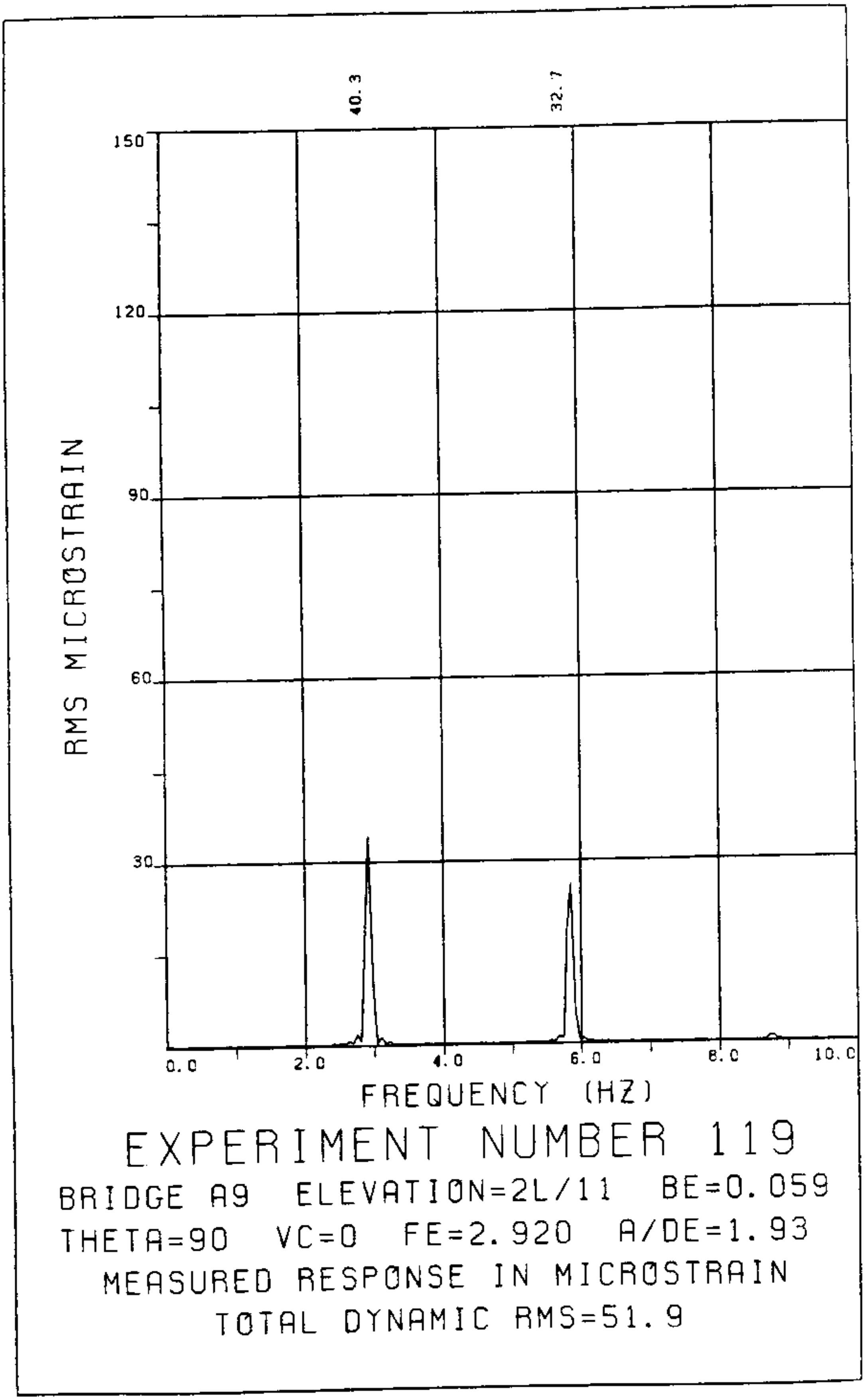
40.3
32.7
150
120
90
60
30
RMS MICRØSTRAIN
0.0
2.0
4.0
6.0
8.0
10.0
FREQUENCY (HZ)
EXPERIMENT NUMBER 119
BRIDGE A9 ELEVATIØN=2L/11 BE=0.059
THETA=90 VC=0 FE=2.920 A/DE=1.93
MEASURED RESPØNSE IN MICRØSTRAIN
TOTAL DYNAMIC RMS=51.9

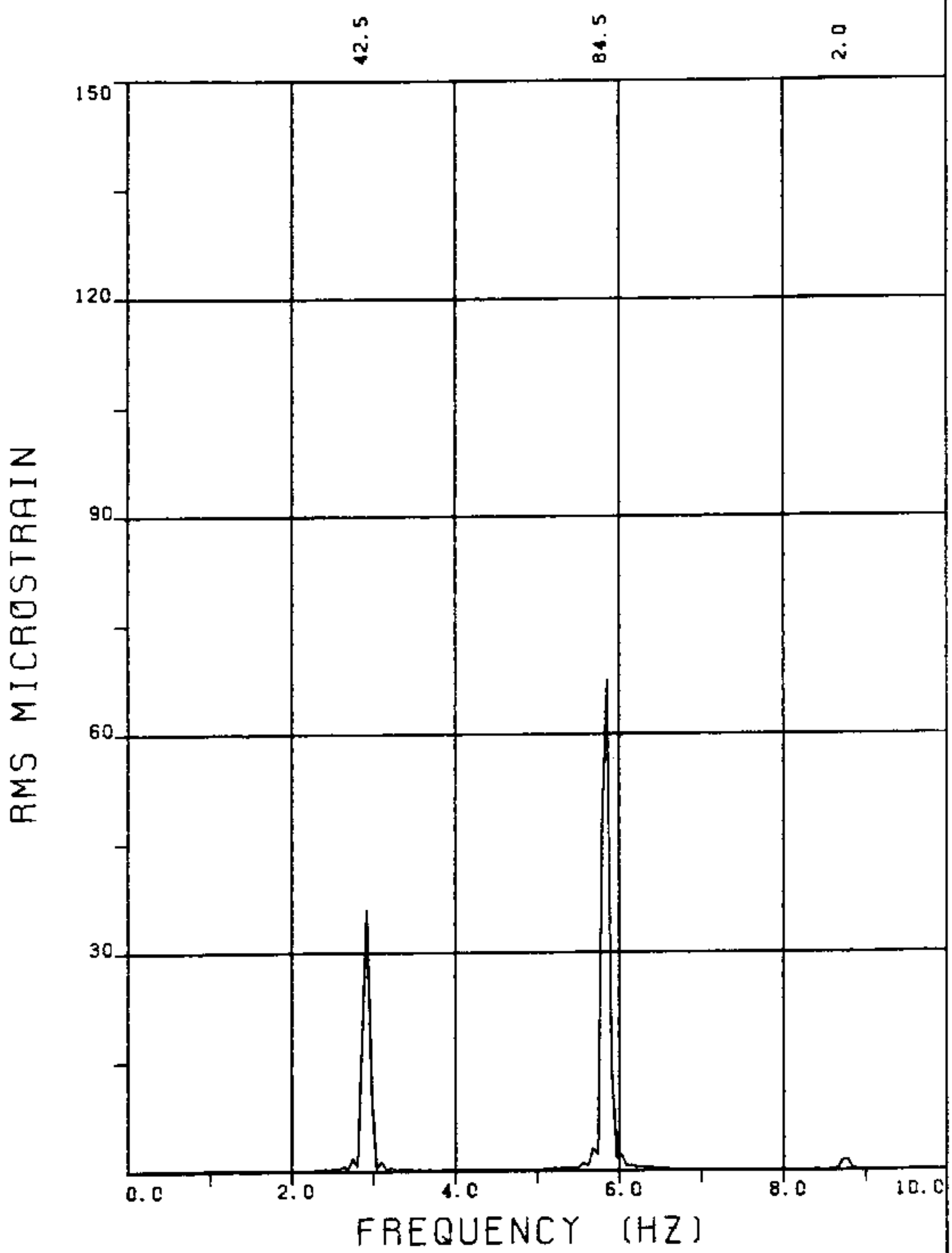

EXPERIMENT NUMBER 119

BRIDGE A7 ELEVATION=4L/11 BE=0.059

THETA=90 VC=0 FE=2.920 A/DE=1.93

MEASURED RESPONSE IN MICROSTRAIN

TOTAL DYNAMIC RMS=94.6

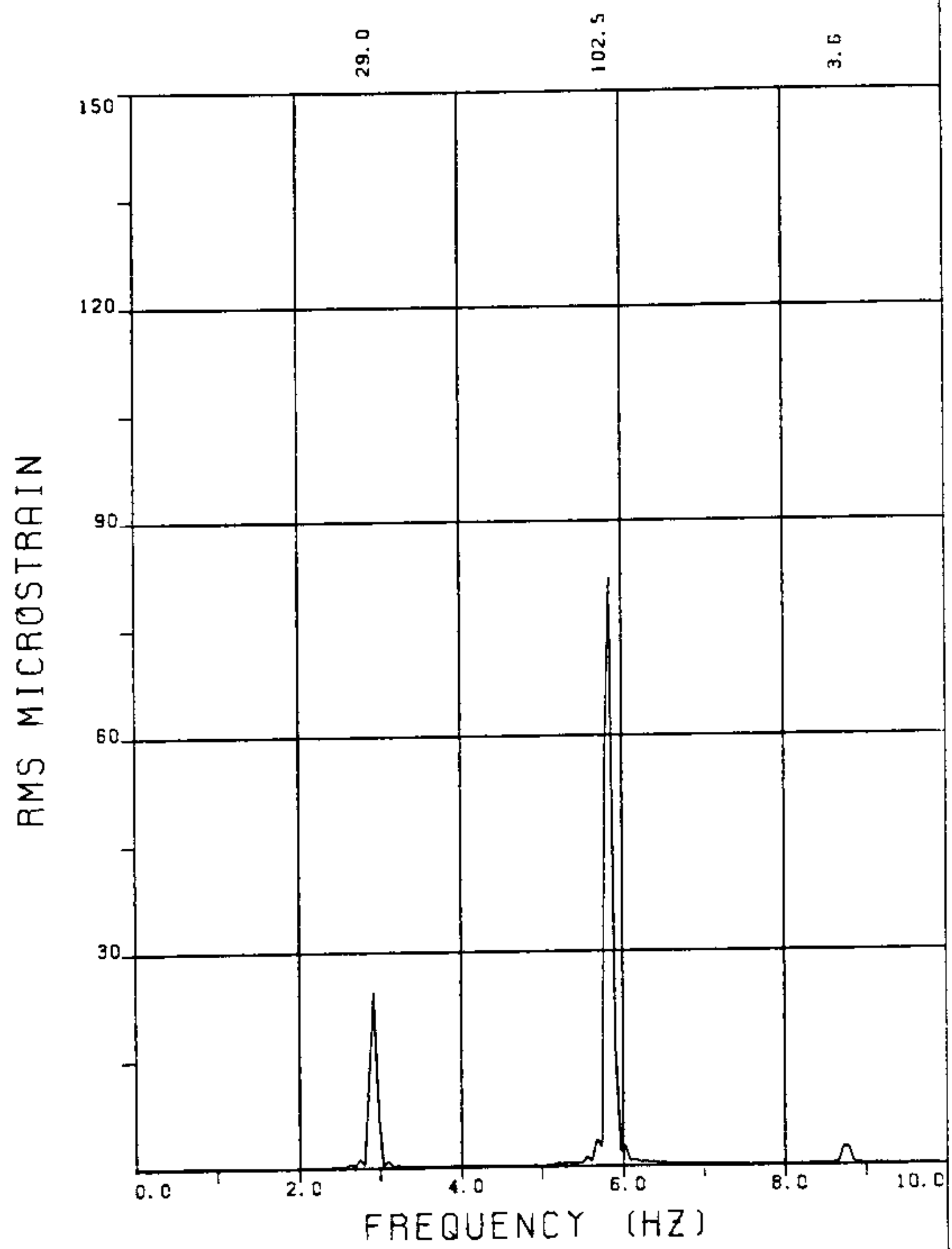

EXPERIMENT NUMBER 119

BRIDGE A6 ELEVATION=5L/11 BE=0.059

THETA=90 VC=0 FE=2.920 A/DE=1.93

MEASURED RESPONSE IN MICROSTRAIN

TOTAL DYNAMIC RMS=106.6

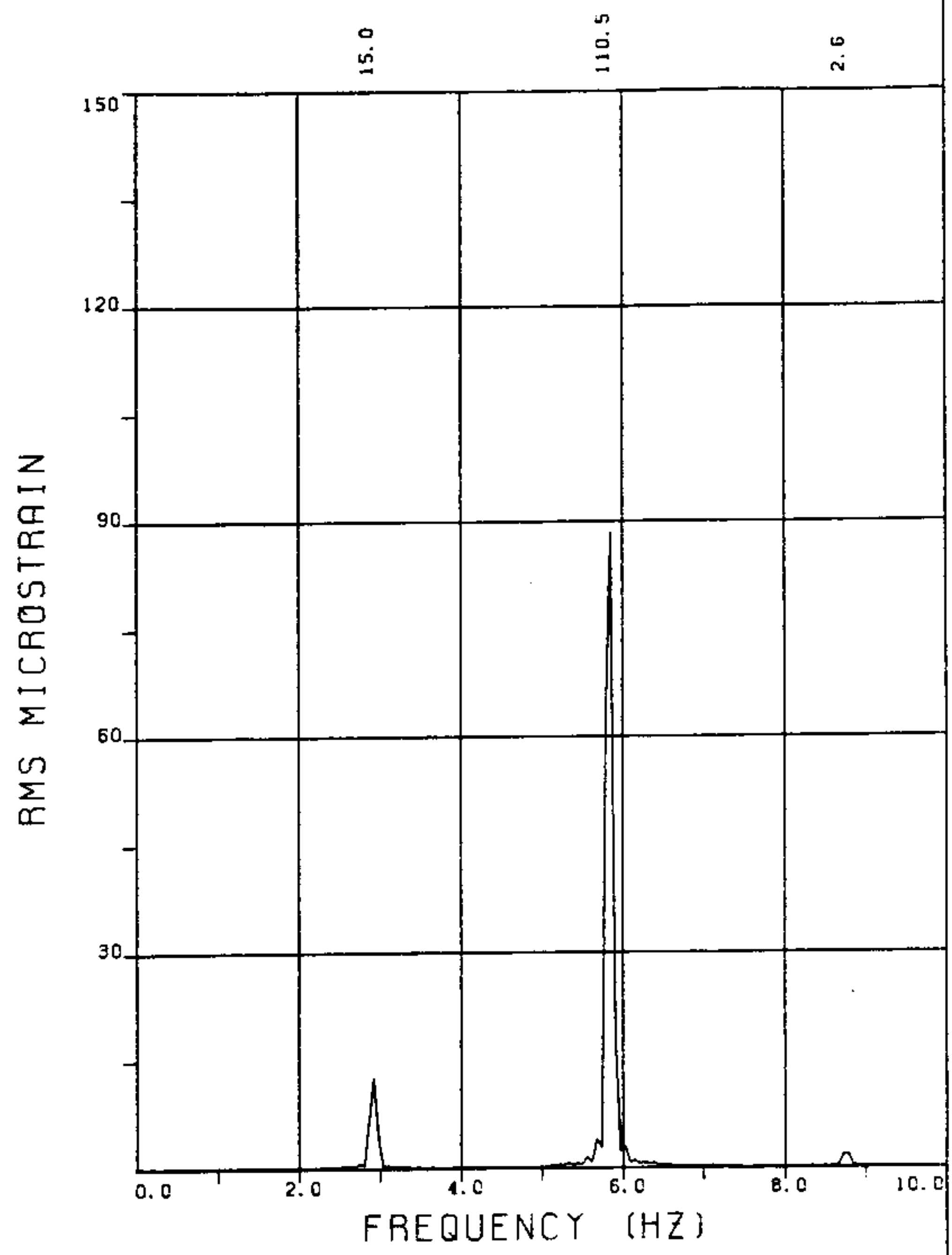

EXPERIMENT NUMBER 119

BRIDGE A3 ELEVATION=8L/11 BE=0.059

THETA=90 VC=0 FE=2.920 A/DE=1.93

MEASURED RESPONSE IN MICROSTRAIN

TOTAL DYNAMIC RMS=111.4

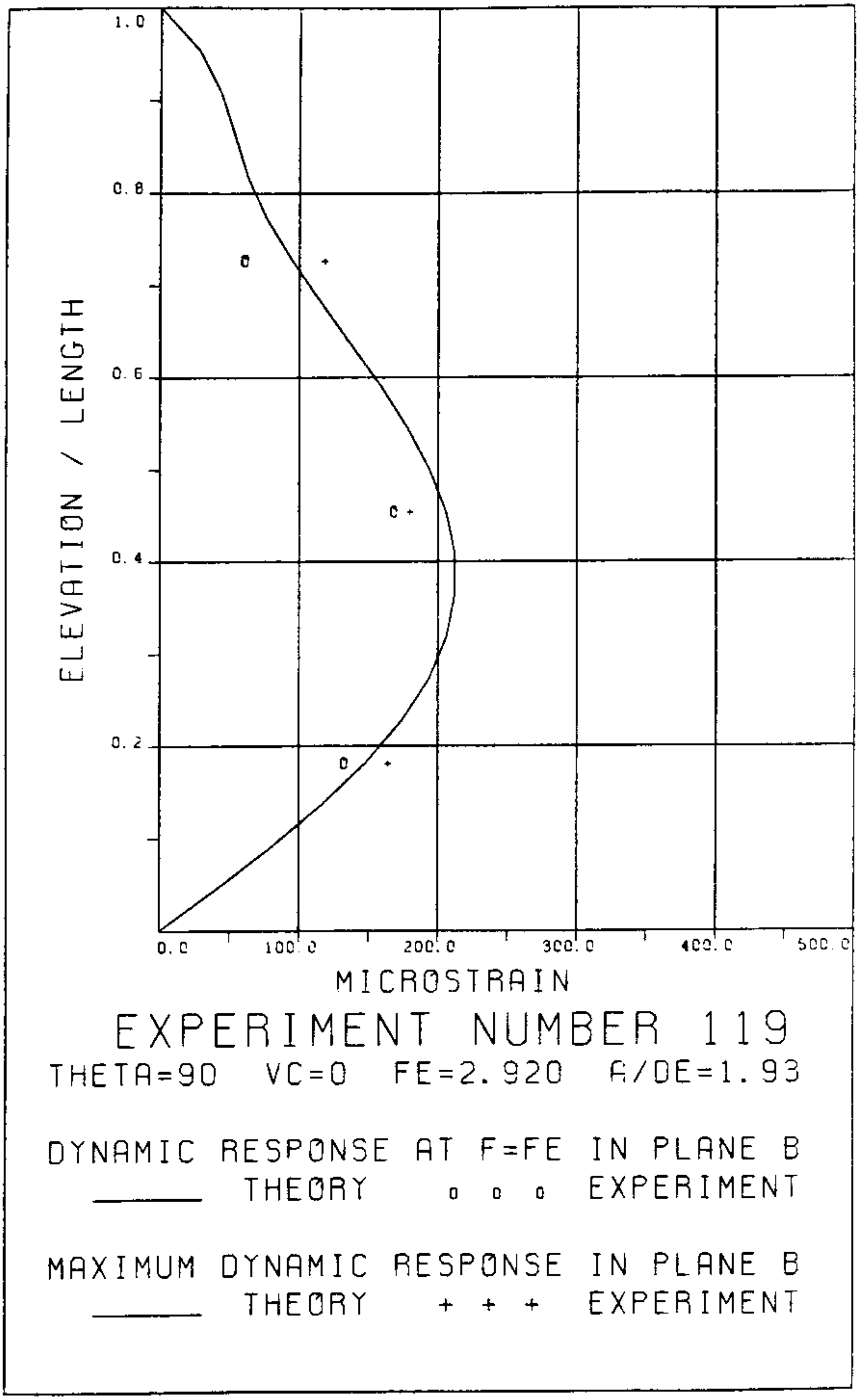
1.0
0.8
0.6
0.4
0.2
ELEVATION / LENGTH
0.0
100.0
200.0
300.0
400.0
500.0
MICROSTRAIN
EXPERIMENT NUMBER 119
THETA=90 VC=0 FE=2.920 A/DE=1.93
DYNAMIC RESPONSE AT F=FE IN PLANE B
THEORY o o o EXPERIMENT
MAXIMUM DYNAMIC RESPONSE IN PLANE B
THEORY + + + EXPERIMENT

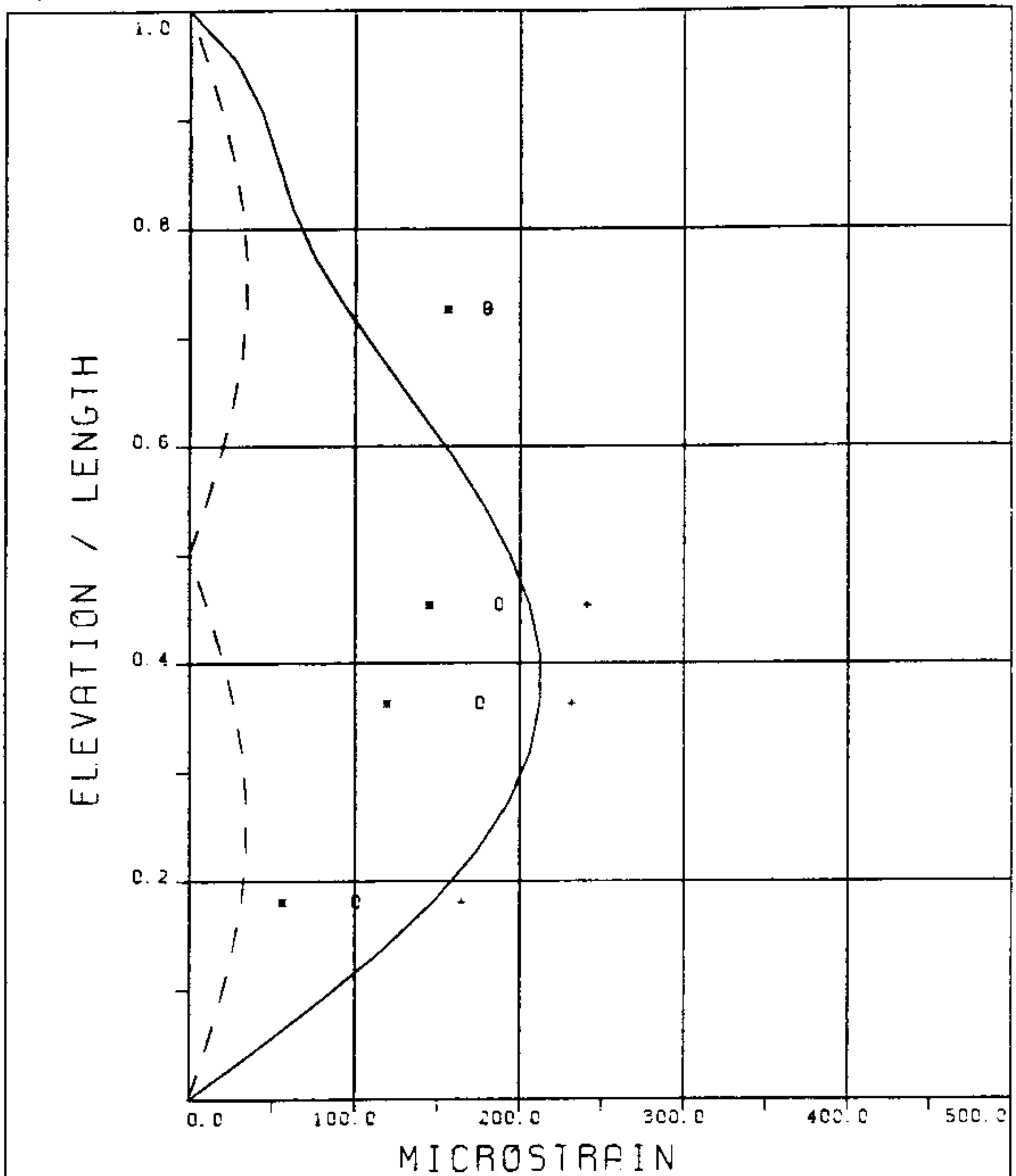

EXPERIMENT NUMBER 119

THETA=90 VC=0 FE=2.920 A/DE=1.93

DYNAMIC RESPONSE IN PLANE A AT F=2FE

----- THEORY * * * EXPERIMENT

MAXIMUM RESPONSE IN PLANE A

o o o EXPERIMENT

MAXIMUM RESPONSE

_____ THEORY + + + EXPERIMENT

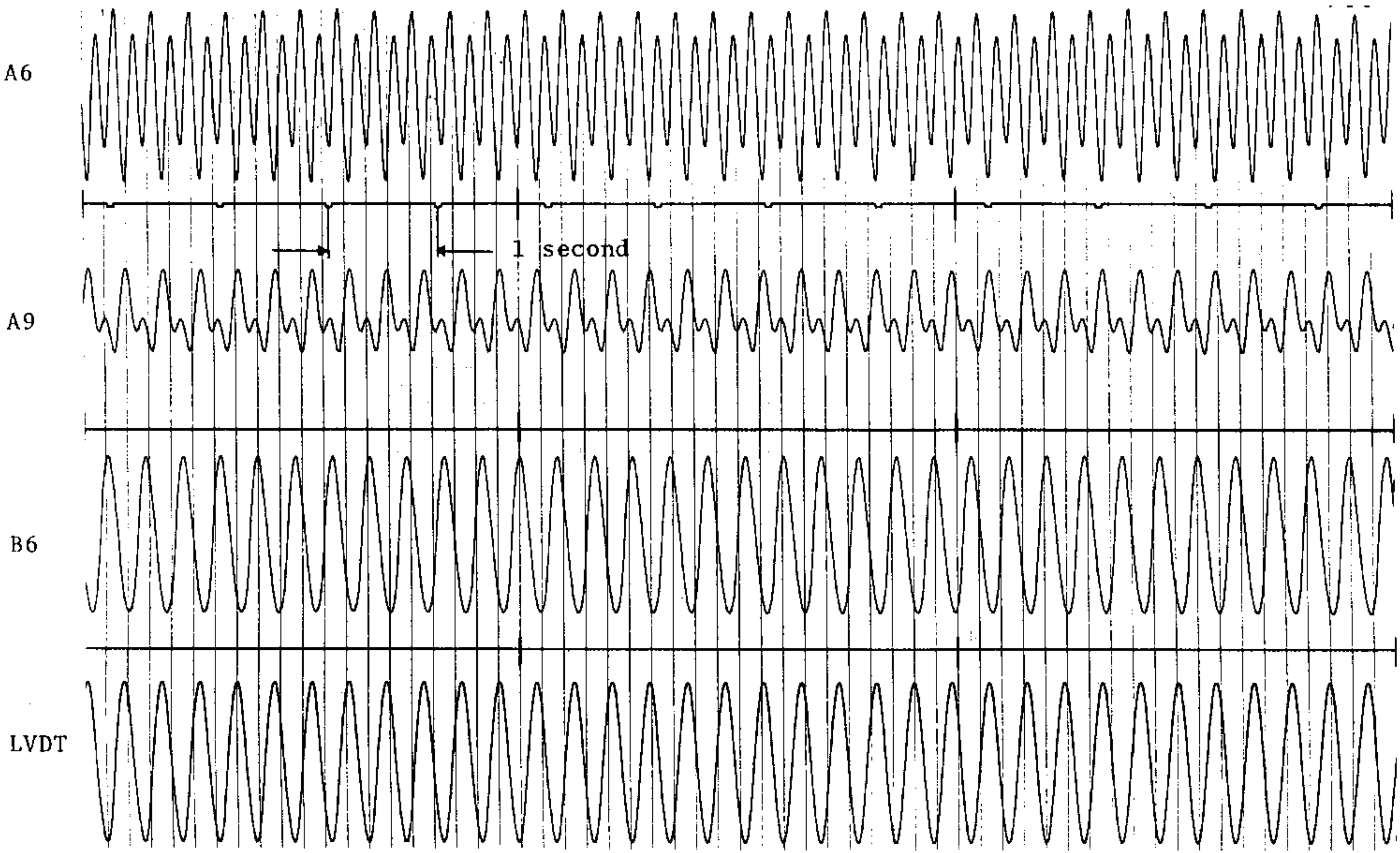

FIGURE 119T: LVDT: 0.087 D_e/DIVISION; STRAINS: 7.64 MICROSTRAIN/DIVISION

EXPERIMENT 15

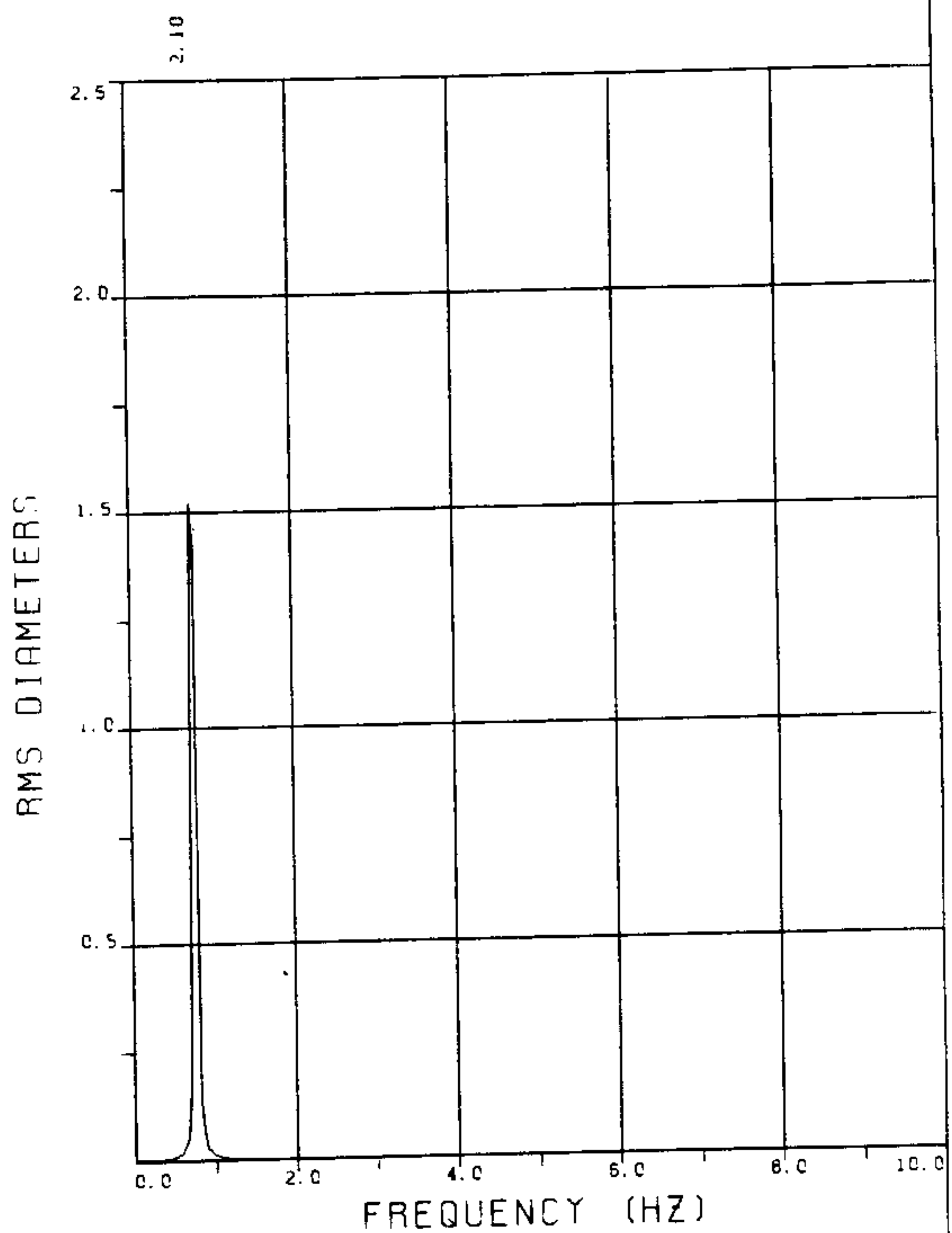

EXPERIMENT NUMBER 15

LVDT

THETA=0 VC=0 FE=0.750 BE=0.039

MEASURED A/DE=2.97

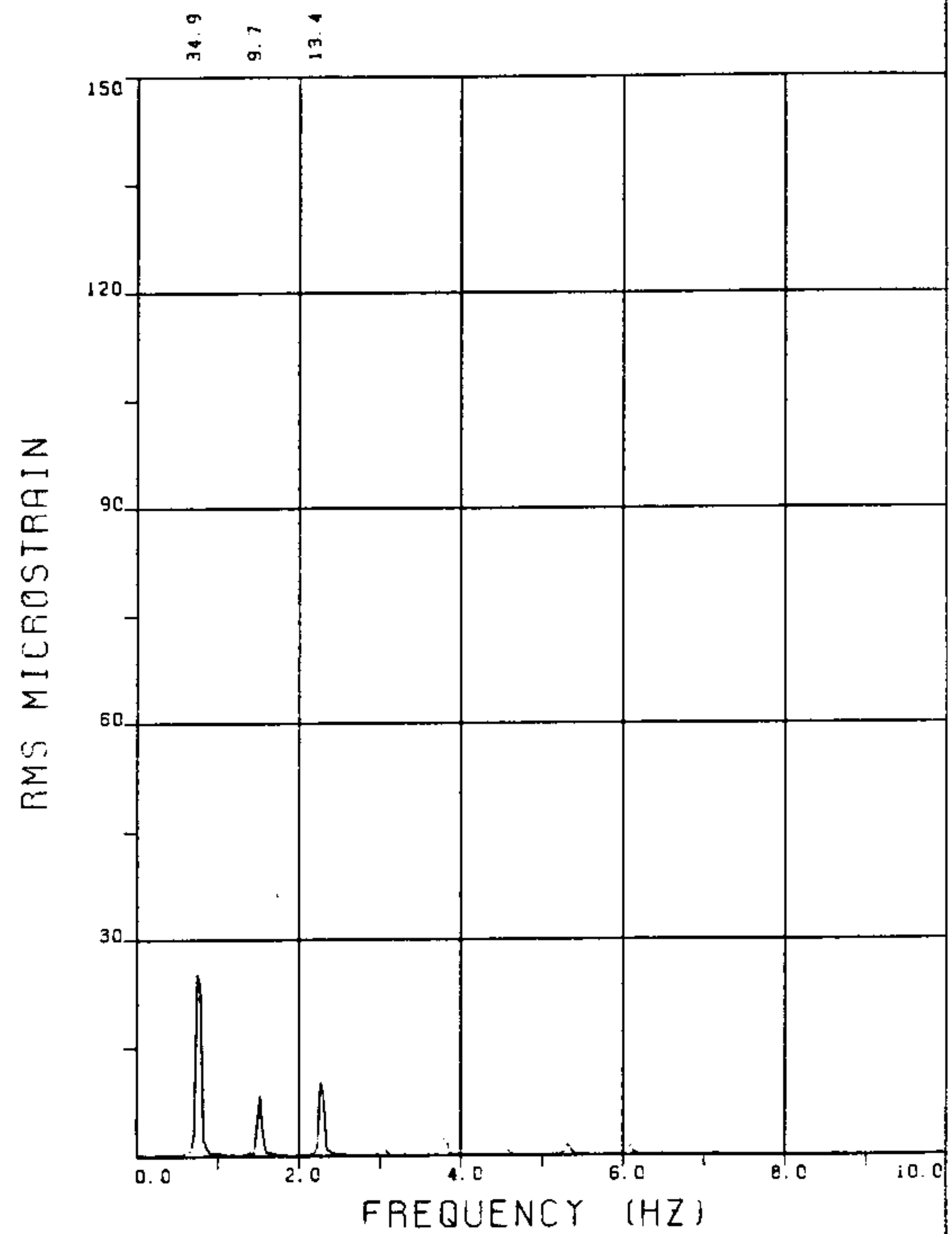

EXPERIMENT NUMBER 15

BRIDGE A8 ELEVATION=3L/11 BE=0.039

THETA=0 VC=0 FE=0.750 A/DE=2.97

MEASURED RESPONSE IN MICROSTRAIN

TOTAL DYNAMIC RMS=39.2

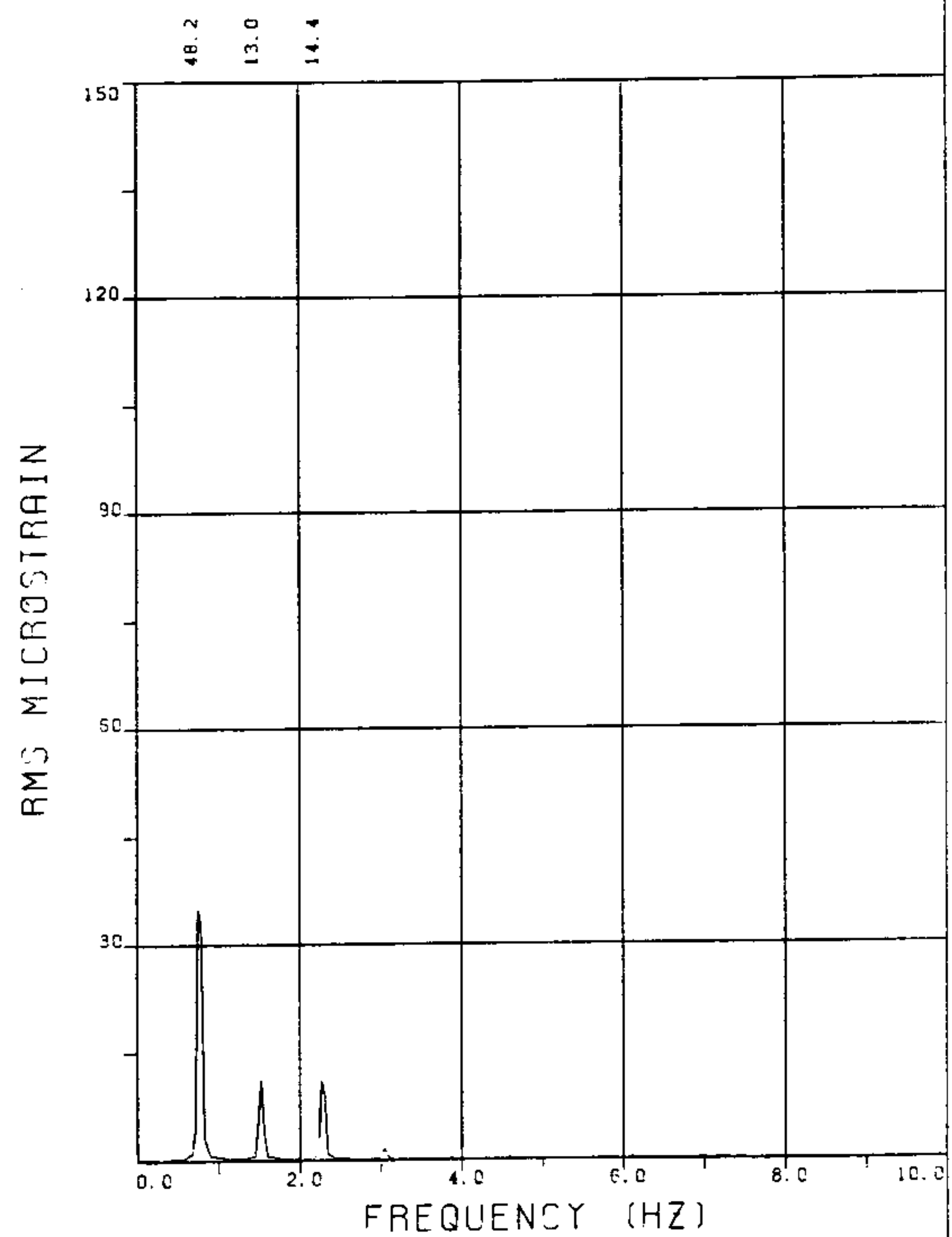

EXPERIMENT NUMBER 15

BRIDGE A6 ELEVATION=5L/11 BE=0.039

THETA=0 VC=0 FE=0.750 A/DE=2.97

MEASURED RESPONSE IN MICROSTRAIN

TOTAL DYNAMIC RMS=52.4

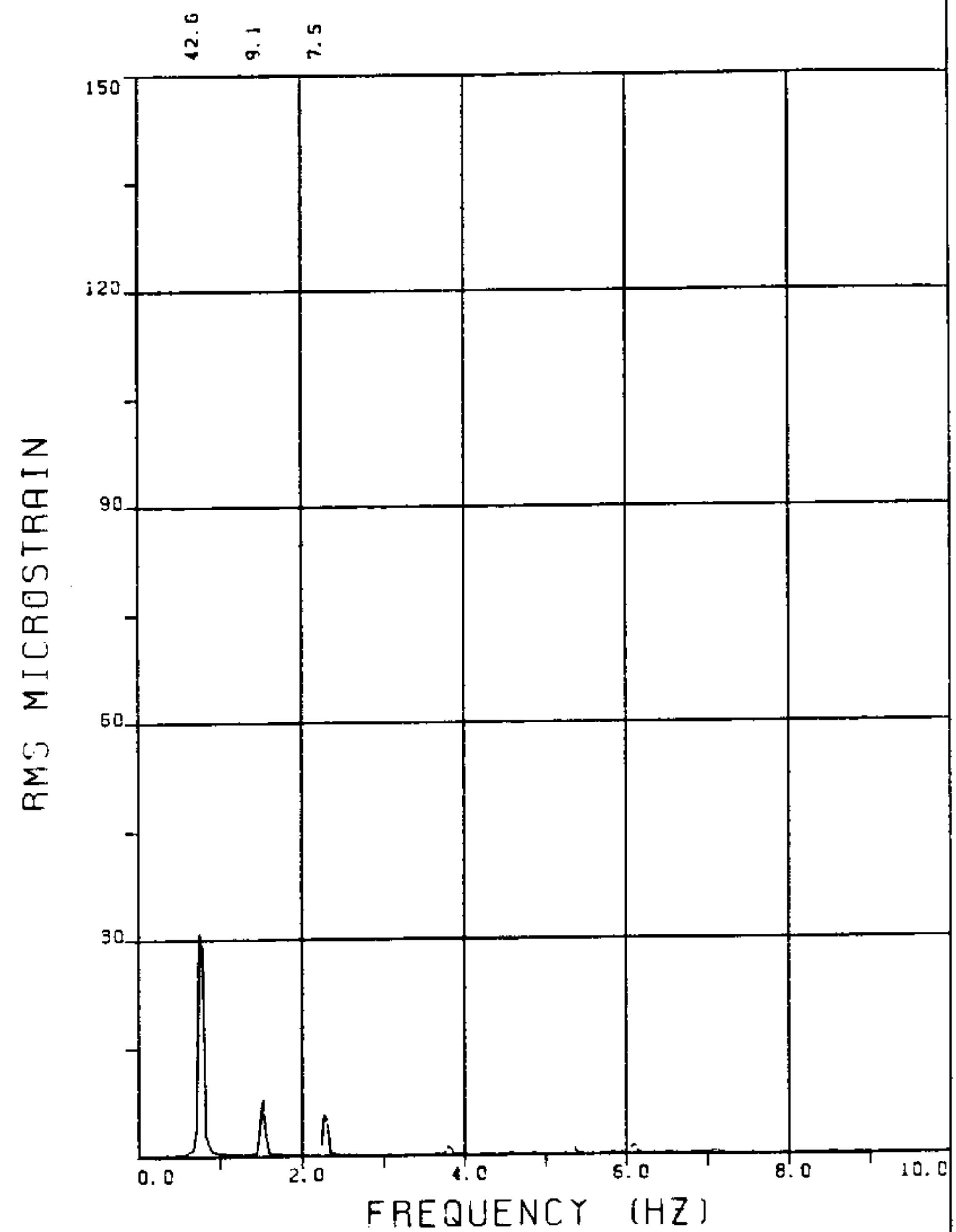

EXPERIMENT NUMBER 15

BRIDGE A3 ELEVATION=8L/11 BE=0.039

THETA=0 VC=0 FE=0.750 A/DE=2.97

MEASURED RESPONSE IN MICROSTRAIN

TOTAL DYNAMIC RMS=44.5

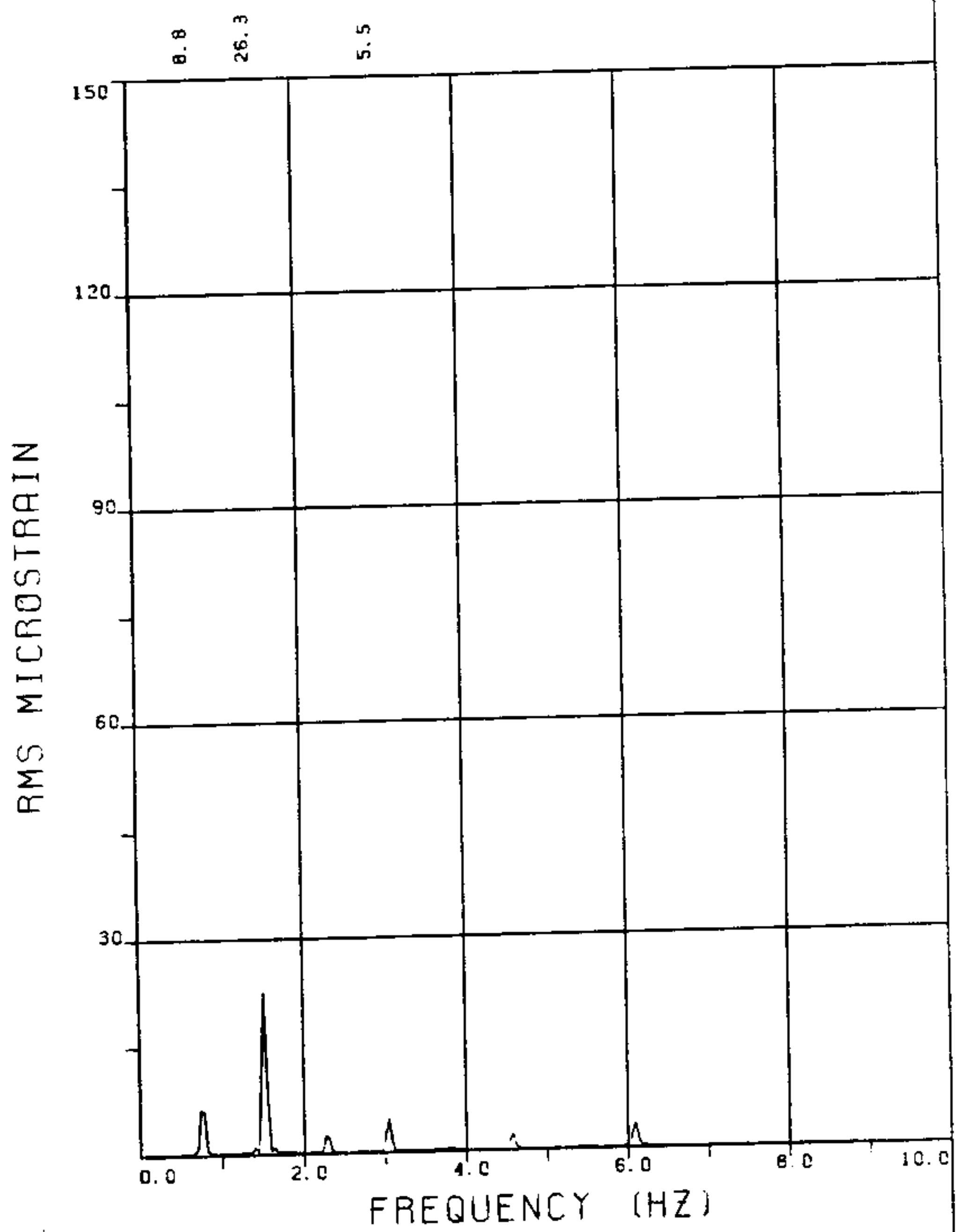

EXPERIMENT NUMBER 15

BRIDGE B8 ELEVATION=3L/11 BE=0.039

THETA=0 VC=0 FE=0.750 A/DE=2.97

MEASURED RESPONSE IN MICROSTRAIN

TOTAL DYNAMIC RMS=28.9

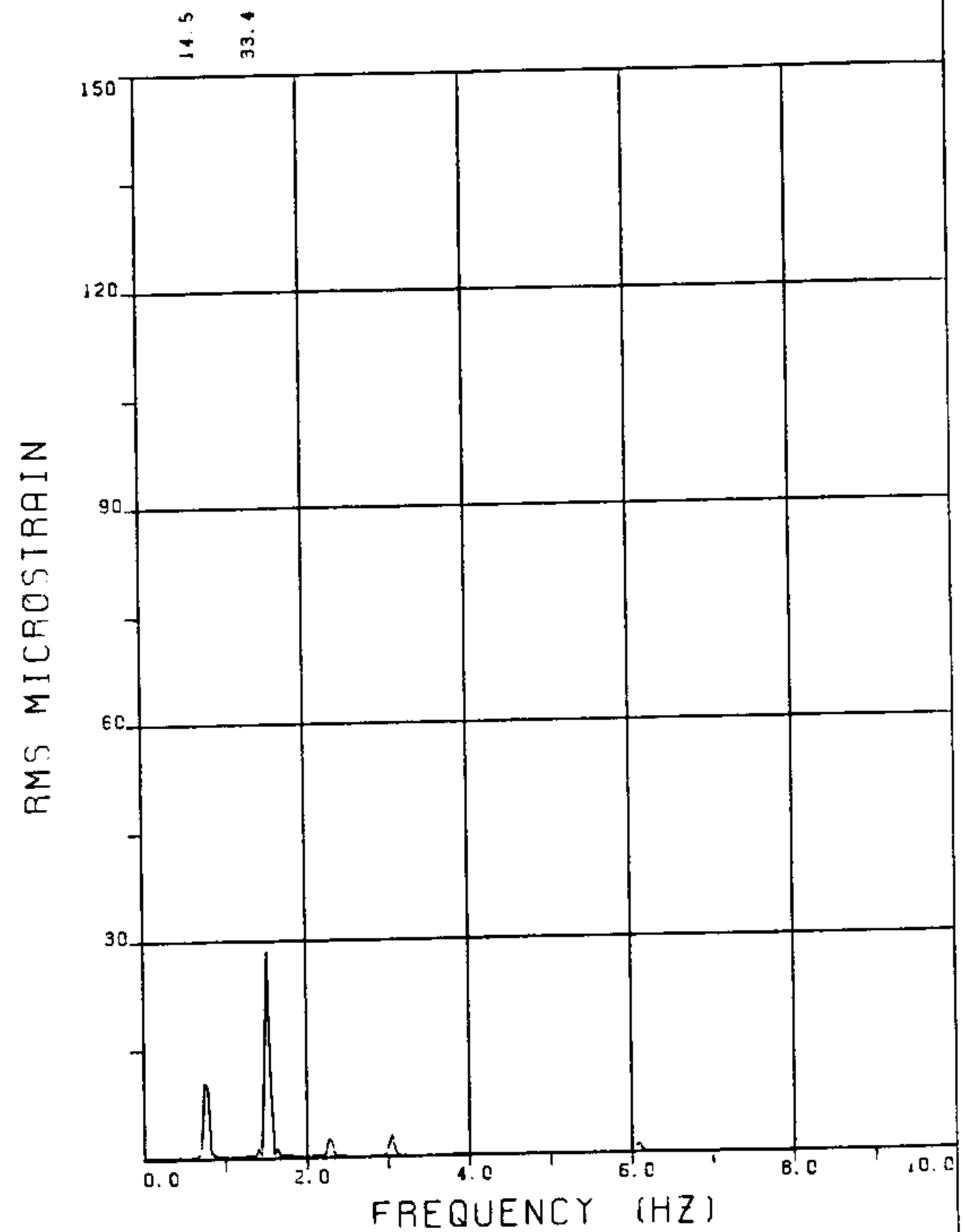

EXPERIMENT NUMBER 15

BRIDGE B5 ELEVATION=6L/11 BE=0.039

THETA=0 VC=0 FE=0.750 A/DE=2.97

MEASURED RESPONSE IN MICROSTRAIN

TOTAL DYNAMIC RMS=36.8

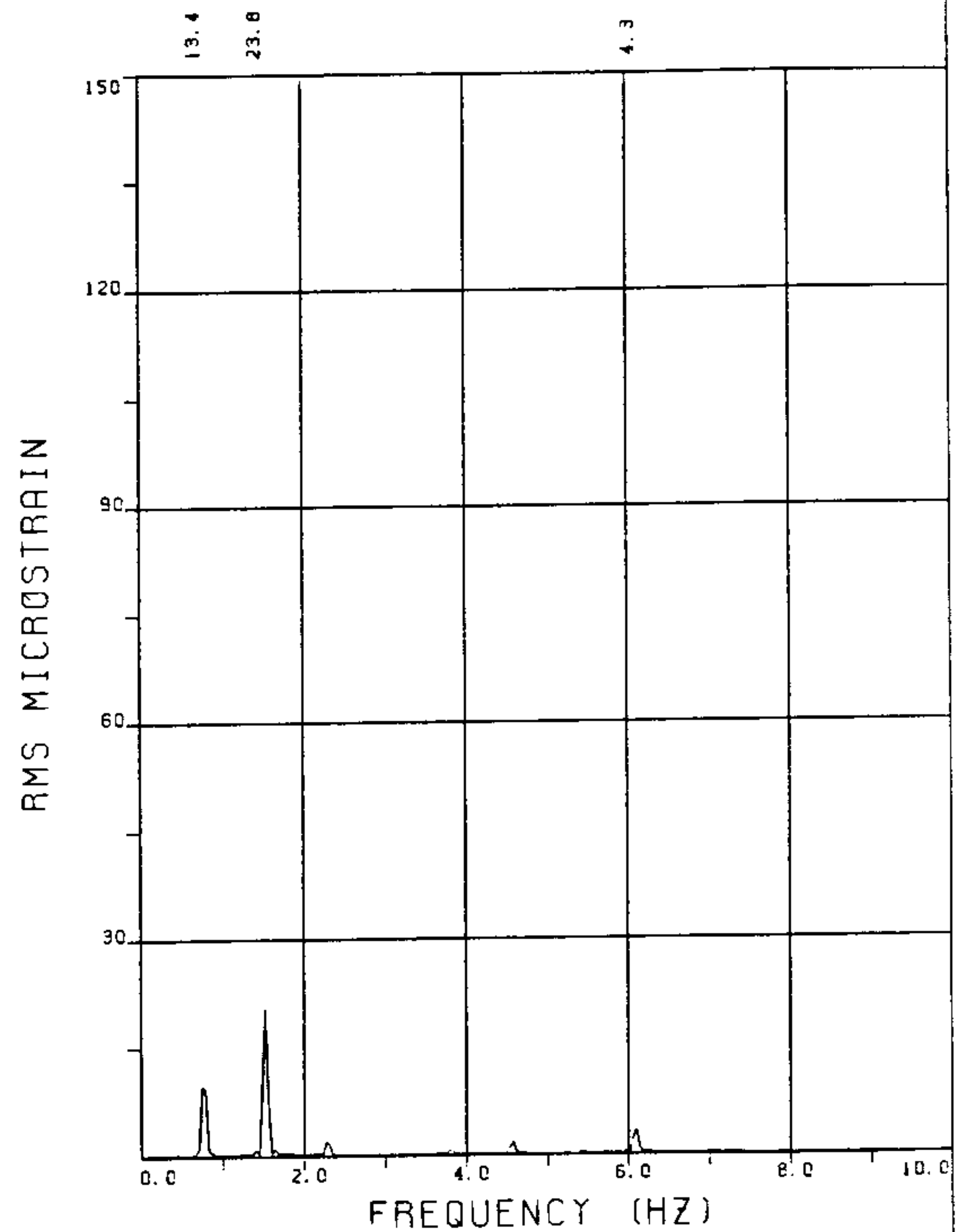

EXPERIMENT NUMBER 15

BRIDGE B3 ELEVATION=8L/11 BE=0.039

THETA=0 VC=0 FE=0.750 A/DE=2.97

MEASURED RESPONSE IN MICROSTRAIN

TOTAL DYNAMIC RMS=28.0

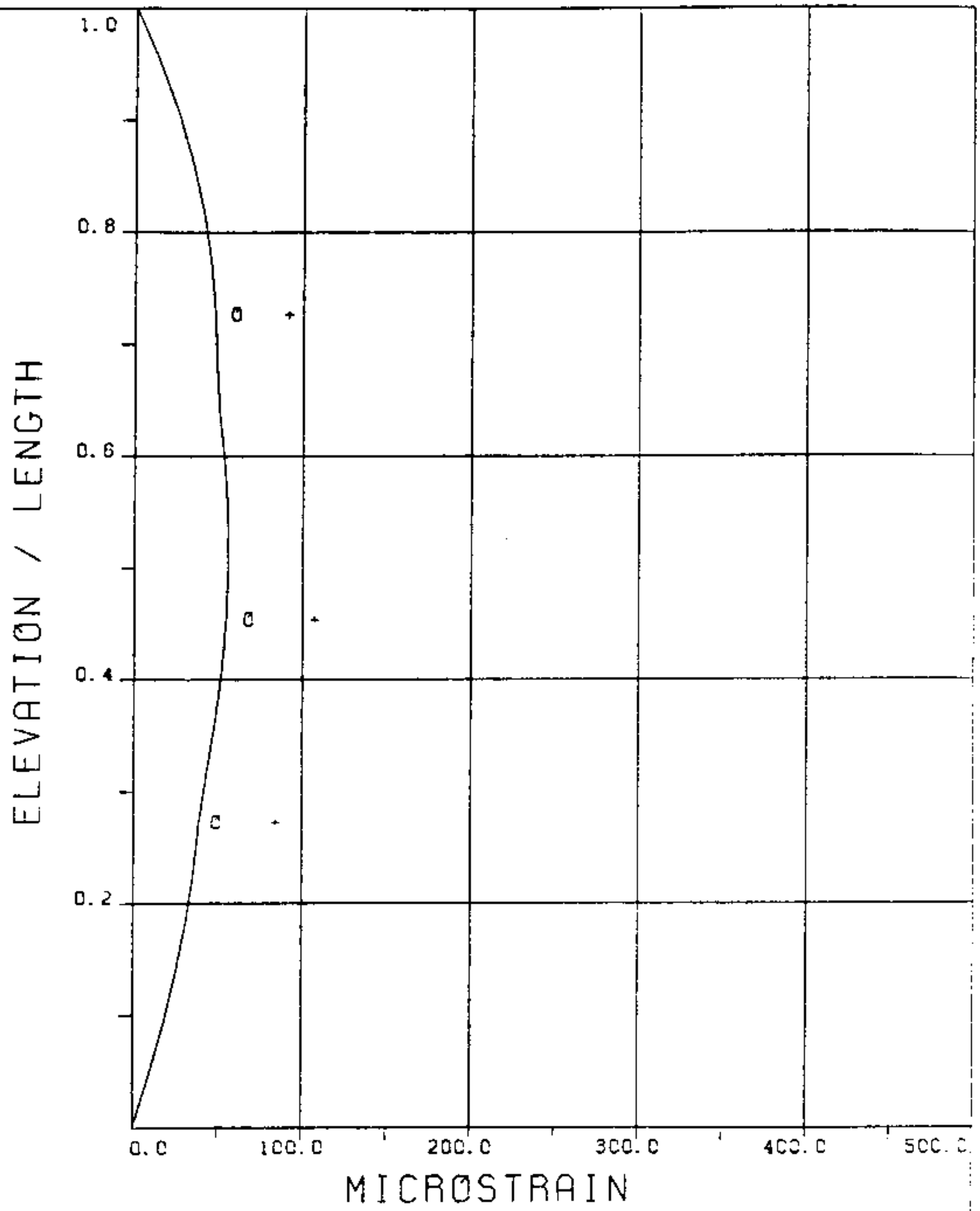

EXPERIMENT NUMBER 15

THETA=0 VC=0 FE=0.750 A/DE=2.97

DYNAMIC RESPONSE AT F=FE IN PLANE A
______ THEORY o o o EXPERIMENT

MAXIMUM DYNAMIC RESPONSE IN PLANE A
______ THEORY + + + EXPERIMENT

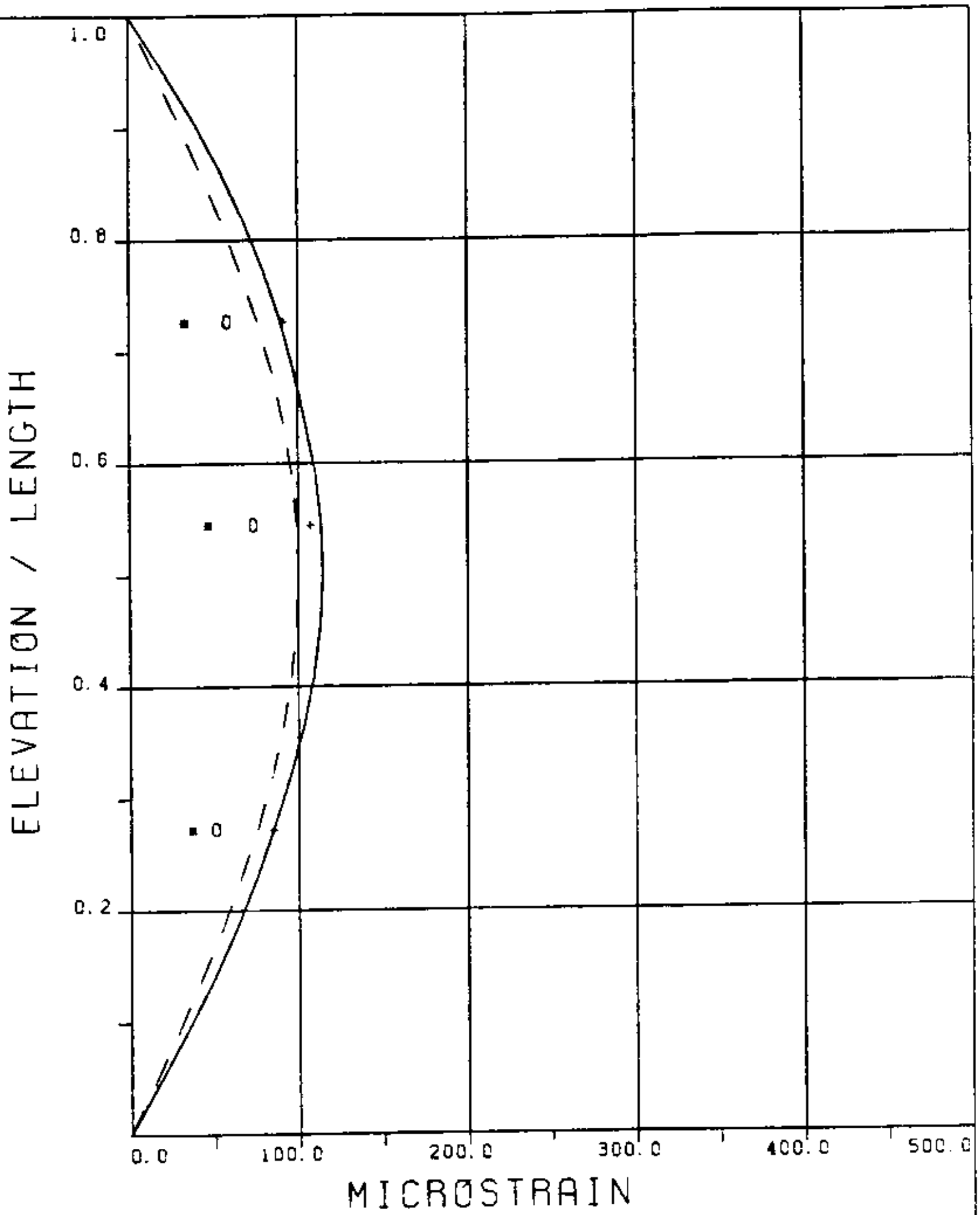

EXPERIMENT NUMBER 15

THETA=0 VC=0 FE=0.750 A/DE=2.97

DYNAMIC RESPONSE IN PLANE B AT F=2FE

----- THEORY * * * EXPERIMENT

MAXIMUM RESPONSE IN PLANE B

o o o EXPERIMENT

MAXIMUM RESPONSE

——— THEORY + + + EXPERIMENT

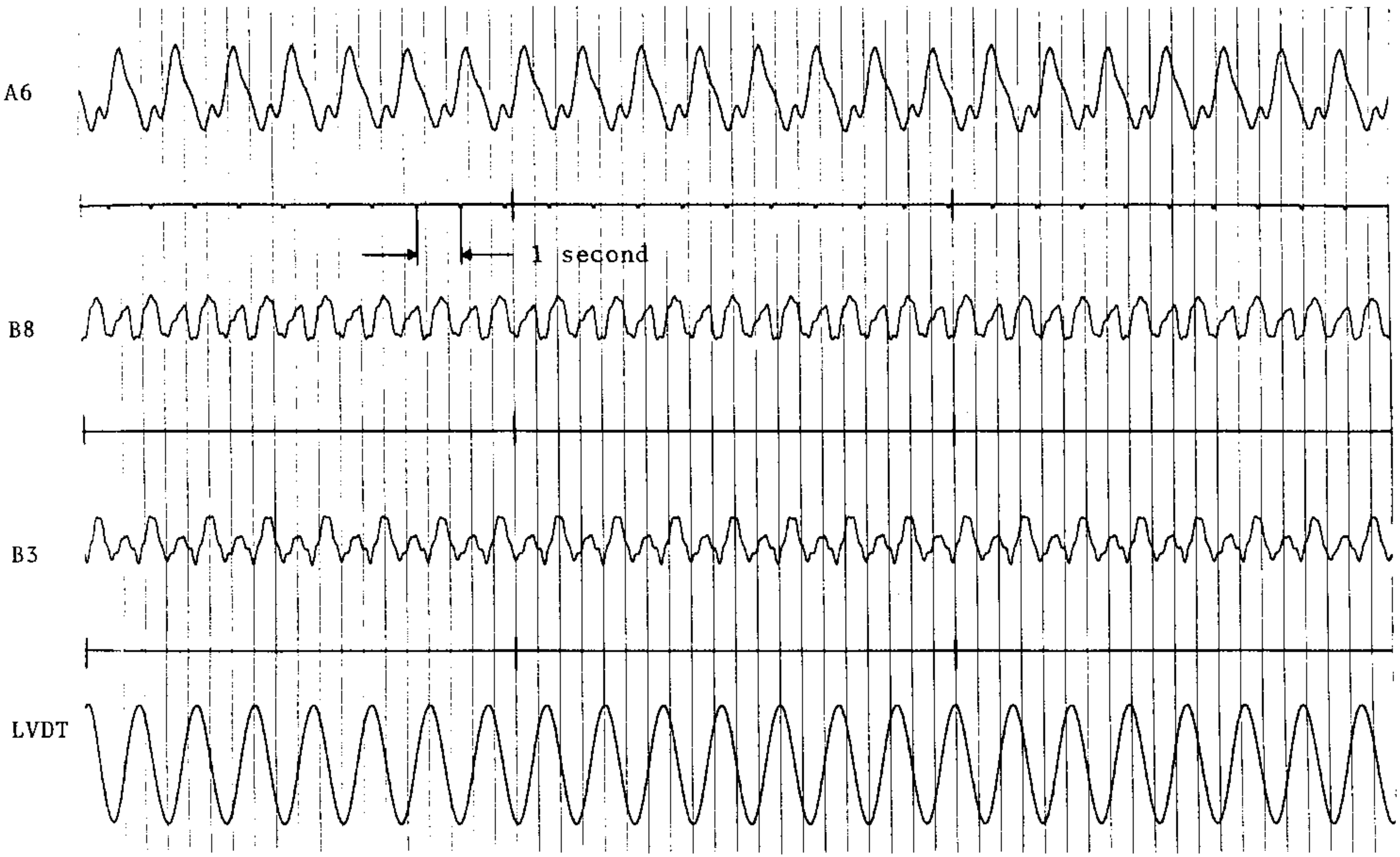

FIGURE 15T: LVDT: 0.174 D_e/DIVISION; STRAINS: 7.64 MICROSTRAIN/DIVISION

EXPERIMENT 18

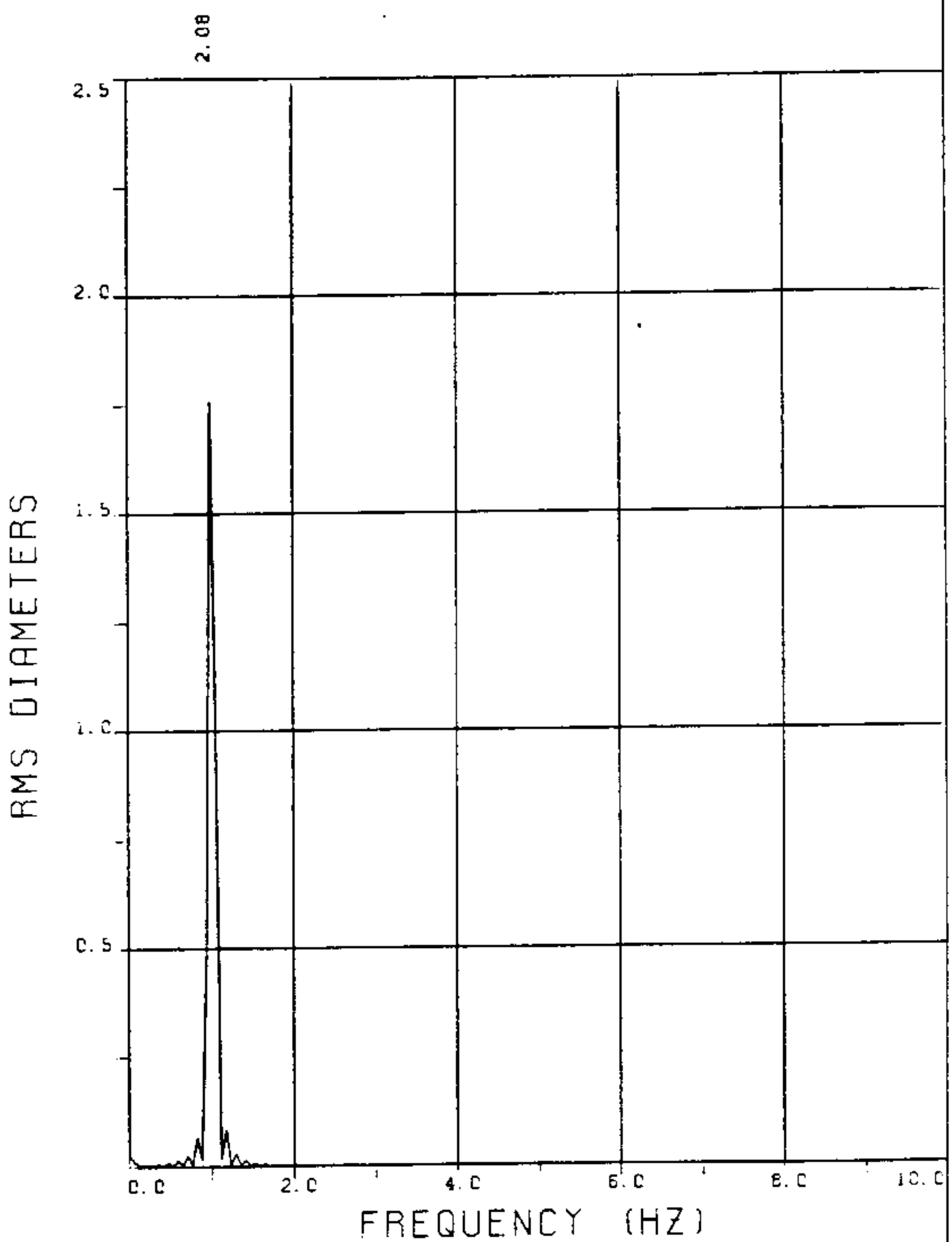

EXPERIMENT NUMBER 18

LVDT

THETA=0 VC=0 FE=1.000 BE=0.059

MEASURED A/DE=2.95

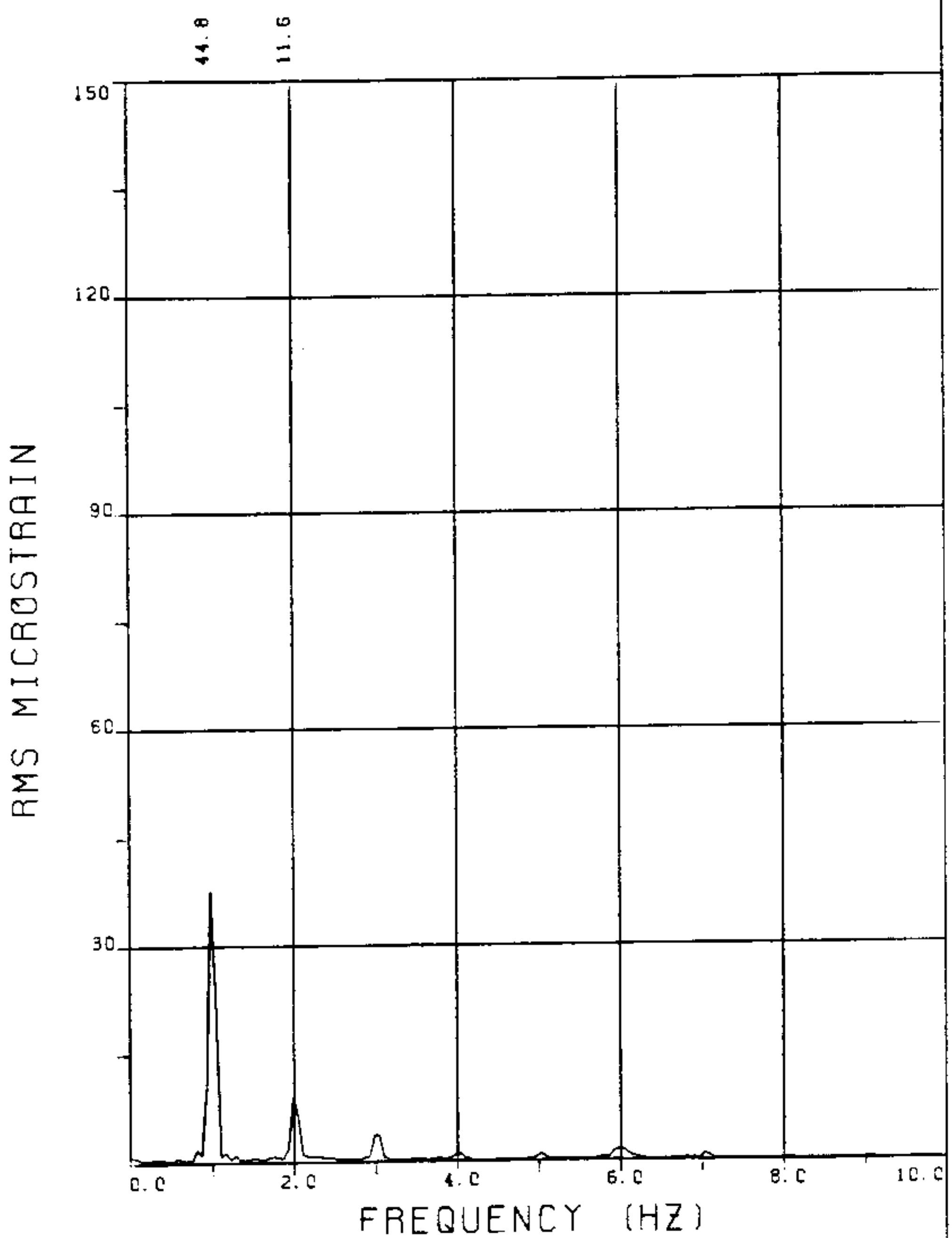

EXPERIMENT NUMBER 18

BRIDGE A8 ELEVATION=3L/11 BE=0.059

THETA=0 VC=0 FE=1.000 A/DE=2.95

MEASURED RESPONSE IN MICROSTRAIN

TOTAL DYNAMIC RMS=46.8

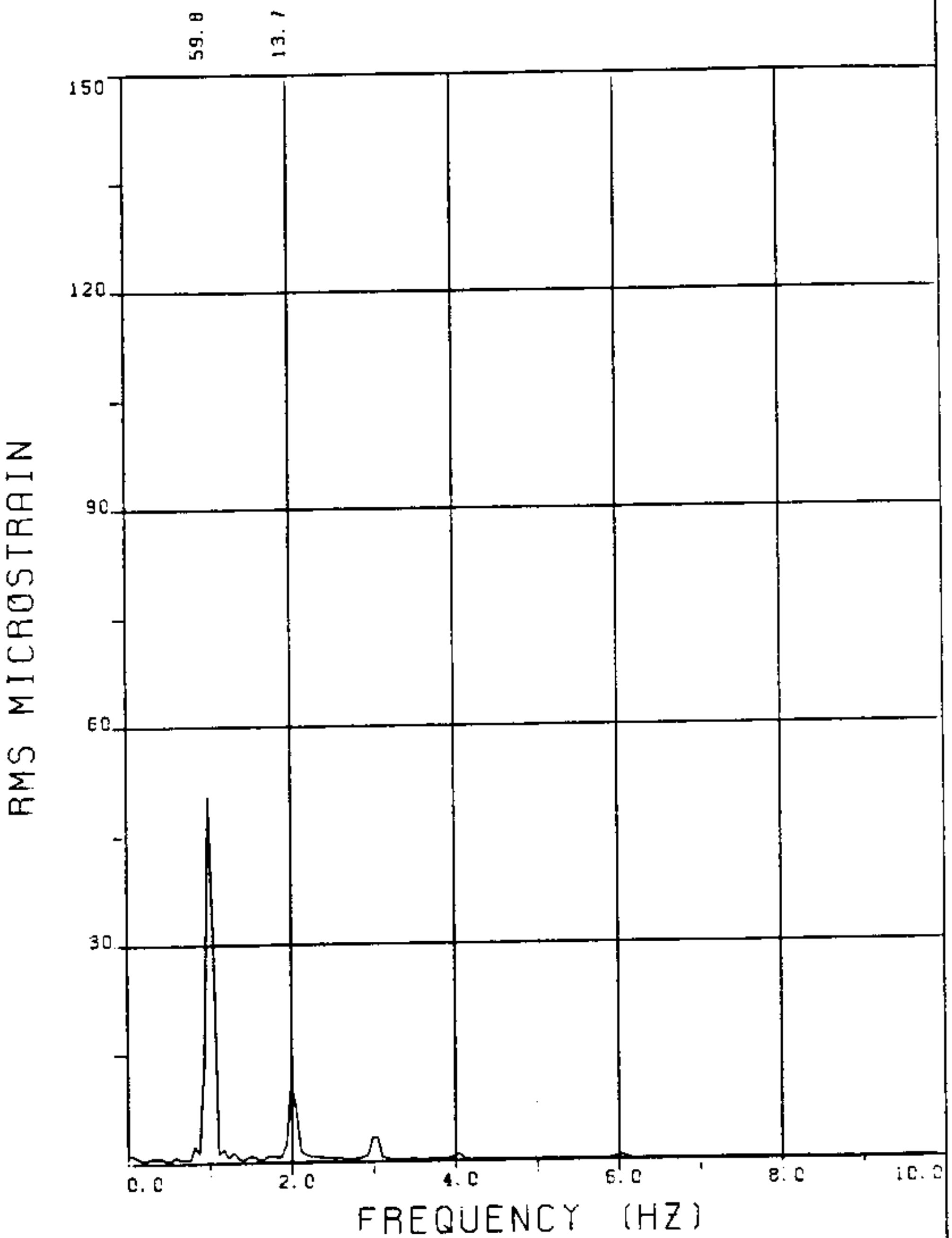

EXPERIMENT NUMBER 18

BRIDGE A6 ELEVATION=5L/11 BE=0.059

THETA=0 VC=0 FE=1.000 A/DE=2.95

MEASURED RESPONSE IN MICROSTRAIN

TOTAL DYNAMIC RMS=61.6

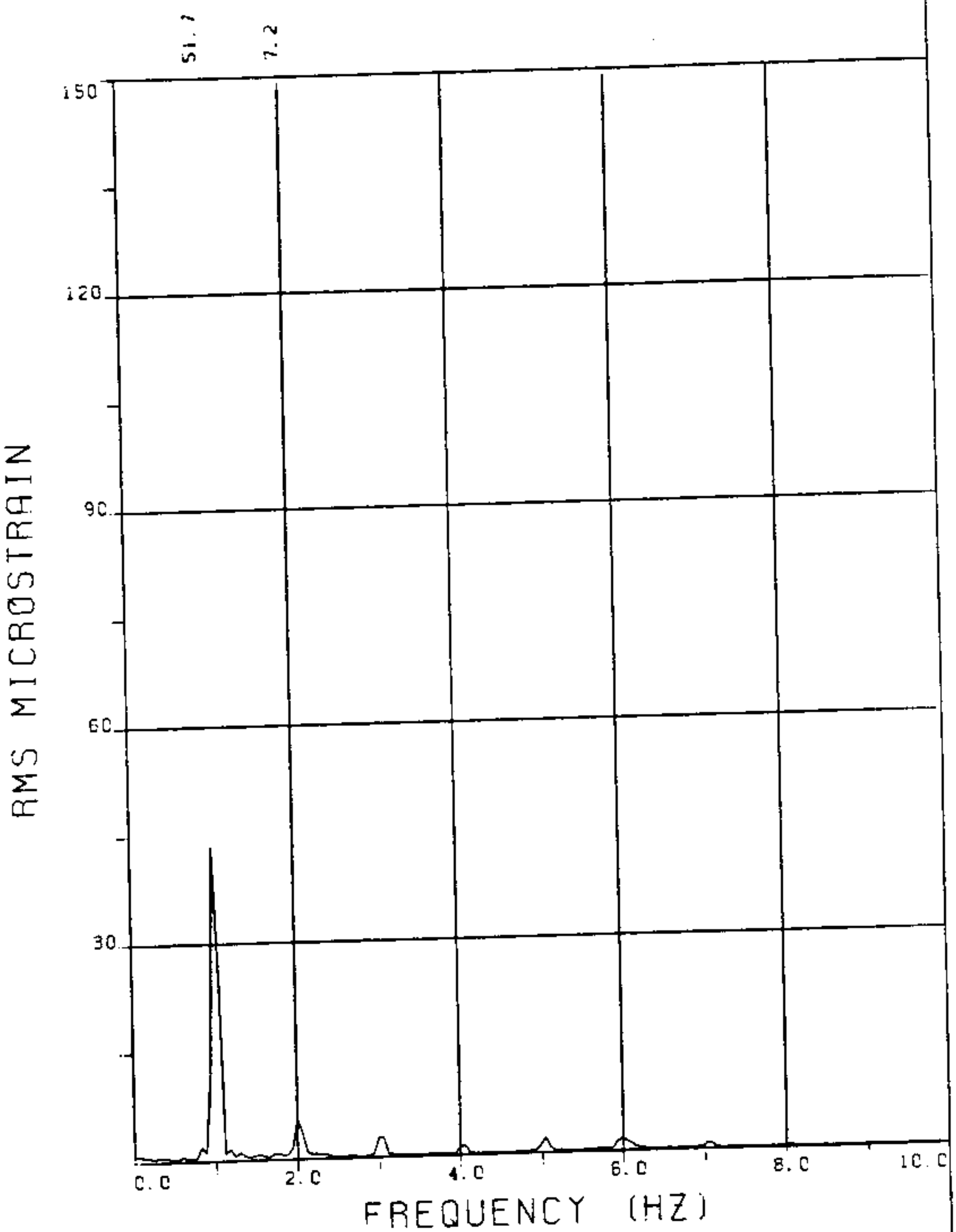

EXPERIMENT NUMBER 18

BRIDGE A3 ELEVATION=8L/11 BE=0.059

THETA=0 VC=0 FE=1.000 A/DE=2.95

MEASURED RESPONSE IN MICROSTRAIN

TOTAL DYNAMIC RMS=52.6

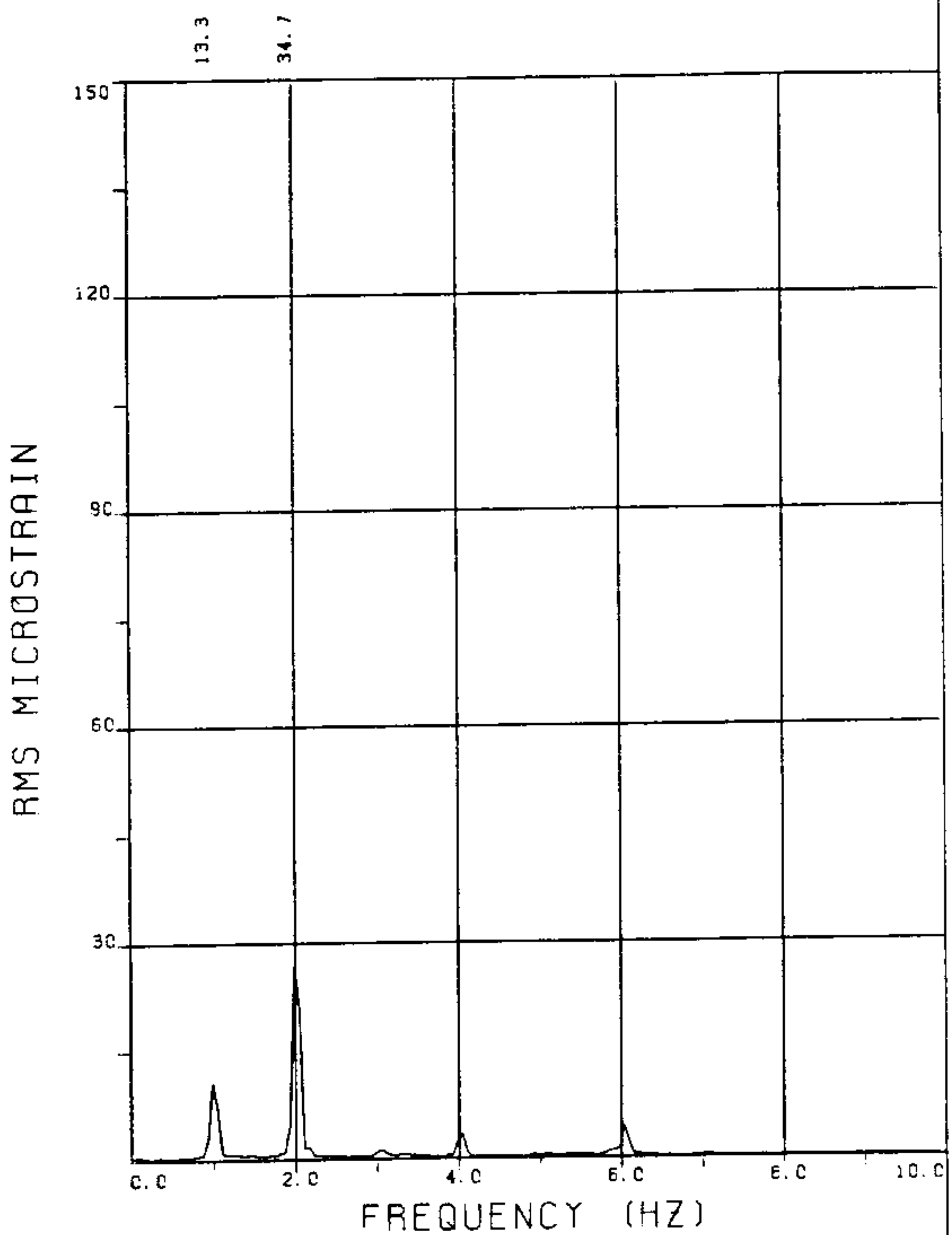

EXPERIMENT NUMBER 18

BRIDGE B8 ELEVATION=3L/11 BE=0.059

THETA=0 VC=0 FE=1.000 A/DE=2.95

MEASURED RESPONSE IN MICROSTRAIN

TOTAL DYNAMIC RMS=37.8

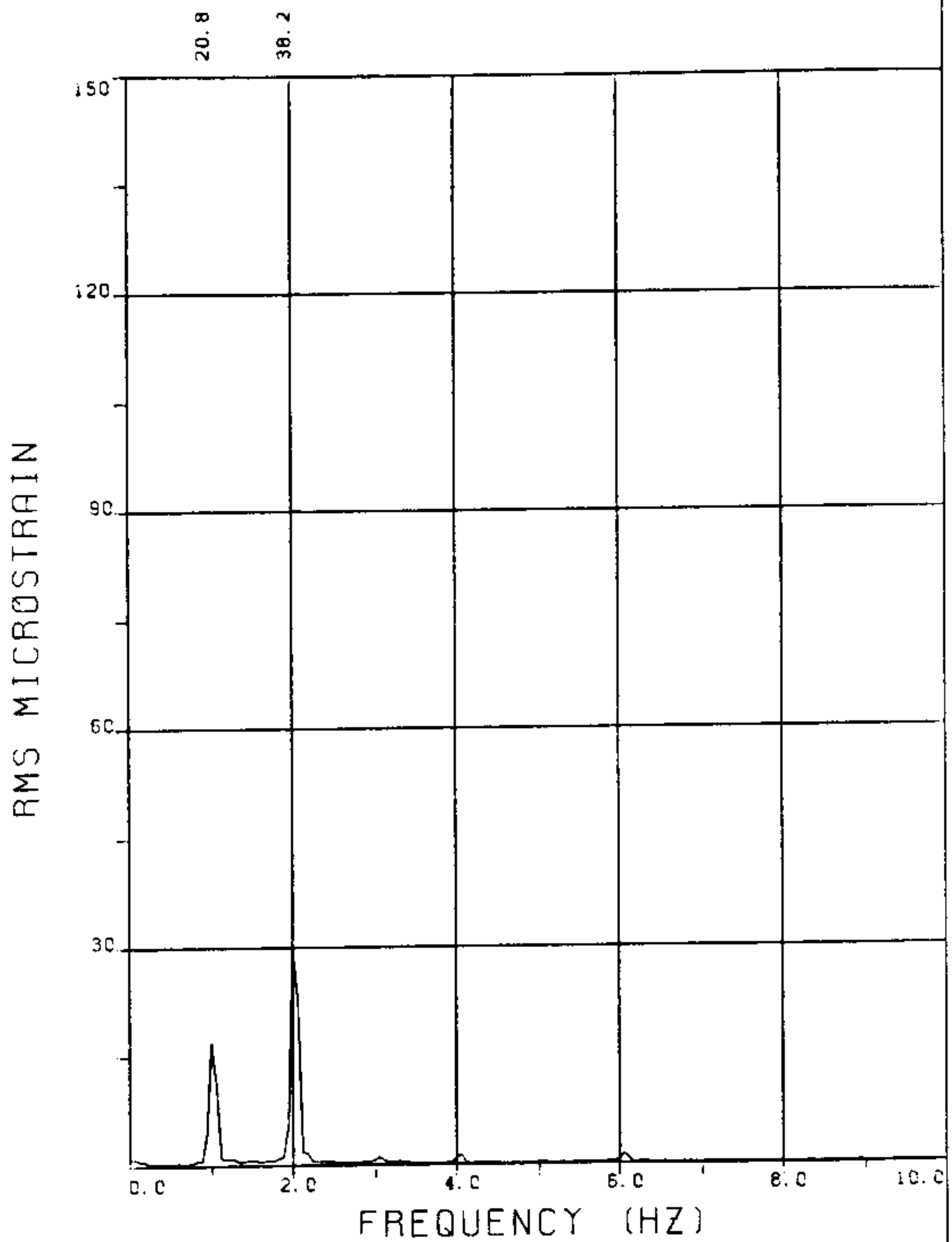

EXPERIMENT NUMBER 18

BRIDGE B5 ELEVATION=6L/11 BE=0.059

THETA=0 VC=0 FE=1.000 A/DE=2.95

MEASURED RESPONSE IN MICROSTRAIN

TOTAL DYNAMIC RMS=43.6

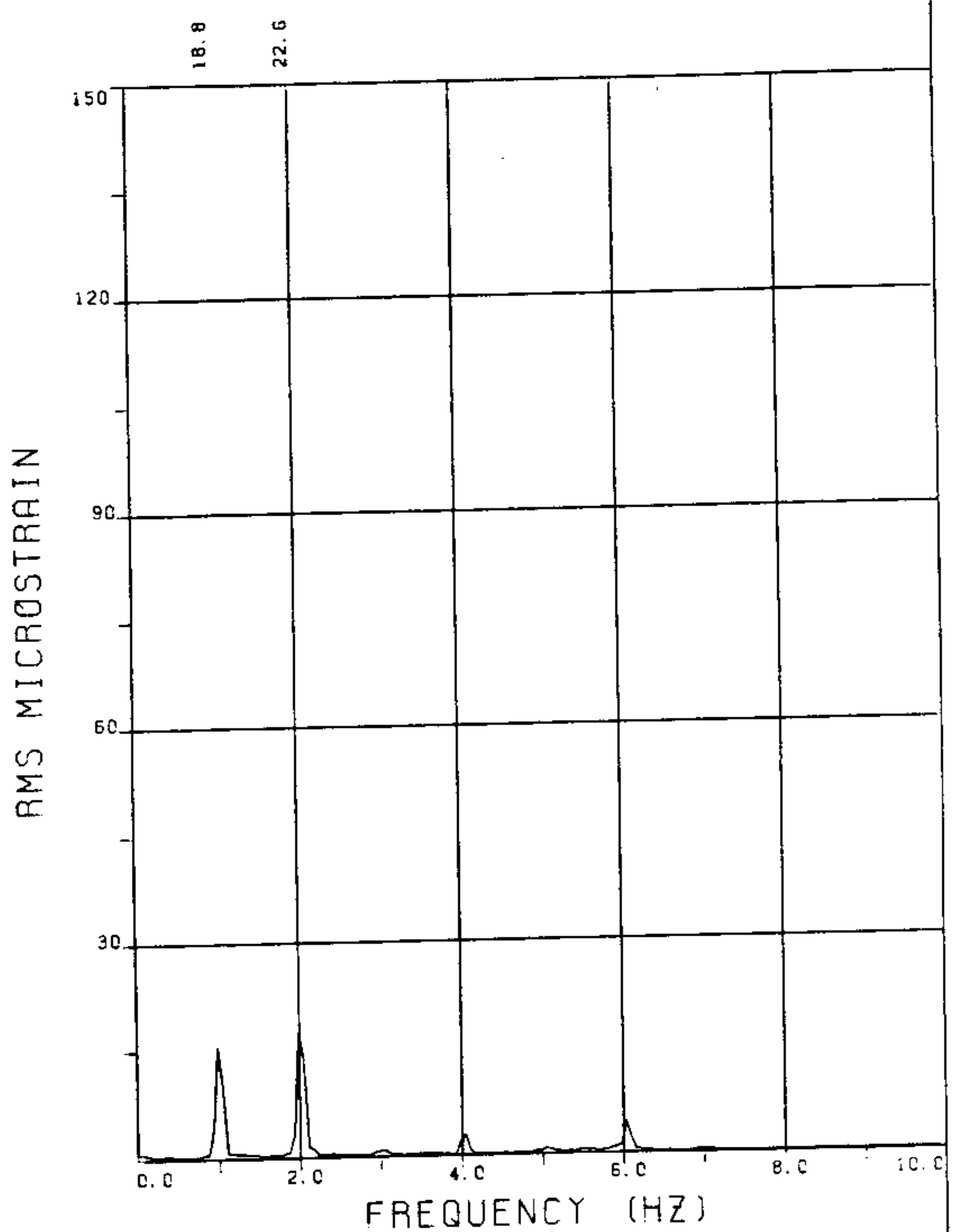

EXPERIMENT NUMBER 18

BRIDGE B3 ELEVATION=8L/11 BE=0.059

THETA=0 VC=0 FE=1.000 A/DE=2.95

MEASURED RESPONSE IN MICROSTRAIN

TOTAL DYNAMIC RMS=30.3

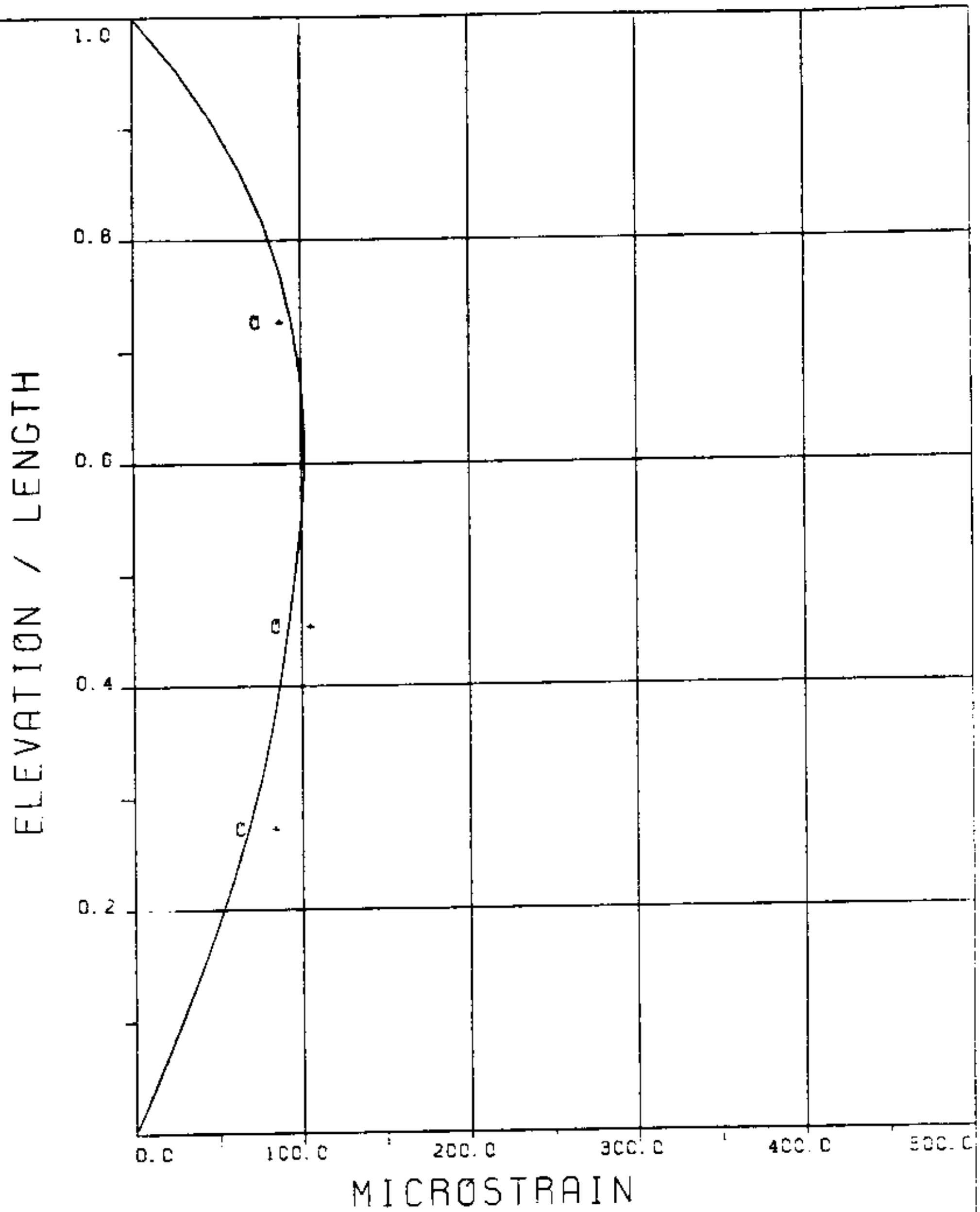

EXPERIMENT NUMBER 18

THETA=0 VC=0 FE=1.000 A/DE=2.95

DYNAMIC RESPONSE AT F=FE IN PLANE A

——— THEORY o o o EXPERIMENT

MAXIMUM DYNAMIC RESPONSE IN PLANE A

——— THEORY + + + EXPERIMENT

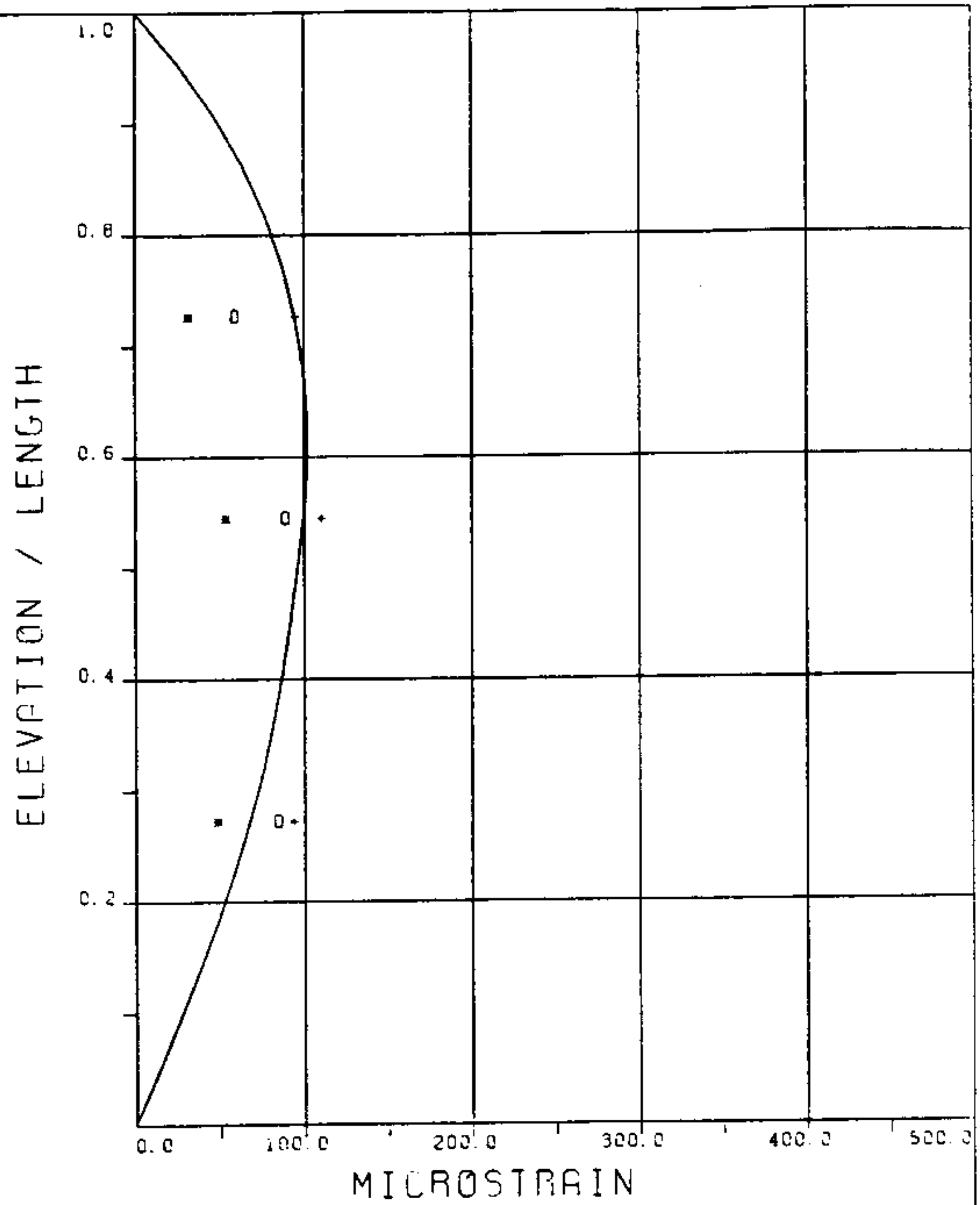

EXPERIMENT NUMBER 18

THETA=0 VC=0 FE=1.000 A/DE=2.95

DYNAMIC RESPONSE IN PLANE B AT F=2FE

* * * EXPERIMENT

MAXIMUM RESPONSE IN PLANE B

o o o EXPERIMENT

MAXIMUM RESPONSE

———— THEORY + + + EXPERIMENT

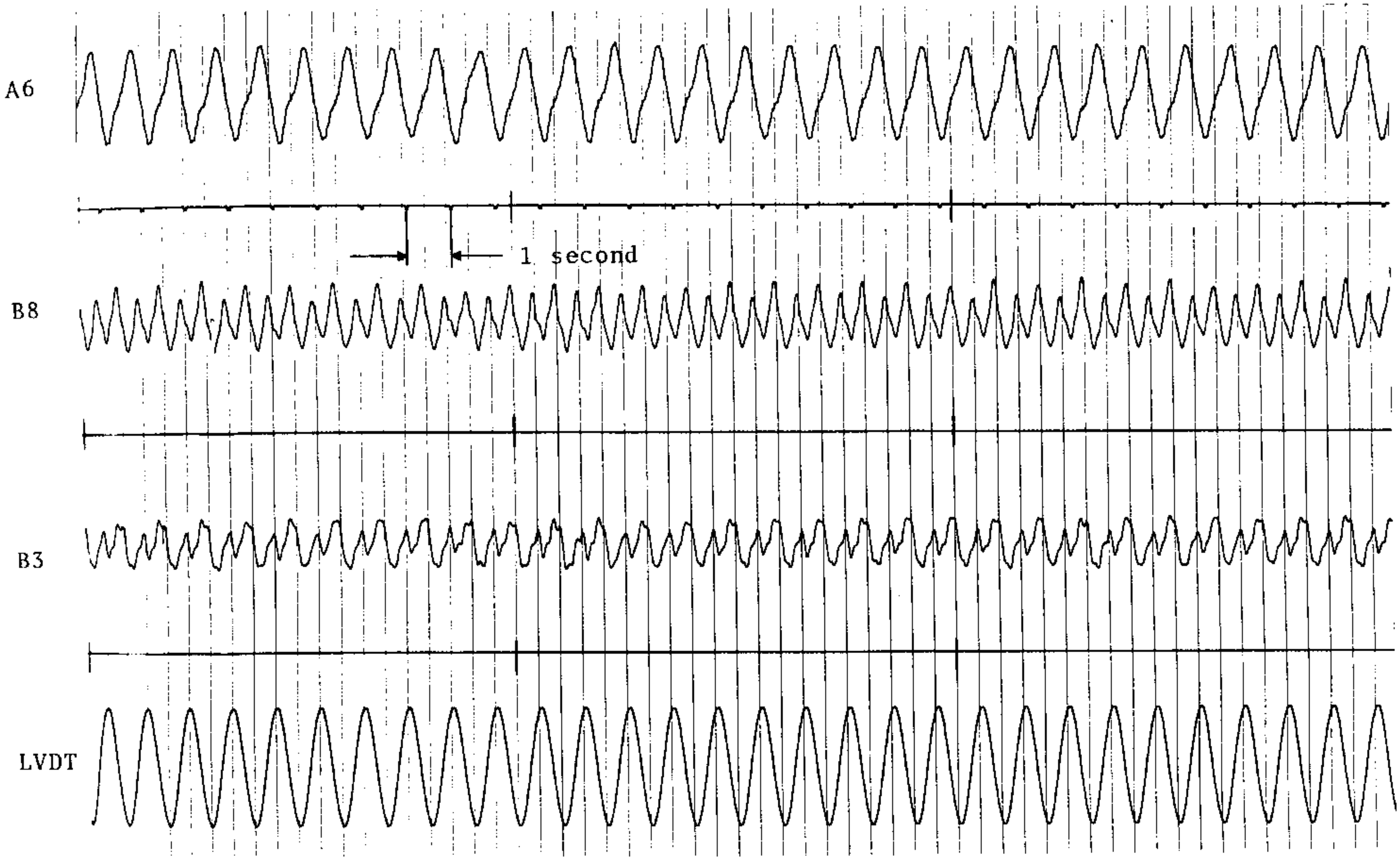

FIGURE 18T: LVDT: 0.174 D_e/DIVISION; STRAINS: 7.64 MICROSTRAIN/DIVISION

EXPERIMENT 21

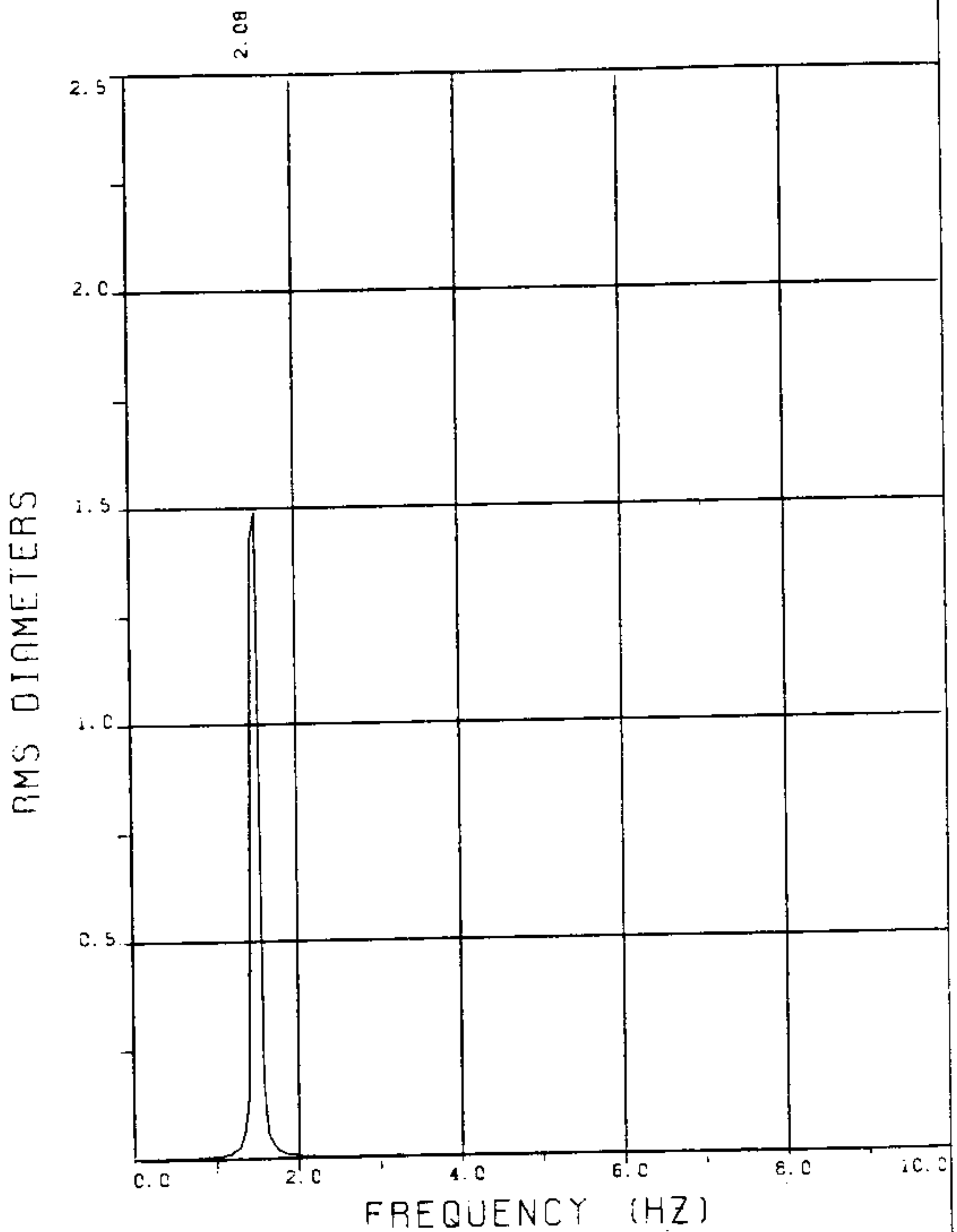

EXPERIMENT NUMBER 21

LVDT

THETA=0 VC=0 FE=1.500 BE=0.059

MEASURED A/DE=2.94

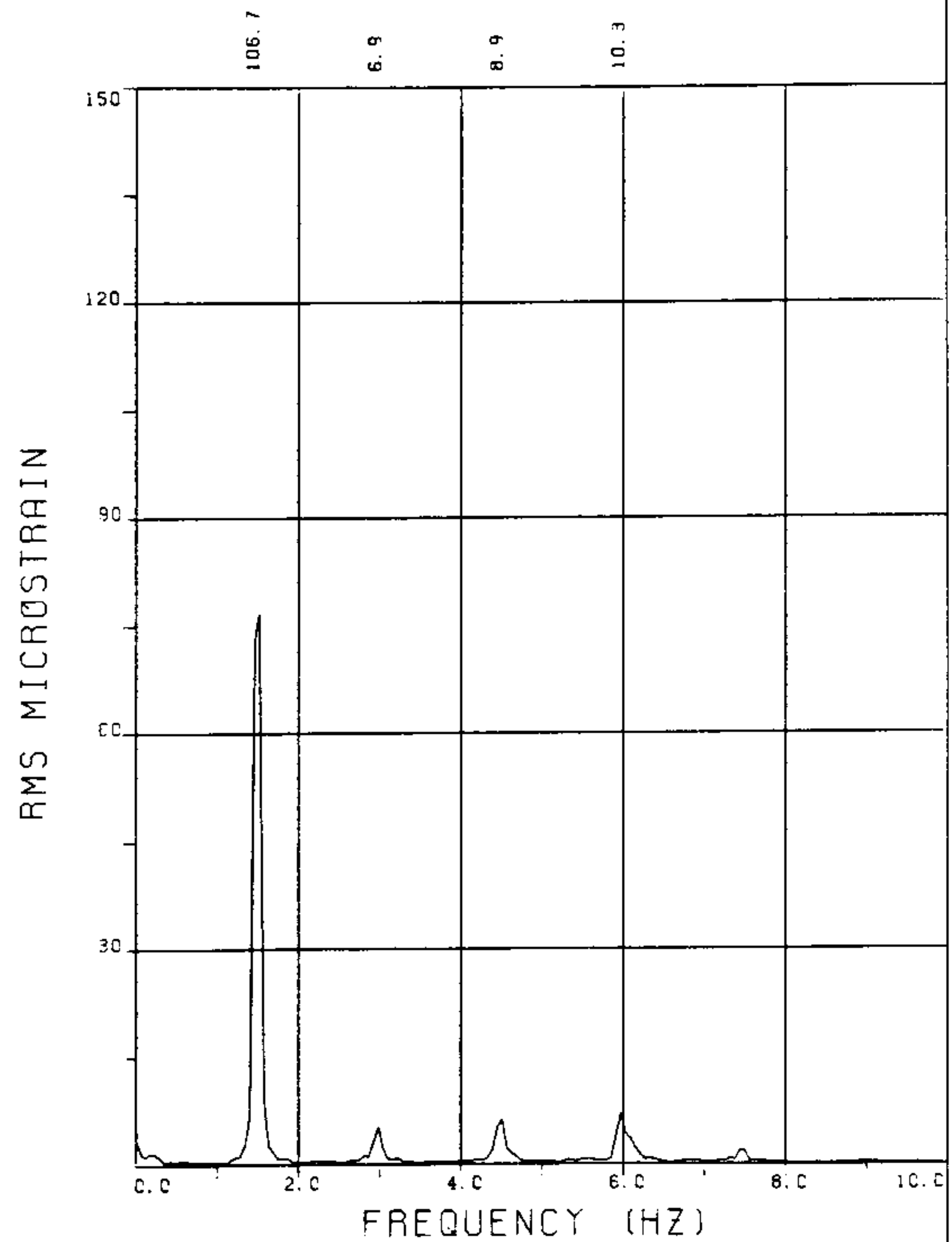

EXPERIMENT NUMBER 21

BRIDGE A8 ELEVATION=3L/11 BE=0.059

THETA=0 VC=0 FE=1.500 A/DE=2.94

MEASURED RESPONSE IN MICROSTRAIN

TOTAL DYNAMIC RMS=108.0

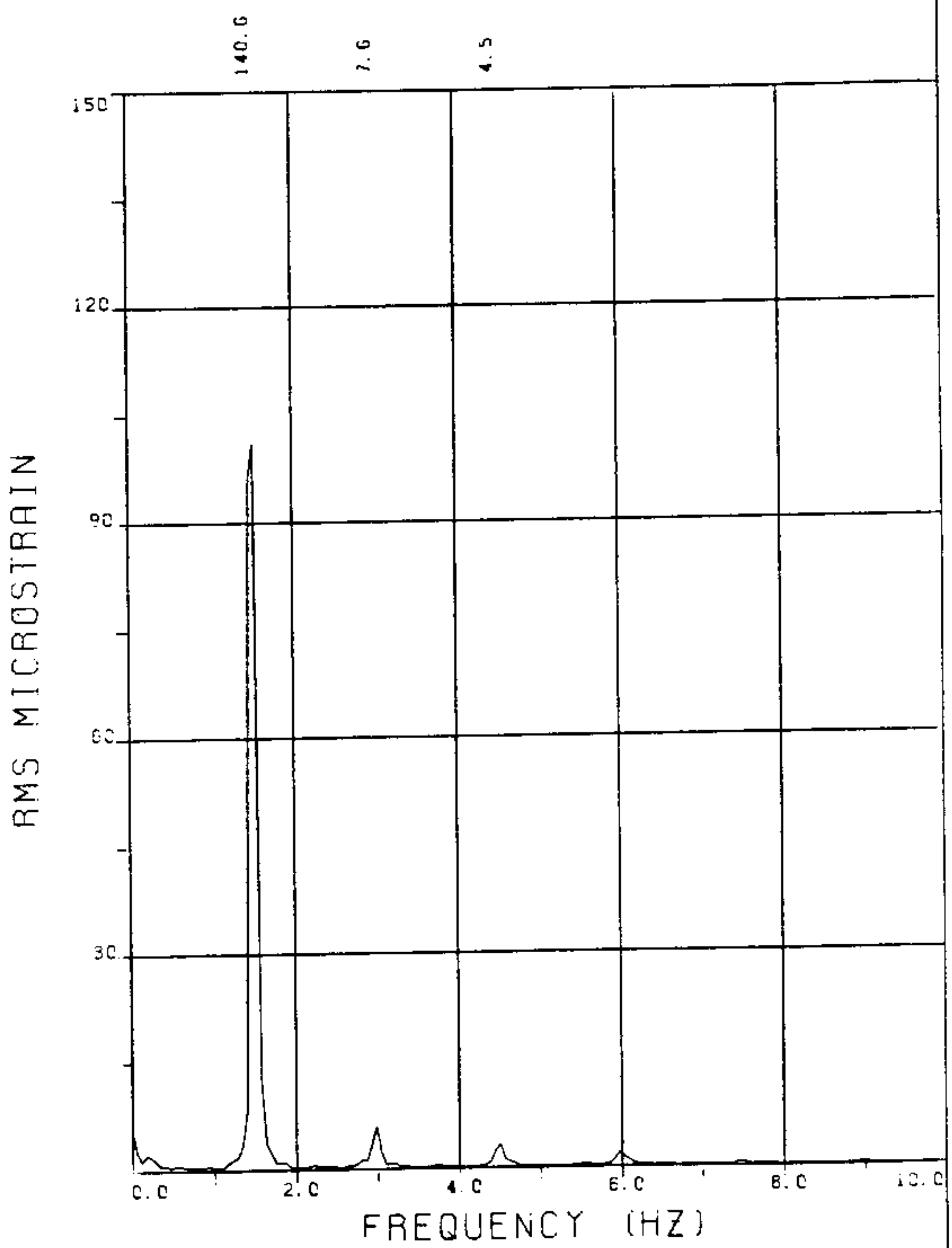

EXPERIMENT NUMBER 21

BRIDGE A6 ELEVATION=5L/11 BE=0.059

THETA=0 VC=0 FE=1.500 A/DE=2.94

MEASURED RESPONSE IN MICROSTRAIN

TOTAL DYNAMIC RMS=141.2

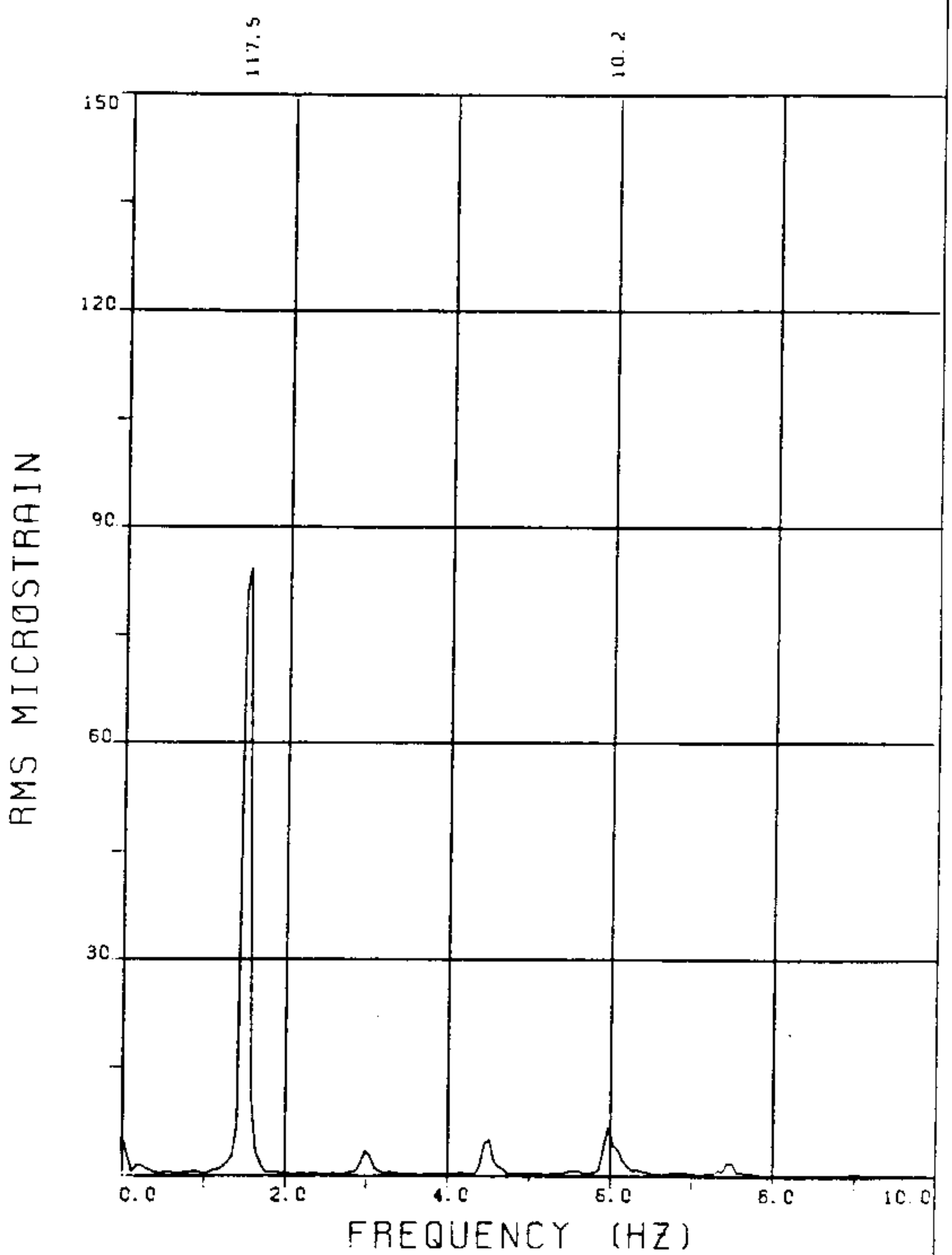

EXPERIMENT NUMBER 21

BRIDGE A3 ELEVATION=8L/11 BE=0.059

THETA=0 VC=0 FE=1.500 A/DE=2.94

MEASURED RESPONSE IN MICROSTRAIN

TOTAL DYNAMIC RMS=118.6

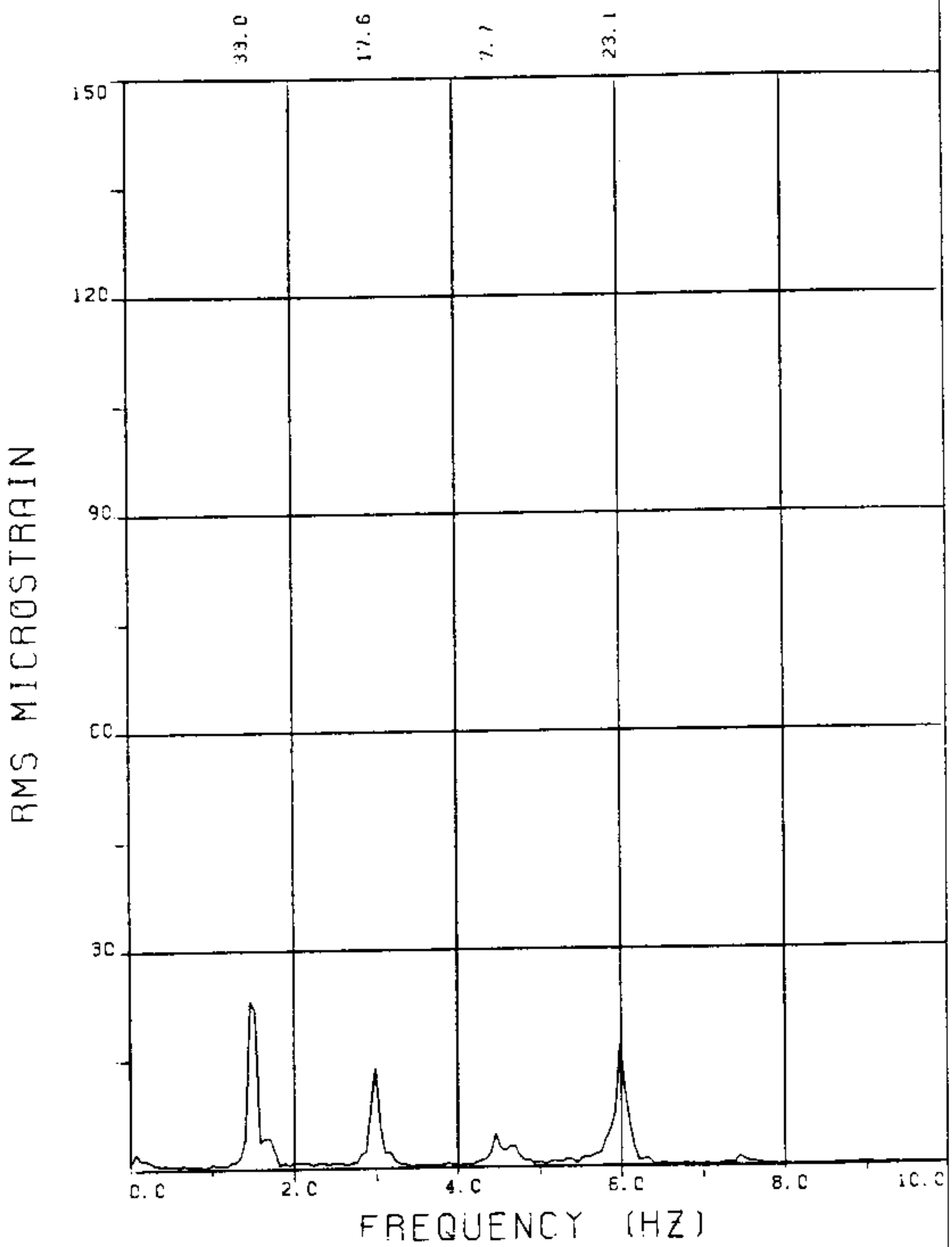

EXPERIMENT NUMBER 21

BRIDGE B8 ELEVATION=3L/11 BE=0.059

THETA=0 VC=0 FE=1.500 A/DE=2.94

MEASURED RESPONSE IN MICROSTRAIN

TOTAL DYNAMIC RMS=44.9

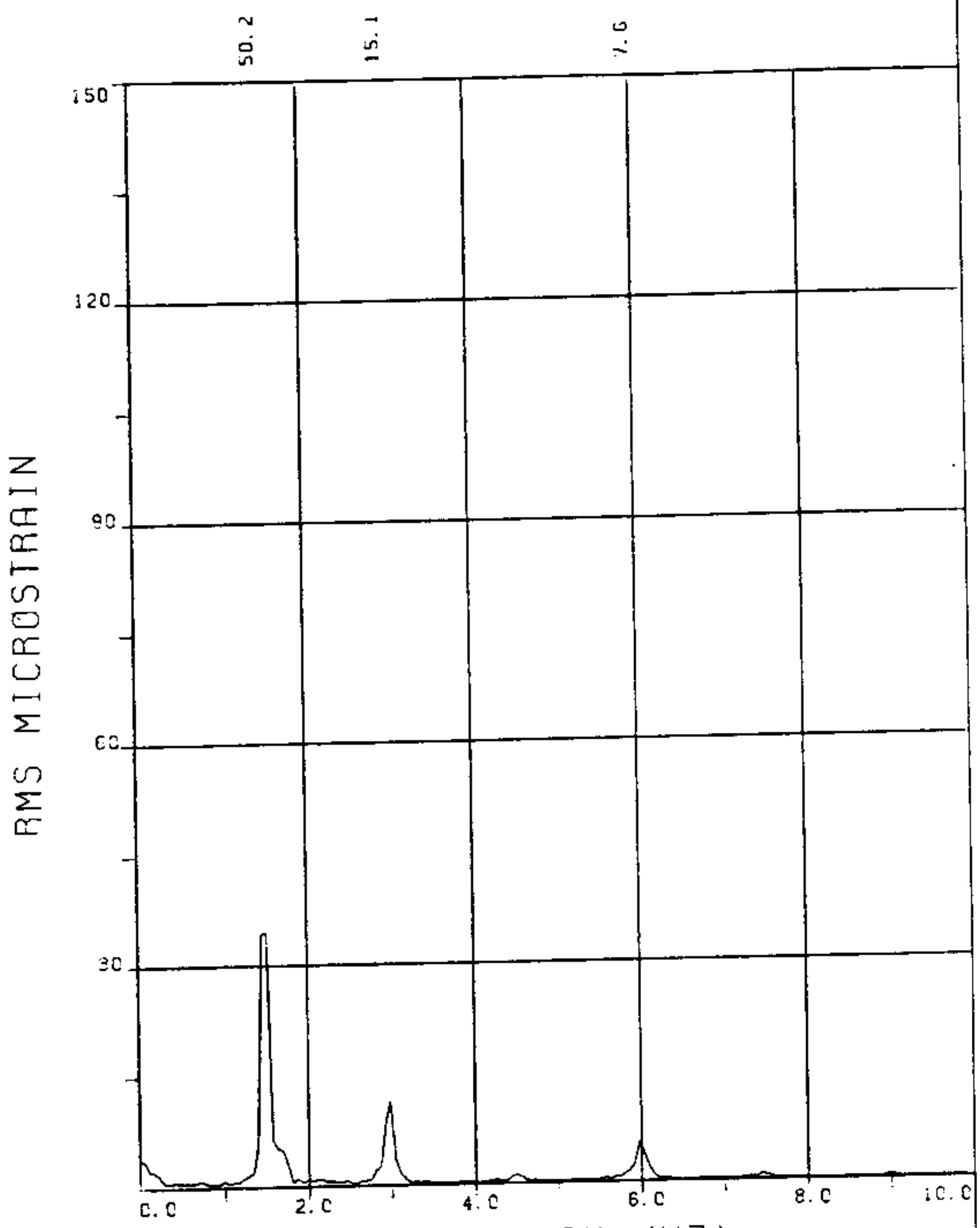

EXPERIMENT NUMBER 21

BRIDGE B5 ELEVATION=6L/11 BE=0.059

THETA=0 VC=0 FE=1.500 A/DE=2.94

MEASURED RESPONSE IN MICROSTRAIN

TOTAL DYNAMIC RMS=53.5

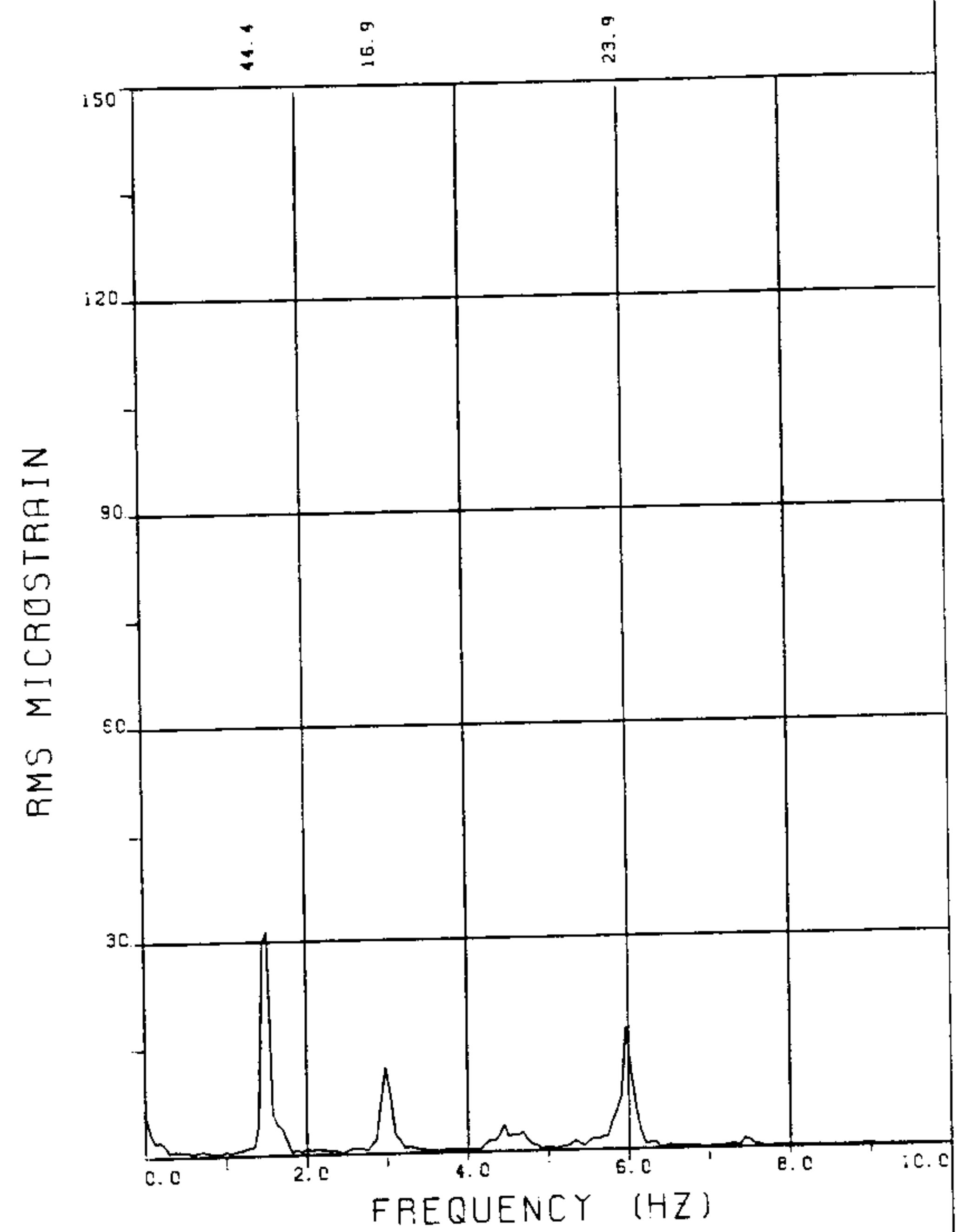

EXPERIMENT NUMBER 21

BRIDGE B3 ELEVATIØN=8L/11 BE=0.059

THETA=0 VC=0 FE=1.500 A/DE=2.94

MEASURED RESPONSE IN MICRØSTRAIN

TØTAL DYNAMIC RMS=54.4

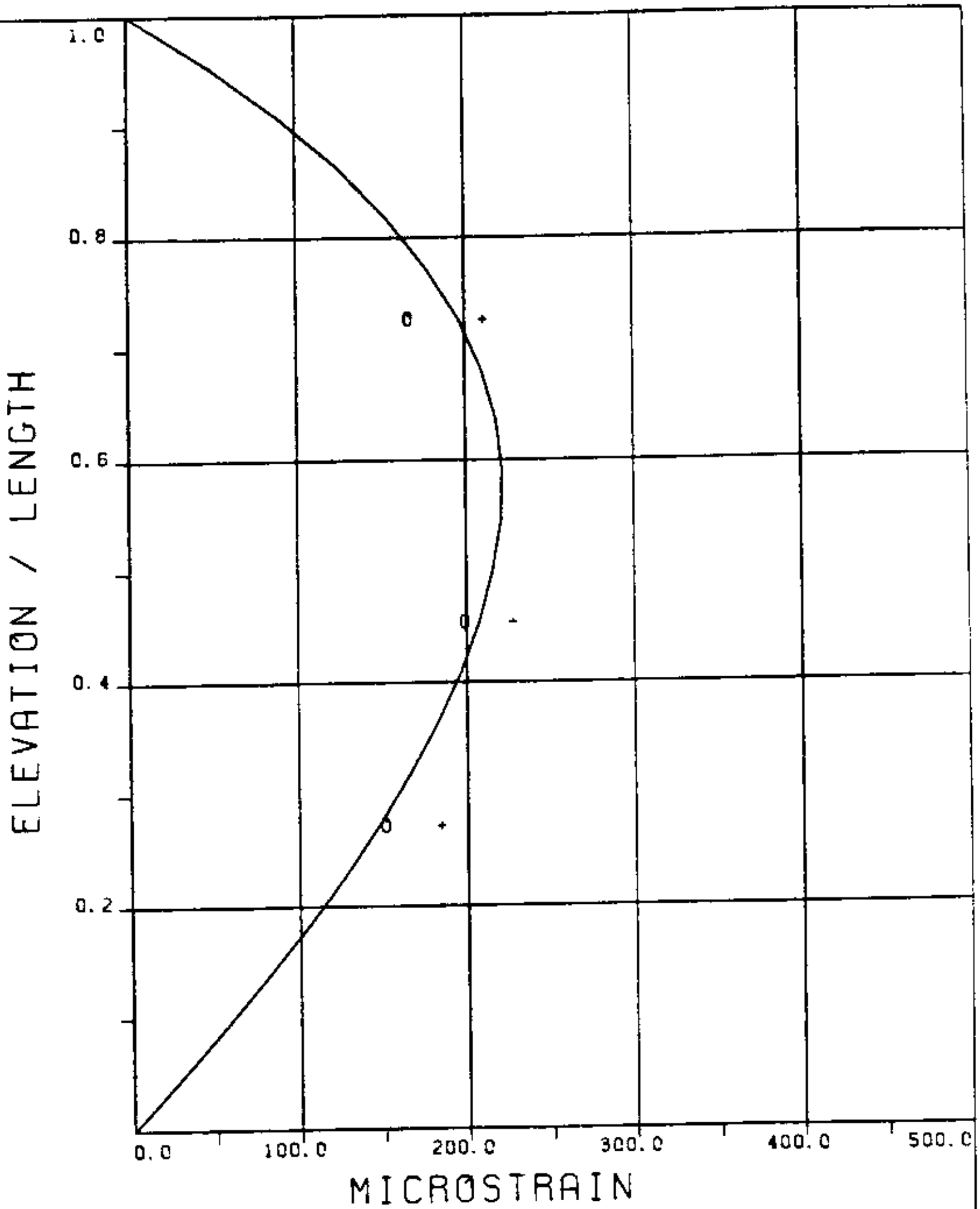

EXPERIMENT NUMBER 21

THETA=0 VC=0 FE=1.500 A/DE=2.94

DYNAMIC RESPONSE AT F=FE IN PLANE A

______ THEORY o o o EXPERIMENT

MAXIMUM DYNAMIC RESPONSE IN PLANE A

______ THEORY + + + EXPERIMENT

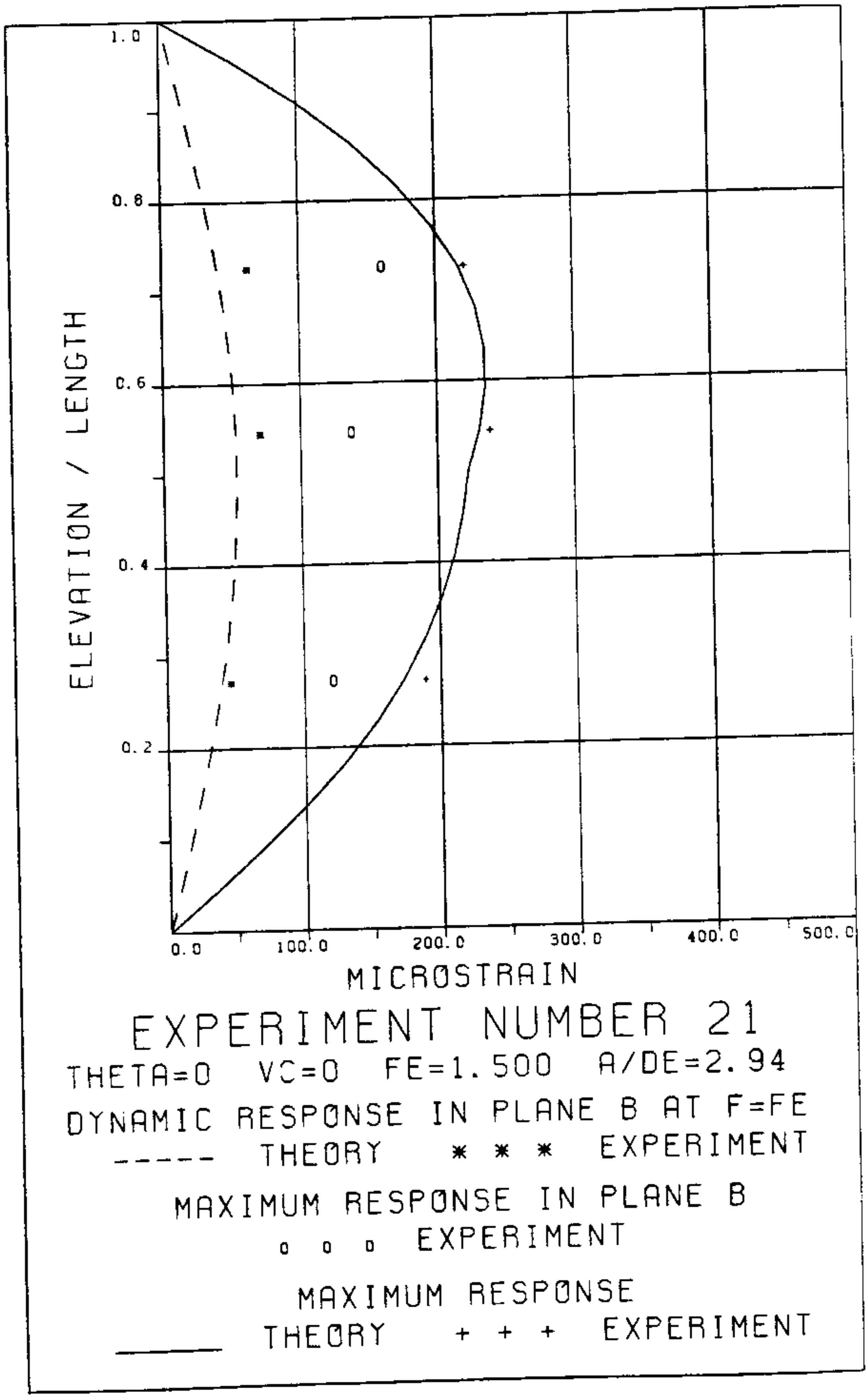
1.0
0.8
0.6
0.4
0.2
0.0
100.0
200.0
300.0
400.0
500.0
ELEVATION / LENGTH
MICROSTRAIN
EXPERIMENT NUMBER 21
THETA=0 VC=0 FE=1.500 A/DE=2.94
DYNAMIC RESPONSE IN PLANE B AT F=FE
----- THEORY * * * EXPERIMENT
MAXIMUM RESPONSE IN PLANE B
o o o EXPERIMENT
MAXIMUM RESPONSE
THEORY + + + EXPERIMENT

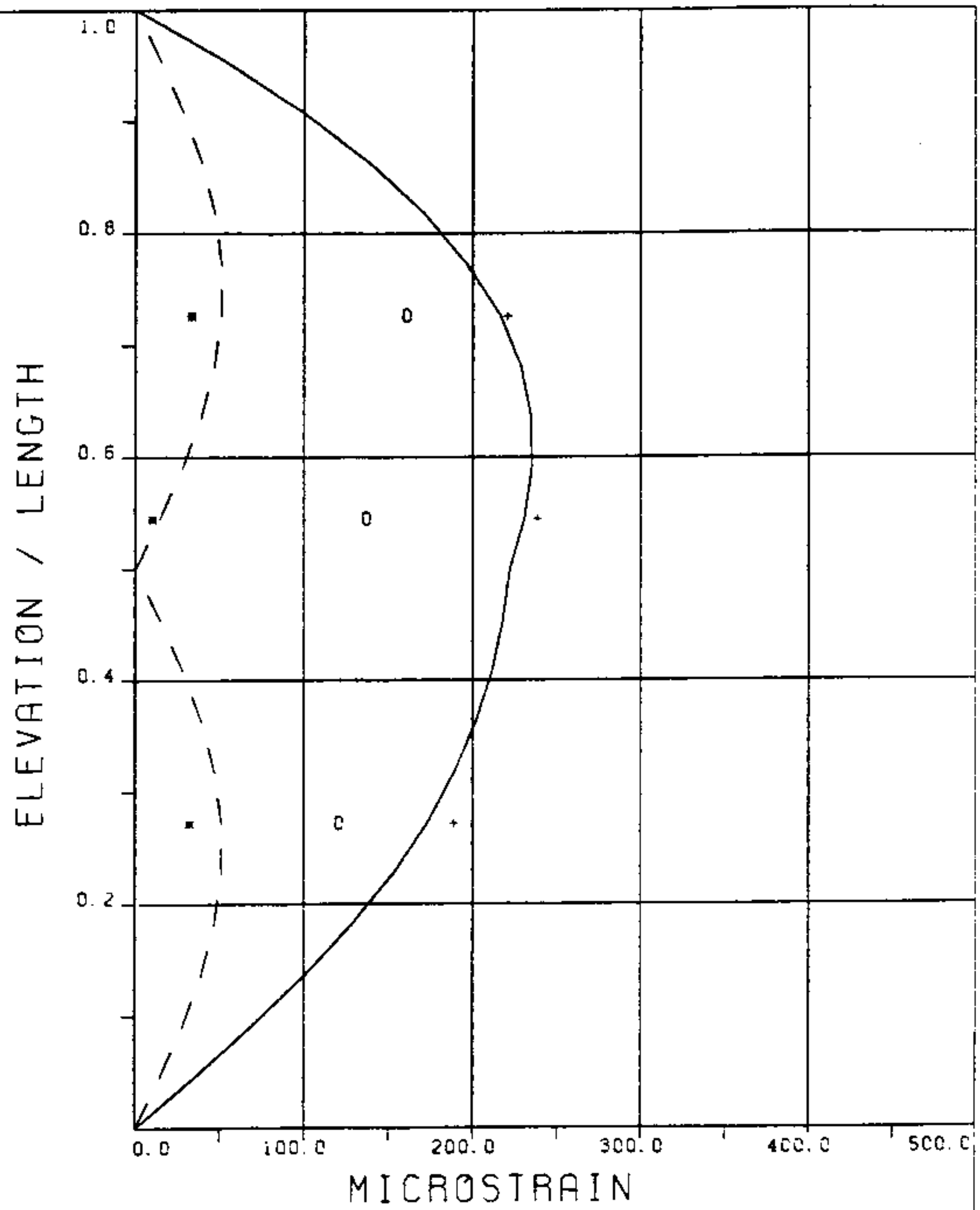

EXPERIMENT NUMBER 21

THETA=0 VC=0 FE=1.500 A/DE=2.94

DYNAMIC RESPONSE IN PLANE B AT F=4FE

----- THEORY * * * EXPERIMENT

MAXIMUM RESPONSE IN PLANE B

o o o EXPERIMENT

MAXIMUM RESPONSE

——— THEORY + + + EXPERIMENT

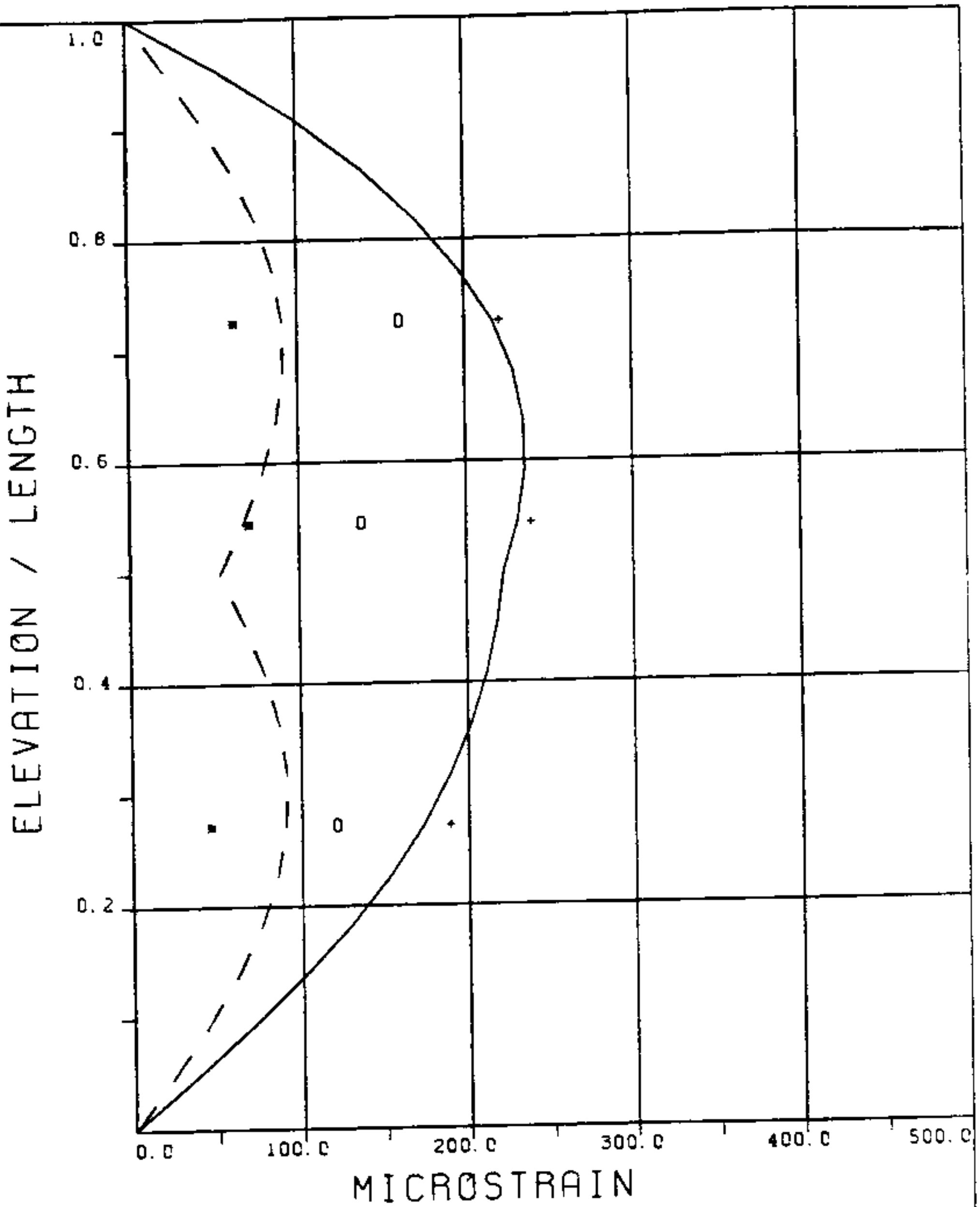

EXPERIMENT NUMBER 21

THETA=0 VC=0 FE=1.500 A/DE=2.94

DYNAMIC RESPONSE IN PLANE B AT F=FE

* * * EXPERIMENT

MAXIMUM RESPONSE IN PLANE B

----- THEORY o o o EXPERIMENT

MAXIMUM RESPONSE

______ THEORY + + + EXPERIMENT

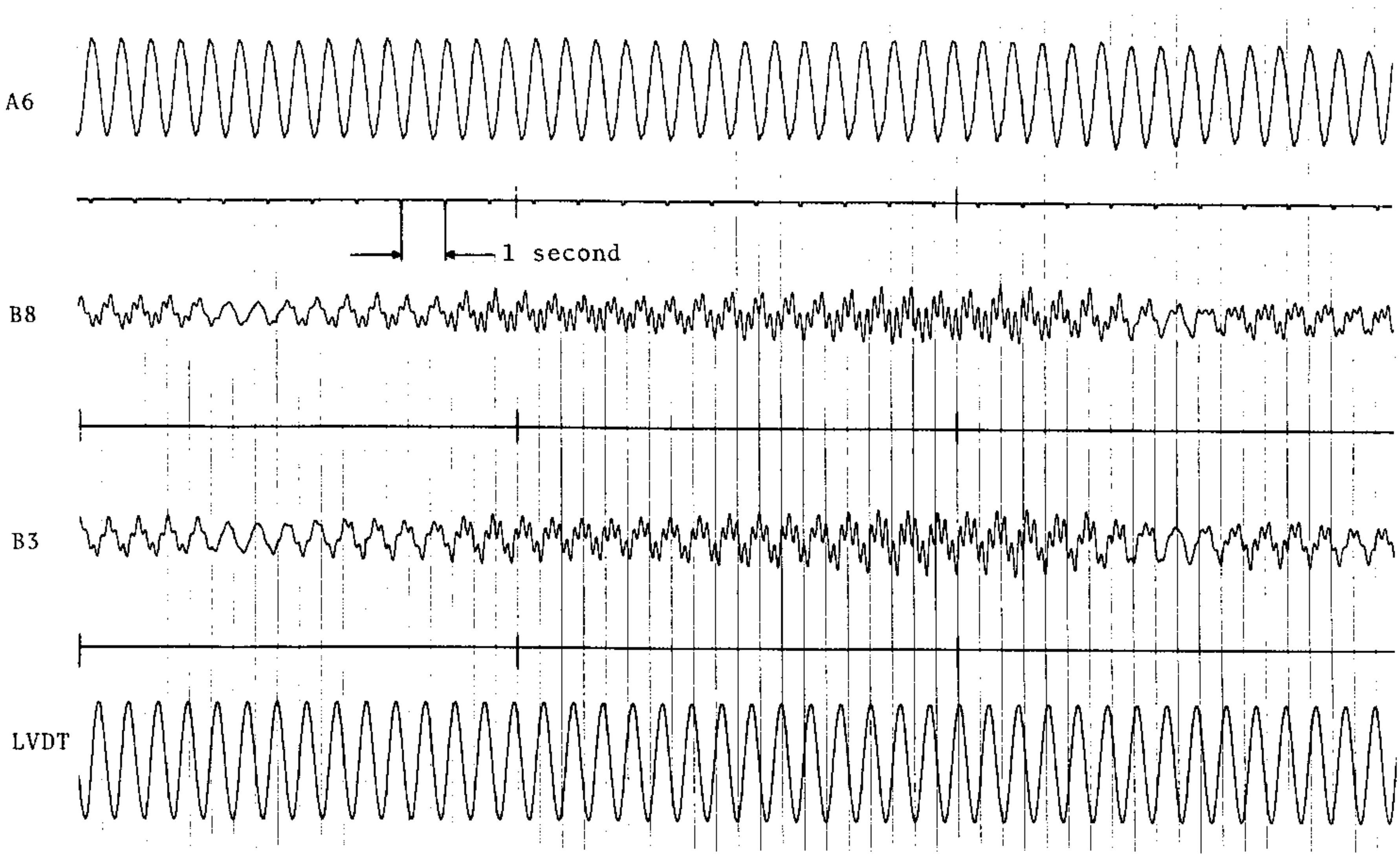

FIGURE 21Ta: LVDT: 0.174 D_e/DIVISION; STRAINS: 15.3 MICROSTRAIN/DIVISION

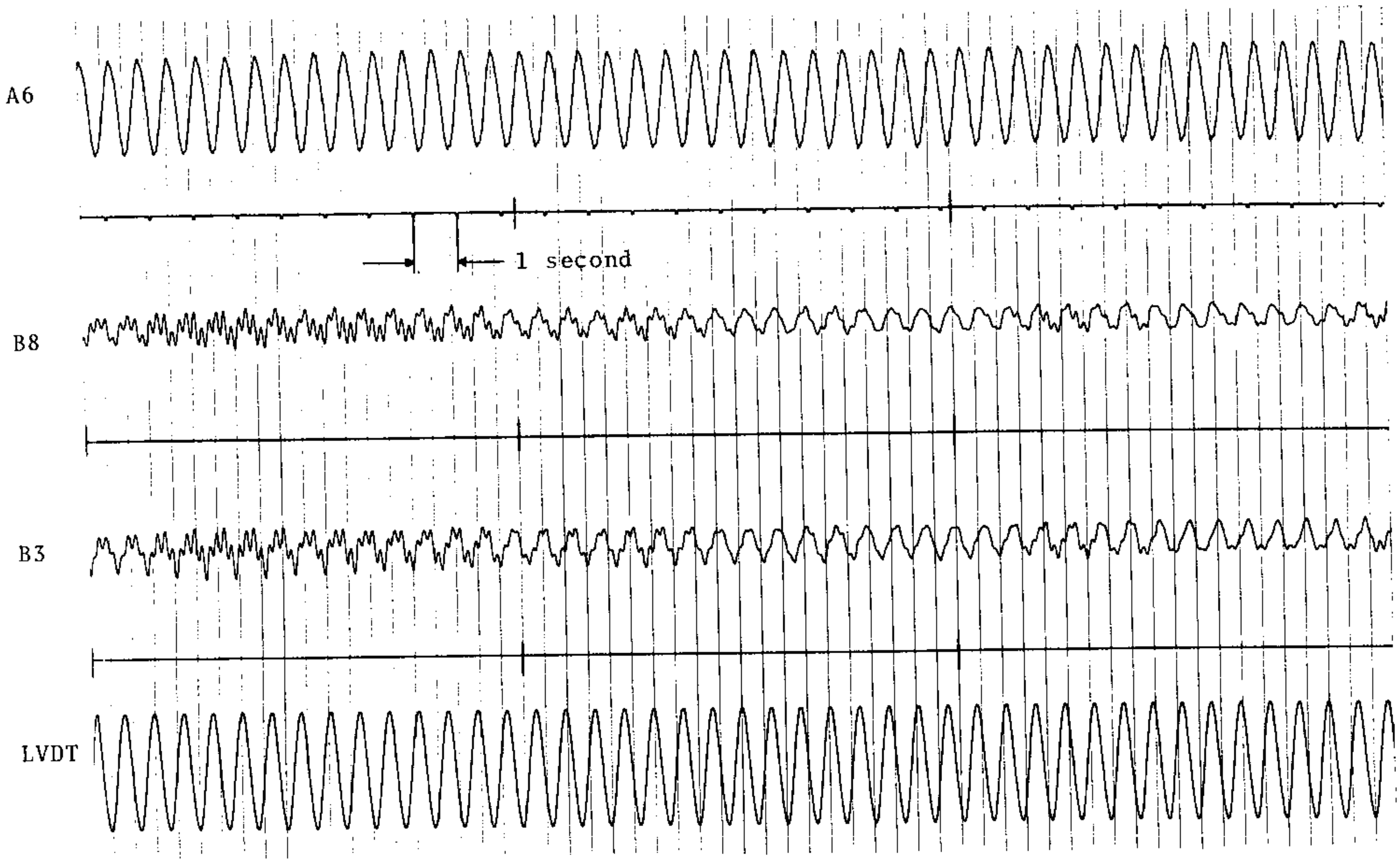

FIGURE 21Tb: LVDT: 0.174 D_e/DIVISION; STRAINS: 15.3 MICROSTRAIN/DIVISION

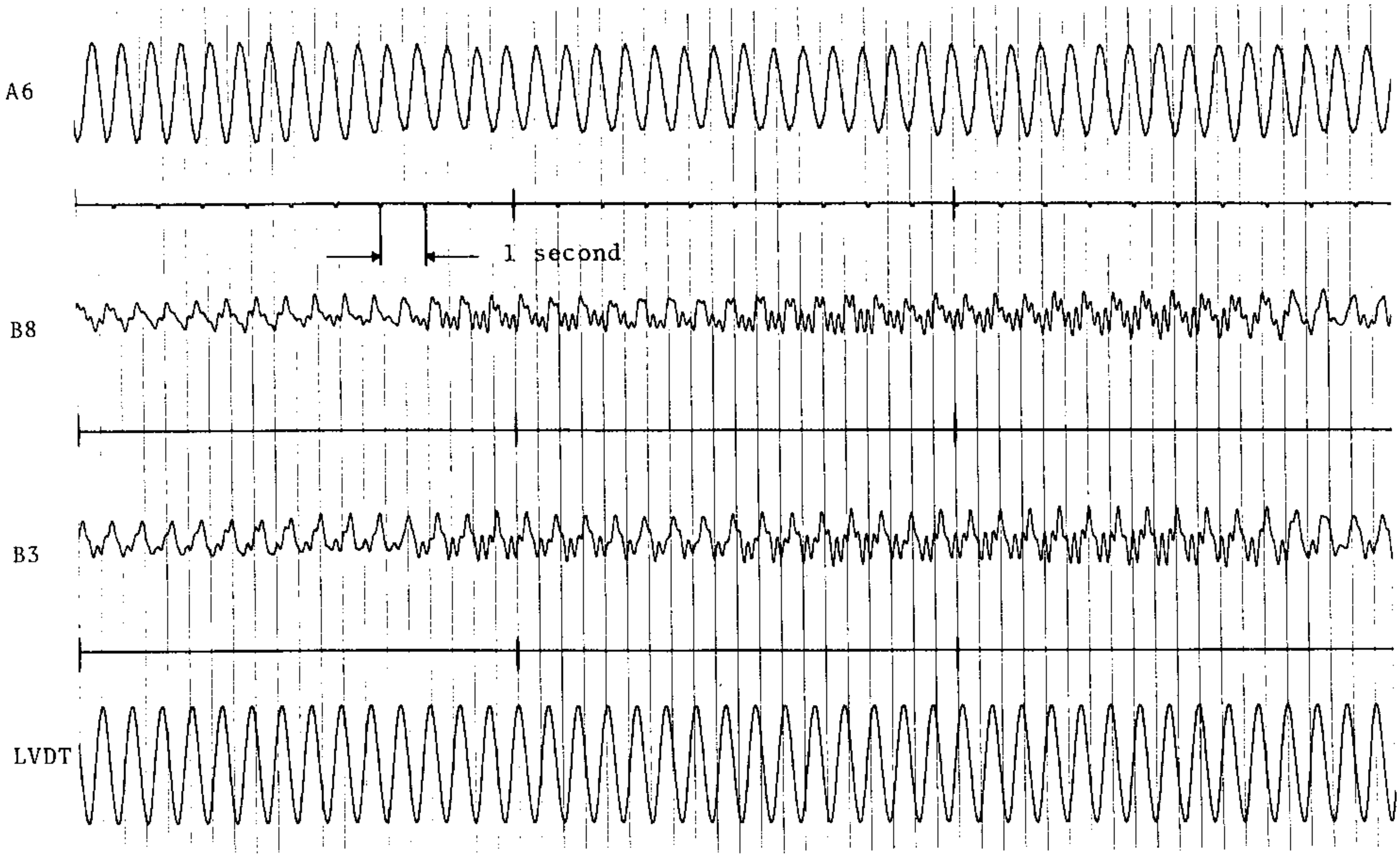

FIGURE 21Tc: LVDT: 0.174 D_e/DIVISION; STRAINS: 15.3 MICROSTRAIN/DIVISION

EXPERIMENT 48

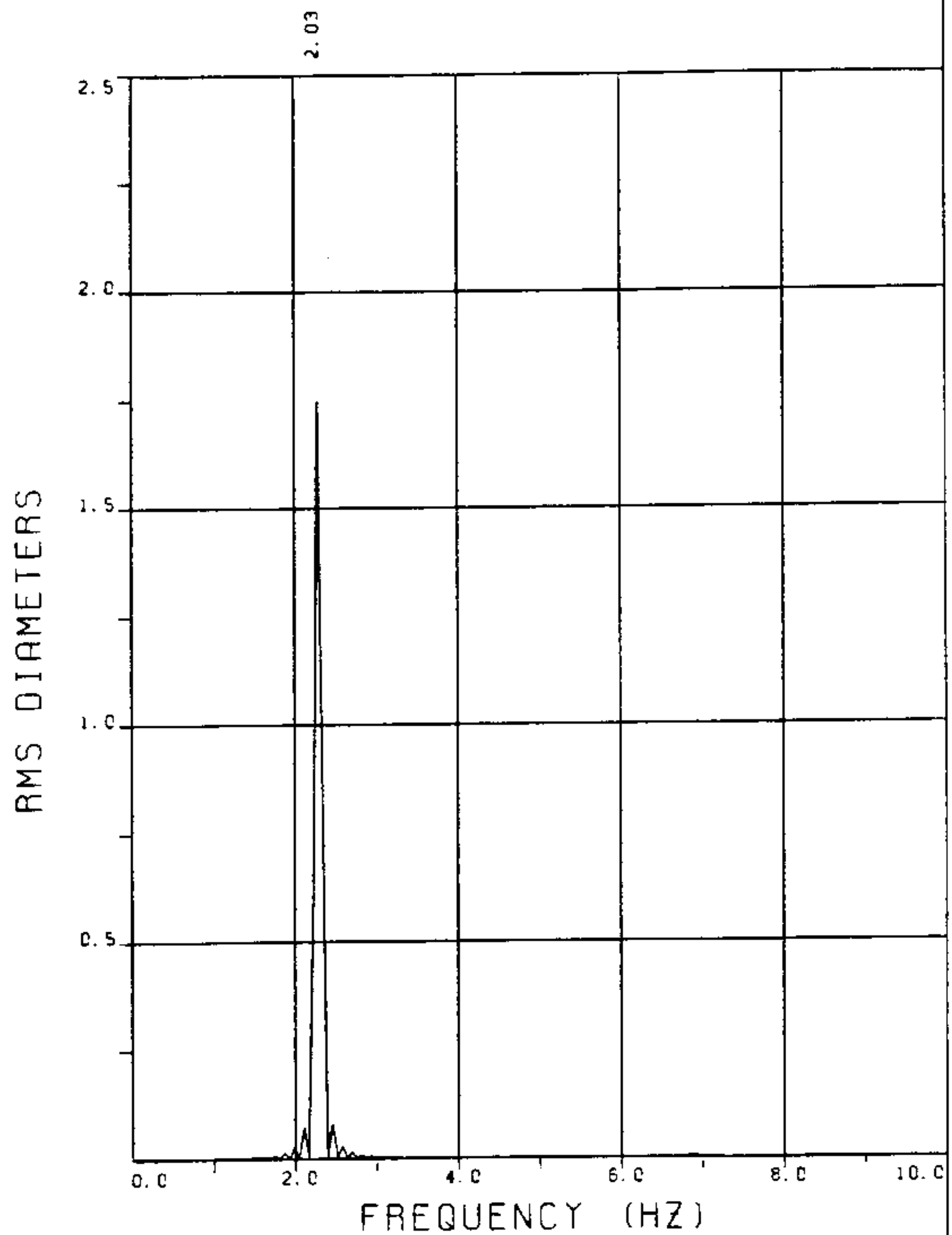

EXPERIMENT NUMBER 48

LVDT

THETA=0 VC=0 FE=2.300 BE=0.059

MEASURED A/DE=2.87

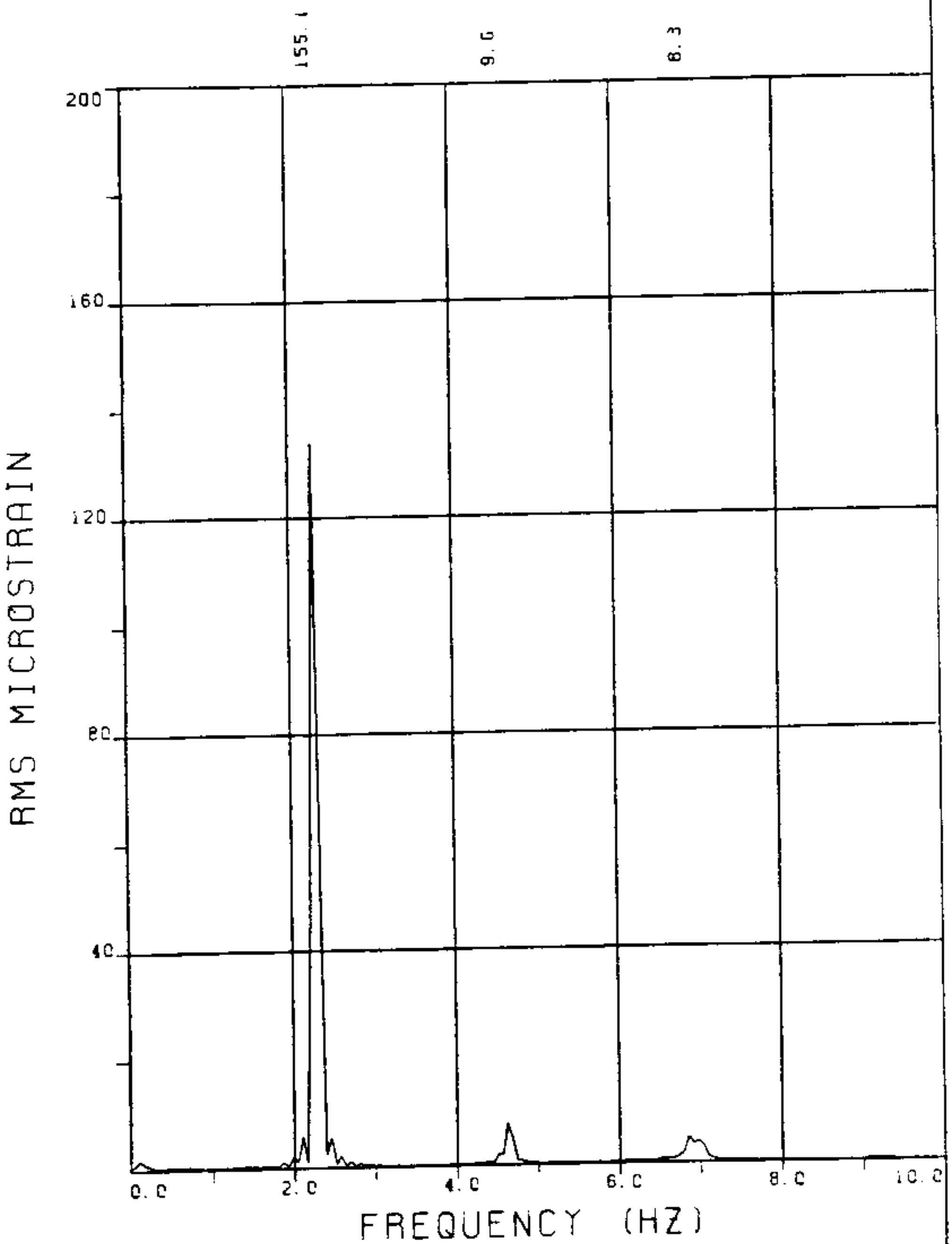

EXPERIMENT NUMBER 48

BRIDGE A8 ELEVATION=3L/11 BE=0.059

THETA=0 VC=0 FE=2.300 A/DE=2.87

MEASURED RESPONSE IN MICROSTRAIN

TOTAL DYNAMIC RMS=156.1

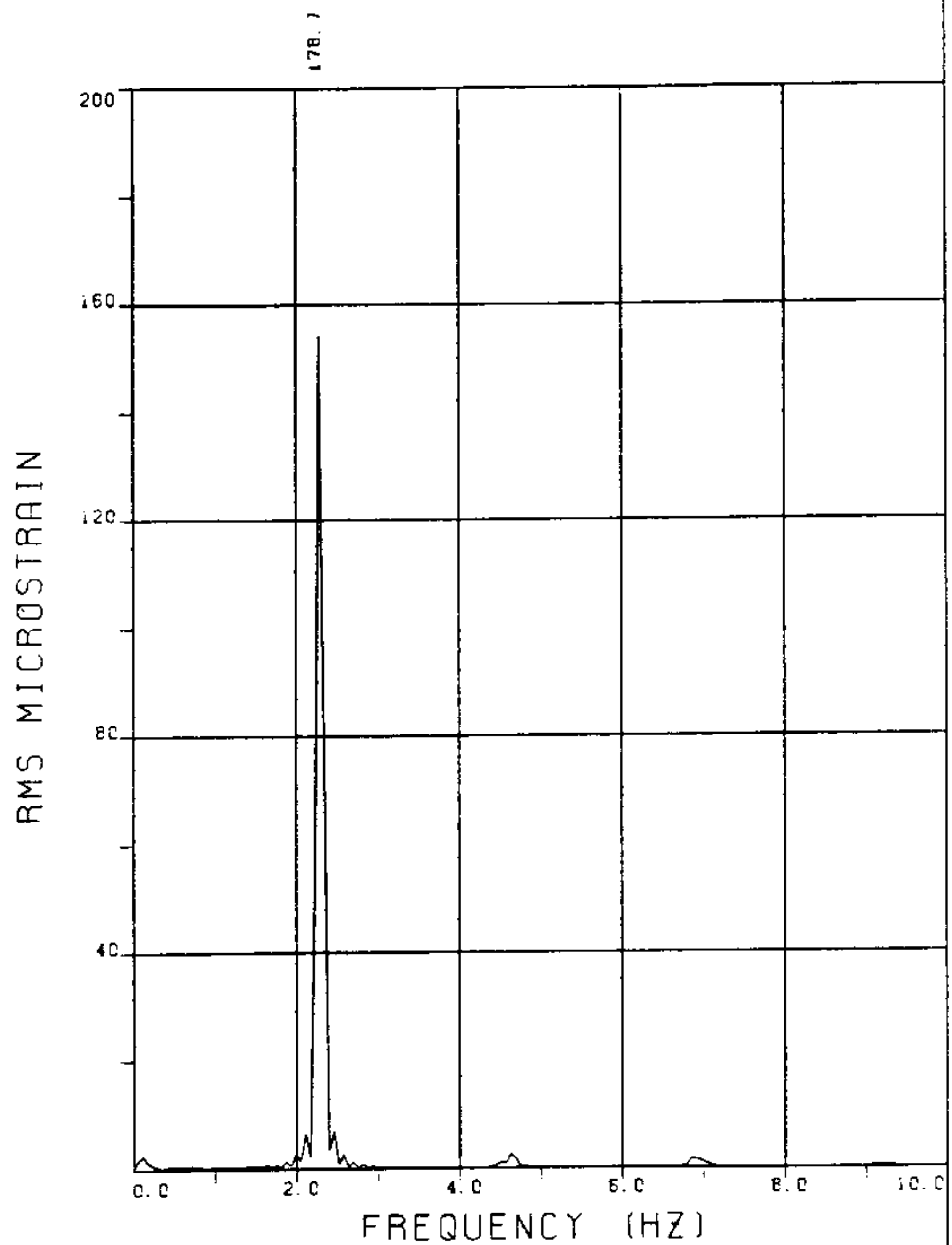

EXPERIMENT NUMBER 48

BRIDGE A6 ELEVATION=5L/11 BE=0.059

THETA=0 VC=0 FE=2.300 A/DE=2.87

MEASURED RESPONSE IN MICROSTRAIN

TOTAL DYNAMIC RMS=179.4

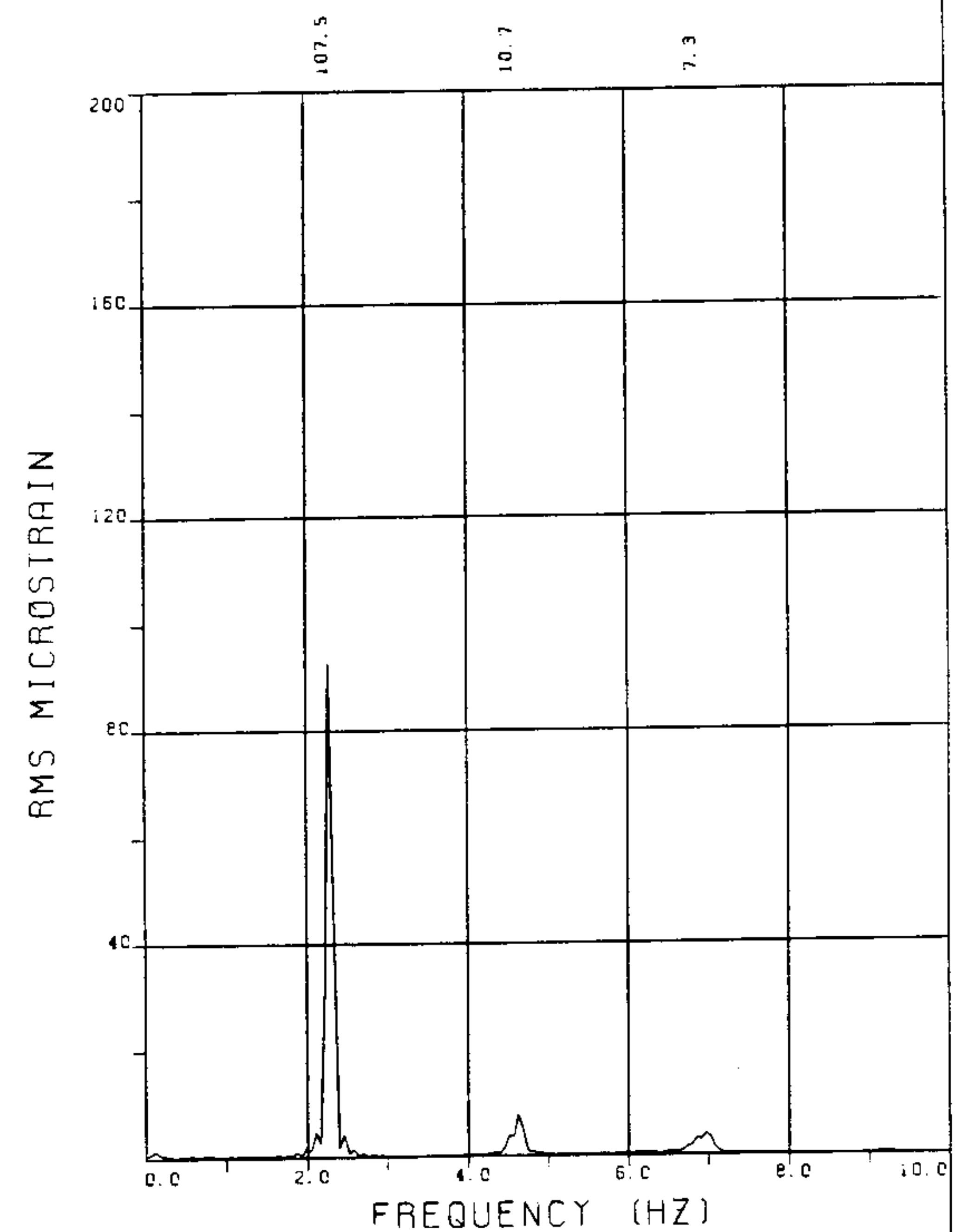

EXPERIMENT NUMBER 48

BRIDGE A3 ELEVATION=8L/11 BE=0.059

THETA=0 VC=0 FE=2.300 A/DE=2.87

MEASURED RESPONSE IN MICROSTRAIN

TOTAL DYNAMIC RMS=108.0

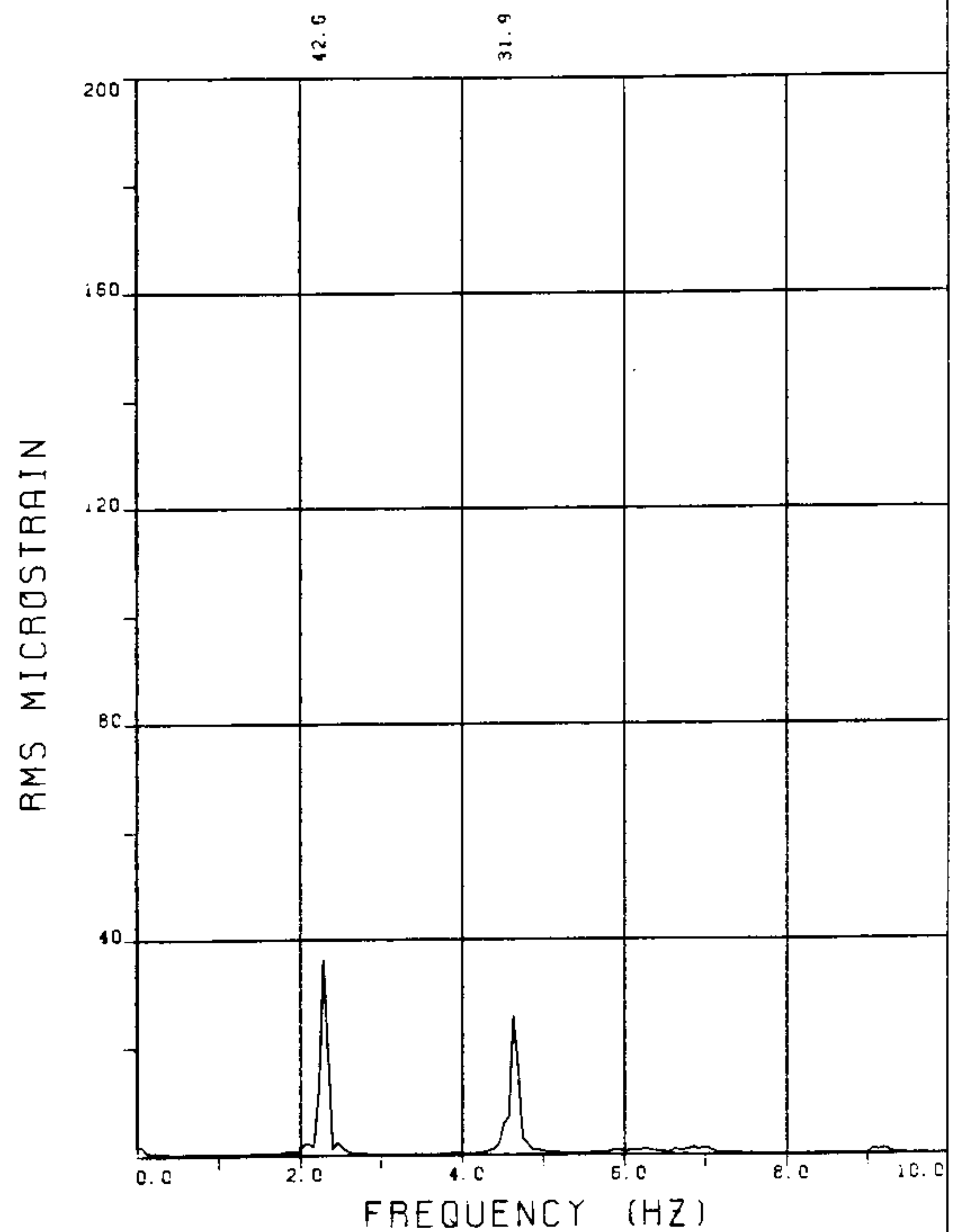

EXPERIMENT NUMBER 48

BRIDGE B8 ELEVATION=3L/11 BE=0.059

THETA=0 VC=0 FE=2.300 A/DE=2.87

MEASURED RESPONSE IN MICROSTRAIN

TOTAL DYNAMIC RMS=52.9

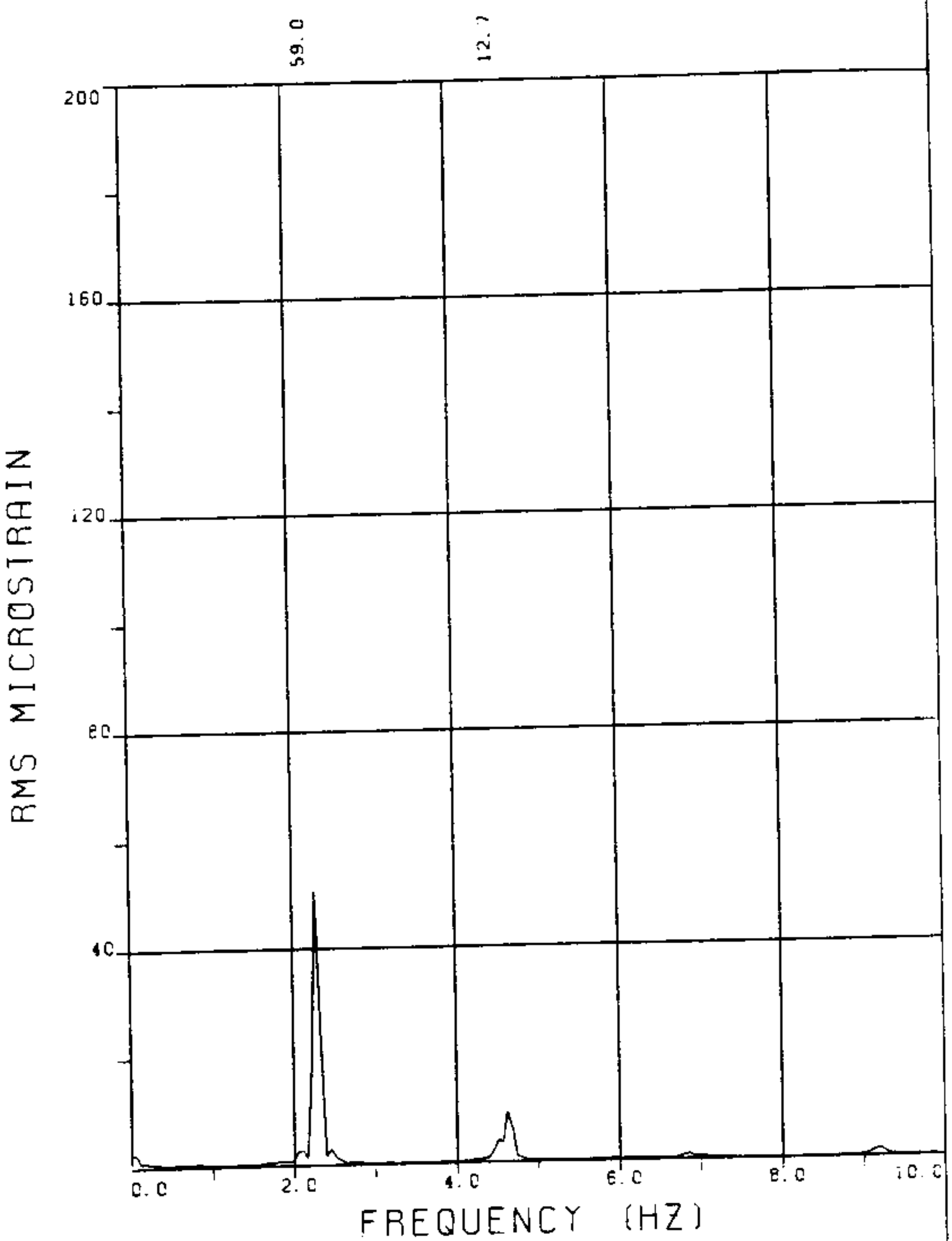

EXPERIMENT NUMBER 48

BRIDGE B6 ELEVATION=5L/11 BE=0.059

THETA=0 VC=0 FE=2.300 A/DE=2.87

MEASURED RESPONSE IN MICROSTRAIN

TOTAL DYNAMIC RMS=59.9

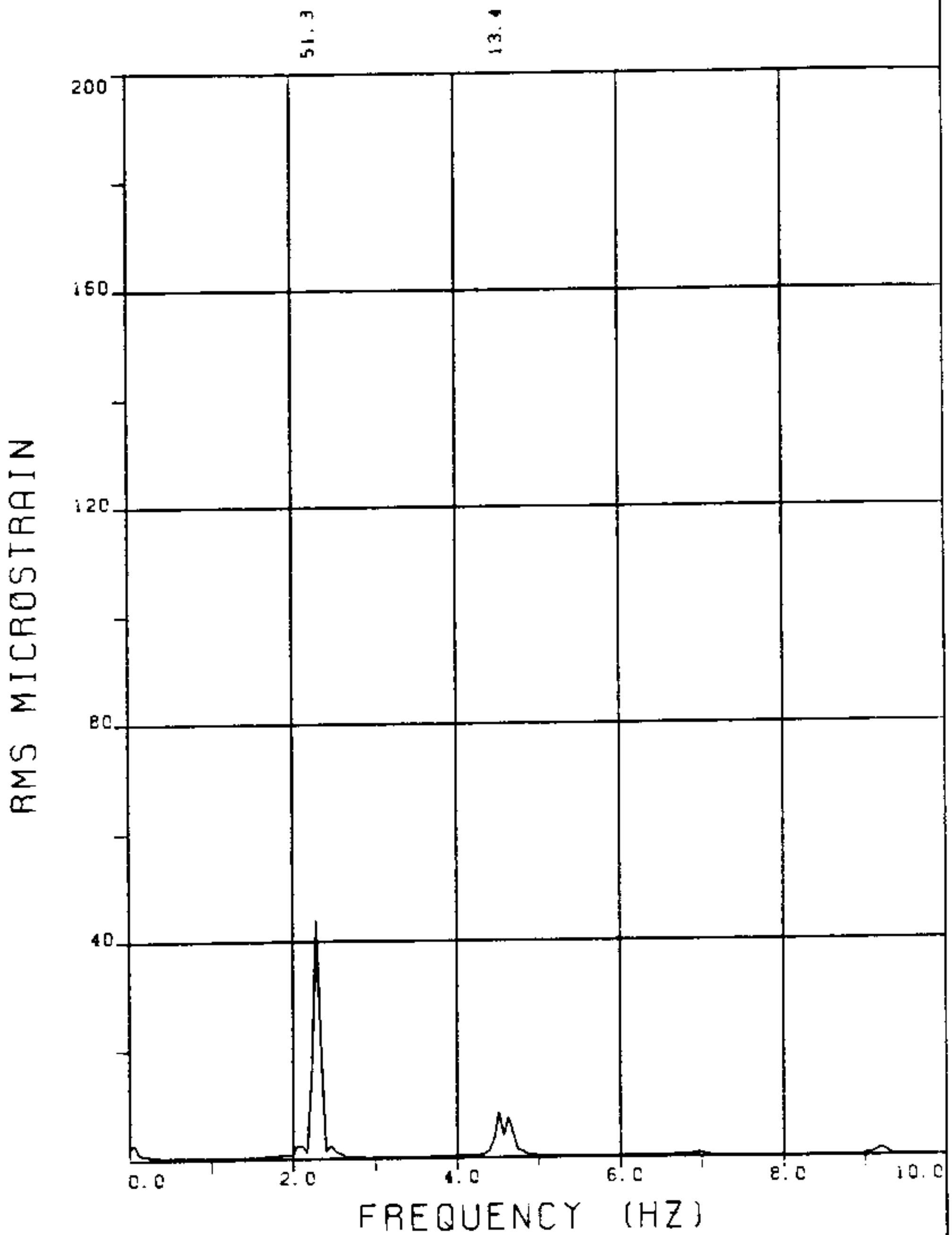

EXPERIMENT NUMBER 48

BRIDGE B5 ELEVATION=6L/11 BE=0.059

THETA=0 VC=0 FE=2.300 A/DE=2.87

MEASURED RESPONSE IN MICROSTRAIN

TOTAL DYNAMIC RMS=52.7

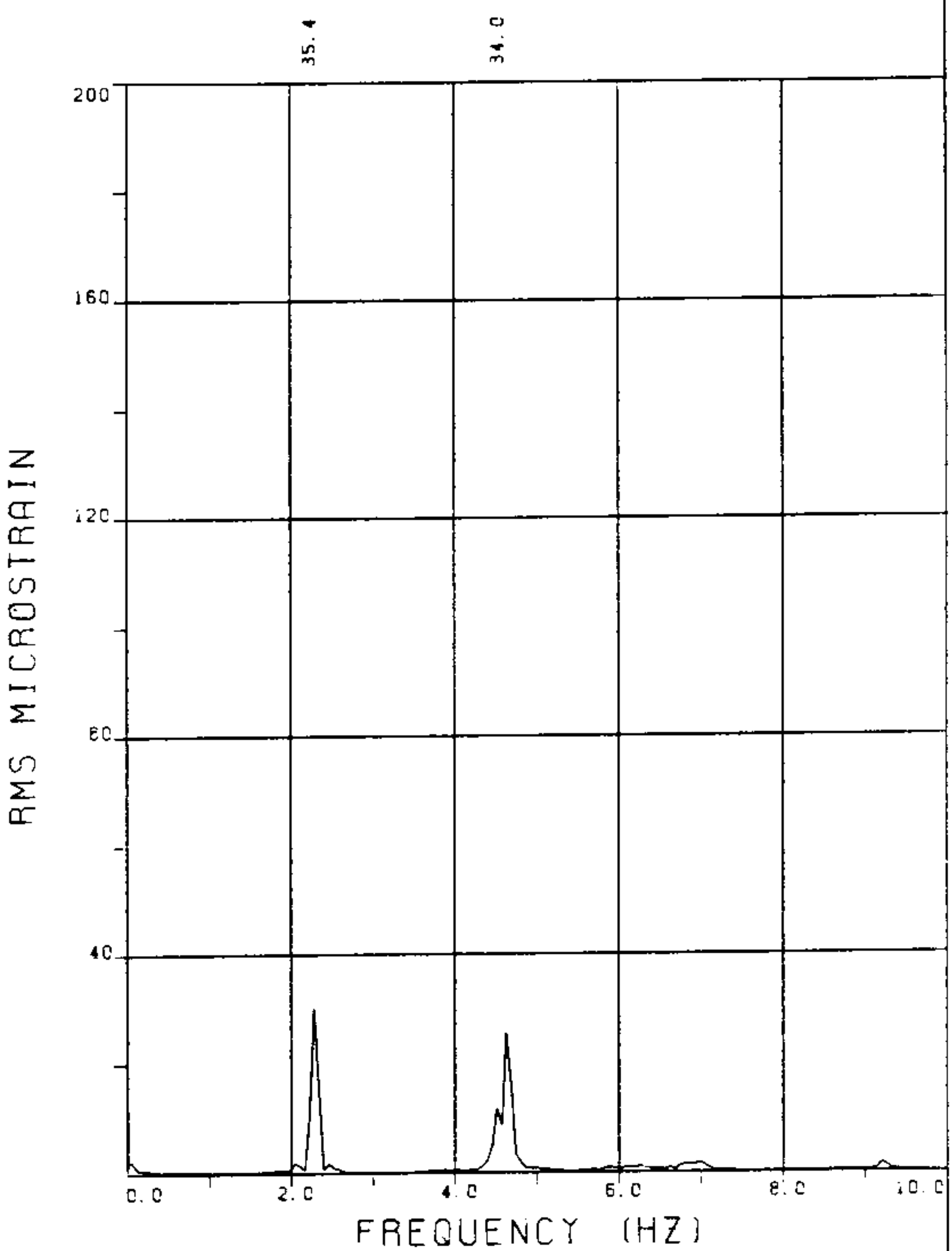

EXPERIMENT NUMBER 48

BRIDGE B3 ELEVATION=8L/11 BE=0.059

THETA=0 VC=0 FE=2.300 A/DE=2.87

MEASURED RESPONSE IN MICROSTRAIN

TOTAL DYNAMIC RMS=47.9

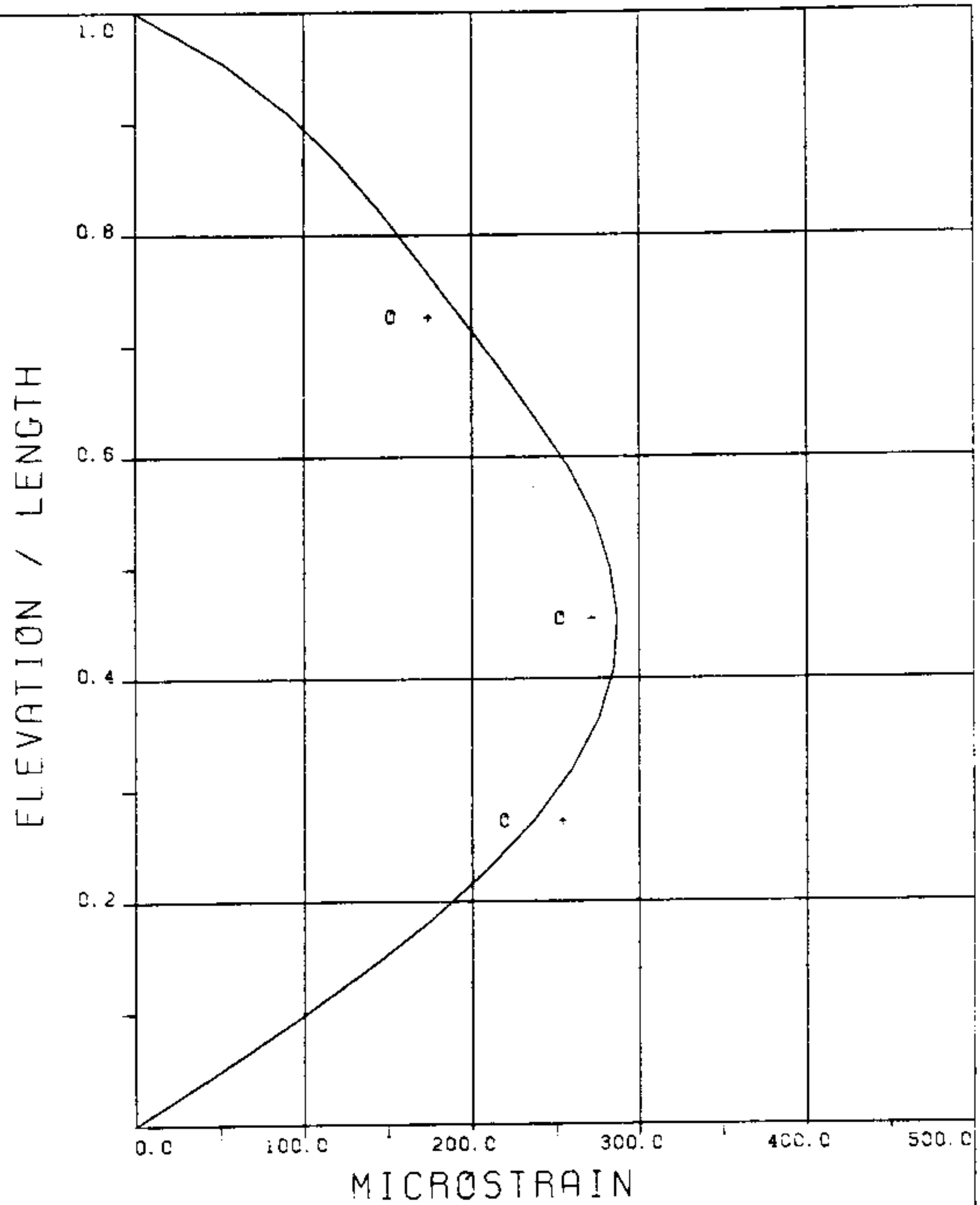

EXPERIMENT NUMBER 48

THETA=0 VC=0 FE=2.300 A/DE=2.87

DYNAMIC RESPONSE AT F=FE IN PLANE A
_______ THEORY o o o EXPERIMENT

MAXIMUM DYNAMIC RESPONSE IN PLANE A
_______ THEORY + + + EXPERIMENT

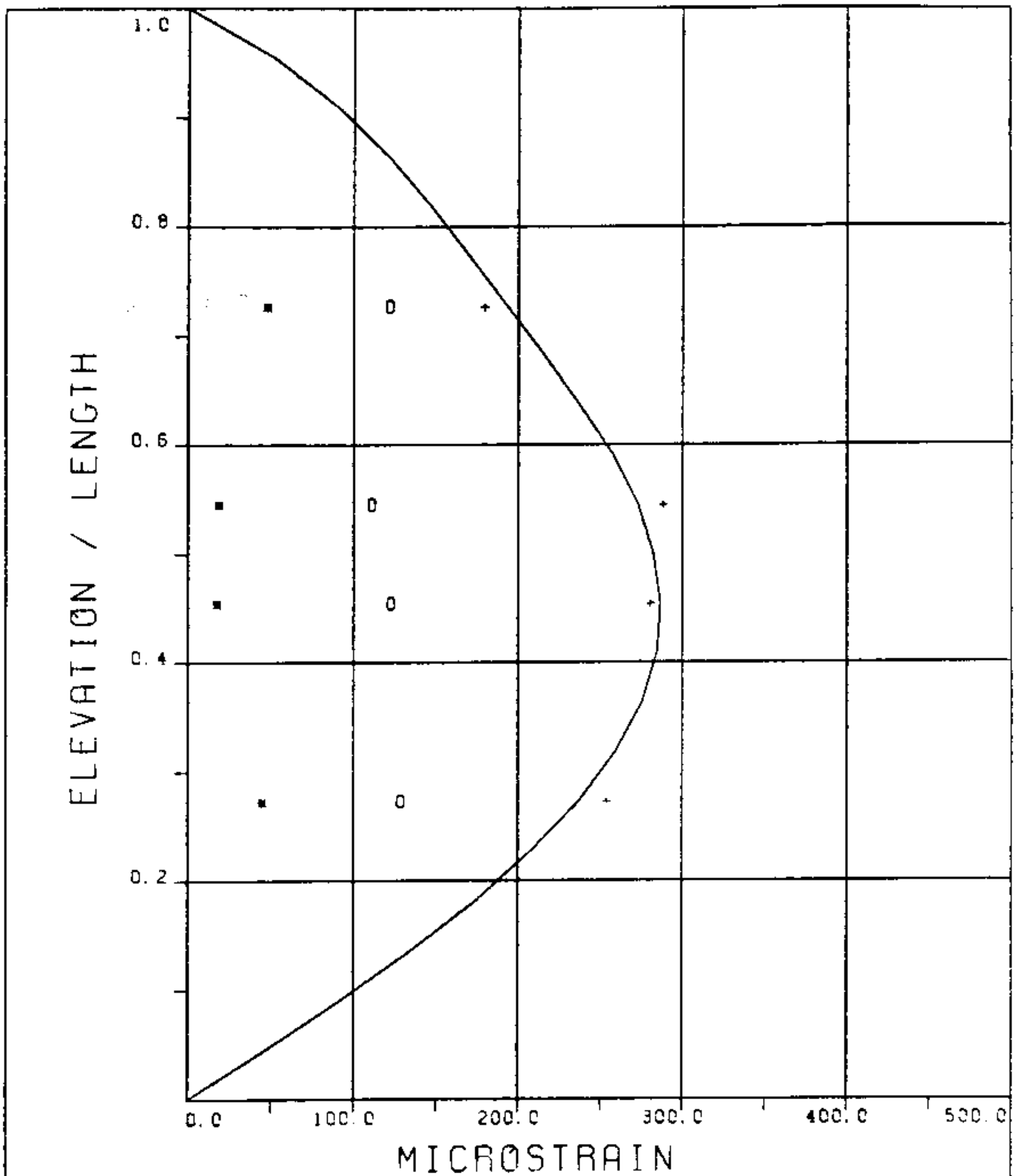

EXPERIMENT NUMBER 48

THETA=0 VC=0 FE=2.300 A/DE=2.87

DYNAMIC RESPONSE IN PLANE B AT F=2FE

* * * EXPERIMENT

MAXIMUM RESPONSE IN PLANE B

o o o EXPERIMENT

MAXIMUM RESPONSE

——— THEORY + + + EXPERIMENT

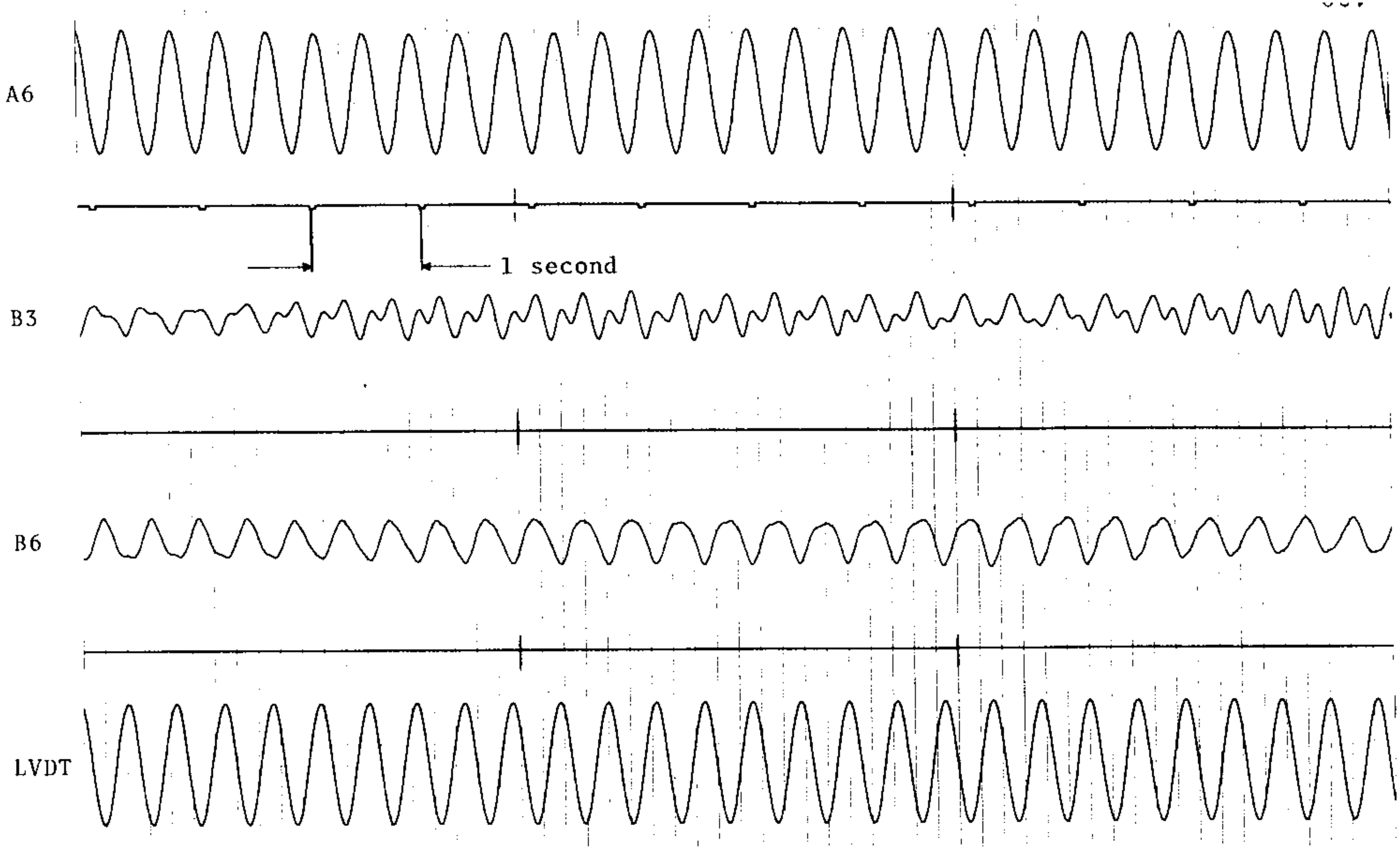

FIGURE 48Ta: LVDT: 0.174 D_e/DIVISION; STRAINS: 15.3 MICROSTRAIN/DIVISION

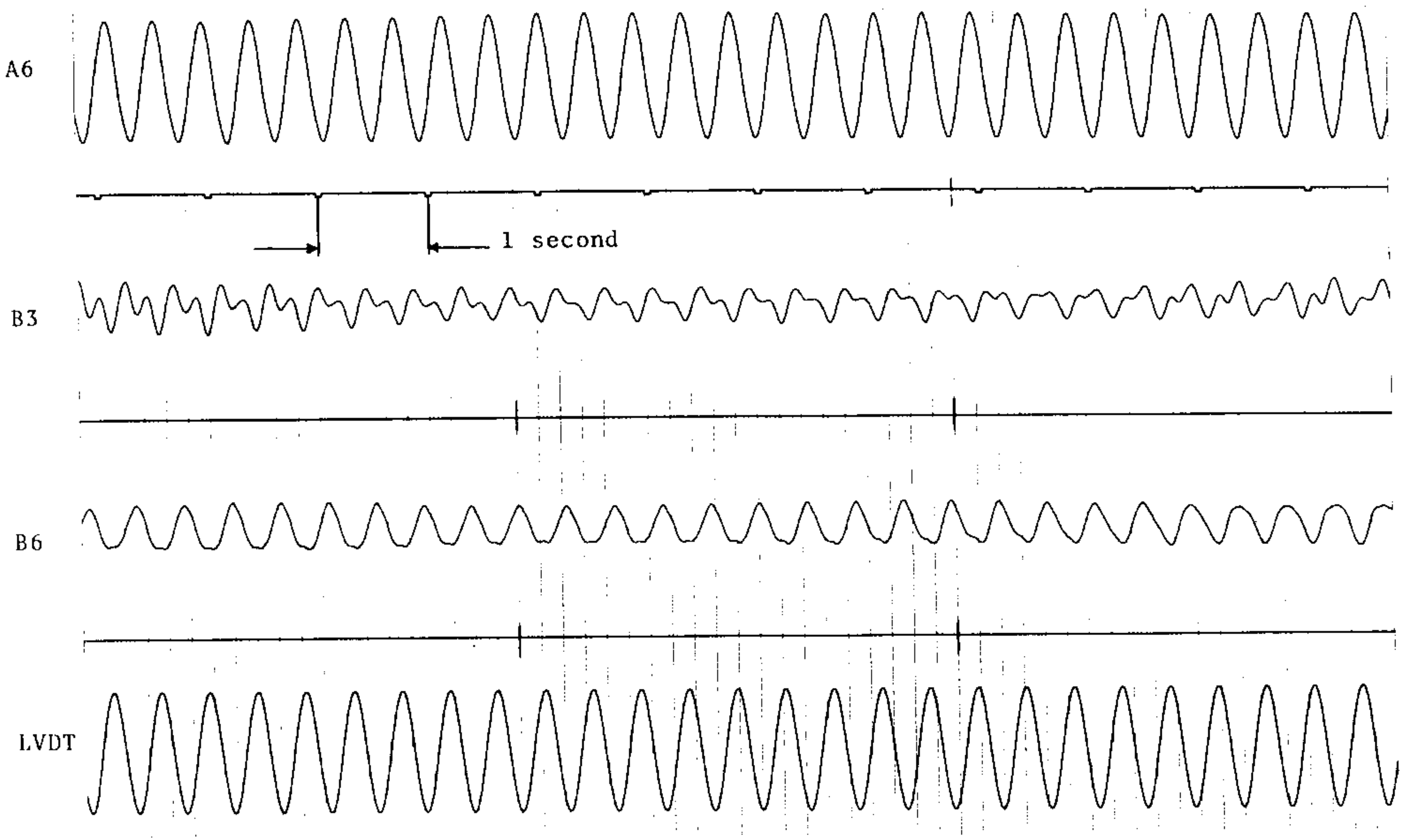

FIGURE 48Tb: LVDT: 0.174 D_e/DIVISION; STRAINS: 15.3 MICROSTRAIN/DIVISION

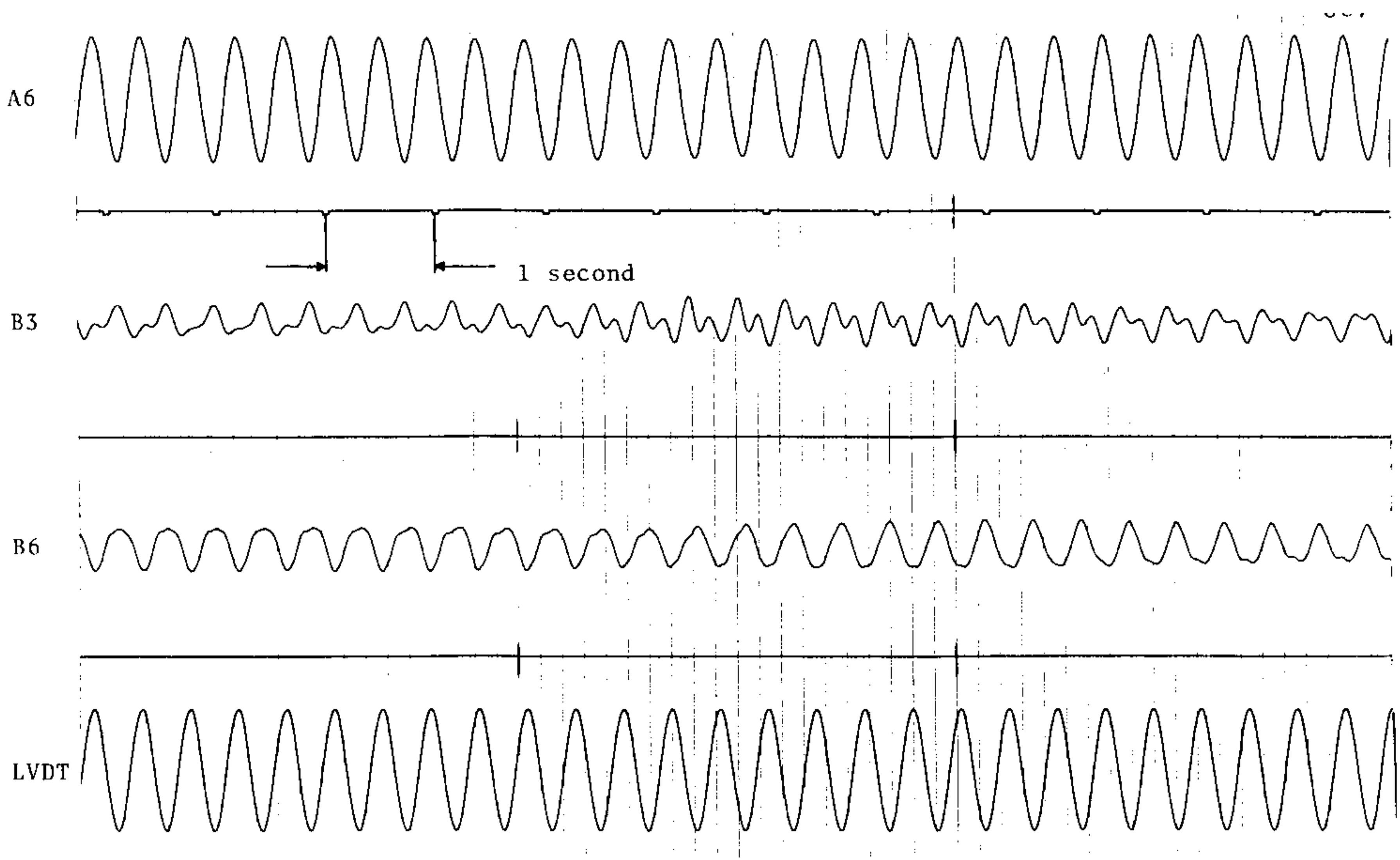

FIGURE 48Tc: LVDT: 0.174 D_e/DIVISION; STRAINS: 15.3 MICROSTRAIN/DIVISION

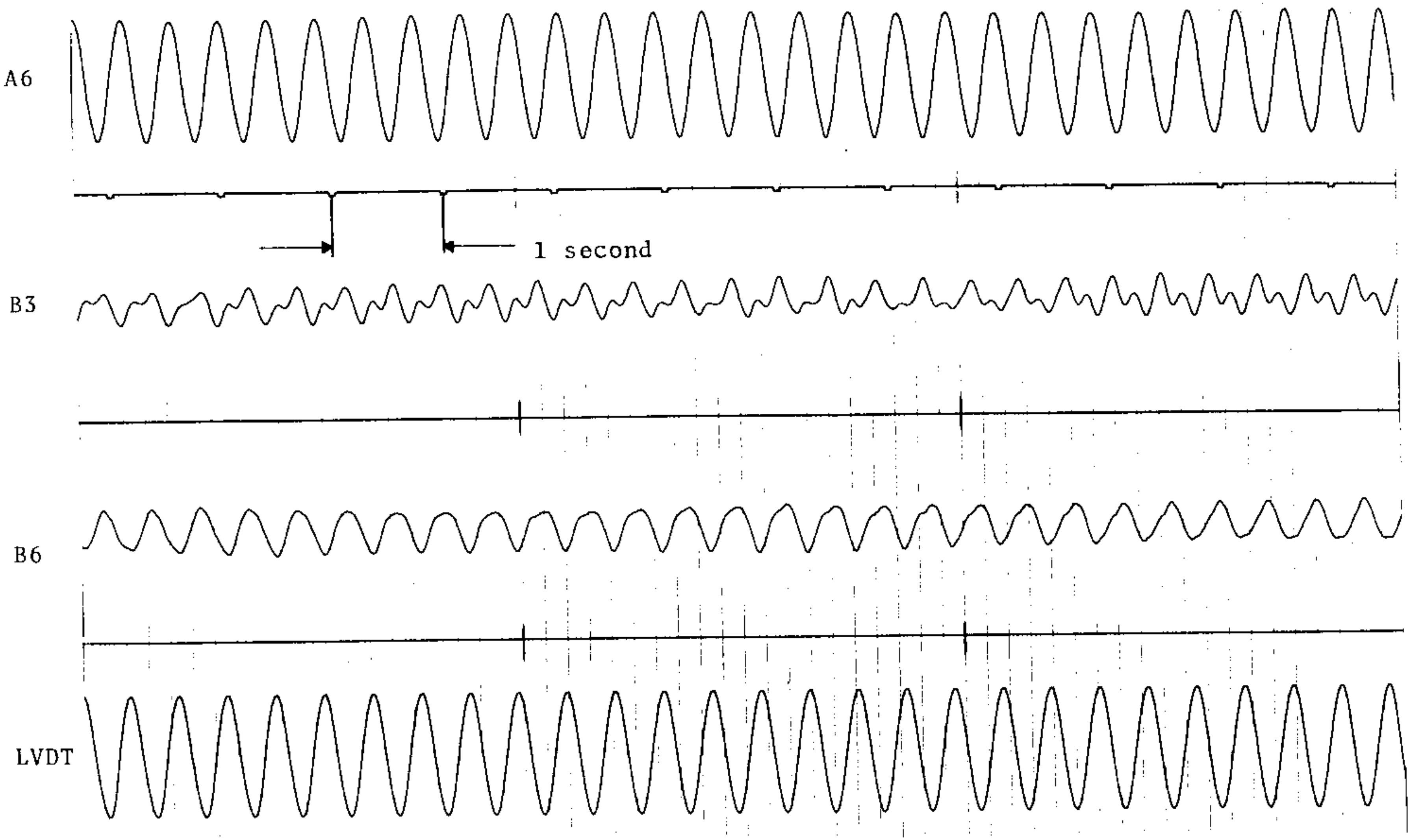

FIGURE 48Td: LVDT: 0.174 D_e/DIVISION; STRAINS: 15.3 MICROSTRAIN/DIVISION

EXPERIMENT 24

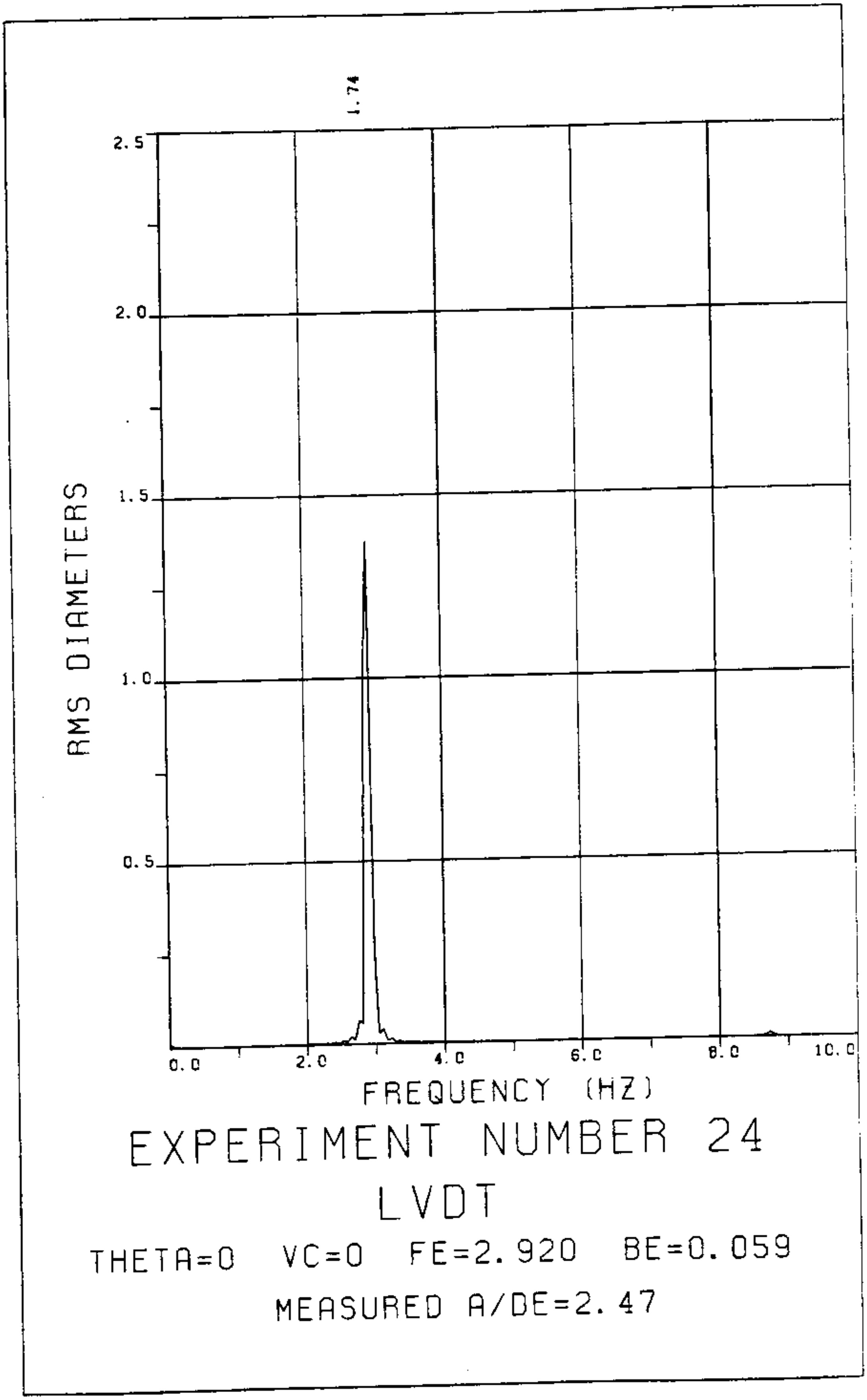
1.74
2.5
2.0
1.5
1.0
0.5
RMS DIAMETERS
0.0
2.0
4.0
6.0
8.0
10.0
FREQUENCY (HZ)
EXPERIMENT NUMBER 24
LVDT
THETA=0 VC=0 FE=2.920 BE=0.059
MEASURED A/DE=2.47

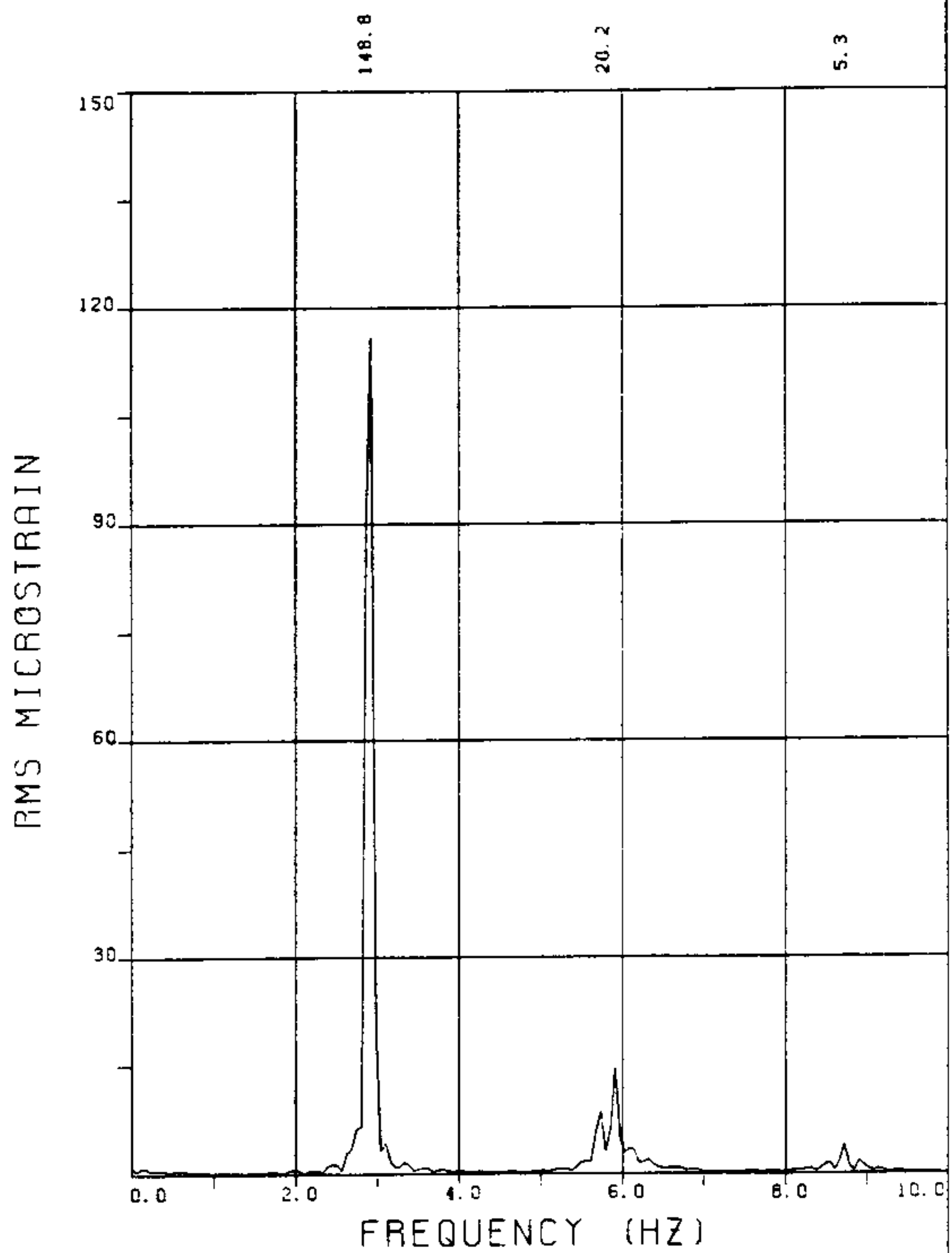

EXPERIMENT NUMBER 24

BRIDGE A8 ELEVATION=3L/11 BE=0.059

THETA=0 VC=0 FE=2.920 A/DE=2.47

MEASURED RESPONSE IN MICROSTRAIN

TOTAL DYNAMIC RMS=150.4

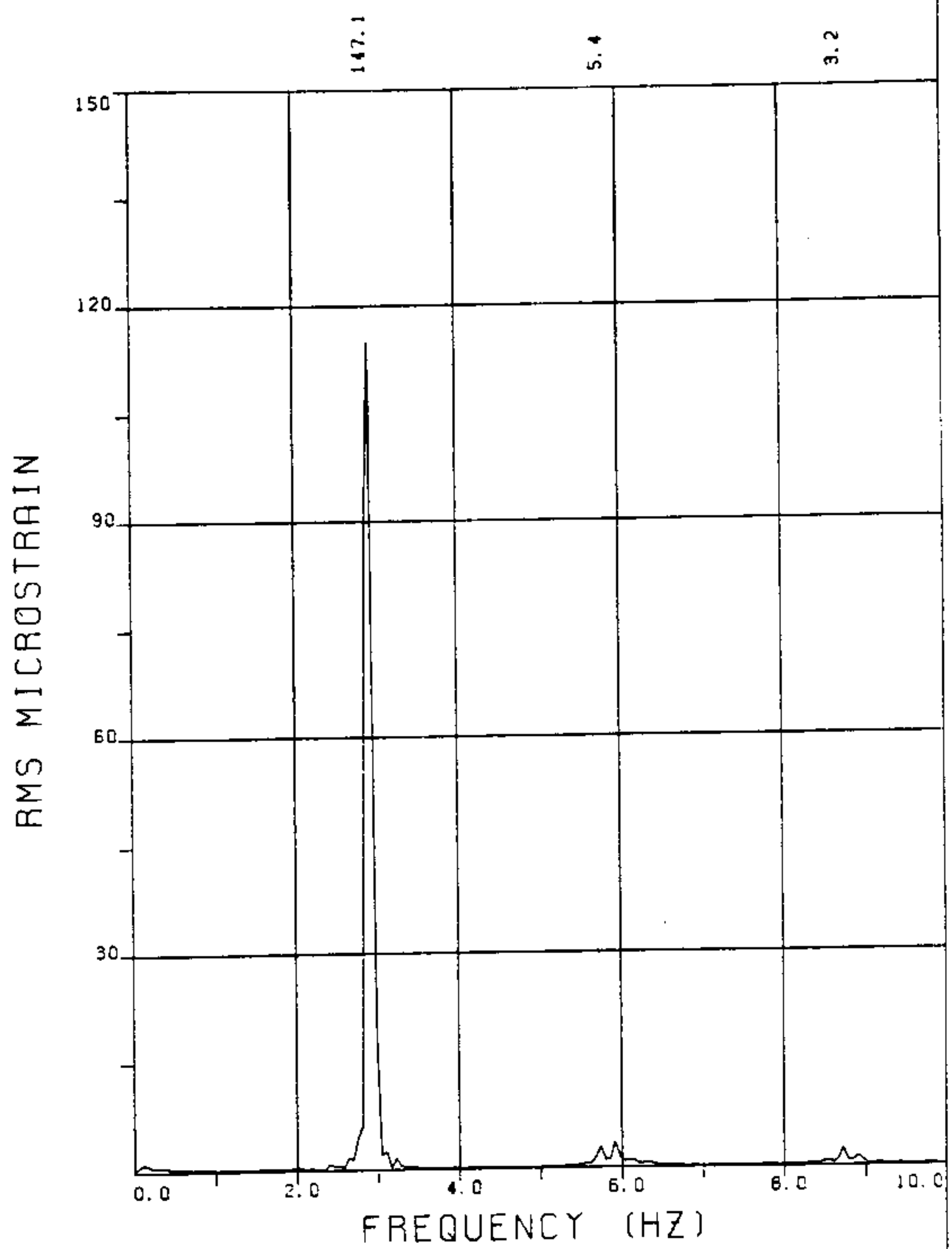

EXPERIMENT NUMBER 24

BRIDGE A6 ELEVATION=5L/11 BE=0.059

THETA=0 VC=0 FE=2.920 A/DE=2.47

MEASURED RESPONSE IN MICROSTRAIN

TOTAL DYNAMIC RMS=147.3

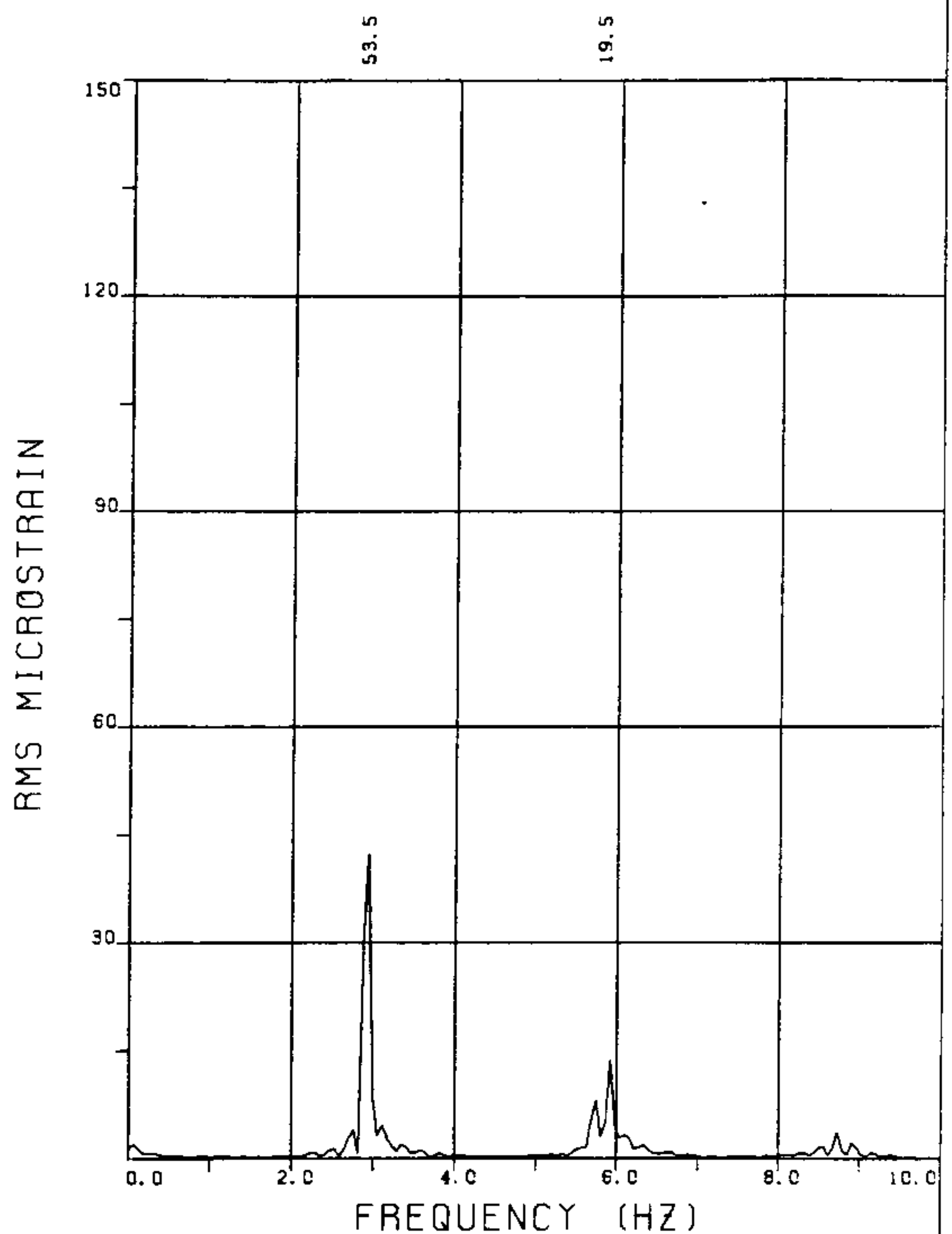

EXPERIMENT NUMBER 24

BRIDGE A3 ELEVATION=8L/11 BE=0.059

THETA=0 VC=0 FE=2.920 A/DE=2.47

MEASURED RESPONSE IN MICROSTRAIN

TOTAL DYNAMIC RMS=57.5

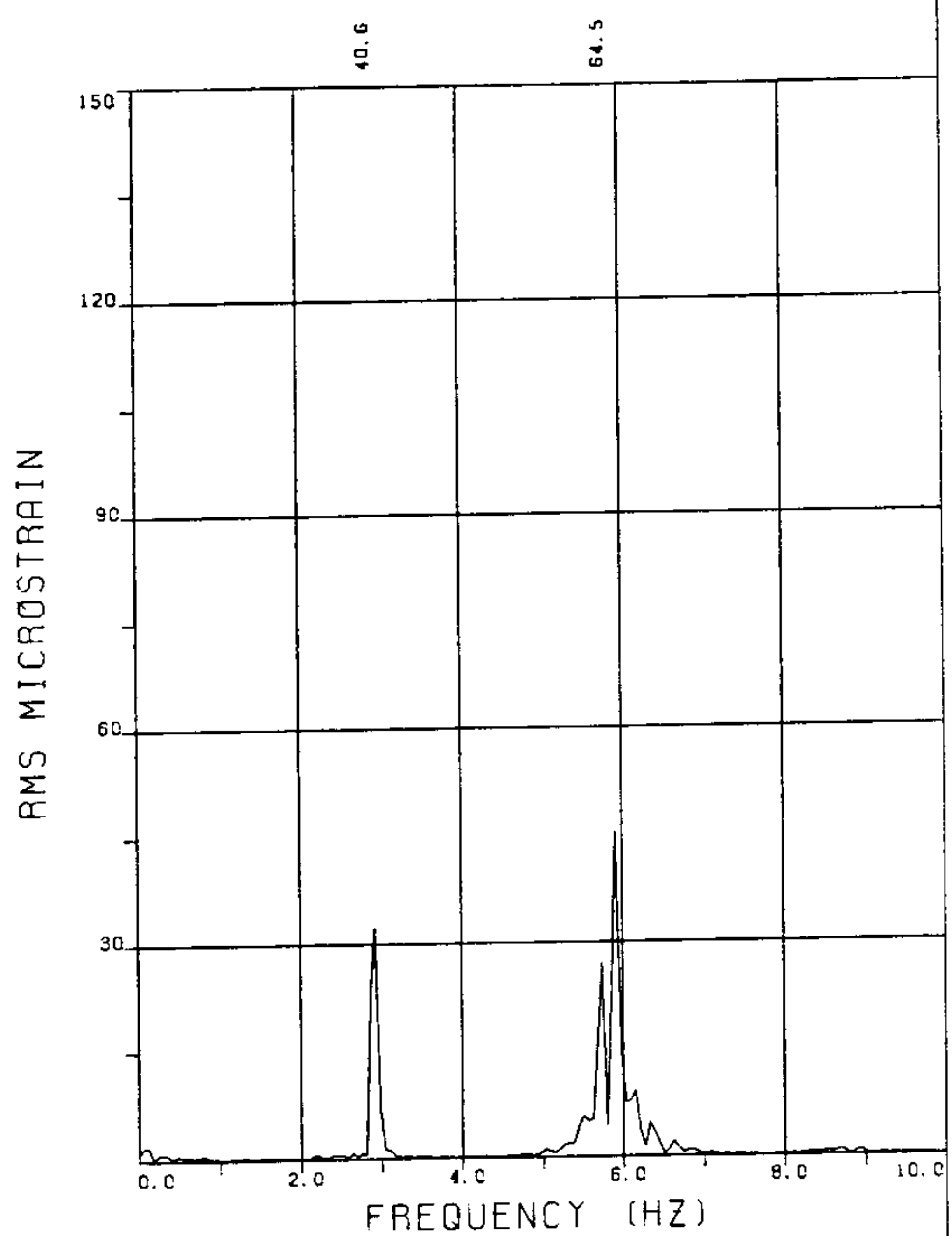

EXPERIMENT NUMBER 24

BRIDGE B8 ELEVATION=3L/11 BE=0.059

THETA=0 VC=0 FE=2.920 A/DE=2.47

MEASURED RESPONSE IN MICROSTRAIN

TOTAL DYNAMIC RMS=76.5

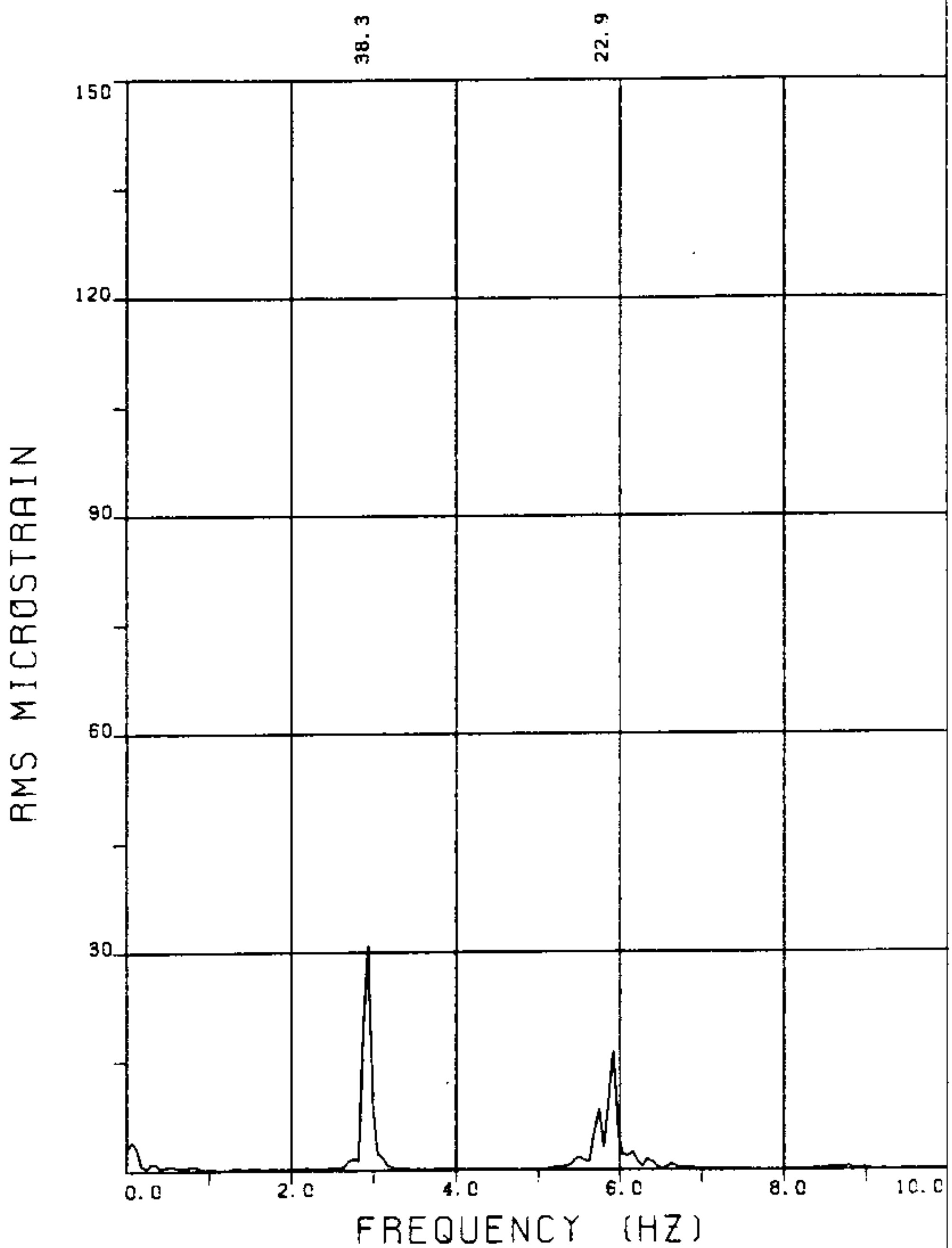

EXPERIMENT NUMBER 24

BRIDGE B5 ELEVATION=6L/11 BE=0.059

THETA=0 VC=0 FE=2.920 A/DE=2.47

MEASURED RESPONSE IN MICROSTRAIN

TOTAL DYNAMIC RMS=45.1

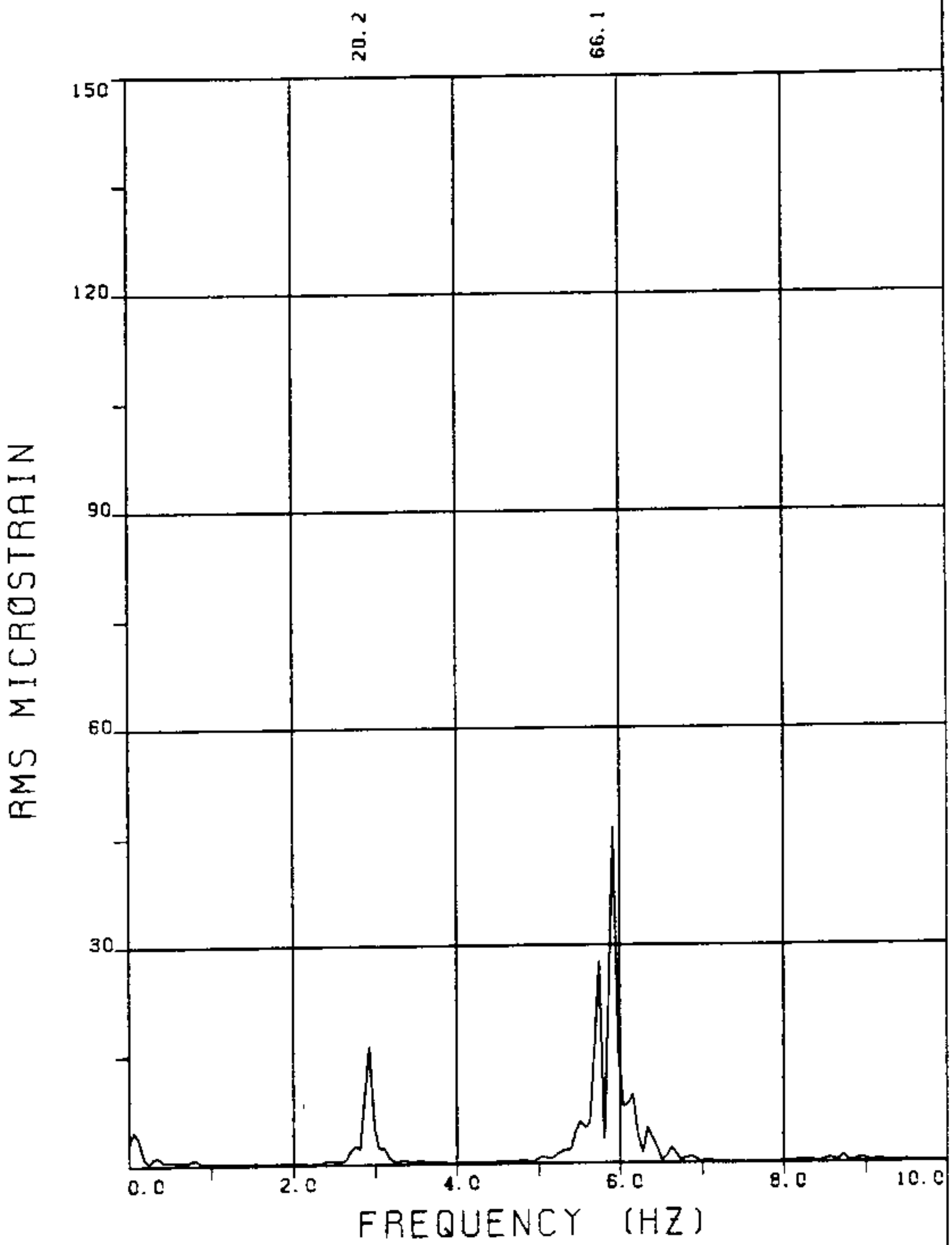

EXPERIMENT NUMBER 24

BRIDGE B3 ELEVATION=8L/11 BE=0.059

THETA=0 VC=0 FE=2.920 A/DE=2.47

MEASURED RESPONSE IN MICROSTRAIN

TOTAL DYNAMIC RMS=69.7

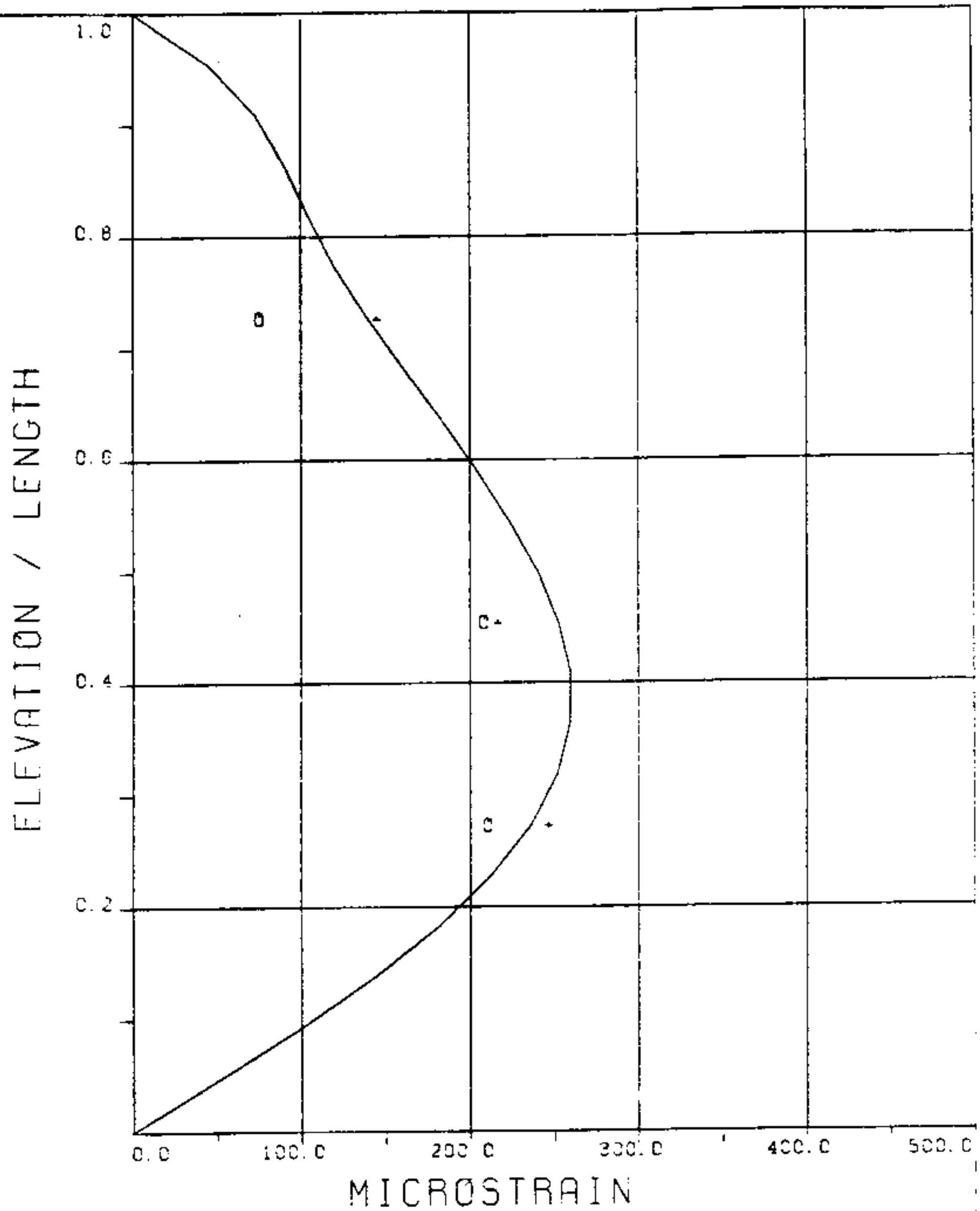

EXPERIMENT NUMBER 24

THETA=0 VC=0 FE=2.920 A/DE=2.47

DYNAMIC RESPONSE AT F=FE IN PLANE A

______ THEORY o o o EXPERIMENT

MAXIMUM DYNAMIC RESPONSE IN PLANE A

______ THEORY + + + EXPERIMENT

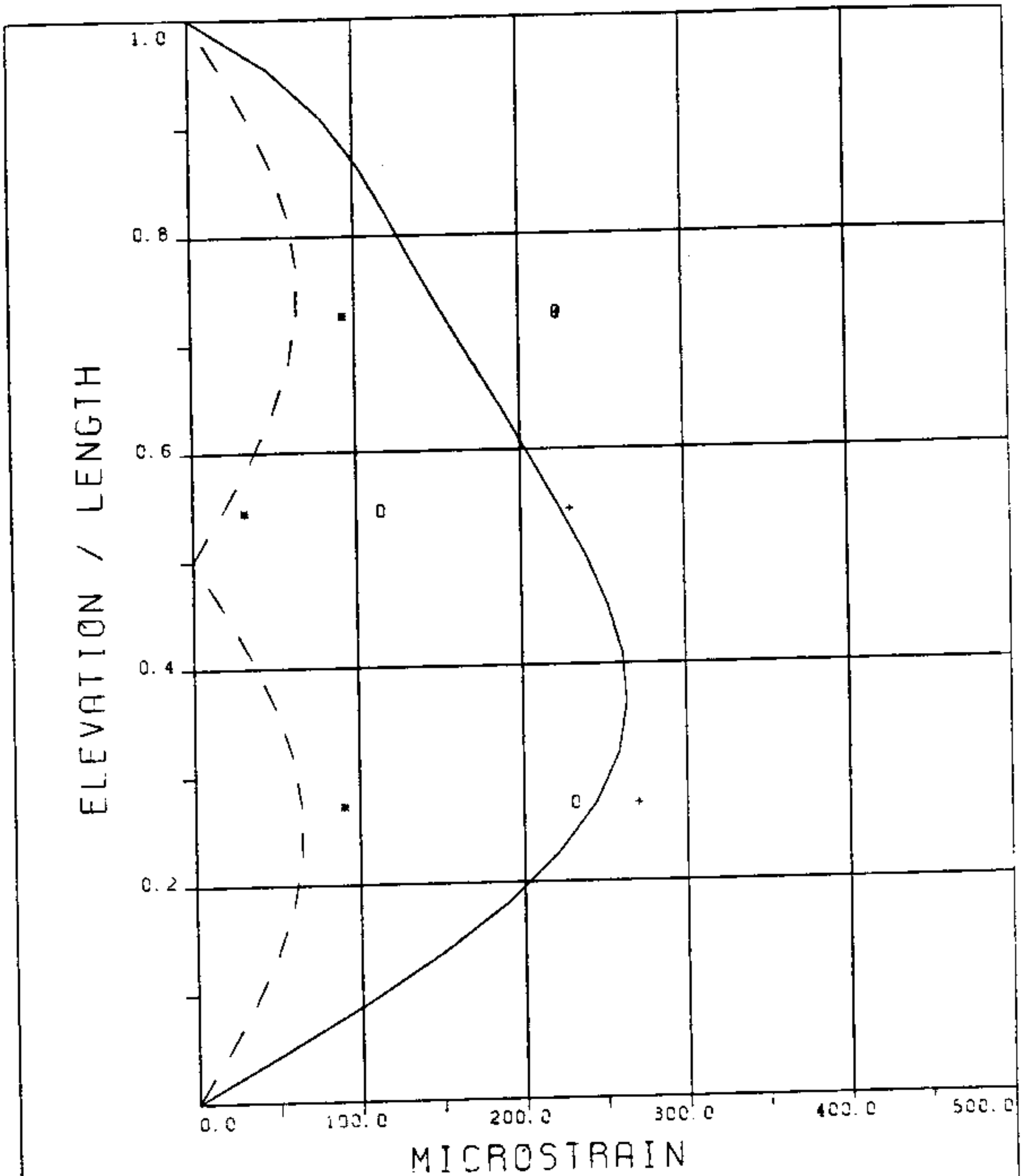

EXPERIMENT NUMBER 24

THETA=0 VC=0 FE=2.920 A/DE=2.47

DYNAMIC RESPONSE IN PLANE B AT F=2FE

----- THEORY * * * EXPERIMENT

MAXIMUM RESPONSE IN PLANE B

o o o EXPERIMENT

MAXIMUM RESPONSE

——— THEORY + + + EXPERIMENT

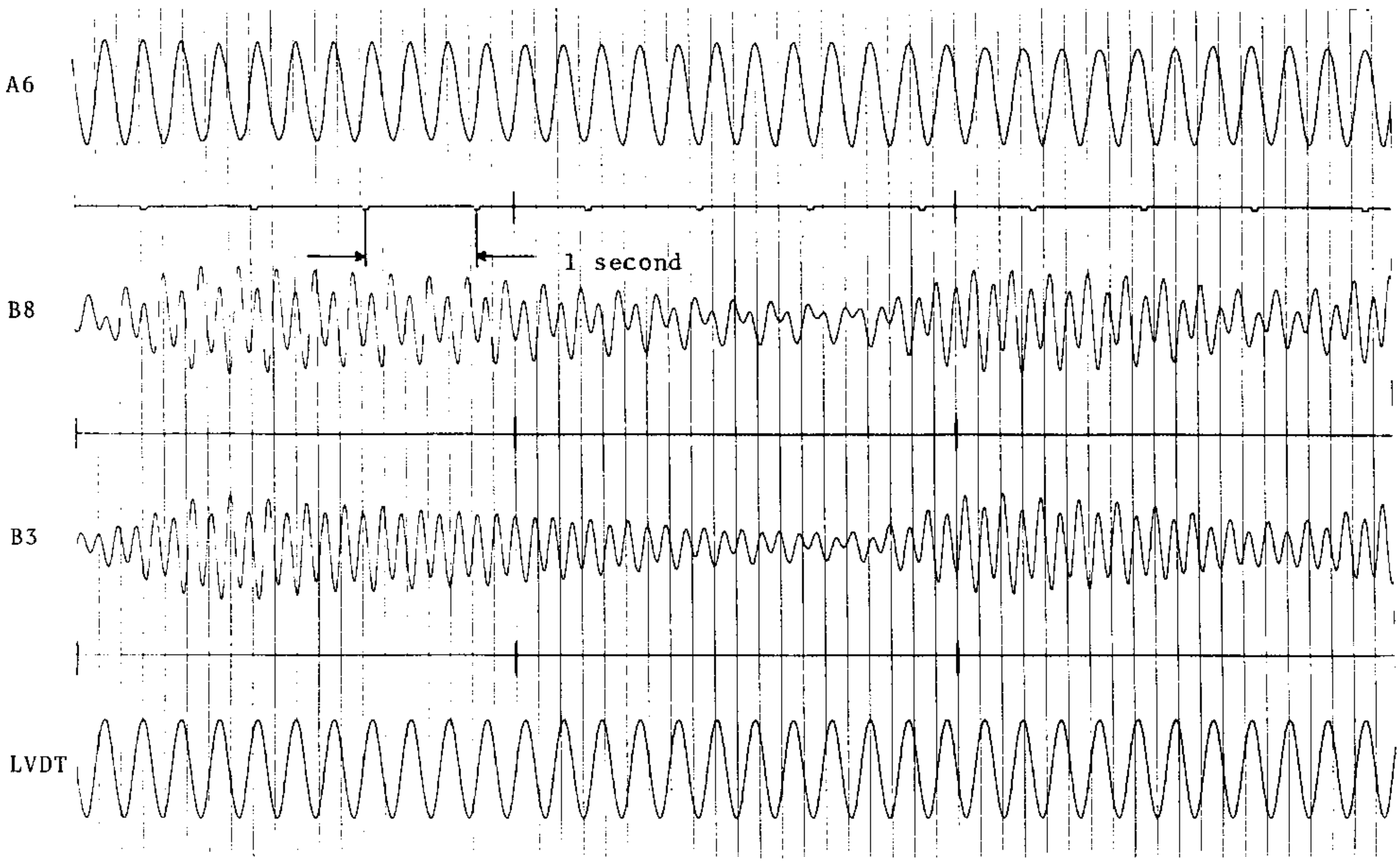

FIGURE 24Ta: LVDT: 0.174 D_e/DIVISION; STRAINS: 15.3 MICROSTRAIN/DIVISION

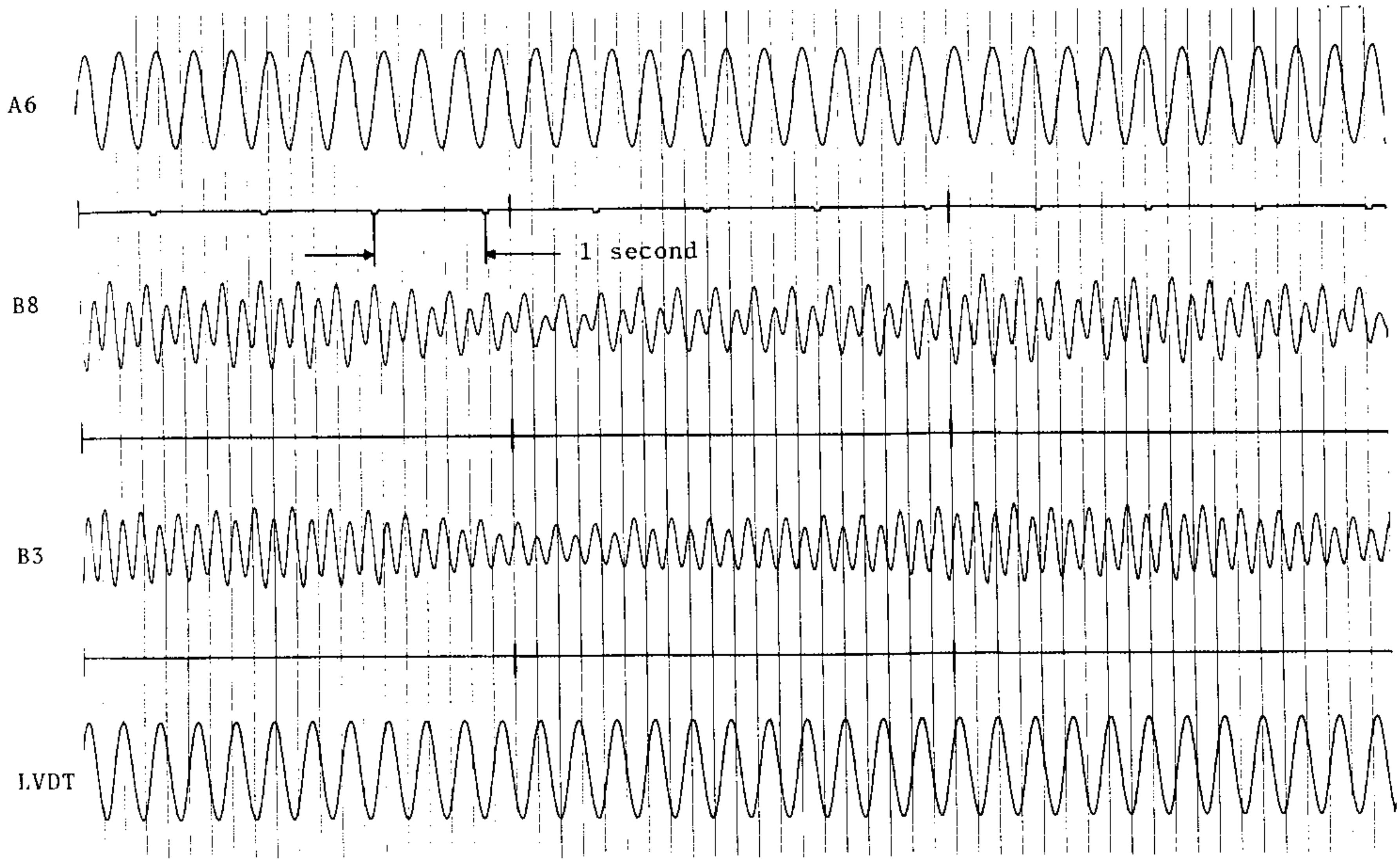

FIGURE 24Tb: LVDT: 0.174 D_e/DIVISION; STRAINS: 15.3 MICROSTRAIN/DIVISION

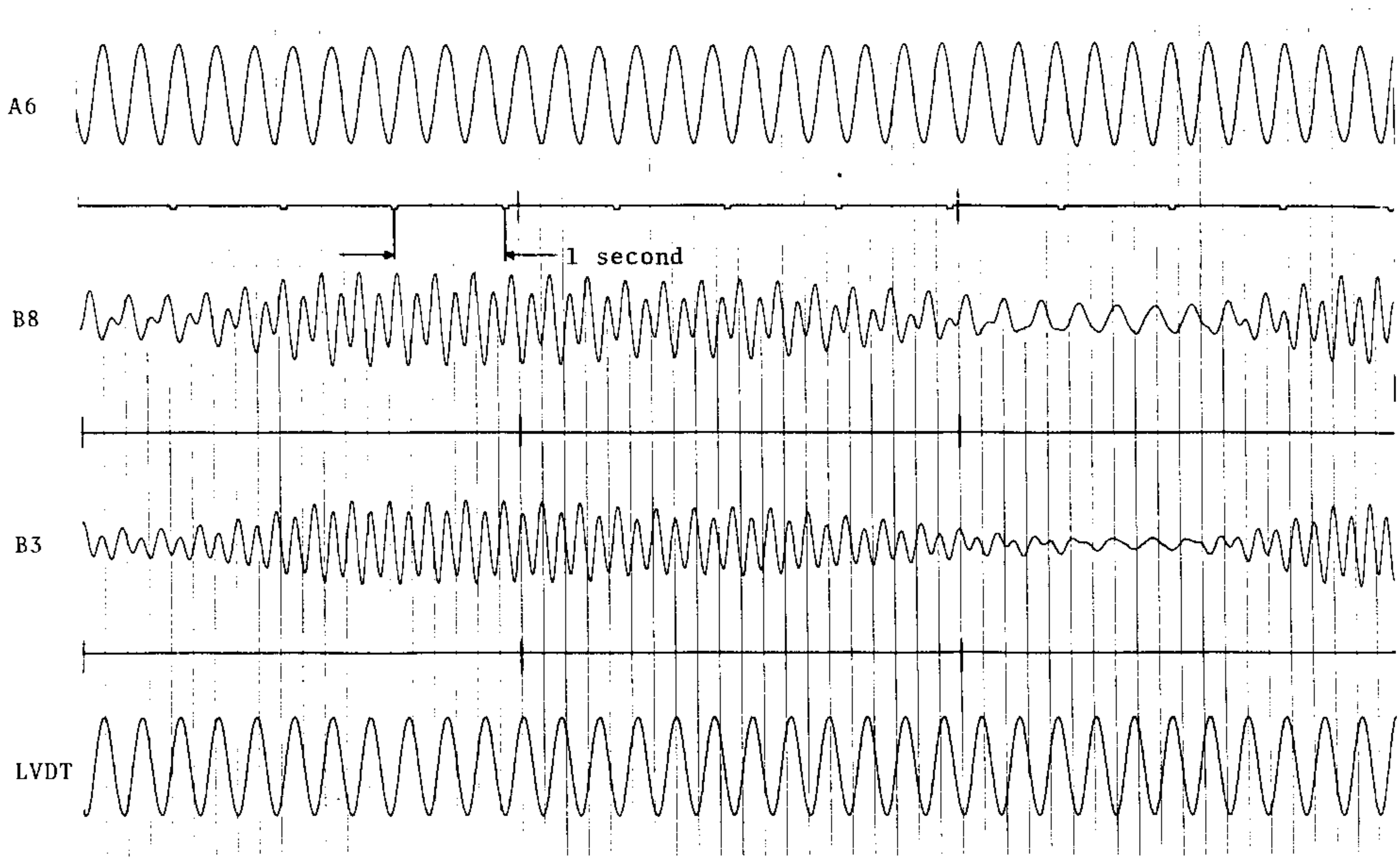

FIGURE 24Tc: LVDT: 0.174 D_e/DIVISION; STRAINS: 15.3 MICROSTRAIN/DIVISION

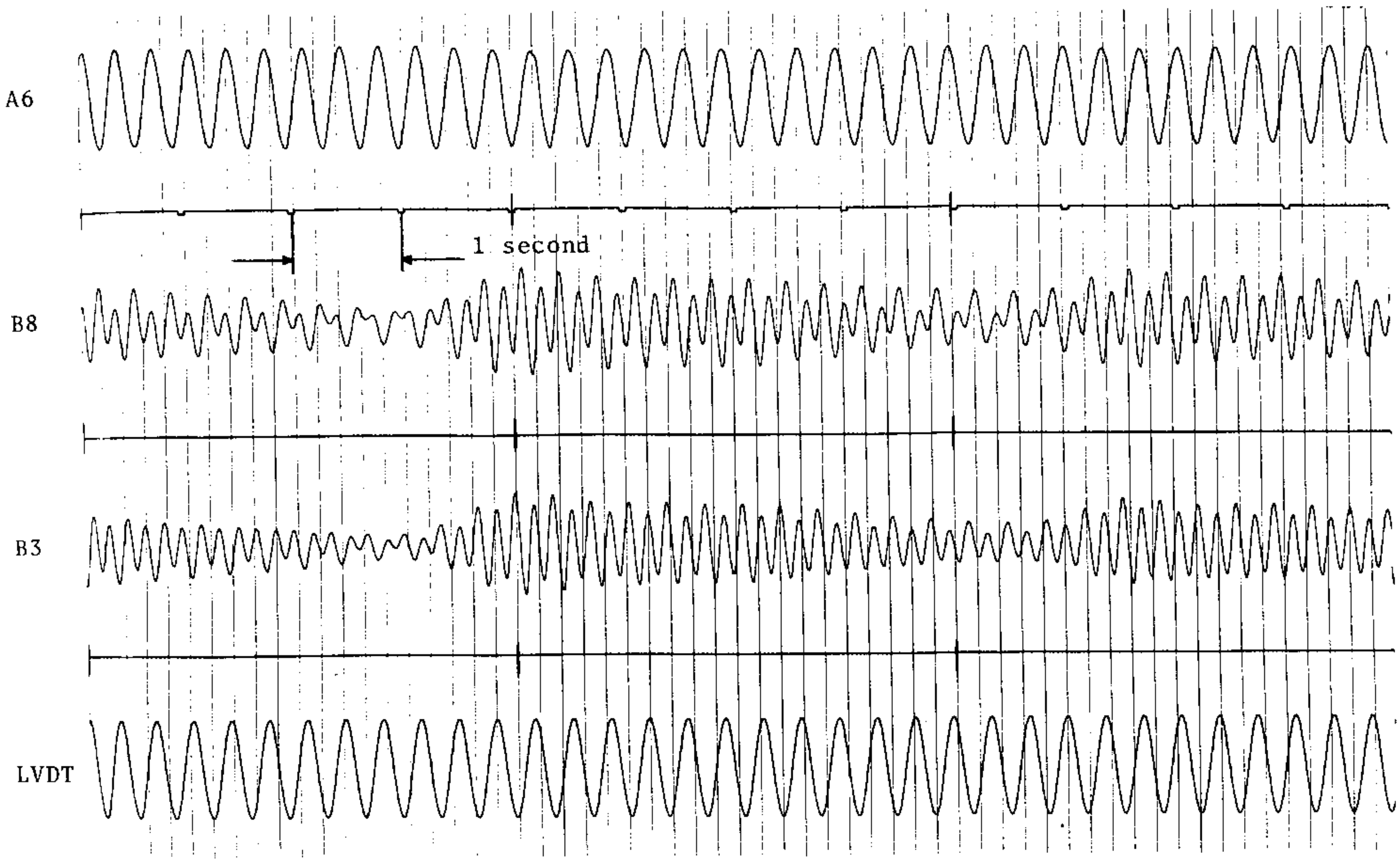

FIGURE 24Td: LVDT: 0.174 D_e/DIVISION; STRAINS: 15.3 MICROSTRAIN/DIVISION

3. REFERENCES

1. Chryssostomidis, C., and Patrikalakis, N. M., 1982, Experimental and Theoretical Prediction of the Response of a Marine Riser System Supported by a Tension Leg Platform Subjected to Surface Wave Excitation, MIT Design Laboratory Report No. 82-1, September 1982.

2. Chryssostomidis, C., Patrikalakis, N. M., and Vrakas, E. A., 1983, Theoretical and Experimental Prediction of the Response of a Marine Riser Model Subjected to Sinusoid Excitation of its Top End with Amplitude Equal to Two Diameters, MIT Sea Grant Report No. 83-2, March 1983.

3. International Mathematical and Statistical Library (IMSL), Reference Manual, 1981, Edition 8, IMSL, Inc.

4. Patrikalakis, N. M., 1983, Theoretical and Experimental Procedures for the Prediction of the Dynamic Behavior of Marine Risers," Ph.D. Thesis, MIT, Department of Ocean Engineering.

5. Patrikalakis, N. M. and Chryssostomidis, C., 1983, Theoretical and Experimental Prediction of the Response of a Marine Riser Model in a Uniform Stream, MIT Sea Grant Report No. 83-15, August 1983.

6. Sarpkaya, T., 1977, "In-Line and Transverse Forces on Cylinders in Oscillatory Flow at High Reynolds Numbers," Journal of Ship Research, Vol. 21, No. 4, 200-216.

7. Sarpkaya, T., 1980, "Hydroelastic Response of Cylinders in Harmonic Flow," Naval Architect, No. 3, pp. 103-110.

APPENDIX A

Figure A-1: Time Averaged Inertia Coefficient, c_M, Versus Reynolds Number Parametrically with Respect to Keulegan-Carpenter Number, K, for a Sinusoid Stream Orthogonal to a Fixed Rigid Smooth Circular Cylinder, Sarpkaya (1977).

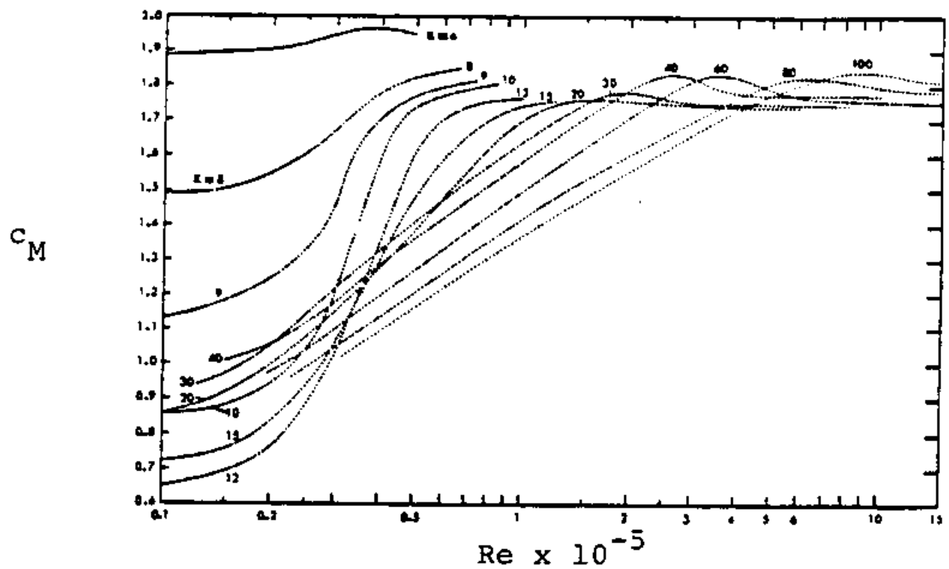

Figure A-2: Time Averaged Drag Coefficient, c_d, Versus Reynolds Number Parametrically with Respect to Keulegan-Carpenter Number, K, for a Sinusoid Stream Orthogonal to a Fixed Rigid Smooth Circular Cylinder, Sarpkaya (1977).

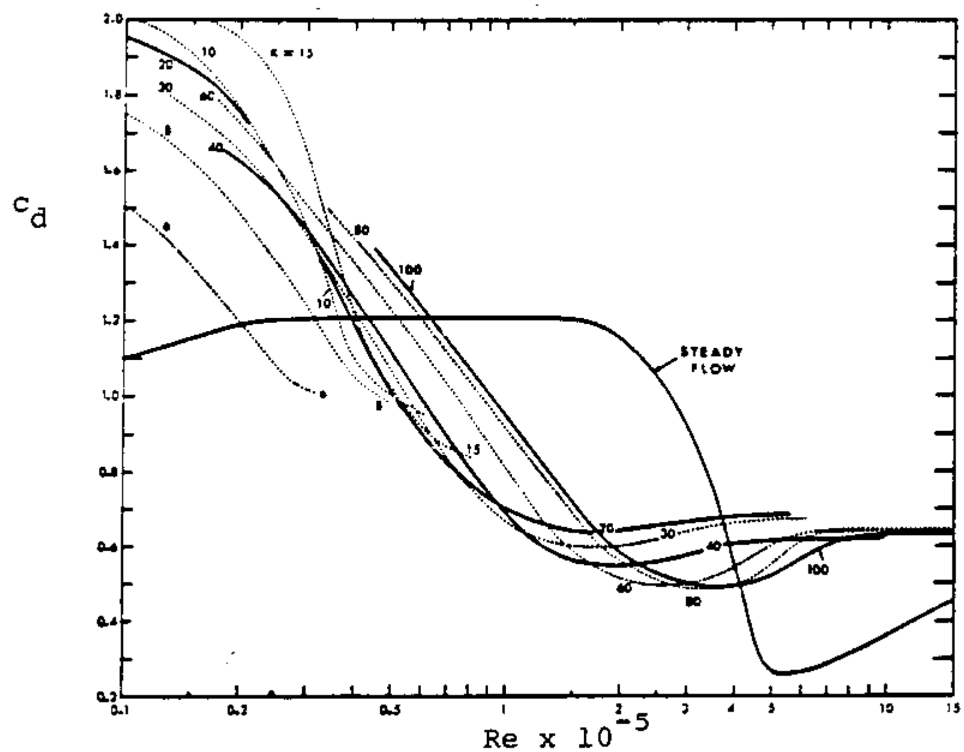

Figure A-3: Maximum Lift Coefficient, c_L, Versus Keulegan-Carpenter Number, K, Parametrically with Respect to Reynolds Number for a Sinusoid Stream Orthogonal to a Fixed Rigid Smooth Circular Cylinder, Sarpkaya (1977).

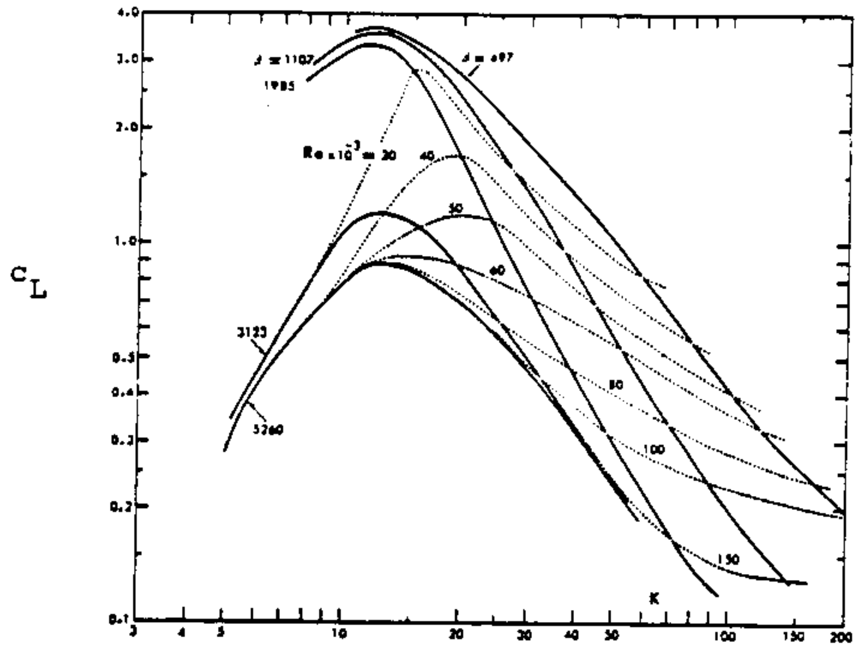

Figure A-4: Plot of the Non-Dimensional Response Amplitude (Half Height) Orthogonal to a Sinusoid Stream, Y_M/D, at Synchronization, as a Function of the Response Parameter, R_p, for Spring Mounted Smooth and Rough Cylinders, Sarpkaya (1980).

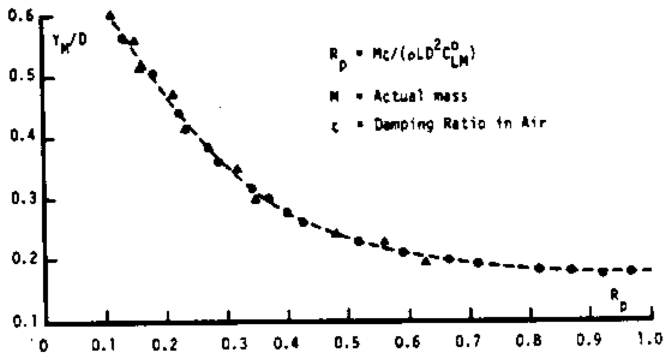

Figure A-5: Typical Plot of the Maximum Response Amplitude Orthogonal to a Sinusoid Stream Divided by the Diameter as a Function of U^*_n for a Sand-Roughened Cylinder with k/D=0.01, Sarpkaya (1980).